A molecular basis for differential Ca^{2+} signalling in B lymphocytes

Dissertation
zur Erlangung des
naturwissenschaftlichen Doktorgrades

der Fakultät für Chemie
der Universität Bielefeld

vorgelegt von
Björn Stork

Juli 2006

Danksagung

Meinem Doktorvater, Herrn Prof. Dr. Jürgen Wienands, möchte ich für das Vertrauen in den vergangenen Jahren danken. Dieses gilt im Besonderen für die ständige Diskussionsbereitschaft und seinen fachlichen Rat. Seine große Kooperationsbereitschaft und engagierte Unterstützung haben entscheidend zum Gelingen dieser Arbeit beigetragen

Ich danke Herrn Prof. Dr. Jürgen Frey und Herrn Prof. Dr. Schraven für die perfekte Zusammenarbeit im NTAL/Grb2-Projekt.

Prof. Dr. Naumann und Dr. Thilo Kähne danke ich für ihren entscheidenden Beitrag im Dok-3-Projekt.

I would like to thank Prof. Dr. Tomohiro Kurosaki for giving me the opportunity to work in his laboratory for eight months. I learned many things and I enjoyed the time in Osaka enormously. I also would like to thank my colleagues Satoko Nishikiori, Yumiko Nishikawa, Sachiko Johmura, Mayuko Takezaki, Yukari Shima, Mari Kurosaki, Tsuyoshi Nakamoto, Tetsuo Yamazaki, Masatsugu Oh-hora, and Masaki Hikida.

Für die Überlassung von Plasmiden und Zelllinien, die in dieser Arbeit Einsatz gefunden haben, danke ich Prof. Dr. H.M. Jäck, Prof. Dr. M. Jücker, Prof. Dr. V. Horejsi und Prof. Dr. M. Reth.

Ich möchte mich bei Anette, Herbert, Rainer, Markus sowie bei allen anderen ehemaligen Kollegen aus Bielefeld für die schöne Zeit bedanken.

Amina, Anna, Annika, Cora, Ilona, Nadine, Verena, Alex, Konstantin und Niklas danke ich für die gute Zusammenarbeit und viele lustige Momente in all den Jahren. Einen besonderen Dank möchte ich auch Frau Döhne und Frau Teuteberg aussprechen.

Den BlockpraktikantINNen Sabrina, Marion, Sven und Sebastian möchte für ihr enormes Engagement danken.

Ein ganz besonderer Dank gilt Ines und Nadine, die meine Arbeit in Göttingen bzw. Bielefeld entscheidend unterstützt haben. Ohne ihre Hilfe wäre diese Arbeit in dieser Form nicht zustande gekommen. Des Weiteren möchte ich herzlich Ines und Konstantin danken, die mich speziell in der Phase des Zusammenschreibens tatkräftig unterstützt haben.

I would like to thank Linda Tremblay for reading this thesis and for the wonderful time I had in Montréal. It was great to return to Montréal in 2004. I also would like to thank Michel, Pedro, Barry, and Prof. Herscovics.

Meinen ehemaligen Bielefelder Kommilitonen Nicole, Sylke, Tabea, Veronika, Dirk, Norman und Elmar danke ich für eine schöne Studiumszeit.

Ein ganz besonderer Dank gilt meinen Freunden Maren und Sebastian, Wiebke und Ingo, Gökhan, Kai, Steffi und Konstantin, Michele und Hans Peter, Berit und Ansgar, Wiebke und Jens, Svenja und Christian, Sabrina und Bernd. Sie alle sorgen für einen wundervollen Ausgleich.

Ich möchte mich besonders bei meinem Freund und „Vorgesetzten“ Michael bedanken. Seit dem Ende meiner Diplomarbeit hat er entscheidenden Anteil an dem roten Faden, der diese Arbeit (hoffentlich) durchzieht. Vielen Dank für deine Hilfe und deine Ideen!

Heide, Melanie, Christoph und Lars danke ich für ihre tiefe Freundschaft. Sie haben mich immer unterstützt und motiviert.

Miriam, Michael, Thomas, Mama und Papa danke ich von ganzem Herzen. Sie alle haben es erst ermöglicht, dass ich diese Arbeit fertig stellen konnte. Vielen Dank für den Halt, den ihr mir in meinem Leben gebt!

Bei Simone möchte ich mich für ihr Verständnis und ihre Liebe bedanken. Es ist schön, einen Menschen an seiner Seite zu haben, der einem das Gefühl und die Gewissheit gibt, das Ziel gefunden zu haben. Meiner Familie und ihr möchte ich diese Arbeit widmen.

Die vorliegende Arbeit wurde in der Zeit von Juli 2002 bis Juli 2006 in den Abteilungen Biochemie & Molekulare Immunologie der Universität Bielefeld, dem Department of Molecular Genetics der Kansai Medical University (Osaka, Japan) und der Abteilung Zelluläre und Molekulare Immunologie der Universität Göttingen unter der wissenschaftlichen Anleitung von Prof. Dr. Jürgen Wienands und Prof. Dr. Tomohiro Kurosaki angefertigt. Während dieser Zeit wurde ich vom Deutschen Akademischen Austauschdienst (DAAD) und dem Boehringer Ingelheim Fonds unterstützt.

Parts of this thesis were published in:

Stork, B., Engelke, M., Frey, J., Horejsi, V., Hamm-Baarke, A., Schraven, B., Kurosaki, T., and Wienands, J. (2004). Grb2 and the non-T cell activation linker NTAL constitute a Ca^{2+}-regulating signal circuit in B lymphocytes. *Immunity* **21**, 681-691.

Contents

I Abbreviations

Ab	antibody
AM	acetoxymethyl (esters)
Amp	ampicillin
AP	affinity purification
AP-1	activating protein 1
2-APB	2-aminoethoxydiphenylborane
APS	ammonium persulphate
ATCC	American type culture collection
ATP	adenosine trisphosphate
ATPase	adenosine trisphosphatase
att site	*att*achment site
BASH	B cell adaptor containing an SH2 domain
BCA	B cell activation-related gene
BCAP	B cell adaptor for PI3K
BCR	B cell antigen receptor
Blk	B cell lymphoma kinase
BLNK	B cell linker protein
Bmx	bone marrow tyrosine kinase gene on chromosome X
bp	base pair
BSA	bovine serum albumine
Btk	Bruton's tyrosine kinase
C2	conserved 2 domain
$[Ca^{2+}]_i$	intracellular Ca^{2+} concentration
CaMK	Ca^{2+}/calmodulin-dependent protein kinase
Cbl	Casitas B-lineage lymphoma
Cbp	Csk binding protein
CCE	capacitative Ca^{2+} entry
CCL	cleared cell lysate
CD	cluster of differentiation
Cdc42	cell division cycle 42
cDNA	complementary DNA/ copy DNA
CDR	complementarity determining region
ch	chicken
CICR	Ca^{2+}-induced Ca^{2+} release
CIF	Ca^{2+} influx factor
CIP	calf intestine phosphatase
CRAC	Ca^{2+} release activated Ca^{2+} channel
CS	chicken serum
Csk	C-terminal Src kinase
Δ	deletion
Da	Dalton

DAG	diacylglycerol
DEPC	diethylpyrocarbonate
DIG	detergent-insoluble glycolipid-rich membranes
DMEM	Dulbecco's modified Eagle's medium
DMP	dimethyl pimelimidate
DMSO	dimethylsulfoxide
DNA	deoxyribonucleic acid
dNTP	2'-deoxynucleoside-5'-trisphosphate
Dok	downstream of tyrosine kinase
Dok-L	Dok-like
Dok-R	Dok-related
DRM	detergent-resistant membranes
DTT	1,4-dithiothreitol
E. coli	*Escherichia coli*
ECL	enhanced chemical luminescence
EDTA	ethylenediamine tetraacetic acid
EGF	epidermal growth factor
EGFP	enhanced green fluorescent protein
EGFR	EGF receptor
EGTA	ethylene-glycol-bis(2-aminoethyl ether)-N,N,N',N'-tetraacetic acid
env	envelope; gene encoding glycoprotein160
ER	endoplasmic reticulum
ERK	extracellular signal-regulated kinase
$F(ab')_2$	bivalent antigen-binding fragment
FACS	fluorescence-activated cell sorter
Fc	fragment crystalline
FcR	Fc receptor
FCS	fetal calf serum
FITC	fluorescein-5-isothiocyanate
Fluo-3-AM	glycine, N-[4-[6-[(acetyloxy)methoxy]-2,7-dichloro-3-oxo-3H-xanthen-9-yl]-2-[2-[2-[bis[2-[(acetyloxy)methoxy]-2-oxyethyl]amino]-5-methylphenoxy]ethoxy]phenyl]-N-[2-[(acetyloxy)methoxy]-2-oxyethyl]-, (acetyloxy)methyl ester
FRIP	IL-four receptor interacting protein
Fyn	fgr/yes-related novel PTK
Gab	Grb2-associated binder
Gads	Grb2-related adaptor downstream of Shc
gag	gene encoding p55 (core protein)
GAPDH	glyceraldehyde-3-phosphate dehydrogenase
GEF	guanine-nucleotide exchange factor
GEM	glycophospholipid-enriched microdomain
Gga	*gallus gallus*

Grb2	growth factor receptor-bound protein 2
GST	glutathione-S-transferase
GTPase	guanosine trisphosphatase
HA	peptide from influenza hemagglutinin protein (YPYDVPDYA)
HEK	human embryonic kidney
HEL	hen egg lysozyme
HEPES	2-[4-(2-Hydroxyethyl)-1-piperazinyl]-ethanesulfonic acid
hisD	histidinol
HIV	human immunodeficiency virus
HPK1	hematopoietic progenitor kinase 1
HRPO	horseradish peroxidase
IB	immunoblot
I_{CRAC}	Ca^{2+} release activated Ca^{2+} current
Ig	immunoglobulin
IgH chain	Ig heavy chain
IgL chain	Ig light chain
IHF	integration host factor
IL	interleukin
Indo-1	1H-indole-6-carboxylic acid, 2-[4-[bis[2-[(acetyloxy)methoxy]-2-oxoethyl]amino]-3-[2-[2-[bis[2-[(acetyloxy)methoxy]-2-oxoethyl]amino]-5-methylphenoxy]ethoxy]phenyl]-, (acetyloxy)methyl ester
INS	insertion
Int	integrase
IP	immunoprecipitation
IP_3	inositol 1,4,5-trisphosphate
IP_3R	IP_3 receptor
IPTG	isopropyl-β-D-thiogalactopyranoside
IRES	internal ribosome entry site
IRS	insulin receptor substrate
ITAM	immunoreceptor tyrosine-based activation motif
ITIM	immunoreceptor tyrosine-based inhibitory motif
Itk	IL-2-inducible T-cell kinase
JNK	c-Jun N-terminal kinase
Kan	kanamycin
KAR	killer activating receptor
KIR	killer inhibitory receptor
LA	left arm
LAB	linker for activation of B cells
LAT	linker for activation of T cells
LAX	linker for activation of X cells

LB	lysogeny broth (incorrect: Luria broth; Lennox broth; Luria Bertani medium)
Lck	lymphocyte-specific protein tyrosine kinase
LGCC	ligand-gated non-specific cation channel
LIME	Lck-interacting molecule
Lyn	lck/yes-related novel PTK
mAb	monoclonal antibody
MAPK	mitogen-activated protein kinase
mIg	membrane Ig
MMLV	moloney murine leukemia virus
MS	mass spectrometry
NCBI	National Center for Biotechnology information
Nck	non-catalytic region of tyrosine kinase
NCR	natural cytotoxicity receptor
NEF	negative factor
neo	neomycin
NFAT	nuclear factor of activated T cells
NFκB	nuclear factor for κ gene in B lymphocytes
NK cells	natural killer cells
NTAL	non-T cell activation linker
OD	optical density
p	protein
P	phosphate
PAG	phosphoprotein associated with glycosphingolipid-enriched microdomains
PAGE	polyacrylamide gel electrophoresis
PBL	peripheral blood leukocyte
PBS	phosphate-buffered saline
PCMV	PCC4-cell-passaged myeloproliferative sarcoma virus
PCR	polymerase chain reaction
PDGF	platelet-derived growth factor
PH domain	pleckstrin homology domain
PI3K	phosphatidylinositol 3'-kinase
$PI(3,4)P_2$	phosphatidylinositol 3,4-bisphosphate
$PI(4,5)P_2$	phosphatidylinositol 4,5-bisphosphate
$PI(3,4,5)P_3$	phosphatidylinositol 3,4,5-trisphosphate
PIR-B	paired immunoglobulin-like receptor
PKC	protein kinase C
PLA	phospholipase A
PLC-γ1/2	phospholipase C-γ1/2
PMSF	phenylmethanesulfonyl fluoride
PNGase F	peptide:N-glycosidase F

pol	gene encoding protease, reverse transcriptase, and integrase
PTB domain	phosphotyrosine binding domain
PTK	protein tyrosine kinase
PTP	protein tyrosine phosphatase
pTyr	phosphotyrosine
pY	phosphotyrosine
RA	right arm
Rac	Ras-related C3 botulinum toxin substrate
RACC	receptor-activated Ca^{2+} channel
Ras	abbreviation originated from rat sarcoma
RasGAP	Ras GTPase-activating protein
RasGRP	Ras guanine nucleotide releasing protein
REP	replacement
Ret	rearranged during transfection
Rho	Ras homology
RNA	ribonucleic acid
RNAi	RNA interference
RNase	ribonuclease
ROC	receptor-operated channel
rpm	rounds per minute
RPMI	Roswell Park Memorial Institute
RT	reverse transcription/transcriptase or room temperature
RTK	receptor tyrosine kinase
RYR	ryanodine receptor
SDS	sodium dodecylsulfate
SERCA	sarcoplasmic/endoplasmic reticulum Ca^{2+}-ATPase
Shc	SH2-containing sequence
SH domain	Src homology domain
SHIP	SH2 domain-containing inositol 5'-phosphatase
SHP-1/2	SH2 domain-containing protein tyrosine phosphatases 1/2
SIT	SHP-2 interacting transmembrane adaptor protein
SLC	surrogate light chain
SLP-65	SH2 domain-containing leukocyte adaptor protein of 65 kDa
SLP-76	SH2 domain-containing leukocyte adaptor protein of 76 kDa
SMOC	second messenger-operated channel
SNP	single nucleotide polymorphism
SOC	store-operated channel
SOE	splicing by overlap extension
SOS	son of sevenless
SSC	sodium chloride sodium citrate
SSPE	sodium chloride sodium phosphate & EDTA

SR	sarcoplasmic reticulum
src	Rous sarcoma oncogene
STIM1	stromal interaction molecule 1
Syk	Spleen tyrosine kinase
t	time
T	temperature
TAE	Tris acetate EDTA buffer
TBE	Tris borate EDTA buffer
TBS	Tris-buffered saline
TCR	T cell antigen receptor
Tec	Tyrosine kinase expressed in hepatocellular carcinoma
TEMED	N,N,N',N'-tetramethylethylene-diamine
T_m	melting temperature
TM	transmembrane
TRIM	T-cell receptor interacting molecule
Tris	Tris-(hydroxymethyl)-aminomethane
Triton X-100	4-(2',2',4',4'-tetramethylbutyl)phenyldecaethylene-glycol-ether
TRP	transient receptor potential
Tween-20	polyoxyethylene sorbitan monolaurate
U	Units
US	unstimulated
UTR	untranslated region
UV	ultraviolet
Vav	six (Hebrew); adapter protein with GEF activity
VOCC	voltage-operated Ca^{2+} channel
VSV-G	vesicular stomatitis virus glycoprotein
v/v	volume per volume
w/o	without
w/v	weight per volume
wt	wild-type
X-Gal	5-bromo-4-chloro-3-indoxyl-β-D-galactopyranoside
Xis	excisionase
ZAP-70	zeta-chain associated protein of 70 kDa

II Amino acids

Amino Acid	3-letter code	symbol
Alanine	Ala	A
Cysteine	Cys	C
Aspartic Acid	Asp	D
Glutamic Acid	Glu	E
Phenylalanine	Phe	F
Glycine	Gly	G
Histidine	His	H
Isoleucine	Ile	I
Lysine	Lys	K
Leucine	Leu	L
Methionine	Met	M
Asparagine	Asn	N
Proline	Pro	P
Glutamine	Gln	Q
Arginine	Arg	R
Serine	Ser	S
Threonine	Thr	T
Valine	Val	V
Tryptophan	Trp	W
Tyrosine	Tyr	Y

III Deoxyribonucleotides

Deoxyribonucleotides	symbols
deoxyadenosine monophosphate	a, A
deoxycytidine monophosphate	c, C
deoxyguanosine monophospate	g, G
deoxythymidine monophosphate	t, T

IV Prefixes & Units

M	mega	m	meter	Bq	becquerel
k	kilo	L	liter	Ci	Curie
c	centi	M	molar	V	volt
m	milli	g	gram	A	ampere
µ	micro	b	base	F	farad
n	nano	bp	base-pair	h	hour
p	pico	Da	Dalton	min	minute
		U	unit	s	second
		°C	degree Celsius		
		g	acceleration of gravity		
		rpm	rounds per minute		

1. Summary

The generation of antigen-specific B lymphocytes is essential for the humoral immune response. B cell activation depends on signals generated upon engagement of the B cell antigen receptor (BCR). Proximal BCR effector proteins are cytoplasmic protein tyrosine kinases (PTKs) which phosphorylate cytoplasmic and transmembrane adaptor proteins such as SLP-65 or NTAL, respectively. Phosphorylated SLP-65 forms the scaffold for the assembly and activation of a protein complex which initiates Ca^{2+} release from intracellular stores. This Ca^{2+} initiation complex is composed of at least Bruton's tyrosine kinase (Btk) and phospholipase C-γ2 (PLC-γ2). BCR-induced Ca^{2+} mobilization arises by both release from intracellular Ca^{2+} stores, and Ca^{2+} influx through plasma membrane channels. The extent of Ca^{2+} mobilization from these two sources varies depending on the developmental stage of the B lymphocyte. Shaping Ca^{2+} profiles in the dimensions of space and time can determine different B cell responses, i.e. proliferation, differentiation, anergy or apoptosis. Currently, central questions of BCR-induced Ca^{2+} mobilization are: (1) how the Ca^{2+} initiation complex is targeted to the plasma membrane, (2) what is the exact mechanism of BCR-triggered PLC-γ2 activation, (3) how the intracellular Ca^{2+} release is connected to Ca^{2+} influx across the plasma membrane, and (4) how Ca^{2+} mobilization is differentially regulated during B cell lymphopoiesis. In this study, these questions were addressed by gene targeting experiments and subsequent reconstitutions in the chicken B cell line DT40. It was demonstrated that the SH2/SH3 adaptor Grb2 negatively regulates Ca^{2+} mobilization from intra- and extracellular sources. This function depends on the central SH2 and the C-terminal SH3 domain. Tyrosine-phosphorylated NTAL counter-acts Grb2 by recruiting it into lipid rafts. It was further shown that the NTAL/Grb2 module does not affect the phosphorylation state of the central components of the Ca^{2+} initiation complex, i.e. SLP-65 or PLC-γ2. However, it appeared that PLC-γ2 activation and/or retention at the plasma membrane are controlled by NTAL/Grb2. The downstream effector of Grb2 was determined to be the major tyrosine phosphorylated protein in DT40 B cells, and was subsequently identified as the cytosolic adaptor Dok-3. Phosphorylation of Dok-3 by Lyn depends on Grb2 and requires its central SH2 and C-terminal SH3 domain. Collectively, Grb2 seems to be a molecular switch in BCR-induced Ca^{2+} mobilization. The SH2 domain-dependent binding of Grb2 to either tyrosine phosphorylated NTAL or Dok-3 ultimately leads to positive or negative modulation of antigen receptor-induced Ca^{2+} mobilization in B cells. Thus, in this study a novel Ca^{2+} regulation pathway in B lymphocytes was identified. The adaptor-mediated modulation of Ca^{2+} mobilization may critically influence B cell signalling by supporting either activation or tolerance induction.

1.1. Zusammenfassung

Die Generierung Antigen-spezifischer B-Lymphozyten ist essentiell für die humorale Immunantwort. Die Aktivierung von B-Zellen ist von Signalen abhängig, die über den B-Zell-Antigenrezeptor (BCR) vermittelt werden. Cytoplasmatische Protein-Tyrosinkinasen (PTKs) sind BCR-proximale Effektorproteine, die cytoplasmatische und transmembrane Adapterproteine wie SLP-65 oder NTAL phosphorylieren. Phosphoryliertes SLP-65 bildet das Gerüst für die Assemblierung und Aktivierung eines Proteinkomplexes, der die Ca^{2+}-Freisetzung aus intrazellulären Speichern initiiert. Dieser Ca^{2+}-Initiationskomplex besteht mindestens aus Brutons Tyrosinkinase (Btk) und Phospholipase C-γ2 (PLC-γ2). Die BCR-induzierte Ca^{2+}-Mobilisierung beinhaltet sowohl die Freisetzung aus intrazellulären Ca^{2+}-Speichern als auch den Einstrom über die Plasmamembran. Das Ausmaß der Ca^{2+}-Mobilisierung aus diesen beiden Speichern hängt von dem Entwicklungsstadium des B-Lymphozyten ab. Die räumliche und zeitliche Veränderung von Ca^{2+}-Profilen kann zu verschiedenen B-Zell-Antworten führen, d.h. Proliferation, Differenzierung, Anergie oder Apoptose. Gegenwärtig sind zentrale Fragen in der BCR-induzierten Ca^{2+}-Mobilisierung: (1) wie wird der Ca^{2+}-Initiationskomplex an die Membran rekrutiert, (2) was ist der exakte Mechanismus der BCR-vermittelten PLC-γ2 Aktivierung, (3) wie ist die intrazelluläre Ca^{2+}-Freisetzung mit dem Ca^{2+}-Einstrom über die Plasmamembran verbunden, und (4) wie erfolgt die differentielle Regulierung der Ca^{2+}-Mobilisierung während der B-Zell-Lymphopoese? In dieser Studie wurden diese Fragen mittels zielgerichteter Gen-Inaktivierung und nachfolgenden Rekonstitutionen analysiert. Es konnte gezeigt werden, dass der SH2/SH3-Adapter Grb2 die Ca^{2+}-Mobilisierung aus intra- und extrazellulären Quellen negativ reguliert. Diese Funktion ist von der zentralen SH2- und der C-terminalen SH3-Domäne abhängig. Tyrosin-phosphoryliertes NTAL wirkt dieser Funktion durch die Grb2-Rekrutierung in *lipid rafts* entgegen. Es konnte des weiteren gezeigt werden, dass das NTAL/Grb2-Modul nicht den Phosphorylierungsgrad der zentralen Komponenten des Ca^{2+}-Initiationskomplexes, d.h. SLP-65 oder PLC-γ2, beeinflusst. Allerdings scheinen NTAL/Grb2 die PLC-γ2-Aktivierung und/oder dessen Retention an der Plasmamembran zu kontrollieren. Es konnte im Rahmen dieser Arbeit herausgefunden werden, dass das Hauptphosphoprotein in DT40 das Grb2-Effektorprotein ist. Nachfolgend wurde dieses als das cytosolische Adapterprotein Dok-3 identifiziert. Die Phosphorylierung von Dok-3 durch Lyn ist abhängig von Grb2 und benötigt dessen zentrale SH2- und die C-terminale SH3-Domäne. Zusammenfassend deuten diese Studien darauf hin, dass Grb2 ein molekularer Schalter in der BCR-induzierten Ca^{2+}-Mobilisierung ist. Die SH2-Domänen-abhängige Bindung von Grb2 an entweder Tyrosin-phosphoryliertes NTAL oder Dok-3 führt letztendlich zur positiven bzw. negativen Modulation der Antigenrezeptor-induzierten Ca^{2+}-Mobilisierung in B-Zellen. In dieser Studie wurde ein neuer Ca^{2+}-Regulationsmechanismus identifiziert. Die Adapter-vermittelte Modulation der Ca^{2+}-Mobilisierung könnte durch die Unterstützung von entweder Aktivierung oder Toleranzinduktion die B-Zell-Signaltransduktion kritisch beeinflussen.

2. Introduction

Immune responses are mediated by leukocytes, which originate from pluripotent hematopoietic stem cells in the bone marrow. These stem cells give rise to myeloid cell lineages including granulocytes, macrophages, dendritic cells and mast cells, as well as lymphoid cell lineages such as B lymphocytes, T lymphocytes and natural killer (NK) cells. B lymphocytes (B cells) mature in the bone marrow or in the avian Bursa of Fabricius, whereas T lymphocytes (T cells) mature in the thymus. Lymphocytes represent the foundation for the adaptive immune response which specifically recognizes all pathogens and guarantees protective immunity against re-infection. This is accomplished by mature lymphocytes each bearing a monospecific variant of a prototype antigen receptor on its surface.

2.1. Structure and functions of the antigen receptors on B lymphocytes

The B cell antigen receptor (BCR) is composed of several subunits with separate functions for signal reception and signal transduction (RETH, 1992; NEUBERGER et al., 1993). Membrane-bound immunoglobulins (mIgs) recognize and bind extracellular antigen. Immunoglobulins (Igs) are tetrameric proteins consisting of two Ig heavy (IgH) chains and two Ig light (IgL) chains. One IgL chain is covalently associated with one IgH chain by a disulfide bond, and the two IgH chains are connected by disulfide bonds. The juxtaposition of the IgH and IgL complementarity-determining regions (CDRs) form the antigen binding region (RETH, 1992; WIENANDS, 2000a), and each individual B cell carries BCRs of a single antigen specificity. According to the Ig heavy chain, Igs are divided into five isotypes: IgM, IgD, IgG, IgA, and IgE (RETH, 1992). In pre-B cells, the pre-BCR is generated by the association of the μm-heavy chain (m = membrane) with the surrogate light chain (SLC) which is composed of the invariant polypeptides λ5 and $V_{pre}B$ (RETH, 1992). BCR signal transduction is mediated through the transmembrane proteins Ig-α (CD79a, *mb-1* gene product) and Ig-β (CD79b, *B29* gene product). A disulfide-linked Ig-α/Ig-β heterodimer is non-covalently associated with the mIg in a 1:1 complex (RETH et al., 2000; SCHAMEL and RETH, 2000).

The main function of B lymphocytes is to contribute to the elimination of foreign antigens by producing soluble antibodies. However, the BCR does not only play a central role in the antigen-induced activation of mature B lymphocytes during adaptive humoral immune responses, but also in B cell development, B cell maintenance, and in the apoptotic elimination of B cells reactive to self-antigens (reviewed in WIENANDS, 2000a).

2.2. BCR-mediated signalling

2.2.1. Signalling via the Ig-α/Ig-β heterodimer

Ig-α and Ig-β each contain in their cytoplasmic tail a single copy of a specific amino acid motif which is necessary for the signalling functions of both the pre-BCR and the BCR (RETH, 1989; CAMBIER, 1995). This motif is called the immunoreceptor tyrosine-based activation motif (ITAM) and is characterized by the consensus amino acid sequence D/Ex$_7$D/ExxYxxI/Lx$_7$YxxI/L (single-letter amino acid code, x denotes any residue) (RETH, 1989). Upon BCR engagement, the two tyrosine residues of the ITAM become phosphorylated by intracellular protein tyrosine kinases (PTKs). ITAM phosphorylation is initiated by Src family PTKs (Lyn, Fyn and/or Blk), which can be found in close association with unligated BCRs (YAMANASHI et al., 1991; CAMPBELL and SEFTON, 1992). A phosphorylated ITAM-tyrosine provides a binding motif for proteins containing a Src homology 2 (SH2) domain. SH2 domains bind sequence-specifically to tyrosine-phosphorylated proteins (SONGYANG et al., 1993). A doubly phosphorylated ITAM is bound by the tandemly arranged SH2 domains of the cytoplasmic PTK Syk (see figure 2.1) (KUROSAKI et al., 1995; WIENANDS et al., 1995; FUTTERER et al., 1998). Syk is expressed in most hematopoietic cells, and forms together with ZAP-70 that is expressed in T lymphocytes and NK cells the Syk family PTKs (reviewed in TURNER et al., 2000). The kinase activity of Syk is activated by a combination of SH2-mediated recruitment, transphosphorylation through Src family PTKs, and autophosphorylation processes (KUROSAKI et al., 1994; KUROSAKI et al., 1995; ROWLEY et al., 1995; KIMURA et al., 1996). The phosphorylation of a tyrosine residue in the activation loop of the kinase domain (Y^{520}) is central to Syk activation, whereas phosphorylation of Y^{317} in the linker region between C-terminal SH2 domain and kinase domain inhibits Syk function (HIKIDA and KUROSAKI, 2005).

PTKs of the Src family and Syk couple the BCR to multiple signal transduction pathways including the mobilization of Ca^{2+} ions, activation of protein kinase C (PKC), and activation of small G proteins (Ras and Rho/Rac/Cdc42), and mitogen-activated protein kinases (MAPKs) such as extracellular signal-regulated kinase (Erk), c-Jun N-terminal kinase (Jnk), or p38. Ultimately, antigen recognition leads to the activation of transcription factors (e.g. nuclear factor of activated T cells, NFAT; nuclear factor for κ gene in B lymphocytes, NF-κB; activating protein-1, AP-1) and subsequent changes in gene expression (see also section 2.6).

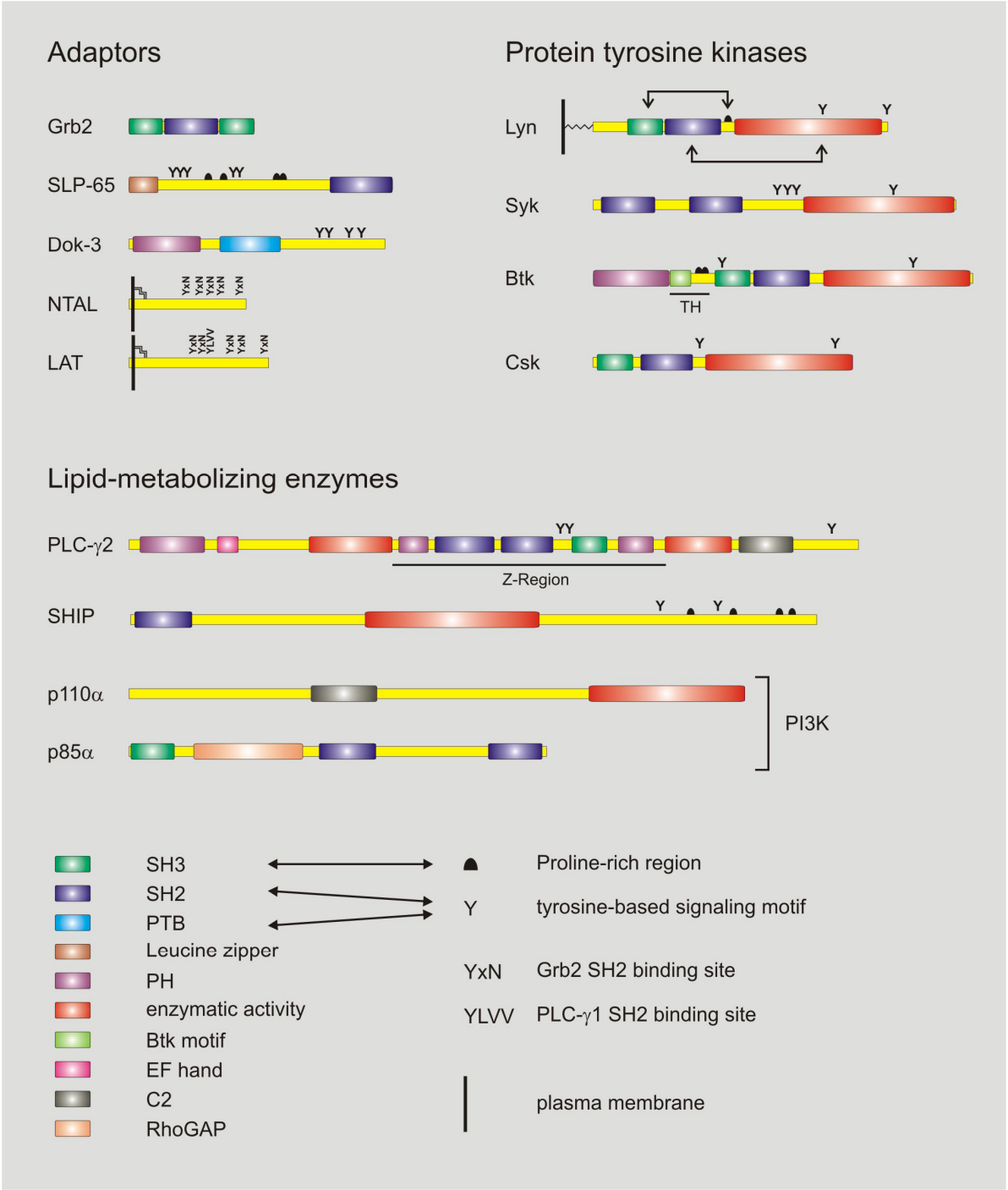

Figure 2.1: Signalling molecules in B lymphocytes
A selection of signalling molecules found in B lymphocytes is schematically depicted to visualize their modular structure and their protein-protein and protein-lipid interaction domains. In this figure murine orthologs are illustrated. SH2 and PTB domains bind to phosphotyrosines (shown as Y), SH3 domains bind to proline-rich peptide motifs (illustrated as black semi-ellipses), and PH domains associate with phospholipids. Binding sites for the Grb2 SH2 domain are designated as YxN. Intramolecular interactions in PTK Lyn are illustrated as black doubleheaded arrows. The relative size of the molecules is scaled down. Btk, Bruton's tyrosine kinase; Csk, C-terminal Src kinase; Dok-3, downstream of kinase 3; Grb2, growth factor receptor bound protein 2; LAT, linker for activation of T cells; Lyn, Lck/Yes-related novel tyrosine kinase; NTAL, non-T cell activation linker; PH, pleckstrin homology domain; PI3K, phosphatidylinositol 3'-kinase; PLC-γ2, phospholipase C-γ2; PTB, phosphotyrosine binding domain; PTK, protein tyrosine kinase; SH2, Src homology domain 2; SH3, Src homology domain 3; SHIP, SH2 domain-containing inositol 5'-phosphatase; SLP-65, SH2-domain-containing leukocyte protein of 65 kDa; Syk, spleen tyrosine kinase; TH, tec homology domain (modified from KUROSAKI, 2002).

2.2.2. Negative regulation of BCR signalling

The intracellular signalling machinery leading to cell activation is shared not only by the BCR and T cell antigen receptor (TCR), but also by receptors for the Fc portion of immunolgobulins (FcRs; e.g. FcεRI, FcγRI, FcγRIIA, FcγRIII), natural cytotoxicity receptors (NCRs) on NK cells, and killer activating receptors (KARs) (VEILLETTE et al., 2002). In order to counterbalance this cell activation machinery, immune cells possess an equally complex machinery aimed at restricting the duration and/or intensity of signalling. This inhibitory machinery includes receptors containing immunoreceptor tyrosine-based inhibitory motifs (ITIMs) (e.g. FcγRIIB; killer inhibitory receptors, KIRs; CD22; CD72; paired immunoglobulin-like receptor B, PIR-B), tyrosine kinases (e.g. C-terminal Src kinase, Csk), tyrosine phosphatases (e.g. SH2 domain-containing protein tyrosine phosphatases 1/2, SHP-1/2), lipid phosphatases (e.g. SH2 domain-containing inositol 5'-phosphatase, SHIP; phosphatase and tensin homolog, PTEN), adaptors (e.g. downstream of tyrosine kinase, Dok), and ubiquitin ligases (e.g. c-Cbl, Cbl-b) (reviewed in VEILLETTE et al., 2002).

The regulation of the activity of Src family PTKs is an example for the interplay between activating and inhibitory machinery. Src family PTKs contain a unique region at the N-terminus, followed by a Src homology 3 (SH3) domain, an SH2 domain, and a kinase domain (also known as SH1 domain) (see figure 2.1). SH3 domains bind to short proline rich sequences with a core PxxP motif (SPARKS et al., 1996, 1998; MAYER, 2001). The activity of Src family PTKs is controlled by two tyrosine phosphorylation sites. Autophosphorylation of a conserved tyrosine in the kinase domain (Y^{397} in murine Lyn) results in activation. In contrast, phosphorylation of the regulatory tyrosine near the C-terminus (Y^{508} in murine Lyn) by Csk leads to intramolecular interactions which stabilize the inactive conformation (NADA et al., 1993; CHONG et al., 2005a, 2005b). These inhibitory intramolecular interactions include the binding of phospho-Y^{508} to the SH2 domain and the association of a polyproline type II helical structure in the SH2-kinase interdomain with the SH3 domain (see figure 2.1) (CHONG et al., 2005a, 2005b). Thus, it has been proposed that Src family PTKs are active upon: (1) interference with the inhibitory intramolecular interactions, (2) autophosphorylation of Y^{397}, and (3) dephosphorylation of Y^{508} (CHONG et al., 2005a, 2005b). CD45 is the phosphatase responsible for the dephosphorylation of both the autophosphorylation and the regulatory tyrosine (YANAGI et al., 1996). Indeed, the regulatory tyrosine of Lyn is hyperphosphorylated in CD45-deficient B cells and hypophosphorylated in Csk-deficient B cells (HATA et al., 1994; YANAGI et al., 1996). Csk is recruited to the plasma membrane via the phosphoprotein associated with

glycosphingolipid-enriched microdomains (PAG; also known as Csk-interacting protein, Cbp) (BRDICKA et al., 2000; KAWABUCHI et al., 2000). Ligands which bind to the SH3 domain of Src family PTKs can efficiently activate them by disrupting the polyproline-SH3 interaction. Examples of these SH3 ligands are the human immunodeficiency virus (HIV)-1 accessory protein Nef (BRIGGS et al., 1997; MOAREFI et al., 1997), SHP-2 (WALTER et al., 1999), and UNC119 (CEN et al., 2003; GORSKA et al., 2004).

2.2.3. BCR complexes and lipid rafts

Upon crosslinking, BCR complexes can be detected in low-density detergent-resistant microdomains called lipid rafts (CHENG et al., 1999; AMAN and RAVICHANDRAN, 2000; DILLON et al., 2000; PETRIE et al., 2000; WEINTRAUB et al., 2000). Lipid rafts (also known as detergent-resistant membranes, DRMs, glycophospholipid-enriched microdomains, GEMs, or detergent insoluble glycolipid-rich membranes, DIGs) are lateral heterogeneities in the plasma membrane which are highly dynamic submicroscopic assemblies that float freely like a raft in the lipid bilayer of cell membranes (reviewed in BROWN and LONDON, 2000; LANGLET et al., 2000; SIMONS and TOOMRE, 2000; RAJENDRAN and SIMONS, 2005). Lipid rafts are enriched in cholesterol as well as glycosphingolipids with saturated fatty acid side chains. Phosphatidyl-4,5-bisphosphate [$PI(4,5)P_2$], the major substrate of activated phospholipase C-γ (PLC-γ) or phosphatidylinositol 3'-kinase (PI3K) (see below), is also a major component of lipid rafts (HOPE and PIKE, 1996; XAVIER et al., 1998). Whereas most transmembrane proteins are excluded from these microdomains, several signalling proteins partition into the lipid rafts upon modification with hydrophobic side chains, e.g. the doubly acylated Src family PTKs or the linker for activation of T cells (LAT, see below) (ZHANG et al., 1998a; LIN et al., 1999; BROWN and LONDON, 2000; LANGLET et al., 2000; SIMONS and TOOMRE, 2000). In mature B cells, few BCR complexes are present in lipid rafts before antigen recognition. It has been postulated that the recruitment of crosslinked BCRs within lipid rafts initiates signalling by co-localizing the BCR with proximal signalling molecules such as Lyn (CHENG et al., 1999) and by exclusion of negative regulators of BCR signalling such as CD22 (WEINTRAUB et al., 2000). However, recent reports question the importance of lipid rafts. The first definition of lipid rafts was biochemical and based on the resistance of lipid rafts to extraction with Triton X-100 at 4 °C (BROWN and ROSE, 1992). It is now accepted that DRMs do not accurately reflect the native state of the lipid microdomains (MUNRO, 2003; LICHTENBERG et al., 2005). Douglass and Vale recently demonstrated that the key regulator of plasma membrane microdomains is a protein-protein network and not

lipid rafts (DOUGLASS and VALE, 2005). Thus, defining the role of membrane microdomains definitely requires further investigation.

2.3. Adaptor proteins in lymphocyte signalling

2.3.1. Cytosolic adaptor proteins

In addition to cell-surface receptors, it is now clear that adaptor molecules participate in the modulation of signal transduction. Adaptor molecules exert their function by mediating protein-protein or protein-lipid interactions via modular interaction domains, without intrinsic enzymatic or transcriptional activities. However, many enzymes also contain protein- or lipid-binding modules and can therefore be considered adaptors (see figure 2.1).

The SH2-domain-containing leukocyte protein of 65 kDa (SLP-65, also known as BLNK, BASH, and BCA) is the central adaptor protein in B cells (FU et al., 1998; GANGI-PETERSON et al., 1998; GOITSUKA et al., 1998; WIENANDS et al., 1998). It is the immediate downstream substrate of Syk and was cloned on the basis of its tyrosine phosphorylation after BCR engagement. SLP-65 is composed of an N-terminal leucine-zipper motif (KOHLER et al., 2005), followed by an acidic region with five tyrosine phosphorylation motifs and several putative recognition motifs for SH3 domains, and a C-terminal SH2 domain (figure 2.1). SLP-65 is mainly expressed in B cells and macrophages and its domain structure is similar to its T-cell paralog SLP-76 (FU et al., 1998; GANGI-PETERSON et al., 1998; GOITSUKA et al., 1998; WIENANDS et al., 1998; BONILLA et al., 2000). The N-terminal tyrosine residues mediate phosphorylation-dependent interactions with the guanine-nucleotide exchange factor (GEF) Vav1, the adaptor non-catalytic region of tyrosine kinase (Nck), the Tec family PTK Bruton`s tyrosine kinase (Btk), and PLC-γ2 (FU et al., 1998; WIENANDS et al., 1998; HASHIMOTO et al., 1999; ISHIAI et al., 1999a; SU et al., 1999). The adaptor molecule growth factor receptor bound protein 2 (Grb2) binds to proline rich regions of SLP-65 (FU et al., 1998; WIENANDS et al., 1998; FUSAKI et al., 2000), and the SLP-65 SH2 domain was shown to interact with hematopoietic progenitor kinase 1 (HPK1) and Ig-α (SAUER et al., 2001; ENGELS et al., 2001; KABAK et al., 2002). One of SLP-65's central tasks in B cell signalling is the organization of the Ca^{2+} initiation complex consisting of SLP-65, Btk, and PLC-γ2 (see below) (reviewed in KORETZKY et al., 2006).

Grb2 is a prototypic adaptor protein containing a central SH2 domain flanked by two SH3 domains (figure 2.1) (CLARK et al., 1992; LOWENSTEIN et al., 1992; OLIVIER et al., 1993). Grb2 is ubiquitously expressed in mutliple tissues and cell lines (OLIVIER et al., 1993), and since its discovery a plethora of Grb2-interacting proteins have been identified (for an overview see: www.signaling-gateway.org). Although the C-terminal SH3 domain of Grb2

can bind to SLP-65 it was shown that these two molecules translocate to lipid rafts independently of each other following BCR engagement (JOHMURA et al., 2003). Both SH3 domains were demonstrated to bind the GEF son of sevenless (SOS) homolog (BUDAY and DOWNWARD, 1993; CHARDIN et al., 1993; EGAN et al., 1993; LI et al., 1993; ROZAKIS-ADCOCK et al., 1993). The Grb2 SH2 domain preferentially binds to the phosphotyrosine (pY)-containing motif pYxN (KESSELS et al., 2002). Ligation of growth-factor receptors leads to tyrosine phosphorylation in the cytoplasmic tail of the receptor tyrosine kinases (RTKs) and subsequent binding of Grb2 via its SH2 domain. Thereby, the Grb2-SOS complex is recruited to the membrane, where SOS can activate membrane-localized Ras (ROGGE et al., 1991; EGAN et al., 1993; GALE et al., 1993; LI et al., 1993; ROZAKIS-ADCOCK et al., 1993; SKOLNIK et al., 1993; DOWNWARD, 1994; MARGOLIS and SKOLNIK, 1994). In BCR signalling, the adaptor protein Shc has been implicated in the recruitment of the Grb2/SOS complex to the membrane (SAXTON et al., 1994; HARMER and DEFRANCO, 1997). Upon BCR stimulation, Shc is recruited to the plasma membrane and becomes tyrosine phosphorylated, thereby creating binding sites for Grb2 (SALCINI et al., 1994; SAXTON et al., 1994; VAN DER GEER et al., 1996; HARMER and DEFRANCO, 1997). Shc/Grb2/SOS complexes were detected in the membrane-enriched particulate fraction of stimulated B cells (SAXTON et al., 1994). However, Oh-hora et al. demonstrated that the BCR activates Ras through Ras guanine nucleotide releasing protein 3 (RasGRP3) rather than via the Grb2/SOS complex (OH-HORA et al., 2003). Thus, the exact role of Grb2 in BCR signal transduction remains to be determined.

Cytosolic adaptor proteins not only serve as scaffolds for the assembly of cell activation complexes, but also play an important role in inhibitory pathways. Members of one adaptor family may sometimes exert both activating and inhibitory functions as exemplified by members of the Dok family. Structural characteristics of this adaptor family make them most similar to the insulin receptor substrate (IRS) family of proteins (CONG et al., 1999). All Dok proteins contain an N-terminal pleckstrin homology (PH) domain, a central phosphotyrosine binding (PTB) domain, and a C-terminal region containing proline-rich regions and tyrosine-based signalling motifs (VEILLETTE et al., 2002).

To date, six members of the Dok-family have been identified. Dok-1 (also known as $p62^{dok}$) was originally shown to be a substrate of activated PTKs and to associate with p120 Ras GTPase-activating protein (p120 RasGAP) when phosphorylated (ELLIS et al., 1990; CARPINO et al., 1997; YAMANASHI and BALTIMORE, 1997). Dok-2 (also known as Dok-R, FRIP, or $p56^{dok}$) has also been shown to inducibly interact with p120 RasGAP (DI CRISTOFANO et al., 1998; JONES and DUMONT, 1998; NELMS et al., 1998). Dok-3 (figure2.1; also known as Dok-L) was reported to play a role in the negative regulation of BCR

signalling, but unlike Dok-1 and Dok-2, Dok-3 cannot bind p120 RasGAP (CONG et al., 1999; LEMAY et al., 2000).

Dok-1, Dok-2, and Dok-3 have all been shown to primarily mediate negative signalling downstream of various receptor and non-receptor kinases (NELMS et al., 1998; CONG et al., 1999; JONES and DUMONT, 1999; LEMAY et al., 2000; YAMANASHI et al., 2000; ZHAO et al., 2001; ROBSON et al., 2004), and all three inducibly interact with both SHIP and Csk (LEMAY et al., 2000; TAMIR et al., 2000; LATOUR and VEILLETTE, 2001; OTT et al., 2002; VAN SLYKE et al., 2005). In contrast, Dok-4, Dok-5 and Dok-6 were identified as targets of Ret and the insulin receptor, and positively regulate RTK signalling pathways (GRIMM et al., 2001; CAI et al., 2003; FAVRE et al., 2003; CROWDER et al., 2004). Dok-1-3 are predominantly expressed in tissues of hematopoietic origin, whereas the other three members are highly expressed in non-hematopoietic tissues, and particularly in the nervous system (LEMAY et al., 2000; GRIMM et al., 2001; CROWDER et al., 2004).

Dok proteins function as scaffolding molecules with regulated membrane-targeting properties (WHITE and YENUSH, 1998; VAN DIJK et al., 2000; JACOBS et al., 2001; ZHAO et al., 2001). PH domains bind phospholipids and therefore serve as membrane-targeting domains (LEMMON and FERGUSON, 1998; LEMMON, 2004). Since most PH domains bind phospholipids with low affinity and specificity, it has been postulated that either post-translational modifications or oligomerization might enable PH domains to bind membranes with greater avidity (LEMMON and FERGUSON, 2000). PTB domains are structurally related to PH domains (BORG and MARGOLIS, 1998; BLOMBERG et al., 1999). Some PTB domains may bind phospholipids (RAVICHANDRAN et al., 1997; HOWELL et al., 1999), but essentially they serve as protein-protein interaction modules (FORMAN-KAY and PAWSON, 1999; SCHLESSINGER and LEMMON, 2003). Recently it was discovered that many PTB domains can bind peptide sequences in a phosphorylation-independent (BORG et al., 1996) or in a tyrosine-independent manner (CHAREST et al., 1996; CHIEN et al., 1998; MEYER et al., 1999; ONG et al., 2000). In IRS and Dok proteins, PH and PTB domains co-exist (BEDIRIAN et al., 2004). So far it seems that recruitment of the Dok family proteins to the plasma membrane can occur by various mechanisms, and is dependent on either the PH domain or the PTB domain or both. Although the interaction of Dok-1-3 with various negative regulators of BCR signalling and their recruitment to the membrane was reported by several groups, the physiologic processes regulated by Dok-1-3 in B lymphocytes remain poorly understood.

2.3.2. Transmembrane adaptor proteins

The second large group of adaptors are integral membrane proteins. They lack modular protein-protein interaction domains present in cytosolic adaptors but contain mutiple

tyrosine-based signalling motifs, which are phosphorylated upon antigen receptor triggering. Based on these structural properties, transmembrane adaptors serve as anchors for SH2- and PTB-domain containing signalling molecules and recruit them to the plasma membrane. Transmembrane adaptor proteins can be further divided into lipid raft-associated and lipid raft-excluded molecules.

To date, four lipid-raft associated transmembrane adaptors have been identified and cloned: LAT, the non-T cell activation linker (NTAL; also called linker for activation of B cells, LAB), PAG/Cbp, and the Lck-interacting molecule (LIME) (ZHANG et al., 1998b; BRDICKA et al., 2002; JANSSEN et al., 2003; BRDICKA et al., 2000; KAWABUCHI et al., 2000; BRDICKOVA et al., 2003; HUR et al., 2003). These four members are monomeric type III transmembrane proteins that share a common structure including a short extracellular domain, a single transmembrane domain, and a cytoplasmic tail possessing a palmitoylation motif (CxxC) juxtaposed to the transmembrane region, as well as multiple tyrosine-based signalling motifs (LINDQUIST et al., 2003; SIMEONI et al., 2005). The CxxC motif is responsible for lipid-raft targeting (ZHANG et al., 1998a; LIN et al., 1999). In contrast, the non-lipid raft transmembrane proteins T-cell receptor interacting molecule (TRIM), SHP-2 interacting transmembrane adaptor protein (SIT), and linker for activation of X cells (LAX) all lack the CxxC motif.

LAT is probably the best-studied transmembrane adaptor molecule and was first cloned in 1998 (ZHANG et al., 1998b). It plays an important role in both TCR signalling and T cell development (ZHANG et al., 1999a). However, LAT is not only expressed in T lymphocytes but also in NK cells, mast cells, megakaryocytes, platelets, and in pre-B cells (GIBBINS et al., 1998; SARKAR, 1998; FACCHETTI et al., 1999; SU and JUMAA, 2003). The four membrane distal tyrosines (Y^{132}, Y^{171}, Y^{191} and Y^{226} in human) are preferentially phosphorylated upon TCR engagement, and serve as binding sites for the SH2 domains of Grb2 (Y^{171}, Y^{191}, and Y^{226}), Grb2-related adaptor downstream of Shc (Gads) (Y^{171} and Y^{191}), and PLC-γ1 (Y^{132}) (FINCO et al., 1998; ZHANG et al., 1998b, 2000; LIN and WEISS, 2001; ZHU et al., 2003). Since the SH2 domains of Gads and Grb2 are flanked by two additional SH3 domains, these two adaptors are capable of recruiting further signalling molecules to LAT. For example, the C-terminal SH3 domain of Gads binds to SLP-76 with high affinity (BERRY et al., 2002; LIU et al., 2003). SLP-76 itself also recruits further effector molecules to this complex such as the Tec family kinase Itk. To summarize, LAT acts as scaffold for several signalling complexes in T cells and couples the immediate signalling events upon TCR engagement to processes leading to T cell activation.

Identification of NTAL led researchers to believe that the B-cell paralog of LAT. This view was mainly supported by the fact that NTAL is closely related to LAT both structurally and evolutionarily (BRDICKA et al., 2002; JANSSEN et al., 2003). NTAL contains five potential Grb2 binding sites of the YxN type. SLP-65 translocates to lipid rafts upon BCR stimulation (FU et al., 1998). Gads and LAT paralogs have been speculated to mediate this translocation. However, NTAL has not been shown to associate with SLP-65 or PLC-γ2 (BRDICKA et al., 2002; JANSSEN et al., 2003). Furthermore, *ntal*$^{-/-}$ mast cells show increased PLC-γ activity, increased inositol 1,4,5-trisphosphate (IP_3) production, and increased Ca^{2+} mobilization (VOLNA et al., 2004; ZHU et al., 2004). Additionally, *ntal*$^{-/-}$ mice have normal B cell development and slightly increased BCR-induced Ca^{2+} mobilization and proliferation (ZHU et al., 2004; WANG et al., 2005). Thus, it was postulated that NTAL does not play a role in BCR signalling paralleling the role played by LAT in TCR signalling (WANG et al., 2005).

Mast cells or NK cells are positive for the endogenous expression of both transmembrane adaptors, whereas in B cells only NTAL is present (BRDICKA et al., 2002; JANSSEN et al., 2003). It was shown that LAT and NTAL exist in distinct and heterogenous lipid raft compartments in mast cells (VOLNA et al., 2004) which could add to the complexity of transmembrane adaptor function. This was emphasized by the observation that LAX, which is excluded from lipid rafts, seems to negatively regulate mast cell signalling through NTAL. In sensitized *lax*$^{-/-}$ mast cells, NTAL expression is down-regulated, whereas LAT expression is not affected (ZHU et al., 2006).

Collectively, the combinatorial expression of different transmembrane adaptor molecules may influence the signalling properties of a single adaptor in a positive or negative way. A final assessment of the redundancy of the transmembrane adaptors remains to be determined.

2.4. Ca^{2+}: a universal second messenger

Ca^{2+} ions are the most widely used second messengers in biology. Ca^{2+} is essential for the early development of organisms, for the diversity and plasticity of immune responses, and even for remembering what you are about to read on the following pages. In B lymphocytes, the intracellular Ca^{2+} concentration $[Ca^{2+}]_i$ is a critical factor involved in the regulation of B cell fates including apoptosis, proliferation, and differentiation. Ca^{2+} ions exert their regulatory function principally via two mechanisms. Several proteins have a specific binding site for Ca^{2+} and their activity directly depends on Ca^{2+} binding, e.g. phospholipase A2 (PLA2) (WHITE et al., 1990) or PKC (reviewed in DEKKER and PARKER, 1994;

NEWTON, 1997; OANCEA and MEYER, 1998). Alternatively, Ca^{2+}-mediated signal transduction is accomplished by its binding to proteins known as Ca^{2+} sensors which function as regulatory subunits of target proteins. Calmodulin is the most extensively studied example of this group of proteins (reviewed in WEINSTEIN and MEHLER, 1994; IKURA, 1996). For example, Ca^{2+}-bound calmodulin regulates the calcineurin phosphatase complex (CRABTREE and OLSON, 2002; PARSONS et al., 2004) or Ca^{2+}/calmodulin-dependent protein kinase (CaMK) family members (MCKINSEY et al., 2000; MEANS, 2000).
Basically, eukaryotic cells can elevate their cytoplasmic Ca^{2+} concentration by two methods: release from intracellular stores (see section 2.4.1) and Ca^{2+} influx through channels in the plasma membrane (see section 2.4.2) (PAREKH and PENNER, 1997; BERRIDGE et al., 2000; PAREKH and PUTNEY, 2005). However, $[Ca^{2+}]_i$ will ultimately be determined by the balance between Ca^{2+} influx, cytoplasmic Ca^{2+} buffering, and Ca^{2+} removal, i.e. changes in the activity of sarcoplasmic/endoplasmic reticulum Ca^{2+}-ATPases (SERCAs), mitochondrial Ca^{2+} uptake, plasmalemmal Na^{+}-Ca^{2+}-exchanger, or Ca^{2+}-ATPases in the plasma membrane will all affect $[Ca^{2+}]_i$ (PAREKH and PUTNEY, 2005). By modulating the spatial or temporal amplitude, a single BCR can use the same second messenger Ca^{2+} to control a plethora of cellular processes. Additionally, Ca^{2+} signals often appear as regular oscillations whose frequency varies with the strength of the incoming signal (BERRIDGE, 1997a). These oscillations also influence the efficiency and specificity of gene expression (see section 2.6) (DOLMETSCH et al., 1998).

2.4.1. PLC-γ activation and Ca^{2+} release from intracellular stores

In 1975 the year of my birth, Michell proposed that PLC is essential for the generation of cellular Ca^{2+} signals in response to hormones or neurotransmitters (MICHELL, 1975). During the interim the molecular basis for this role has been deciphered. PLC isozymes catalyze the hydrolysis of $PI(4,5)P_2$ to the soluble Ca^{2+}-mobilizing second messenger IP_3 and the membrane-bound diacylglycerol (DAG), an activator of PKC.
The mammalian PLCs can be divided into six subfamilies, designated β, γ, δ, ε, ζ, and η (HARDEN and SONDEK, 2006). The two members of the PLC-γ subfamily, PLC-γ1 and -γ2, are mainly regulated by receptor and non-receptor PTKs, and therefore mediate the responses downstream of the antigen receptors on lymphocytes (reviewed in RHEE and CHOI, 1992a, 1992b; REBECCHI and PENTYALA, 2000; KATAN et al., 2003). T lymphocytes mainly express the PLC-γ1 isoform, whereas PLC-γ2 is predominantly expressed in B lymphocytes (PARK et al., 1991; SECRIST et al., 1991; RHEE and BAE, 1997; HASHIMOTO et al., 2000; IRVIN et al., 2000; WANG et al., 2000; HIKIDA and KUROSAKI, 2005).

Both PLC-γ1 and -γ2 possess an N-terminal PH domain, followed by EF-hand motifs, the catalytic domain formed from the separated X and Y regions, and a C-terminal C2 domain. The catalytic regions X and Y are separated by an X/Y-spanning sequence, also known as Z region. The Z region contains an additional PH domain, split by two SH2 and a single SH3 domain (see figure 2.1). The domains of the Z region are critical to extrinsic regulation of the PLC-γ isoforms, but they also exert an intrinsic control on catalytic activity (see below) (reviewed in REBECCHI and PENTYALA, 2000). The precise mechanism of transition from an inactive to active form of PLC-γ remains a mystery, but certain requirements are well established. One such requirement is the translocation of the PLC-γ isoforms to the plasma membrane. The PH domain binds to the non-substrate lipid phosphatidyl-3,4,5-trisphosphate [PI(3,4,5)P_3], which is a product of PI3K (FALASCA et al., 1998). It is also possible, that other PLC-γ domains participate in direct interactions with membrane lipids, e.g. the C2 domain. A further requirement for PLC-γ stimulation is the phosphorylation of specific tyrosine residues (reviewed in REBECCHI and PENTYALA, 2000). *In vitro*, all three types of PTKs (Src, Syk, and Tec) are able to phosphorylate PLC-γ2. However, the kinase(s) involved in BCR-induced PLC-γ2 tyrosine phosphorylation are currently under investigation. By using antibodies specific for each of the putative phosphorylation sites, Kim et al. demonstrated that PLC-γ2 is phosphorylated on Y^{753}, Y^{759}, and Y^{1217} in response to BCR engagement of human Ramos B cells and murine splenic B cells (KIM et al., 2004). It has been proposed that phosphorylation of essential residues in the Z region such as Y^{783} in PLC-γ1, or Y^{753} and Y^{759} in PLC-γ2, and/or other interactions with the SH2 or SH3 domains could result in conformational changes which abolish an intramolecular inhibition imposed by the Z region (HOMMA and TAKENAWA, 1992; REBECCHI and PENTYALA, 2000). The phosphorylation-dependent assembly of the Ca^{2+} initiation complex in B lymphocytes, which is composed of SLP-65, Btk, and PLC-γ2, will be discussed in detail below.

Other ways of PLC-γ activation, which are independent of tyrosine phosphorylation, have also been suggested (SEKIYA et al., 1999). For example, PLC-γ2 is activated *in vitro* by SH2-mediated binding of PI(3,4,5)P_3 (BAE et al., 1998). Recently, Piechulek et al. suggested a novel mechanism of PLC-γ2 activation by Rac GTPases (PIECHULEK et al., 2005). However, a final model of PLC-γ2 activation upon BCR engagement has yet to be established, and will likely include membrane interaction, tyrosine phosphorylation, and association with adaptor molecules.

IP_3-generation by the PLC superfamily is a central process of Ca^{2+} mobilization from intracellular stores. These stores are held within the membrane systems of the endoplasmic reticulum (ER) or the sarcoplasmic reticulum (SR) of muscle cells. Ca^{2+} release from the

stores is controlled by various channels, of which the IP_3 receptor (IP_3R) and ryanodine receptor (RYR) families have been studied in the most detail. Principally, these channels are activated by Ca^{2+} itself, a process known as Ca^{2+}-induced Ca^{2+} release (CICR) (BERRIDGE, 1997b; BERRIDGE et al., 2000). Ca^{2+} mobilizing second messengers such as IP_3 determine whether Ca^{2+} can activate these channels, i.e. the second messengers increase the Ca^{2+} sensitivity (BERRIDGE, 1997b; BERRIDGE et al., 2000). Ca^{2+} can regulate Ca^{2+} release by acting from either the lumenal or the cytoplasmic sides of the channels (BERRIDGE et al., 2000). Cytosolic Ca^{2+} can either be stimulatory or inhibitory, largely depending on its concentration and the IP_3R isoform. Three distinct *ip3r* genes have been identified so far (HIKIDA and KUROSAKI, 2005), and targeted disruption of these three genes in DT40 B cells abolishes BCR-induced Ca^{2+} mobilization from intra- and extracellular sources (see also section 2.4.2) (SUGAWARA et al., 1997). It seems that IP_3 makes IP_3Rs more sensitive to the stimulatory action of Ca^{2+} (BOOTMAN and LIPP, 1999). Another intracellular IP_3R agonist is ATP (IINO, 1991; BEZPROZVANNY and EHRLICH, 1993), and the channel activity of IP_3Rs is further modulated by serine and tyrosine phosphorylation (NAKADE et al., 1994; JAYARAMAN et al., 1996). The Ca^{2+} signalling properties differ significantly among these three IP_3R isoforms, as shown in DT40 cells expressing only a single isoform (MIYAKAWA et al., 1999). These differences in spatiotemporal Ca^{2+} signals might be partially caused by differential Ca^{2+} sensitivity of the IP_3Rs (MIYAKAWA et al., 2001). Therefore, the differential expression and post-translational modifications of the three IP_3Rs contribute to the generation of transient, sustained, or oscillatory Ca^{2+} signals.

2.4.2. Ca^{2+} entry across the plasma membrane

Various Ca^{2+} channels mediate the influx of Ca^{2+} ions across the plasma membrane. They are defined by the method of activation. One can distinguish three major pathways by which extracellular Ca^{2+} can enter cells: voltage-operated Ca^{2+} channels (VOCCs), ligand-gated non-specific cation channels (LGCCs), and receptor-activated Ca^{2+} channels (RACCs) (BARRITT, 1999). VOCCs are found in excitable cells like nerve and muscle cells, but are largely excluded from non-excitable cells and are activated by membrane-depolarization. Since membrane-depolarization does not initiate lymphocyte activation, the role of VOCCs in lymphocytes has been unclear (GALLO et al., 2006). However, emerging evidence suggests that channels with L-type (subtype of VOCCs) Ca^{2+} channel characteristics exist in lymphocytes (SADIGHI AKHA et al., 1996; GRAFTON et al., 2003; GOMES et al., 2004; GALLO et al., 2006). LGCCs channels open in response to binding of an extracellular ligand, typically transmitters such as glutamate, ATP, or acetylcholine (BERRIDGE et al., 2000). RACCs are channels which are sensitive to various signals generated following receptor

activation. They are defined as any Ca^{2+} plasma membrane channel that opens as a result of the binding of an agonist to its receptor, where the receptor protein is distinct from the channel protein, and the activation mechanism does not involve membrane depolarization (BARRITT, 1999). Since receptor activation generates multiple signals, RACCs can be subdivided into receptor-operated channels (ROCs) and store-operated channels (SOCs). The term ROC refers to Ca^{2+} channels whose opening does not depend on store-emptying. Frequently ROCs are activated by intracellular second messengers, e.g. DAG (HOFMANN et al., 1999), arachidonic acid (BROAD et al., 1999; MIGNEN and SHUTTLEWORTH, 2000), cyclic nucleotides (FINN et al., 1996; APPLEGATE et al., 1997; LENZ and KLEINEKE, 1997), or inositol phosphates (BARRITT, 1999; PAREKH and PUTNEY, 2005). Therefore, they are also designated as second messenger-operated channels (SMOCs) (PAREKH and PUTNEY, 2005). Additionally, trimeric G proteins were reported to link receptor proteins to ROCs (FASOLATO et al., 1993; BARRITT, 1999). The SOC-mediated Ca^{2+} entry, also known as capacitative Ca^{2+} entry CCE), is thought to be the major pathway in electrically non-excitable cells, and is activated by the emptying of intracellular stores (PAREKH and PENNER, 1997; PAREKH and PUTNEY, 2005). The best characterized store-operated current is the Ca^{2+} release activated Ca^{2+} current (I_{CRAC}) (HOTH and PENNER, 1992; reviewed in PAREKH and PENNER, 1997; PAREKH and PUTNEY, 2005), which is defined by certain electrophysiological properties. In spite of extensive research, the following aspects of SOC-mediated Ca^{2+} influx remain unclear: 1) the signal that relays the Ca^{2+} store content to the SOCs in the plasma membrane, 2) the molecular indentity of the Ca^{2+} sensor in the stores, and 3) the molecular identity of CRAC?

To address the first question, four different models have been proposed (PUTNEY et al., 2001). In the first model, a **diffusible messenger** is released from the depleted stores into the cytosol where it then diffuses to the plasma membrane and opens SOCs. Various diffusible messengers have been reported, e.g. the Ca^{2+} influx factor (CIF), PKC, lysophospholipid, or calmodulin (reviewed in PAREKH and PUTNEY, 2005). In the second model, plasmalemmal SOCs are activated by the direct binding of IP_3Rs, which sense the fall in Ca^{2+} levels through Ca^{2+} binding sites on their lumenal domains. The physical interaction might occur in a preformed complex (**conformational coupling**), or upon movement of the peripheral ER (**secretion-like coupling**) (IRVINE, 1990; KISELYOV et al., 1999; PATTERSON et al., 1999; PAREKH and PUTNEY, 2005). Basically three lines of evidence have led to the suggestion that IP_3Rs can activate store-operated channels. First, co-immunoprecipitation experiments indicated that IP_3Rs can associate with certain members of the canonical transient receptor potential (TRPC) family (BOULAY et al., 1999; KISELYOV et al., 1999; ROSADO et al., 2002), which are candidates for store-operated

channels (see below). Second, IP_3Rs seem to activate endogenously expressed store-operated channels in excised patches (ZUBOV et al., 1999; KAZNACHEYEVA et al., 2000). Third, the IP_3R antagonist 2-aminoethoxydiphenylborane (2-APB) inhibits store-operated Ca^{2+} influx even when applied following thapsigargin activated Ca^{2+} influx (MA et al., 2000). Thapsigargin is an inhibitor of SERCAs and thapsigargin-induced Ca^{2+} release relies on the passive leak of Ca^{2+} through unidentified channels. However, the conformational/secretion-like coupling model has been challenged by several observations. For example, Ca^{2+} influx induced by thapsigargin-evoked store depletion was not affected in *ip3r*$^{-/-}$ DT40 cells (SUGAWARA et al., 1997). Furthermore, neither CCE in lacrimal cells nor I_{CRAC} in RBL mast cells is blocked by the intracellular application of the competitive IP_3R antagonist heparin (BIRD et al., 1991; BROAD et al., 2001). In the third model for SOC activation, SOCs do not reside in the plasma membrane in the resting state, but are inserted into the membrane upon store depletion via an exocytotic mechanism (**vesicular fusion model**). Finally, it has been postulated that SOCs are maintained in an inactive state due to an elevated Ca^{2+} concentration in their immediate vicinity. Store depletion removes this inhibition by enhancing Ca^{2+} removal from those sites, presumably by the activity of SERCAs (**removal of Ca^{2+} inhibition**) (BARRITT, 1998). However, it is likely that different cell types employ different mechanisms, and that SOCs are regulated by multiple pathways (reviewed in PUTNEY et al., 2001).

Progress has been made in the identification of the molecular Ca^{2+} sensor in the stores. It has been recently postulated that the stromal interaction molecule 1 (STIM1) plays an essential role in SOC activation, possibly by sensing the Ca^{2+} content of the ER (LIOU et al., 2005; ROOS et al., 2005). STIM1 contains a single membrane-spanning domain and is located both in the plasma membrane and intracellular membranes, presumably the ER (MANJI et al., 2000). The N-terminus contains an EF-hand domain and is orientated toward the extracellular space or the ER lumen. Thus, STIM1 may serve as Ca^{2+} sensor (LIOU et al., 2005; ROOS et al., 2005). Since STIM1 was also reported to homo-oligomerize (WILLIAMS et al., 2002), it has been speculated that a STIM1-STIM1 interaction links the ER with the plasma membrane (ROOS et al., 2005), similar to the coupling models of SOC activation described above. In accordance, Liou et al. reported that STIM1 rapidly redistributes into puncta near the plasma membrane after store depletion (LIOU et al., 2005). Subsequently two alternative methods of STIM1 function were proposed. First, STIM1 located in the ER unbinds Ca^{2+} upon store depletion, and translocates to the plasma membrane for SOC activation, similar to the vesicular fusion model of SOC activation described above. Second, STIM1 forms a functional SOC with other STIM1 molecules and perhaps additional components (ZHANG et al., 2005). Taken together, it is possible that STIM1 is the long

sought sensor of Ca^{2+} store content. However, STIM1 communication with SOCs remains at best uncertain.

Members of the transient receptor potential (TRP) family of ion channels have been implicated in store-operated Ca^{2+} entry. The TRP family can be subdivided into six families, i.e. canonical (TRPC), vanilloid (TRPV), melastatin (TRPM), polycystin (TRPP), mucolipin (TRPML), and ankyrinTM1 (TRPA) (CLAPHAM, 2003). Although experimental evidence has suggested that TRPs may be part of SOCs this remains a controversial issue. For example, two different groups expressed TRPC3 in DT40 B lymphocytes. The first group demonstrated that the formed channels were store-operated (VAZQUEZ et al., 2001), whereas the second group observed that the channels were not store-operated but activated by DAG (VENKATACHALAM et al., 2001). Subsequent studies revealed that the expression level of TRPC3 was responsible for these distinct behaviours: at low levels TRPC3 is store-operated, and at high levels receptor-operated (VAZQUEZ et al., 2003). It seems that the exogenous expression of a given TRP protein might not result in the correct stoichiometry needed for the formation of functional complexes with other TRPs or additional components (PAREKH and PUTNEY, 2005). However, it is accepted that there are alternative ways of TRP activation, including lipid metabolites. For example, TRPC3, TRPC6 and TRPC7 are directly activated by DAG (HOFMANN et al., 1999; OKADA et al., 1999; VENKATACHALAM et al., 2001). Conversely, TRPM7 is positively regulated by $PI(4,5)P_2$ and inactivated by $PI(4,5)P_2$ hydrolysis (RUNNELS et al., 2002). Furthermore, it was observed that PLC-γ directly binds to TRPC1 (TU et al., 2005), TRPC2 (TONG et al., 2004), TRPC3 (PATTERSON et al., 2002; CLAPHAM, 2003; VAN ROSSUM et al., 2005) and TRPM7 (RUNNELS et al., 2002), indicating lipase-independent functions of PLC-γ.

Collectively, many questions concerning SOC activation remain unanswered. Hence, future investigations should focus on the expression levels and the native environment of channel components. Furthermore, the regulation of plasma membrane resident Ca^{2+} channels by lipid mediators or lipase-independent functions of PLC-γ merits attention.

2.4.3. Principles of receptor-induced Ca^{2+} mobilization

The three main pathways of receptor-induced Ca^{2+} mobilization are summarized in figure 2.2 (modified from PATTERSON et al., 2005). (1) Agonist binding by plasmalemmal receptors leads to IP_3 production by PLC isozymes. The soluble IP_3 sensitizes IP_3Rs in the ER, resulting in the Ca^{2+} release from the stores. (2) The ER transmits information back to Ca^{2+} channels in the plasma membrane. This might occur via the models described above, or a combination of these. (3) Alternatively, the plasma membrane receptors transduce the

signal directly to the Ca^{2+} channels in the same membrane. This might occur either via conformational changes upon agonist binding or via signalling molecules, i.e. proteins (e.g. PLC itself) or lipid mediators (e.g. DAG, arachidonic acid).

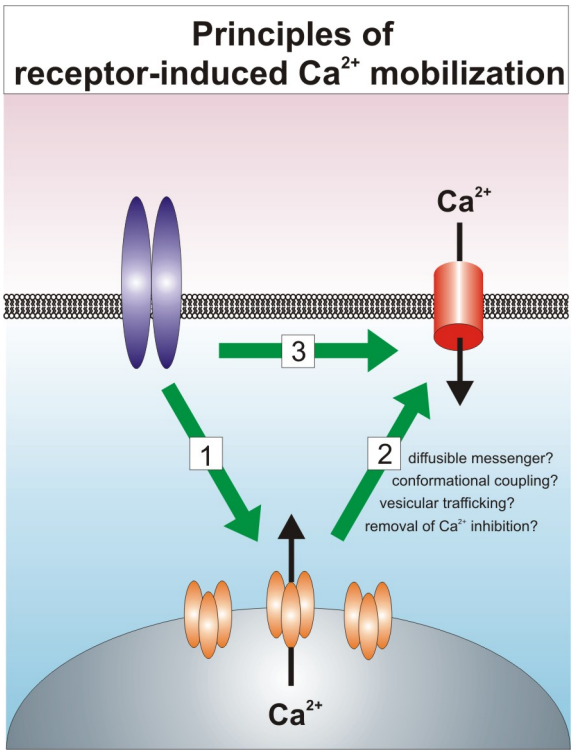

Figure 2.2: Receptor-induced Ca^{2+} mobilization
Principle steps of the receptor-induced Ca^{2+} mobilization from intra- and extracellular sources. (1) Agonist-binding by plasmalemmal receptors leads to PLC-mediated IP_3 production, resulting in Ca^{2+} release from the stores. (2) The ER transmits information back to Ca^{2+} channels in the plasma membrane. Several mechanisms have been proposed for this step, including a diffusible messenger, coupling processes, vesicular trafficking, removal of Ca^{2+} inhibition. (3) The receptors in the plasma membrane might directly activate the Ca^{2+} channels within the same membrane, e.g. via conformational changes or signalling molecules (modified from PATTERSON et al., 2005).

2.5. Antigen receptor-induced Ca^{2+} mobilization in B lymphocytes

The central process of BCR-induced Ca^{2+} mobilization is the phosphorylation-dependent assembly of the Ca^{2+} initiation complex, containing SLP-65, Btk, and PLC-γ2. Upon BCR engagement, SLP-65 becomes tyrosine phosphorylated by activated Syk, and serves as scaffold for the SH2-dependent binding of both Btk and PLC-γ2. Thus Btk and PLC-γ2 are brought into close proximity with each other, resulting in the Btk-dependent PLC-γ2 phosphorylation (KUROSAKI et al., 2000; WIENANDS, 2000b).

It has been previously demonstrated that the PLC-γ2 SH2 domains are essential for coupling BCR to PLC-γ2 activation (TAKATA et al., 1995). In subsequent studies using *slp-65*$^{-/-}$ DT40 B cells, it was shown that SLP-65 is required for the translocation of PLC-γ2 to the membrane and for its subsequent phosphorylation/activation (FU et al., 1998; JUMAA et al., 1999; SU et al., 1999; WOLLSCHEID et al., 1999; ISHIAI et al., 1999a, 1999b; KUROSAKI and TSUKADA, 2000). Furthermore, tyrosine-phosphorylated SLP-65 is also recognized by the SH2 domain of Btk (HASHIMOTO et al., 1999; SU et al., 1999). Association of Btk and PLC-γ2 with the same SLP-65 molecule was demonstrated to elicit functional Ca^{2+} signalling (CHIU et al., 2002).

As described above, the exact mechanism of BCR-induced PLC-γ2 tyrosine phosphorylation remains to be established. Since both SLP-65 phosphorylation, and Btk activation occur downstream of Lyn/Syk activation it is difficult to prove whether PLC-γ2 is a direct substrate for these two kinases. Based on the following two observations it was proposed that PLC-γ2 is a substrate of Btk. First, co-expression of Btk and PLC-γ2 resulted in PLC-γ2 tyrosine phosphorylation (FLUCKIGER et al., 1998), and second, PLC-γ2 tyrosine phosphorylation was substantially (but not completely) decreased in *btk*$^{-/-}$ DT40 cells (TAKATA and KUROSAKI, 1996). As stated above, PLC-γ2 is phosphorylated on Y^{753}, Y^{759}, and Y^{1217} in response to BCR engagement (KIM et al., 2004). It appears that Btk is mainly, but not completely responsible for the phosphorylation of Y^{753} and Y^{759} (KIM et al., 2004). In contrast, Y^{1217} seems to be phosphorylated by a Btk-independent pathway. Collectively, more experiments must be performed to establish a comprehensive model of PLC-γ2 activation within the cellular environment. Greater complexity is further generated by recent observations that PLC-γ isozymes exhibit several lipase-independent activities affecting BCR-induced Ca^{2+} mobilization (PATTERSON et al., 2002; VAN ROSSUM et al., 2005; YU et al., 2005).

To rescue SLP-65 deficiency, SLP-76 has to be co-expressed with LAT and Gads (ISHIAI et al., 2000). This implies that SLP-65 is recruited to the plasma membrane by molecules that cannot interact with SLP-76 or that SLP-65 can mediate its own membrane translocation. A LAT/Gads paralogous pair that is capable of mediating SLP-65 membrane recruitment remains to be described in B lymphocytes. Thus, it was investigated whether SLP-65 is able to mediate its own membrane translocation. In support of this model, two alternative and mutually non-exclusive paths have been reported to date. First, it was shown that the SLP-65 SH2 domain binds to a phosphorylated non-ITAM tyrosine in the cytoplasmic tail of Ig-α (ENGELS et al., 2001; KABAK et al., 2002). Second, recent work indicates that a leucine-zipper motif at the N-terminus of SLP-65 is necessary and sufficient for membrane localization (KOHLER et al., 2005). Since this association of SLP-65 does not require BCR signalling, it might be that there are alternative 'pools' of SLP-65.

Both Btk and PLC-γ2 possess PH domains that bind selectively to the PI3K product $PI(3,4,5)P_3$ (FALASCA et al., 1998; SATTERTHWAITE et al., 1998; MARSHALL et al., 2000). These associations may stabilize the recruitment of the Ca^{2+} initiation complex to the plasma membrane. A PI3K-induced translocation to the membrane and activation of PLC-γ2 has been reported in fibroblasts (RHEE and BAE, 1997; BAE et al., 1998; FALASCA et al., 1998), and PI3K-dependent membrane recruitment of both PLC-γ2 and Btk has been demonstrated in mouse megakaryocytes (BOBE et al., 2001). It was also demonstrated that

$PI(3,4,5)P_3$ acts both at the level of Btk-mediated PLC-γ2 tyrosine phosphorylation, and as an activator of the lipase activity of the phosphorylated PLC-γ2 (KIM et al., 2004). Thus, PI3K activation is generally considered to contribute to PLC-γ2 activation. Heterodimer-type (class Ia) PI3Ks are composed of a catalytic subunit (p110; isoforms α, β, γ and δ) and a regulatory subunit encoded by at least three distinct genes (p85α, p85β, p55γ) (figure 2.1; VANHAESEBROECK et al., 1997; FRUMAN et al., 1998; RAMEH and CANTLEY, 1999; CANTRELL, 2001). Activated Syk phosphorylates the B cell co-receptor CD19, and B-cell adaptor for PI3K (BCAP) which provide binding sites for PI3Ks (TUVESON et al., 1993; OKADA et al., 2000; OKKENHAUG and VANHAESEBROECK, 2003). Thus, Syk has a positive regulatory role in BCR-induced Ca^{2+} mobilization not only through SLP-65 phosphorylation, but also through PI3K activation. The importance of $PI(3,4,5)P_3$ is further evidenced by the deletion of SHIP. This enzyme antagonizes the catalytic activity of PI3K by generating phosphatidyl-3,4-bisphosphate [$PI(3,4)P_2$] from $PI(3,4,5)P_3$. SHIP deficiency leads to increased $PI(3,4,5)P_3$ levels, and thus to enhanced PLC-γ2 activation (BRAUWEILER et al., 2000). Several positive and negative feedback loops in BCR-induced Ca^{2+} mobilization that contribute to fine-tuning Ca^{2+} responses in B lymphocytes have been described, and target the catalytic activities of Syk, Btk, or PLC-γ2, respectively (reviewed in HIKIDA and KUROSAKI, 2005).

Although many details regarding the assembly of the Ca^{2+} initiation complex in B lymphocytes have been clarified during the last years, central aspects remain unclear. What is the exact activation mechanism of PLC-γ2? How is the Ca^{2+} initiation complex translocated to the plasma membrane? What is the role of universal and B cell-specific adaptor proteins in the modulation of BCR-induced Ca^{2+} mobilization?

2.6. Effects of Ca^{2+} on B cell responses

It has been shown that B cells mobilize Ca^{2+} to different extents from intracellular stores and across the plasma membrane depending on their developmental stage. Ca^{2+} entry through channels in the plasma membrane increases with maturation (KONCZ et al., 2002; KOVESDI et al., 2002). The Ca^{2+} signal patterns within a given cell can occur as single transients, as sustained plateau, or as oscillations (BERRIDGE, 1993; CLAPHAM, 1995). It was demonstrated that the different patterns influence the specificity of cellular responses. A major consequence of Ca^{2+} mobilization is activation of Ca^{2+}-sensitive transcription factors, including NFAT and NF-κB (BAEUERLE and HENKEL, 1994; CRABTREE and CLIPSTONE, 1994; FRANTZ et al., 1994; NEGULESCU et al., 1994; RAO, 1994; FANGER et al., 1995; SHIBASAKI et al., 1996; TIMMERMAN et al., 1996). It was reported that the amplitude and

duration of Ca^{2+} signals in B lymphocytes control the differential activation of NFAT and NF-κB (DOLMETSCH et al., 1997). NF-κB is selectively activated by a large transient rise in $[Ca^{2+}]_i$, whereas NFAT activation requires a low sustained Ca^{2+} plateau (DOLMETSCH et al., 1997). Additionally, oscillations reduce the effective Ca^{2+} threshold for the activation of transcription factors (DOLMETSCH et al., 1998). Furthermore, oscillation frequency was shown to control specificity, i.e. rapid oscillations stimulate both NFAT and NF-κB, while infrequent oscillations activate only NF-κB (DOLMETSCH et al., 1998). The importance of differential Ca^{2+} signalling for immune responses could also be demonstrated in different anergy mouse models. In the hen egg lysozyme (HEL) mouse model, mice with B cells specific for HEL are crossed with mice expressing HEL as a soluble 'neo-self antigen'. B cells from those double-transgenic mice are rendered anergic by chronic exposure to HEL *in vivo* (MASON et al., 1992; HEALY and GOODNOW, 1998). These self-tolerant B cells reveal an increased basal level in $[Ca^{2+}]_i$ and a concomitant increase in resting nuclear levels of NFAT (HEALY et al., 1997). Furthermore, the self-tolerant B cells fail to evoke a BCR-induced large Ca^{2+} transient observed in naïve non-tolerant control B cells (COOKE et al., 1994; HEALY et al., 1997). These results were recently extended by using the B cell anergy model of 'Ars/A1' transgenic mice (BENSCHOP et al., 2001). It was shown that maintenance of B cell anergy requires constant BCR occupancy and signalling. Removal of self-antigen reduced basal $[Ca^{2+}]_i$ to normal levels and recovered BCR-induced Ca^{2+} mobilization (GAULD et al., 2005).

The importance of a certain level of PLC-γ activity for B cell development was described. PLC-γ2-deficient mice exhibit a partial block at the developmental transition following pre-BCR signalling and a more complete block at the transition from immature to mature B lymphocytes (HASHIMOTO et al., 2000; WANG et al., 2000; HIKIDA et al., 2003; BELL et al., 2004; HIKIDA and KUROSAKI, 2005). In *plc-γ2*$^{-/-}$ *plc-γ1*$^{+/-}$ mice, the block from pro- to pre-B-cell transition was more complete, and allelic exclusion of the IgH chain locus was perturbated (WEN et al., 2004).

The studies described above support the importance of Ca^{2+} signalling in B cell biology, e.g. in transcriptional regulation, tolerance induction, or allelic exclusion. Thus, a principle focus of this thesis is the regulation and fine-tuning of BCR-induced Ca^{2+} mobilization. In the experiments presented herein, DT40 B lymphocytes and derivatives that were rendered deficient for central components of B cell signalling pathways were applied to gain a greater understanding of the involvement of adaptor proteins in central BCR-triggered processes, i.e. tyrosine phosphorylation and Ca^{2+} mobilization.

3. Aims of work

This thesis addressed the question whether Ca^{2+} mobilization in B cells is controlled by mechanisms that are analogous to TCR-mediated signalling. This working hypothesis was investigated using the DT40 B cell model system, which is prone to a high frequency of homologous recombination, and therefore a suitable tool for gene disruption and subsequent reconstitution experiments.

The hypothesis was investigated by the following two approaches:

1) Defining the role of Grb2 in BCR signal transduction.
Gads is an essential component of TCR-induced Ca^{2+} mobilization but plays only a minor role in BCR signal transduction. Thus, this thesis analyses whether the adaptor Grb2 plays a functionally similar role in BCR-induced Ca^{2+} mobilization using *grb2*$^{-/-}$ DT40 cells. The function of Grb2 after BCR engagement is investigated by reconstitution experiments with different Grb2 mutants. This approach should lead to the elucidation of effector proteins downstream of Grb2. Following the identification of these mediators, their role in BCR signal transduction can be further analysed by gene targeting in DT40 cells.

2) Defining the role of NTAL in BCR-induced Ca^{2+} mobilization.
The recently identified transmembrane adaptor NTAL is closely related to LAT which is instrumental in localizing the TCR-controlled Ca^{2+} initiation complex to the plasma membrane. Thus, the impact of NTAL on BCR-initiated Ca^{2+} signalling was investigated by generating *ntal*$^{-/-}$ DT40 cells, and reconstitution experiments with wild-type chicken NTAL, and derivatives in which lipid raft targeting, and tyrosine-based signalling motifs were inactivated.

4. Material and Methods

4.1. Materials

All chemicals and biologically reactive reagents were purchased from Roth, Sigma/Aldrich (Fluka), Merck, Invitrogen (Gibco; Molecular Probes), Uptima, Becton Dickinson, or Amersham Biosciences. All chemicals were purchased in pA quality unless otherwise indicated.

4.1.1. Antibodies

Table 4.1: Primary antibodies (IB, immunoblot; IP, immunopurification)

antibody	supplier/reference	application
rabbit-anti-Grb2 (C-23)	Santa Cruz Biotechnolgoy	IB, IP
mouse-anti-Grb2 (3F2)	upstate	IB
rabbit-anti-actin	Sigma	IB
rabbit-anti-chicken SLP-65	ISHIAI et al., 1999b	IB, IP
rabbit-anti-PLC-γ2 (Q-20)	Santa Cruz Biotechnolgoy	IB, IP
rabbit-anti-mouse NTAL	this thesis	IB
rabbit-anti-chicken NTAL	this thesis	IB, IP
rabbit-anti-chicken Lyn	TAKATA et al., 1994	IB, IP
rabbit-anti Lyn (44)	Santa Cruz Biotechnolgoy	IB
mouse-anti-phosphotyrosine (pTyr) (4G10)	upstate	IB, IP
mouse-anti-HA* (F-7)	Santa Cruz Biotechnolgoy	IB, IP
rat-anti-HA* (3F10)	Roche	IB, IP
rabbit-anti-LAT (FL-233)	Santa Cruz Biotechnolgoy	IB, IP
rabbit-anti-mouse Dok-3	LEMAY et al., 2000	IB, IP
mouse-anti-chicken IgM (M4)	SouthernBiotech	DT40 stimulation
mouse-anti-chicken IgM (M4)	hybridoma (CHEN et al., 1982) (Riken Cell Bank 1611)	DT40 stimulation
goat-anti-chicken IgM FITC	Bethyl Laboratories	FACS analysis

*HA = eleven amino acid peptide derived from influenza hemagglutinin (YPYDVPDYA)

(continued on next page)

antibody	supplier/reference	application
$F(ab')_2$ fragment goat anti-mouse IgG, $F(ab')_2$ fragment specific	Jackson ImmunoResearch	K46/ IIA1.6 stimulation
$F(ab')_2$ fragment goat anti-mouse IgG + IgM (H+L)	Jackson ImmunoResearch	WEHI231 stimulation
$F(ab')_2$ fragment goat anti-human IgM, $Fc_{5\mu}$ fragment specific	Jackson ImmunoResearch	Ramos stimulation

Table 4.2: Secondary antibodies

antibody	supplier	application
goat-anti-rabbit IgG/HRPO	Pierce	immunoblot
goat-anti-rat IgG/HRPO	Pierce	immunoblot
goat-anti-mouse IgG/HRPO	Pierce	immunoblot

4.1.2. Enzymes

Restriction endonucleases	New England Biolabs, MBI Fermentas, GibcoBRL (Invitrogen)
Calf Intestine Phosphatase (CIP)	New England Biolabs
T4 DNA Ligase	Promega, New England Biolabs
Taq DNA polymerase	New England Biolabs
Taq PCR Master Mix Kit	Qiagen
DNA polymerase I, Large (Klenow) fragment	New England Biolabs
LA-*Taq* DNA Polymerase	Takara (Cambrex)
PrimeStar DNA Polymerase	Takara (Cambrex)
Pfu DNA Polymerase	Promega
Elongase Polymerase Mix	Invitrogen
Moloney murine leukemia virus reverse transcriptase (MMLV-RT)	MBI Fermentas
LR Clonase Mix	Invitrogen
Topoisomerase	Invitrogen
PNGase F	New England Biolabs

4.1.3. Vectors and cDNAs

Table 4.3: Vectors

vector	source/supplier	application
cloning vectors		
pCR2.1-Topo	Invitrogen	T/A cloning (4.2.1.17.)
pCRII-Topo	Invitrogen	T/A cloning (4.2.1.17.)
pENTR/SD/D-Topo	Invitrogen	entry vector (4.2.1.18.)
pBluescript SK II (–)	Stratagene	targeting constructs
p-neo	T. Kurosaki	neomycin resistance cassette for targeting constructs (with β-actin promotor)
p-hisD	T. Kurosaki	histidinol resistance cassette for targeting constructs (with β-actin promotor)
pJG4-5 DT40 cDNA library	T. Kurosaki	amplification of complete chicken dok-3 cDNA ends (see below)
pEGFP-N1	BD Biosciences Clontech	cloning of mLyn/EGFP construct
pcDNA6/TR	Invitrogen	amplification of blasticidin resistance cDNA for generation of pMSCVblast
bacterial expression vectors		
pGEX-3X	Amersham Biosciences	expression of GST/chNTAL(aa150-198) and GST/mNTAL(aa155-203) (4.2.3.1.)
pGEX-4T-1	Amersham Biosciences/ A. Grabbe	expression of GST/mGrb2[SH2] and GST/mGrb2[cSH3] (4.2.3.1.)
mammalian expression vectors		
pApuroII	T. Kurosaki	expression of chicken Dok-3
pApuroII/DEST A	T. Kurosaki	expression of mouse NTAL, chicken NTAL, and chicken NTAL HA
pMSCVpuro	BD Biosciences Clontech	expression of mouse Grb2, chicken Grb2, human LAT, and variants
pMSCVpuro/DEST A	B. Stork	expression of chicken NTAL HA and variants
pMSCVblast	B. Stork	expression of mLyn/EGFP
p5N-M-IRES-hph	M. Jücker	expression of Grb2[R86K] (figure 5.13)
MI165	T. Kurosaki	expression TM-PLC-γ2
pHCMV-VSV-G	M. Jücker	expression of VSV-G/ pseudo-typing of retroviruses(4.2.2.6. and 4.2.2.7.)

DEST = destination vector for Gateway® technology (see 4.2.1.18.)

Table 4.4: cDNAs

cDNA	source/supplied by	expression vector
chicken *grb2*	DT40 wt cells	pMSCVpuro p5N-M-IRES-hph
mouse *grb2*	A. Grabbe	pMSCVpuro
chicken *ntal*	DT40 wt cells	pApuroII/DEST A pMSCVpuro/DEST A
mouse *ntal*	V. Horejsi	pApuroII/DEST A
human *lat*	J. Wienands	pMSCVpuro
mouse *lyn*	M. Reth	pMSCVblast
chicken *dok-3*	DT40 wt cells	pApuroII

Chicken *grb2*, *ntal*, and *dok-3* cDNAs were amplified from wild-type DT40 cDNAs (see 4.2.1.15. and 4.2.1.16.). Complete chicken *dok-3* cDNA ends were amplified from the pJG4-5-based DT40 cDNA library. Coding sequences for variants of chicken Grb2, chicken NTAL, and human LAT, respectively were generated by site-directed mutagenesis (4.2.1.16.). Expression cassettes encoding either C-terminally HA-tagged chicken NTAL or TM-Grb2 were generated by PCR. The *tm-grb2* cDNA encompasses *ntal* base pairs 1-282 and full length *grb2* cDNA at the 3' end (4.2.1.16.).

4.1.4. Oligonucleotides

All oligonucleotides were synthesized by MWG-Biotech (Ebersberg, Germany), Invitrogen (Japan), or Proligo (Japan).

Table 4.5 : Oligonucleotides

Primer	Sequence (5`→3`)	Application
chGrb2for	atg gaa gcc atc gcc aaa tac g	cDNA amplification
chGrb2rev	cta gat gtt ccg gtt cac tg	cDNA amplification
chGrb2_W36Kfor	gaa tgt gat cag aat aag tac aag gca gaa ctc	mutagenesis
chGrb2_W36Kfor	gag ttc tgc ctt gta ctt att ctg atc aca ttc	mutagenesis
chGrb2_R86Kfor	tgc ctt cct tat caa gga gag tga gag tgc	mutagenesis
chGrb2_R86Kfor	gca ctc tca ctc tcc ttg ata agg aag gc	mutagenesis
chGrb2_W193Kfor	aat tct gac ccc aac aag tgg aag gga gcc tg	mutagenesis
chGrb2_W193Kfor	cag gct ccc ttc cac ttg ttg ggg tca gaa ttg	mutagenesis
chNTALfor5	atg tgg ctg ggc cat ggc gca g	cDNA amplification
chNTALrev2	ctt cac ttt gac agc acg acg	cDNA amplification

(continued on next page)

Primer	Sequence (5`→3`)	Application
chNTALentry_for	cac cat ggc gca gcc gga gct gct g	cloning
chNTALentry_rev	tca ctt tga cag cac gac ggc	cloning
chNTALentry_revHA	tca ggc gta gtc tgg cac atc gta ggg gta ctt tga cag cac gac ggc atc	cloning
chNTAL_Y95Ffor	tgc tga gcc ccg ctt cca gaa ctt cct gac	mutagenesis
chNTAL_Y95Frev	gtc agg aag ttc tgg aag cgg ggc tca gca	mutagenesis
chNTAL_Y136Ffor	gga ctc gca ttc ctt cca aaa cgt cat cat tg	mutagenesis
chNTAL_Y136Frev	caa tga tga cgt ttt gga agg aat gcg agt cc	mutagenesis
chNTAL_Y155Ffor	tga tgc aga aga ctt cga gaa cag cac agc	mutagenesis
chNTAL_Y155Frev	gct gtg ctg ttc tcg aag tct tct gca tca	mutagenesis
chNTAL_Y184Ffor	tga gga gcc aga ctt cgt gaa cac gga ccc	mutagenesis
chNTAL_Y184Frev	ggg tcc gtg ttc acg aag tct ggc tcc tca	mutagenesis
chNTAL_C23,26Afor	tgg ctg tca gtg ccg ccg tca ggg ccc agc	mutagenesis
chNTAL_C23,26Arev	gct ggg ccc tga cgg cgg cac tga cag cca	mutagenesis
NTALgenfor1	gct ctc cat gcc tgg att tct cct gg	genomic PCR
NTALgenrev2	cac aca tca ccc tgg gtc act tct ac	genomic PCR
probegenfor2	cgc tgc tta cct gta agt tca cgc ac	probe for Southern
probegenfor2	tca aca ctg tga ggg atc agc gtg g	probe for Southern
chNTALpep3for	gag gaa ttc aga tga tgc aga aga cta c	GST fusion protein
chNTALpep3rev	gag gaa ttc tca ctt tga cag cac gac	GST fusion protein
mNTALpep3for	cag gaa ttc aga gga ctt tga gga tta c	GST fusion protein
mNTALpep3rev	cca gaa ttc cta gat gtt ctc tgc tgc	GST fusion protein
hNTALfor1	tgg agg atc cag cat ctt cca ggt ac	cDNA amplification
hNTALrev1	ggg tga cag ctt atc cta aat cct gc	cDNA amplification
hLATforBgl	aaa aga tct atg gag gag gcc atc ctg	cloning
hLATrevEco	aaa gaa ttc tca gtt cag ctc ctg cag	cloning
hLAT_Y132Ffor	atc aca acc cag gct tcc tgg tgg tgc ttc c	mutagenesis
hLAT_Y132Frev	gaa gca cca cca gga agc ctg ggt tgt gat ag	mutagenesis
NTALfor	atg gcg cag ccg gag ctg ctg	TM-Grb2 construct
bridge2for	gag agc agt gct gag ccc cgc atg gaa gcc atc gcc aaa tac	TM-Grb2 construct
bridge2rev	cgt att tgg cga tgg ctt cca tgc ggg gct cag cac tgc tct c	TM-Grb2 construct
Grb2rev	cta gat gtt ccg gtt cac tg	TM-Grb2 construct
mNTAL_ENTRfor	cac cat gag tgc cga gct gga gct g	cloning

(continued on next page)

Primer	Sequence (5`→3`)	Application
mNTAL_ENTRrev_ut	cta gat gtt ctc tgc tgc ggc	cloning
blast_HindIIIfor	tcc aag ctt acc atg gcc aag cct ttg tc	cloning
blast_ClaIrev	ctg atc gat cag aca tga taa gat aca ttg	cloning
mLynforBglII	tgg aga tct gcc gcc acc atg gga tgt att aaa tca	cloning
mLynrevBamHI	ttt gga tcc ggt tgc tgc tga tac tgc cct tc	cloning
pJG/4-5DT40for	ttg ctg agt gga gat gcc tcc tac c	Dok-3 library screen
pJG/4-5DT40rev	caa gcc gac aac ctt gat tgg aga c	Dok-3 library screen
chDok-3cDNAforSTART	gct ggg ccc atg gag aga cca gtg	cDNA amplification
chDok-3cDNAfor3	cct atg gag gag aac tgc ctc tac	cDNA amplification
chDok-3cDNArev1	ctg atc ttg gcc gaa ttt gcg	cDNA amplification
chDok-3cDNAfor5'UTR	cag ttg ctt tgg ctg aat cag tca c	cDNA amplification
chDok-3cDNArev3'UTR	ttt tgt tac ggc gcc ccc tgg cgg	cDNA amplification
Dok-3_LA_for	tag cac agc tgt aga gat ggc agt g	genomic PCR
Dok-3_LA_rev	agc aca tga agt cat cgc ttc tcc	genomic PCR
Dok-3_RA_for(INS)	gca cgt tat ggg tga cat cat ggc ag	genomic PCR
Dok-3_RA_for(REP)	gag aag ttt gat gca cgg gat cac g	genomic PCR
Dok-3_RA_rev	gaa gat gtt ctc ata gag atg ctc gg	genomic PCR
Dok-3_ATGmut_for	gct gtg ctg ggc cct tgg aga gac cag tg	mutagenesis (left arm)
Dok-3_ATGmut_rev	cac tgg tct ctc caa ggg ccc agc aca gc	mutagenesis (left arm)
Dok-3_Stopexon3_for	cag ccc atc cct atg tag gag aac tgc ctc	mutagenesis (right arm)
Dok-3_Stopexon3_for	gag gca gtt ctc cta cat agg gat ggg ctg	mutagenesis (right arm)
screenLAfor2	gag gaa gcc aag atg gtg tat ctc c	genomic PCR (screen)
screenLAfor3	ccc ttc tct tca gtg caa caa tgc c	genomic PCR (screen)
chDok-3rev2	tgc cat gat gtc acc cat aat gtg c	genomic PCR (screen)
Neo_rev	cgg acc gct atc agg aca tag cgt tg	genomic PCR (screen)
HisD_rev	tgc ccc ttc ttc gct ggt acg agg ag	genomic PCR (screen)
hGAPDHfor	tga agg tcggag tca acg gat ttg	cDNA amplification
hGAPDHrev	cat gtg ggc cat gag gtc cac cac	cDNA amplification
chGAPDHfor	aat gca tcg tgc acc acc aac	cDNA amplification
chGAPDHrev	tca ctc ctt gga tgc cat gtg	cDNA amplification

4.1.5. Solutions, buffers, and media

The compositions of all solutions and buffers used are listed in the sections in which the corresponding experimental procedures are described. All solutions and buffers are aqueous solutions and stored at room temperature unless otherwise indicated. If solutions, buffers, or media had to be autoclaved it is indicated. Autoclaving of liquids was carried out at 125 °C for 30 min. RPMI medium was already endotoxin tested and filter sterilized.

The following common buffers were used:

PBS.....137 mM NaCl; 27 mM KCl; 43 mM $Na_2HPO_4 \cdot 7\ H_2O$; 14 mM KH_2PO_4; pH ~ 7.3

Tris/HCl.....0.5-1.5 M Tris; adjust pH to 6.8-8.8 with HCl

TE buffer..... 10 mM Tris/HCl, pH 8.0; 1 mM EDTA, pH 8.0

4.1.6. Bacteria strains

The following *E. coli* strains were used for the production of expression vectors, production of pCR-Topo or pENTR-Topo plasmids, or expression of recombinant proteins (BL21), respectively. The generation of competent bacteria and their transformation is described in 4.2.1.9.

Table 4.6: Bacteria strains

Strain	Genotype	application
DH5α	F^- endA1 glnV44 thi-1 recA1 relA1 gyrA96 deoR nupG Φ80d*lacZ*ΔM15 Δ(*lacZYA-argF*)U169, hsdR17(r_K^- m_K^+), λ–	plasmid amplification
Top10F’	F'[lacI^q Tn10(tet^R)] mcrA Δ(mrr-hsdRMS-mcrBC) φ80lacZΔM15 ΔlacX74 deoR nupG recA1 araD139 Δ(ara-leu)7697 galU galK rpsL(Str^R) endA1 λ^-	plasmid amplification
XL1 blue	endA1 gyrA96(nal^R) thi-1 recA1 relA1 lac glnV44 F'[::Tn10 $proAB^+$ $lacI^q$ Δ(lacZ)M15] hsdR17(r_K^- m_K^+)	plasmid amplification
BL21(DE3)	F^- ompT gal dcm lon $hsdS_B$(r_B^- m_B^-) λ(DE3)	Expression of GST fusion proteins
DB3.1	F- gyrA462 endA1 glnV44 Δ(sr1-recA) mcrB mrr hsdS20(r_B^-, m_B^-) ara14 galK2 lacY1 proA2 rpsL20(Sm^r) xyl5 Δleu mtl1	amplification of destination vectors

4.1.7. Additional materials

GeneRuler™ 1 kb DNA ladder	MBI Fermentas
λ-DNA/Hind III marker	MBI Fermentas
Rainbow™ coloured protein molecular weight markers (2.5-45 kDa and 14.3-220 kDa)	Amersham Biosciences
Prestained Protein Marker, Broad Range (6.5-175 kDa)	New England Biolabs
Protease Inhibitor Cocktail (P 2714)	Sigma-Aldrich
Tissue culture equipment (dishes, pipettes, tubes etc.)	Greiner, Nunc, Falcon
Electroporation cuvettes (4 mm gap)	Peqlab
Nitrocellulose filter Hybond ECL™	Amersham Biosciences
Nylon Membrane Hybond N^+	Amersham Biosciences
ECL™ Western blotting detection reagents	Amersham Biosciences
Human Immune System MTC™ cDNA Panel	Becton Dickinson

ABI PRISM™ BigDye™ Terminator Cycle Sequencing Ready Reaction Kit

4.1.8. Instruments

Eppendorf Thermomixer comfort

Eppendorf centrifuge 5417R

pH meter inoLab® pH Level 1

Eppendorf BioPhotometer

Eppendorf Mastercycler personal and Eppendorf Mastercycler epgradient

Gel Imager (Intas, Göttingen)

ABI PRISM® 3100 Genetic Analyser

Heraeus HERAcell 150 (cell culture incubators)

INFORS Unitron (37 °C shaker)

Heraeus Kelvitron®t (bacteria incubator)

Centrifuges SORVALL® RC 3B Plus and SORVALL® RC 26 Plus

Trans-Blot SD Semi-Dry Transfer Unit (Bio-Rad)
and T70/T77 semi-dry transfer unit (Amersham Biosciences)

film developer Optimax Typ TR

Chemi Lux Imager (Intas, Göttingen)

HERAsafe (cell culture bench)

Heraeus Multifuge 3 S-R

BIO-RAD Gene Pulser & BIO-RAD Capacitance Extender

Automatic DNA isolation system PI-50alpha (Kurabo Industries, Japan)

FACSCalibur (Becton Dickinson)

LSR II (Becton Dickinson)

Leica Laser Scanning Spectral Confocal Microscope TCS SP2

4.1.9. Software

CellQuest; FlowJo (Ca^{2+} mobilization analysis)

CSX-1400M Camera Controller (Chemi Lux Imager)

Gel documentation software GDS (Gel Imager)

ABI PRISM® GeneScan® Analysis Software (sequencing analysis)

Adobe® Photoshop® CS2 (image editing)

pDRAW 3.1; Clone Manager 7 (*in silico* cloning)

CorelDraw; MS Office

4.1.10. Web-sites and databases

The following databases were used for the identification of avian cDNA orthologs and genomic sequences by blast searches:

http://www.ncbi.nlm.nih.gov

http://www.chick.umist.ac.uk

http://www.ensembl.org

http://www.expasy.org

http://www.tigr.org

http://pheasant.gsf.de/DEPARTMENT/dt40.html

http://www.matrixscience.com

4.2. Experimental Procedures

4.2.1. Methods in Molecular Biology

4.2.1.1. Digestion of DNA with restriction endonucleases

For the sequence-specific cleavage of DNA molecules the samples were incubated with restriction endonucleases following the manufacturer's instructions.

4.2.1.2. Agarose gel electrophoresis of nucleic acids

After restriction endonucleases digestion of DNA the resulting discrete fragments were resolved by agarose gel electrophoresis. Gels were prepared by dissolving 0.8-2 % agarose (w/v) in TAE or TBE buffer, respectively. The agarose was melted in a microvave, ethidium bromide was added to a final concentration of 0.5 µg/mL, and the solution was poured into a sealed gel casting platform. The DNA samples to be resolved were mixed with an appropiate volume of 6x DNA loading buffer. Additionally a DNA molecular weight standard was loaded (GeneRuler™ 1 kb DNA ladder, MBI Fermentas). The electrophoresis was performed in a gel chamber filled with TAE or TBE buffer at a voltage of 5 V/cm electrodal distance.

TAE buffer (50x)..... 2 M Tris/acetic acid, pH 7.8; 0.5 M NaOAc; 50 mM EDTA, pH 8.0

TBE buffer (10x).....0.9 M Tris; 0.9 M boric acid; 10 mM EDTA, pH 8.0

6x DNA loading buffer..... 10 mM Tris/HCl, pH 8.0; 1 mM EDTA, pH 8.0; 0.25 % (w/v) bromophenolblue; 15 % (w/v) Ficoll

4.2.1.3. Extraction of DNA from agarose

Isolation of DNA fragments from agarose gels was achieved with *QIAEX II gel extraction kit* (Qiagen) or *Wizard® SV Gel and PCR Clean-Up System* (Promega) as per manufacturer's instructions. DNA was eluted with an appropriate volume of dH_2O or 10 mM Tris/HCl, pH 8.0.

4.2.1.4. Phenol/chloroform extraction and ethanol precipitation of DNA

The aequous DNA solution was extracted with ½ volume phenol and ½ volume chloroform. The mixture was centrifuged at 16,000 *g* for 5 min at room temperature. The aqueous phase was re-extracted with ½ volume chloroform and centrifuged at 16,000 *g* for 1 min at room

temperature. Subsequently the DNA was concentrated by ethanol precipitation by adding 1/10 volume 3 M NaOAc followed by 2.5 volumes of ice-cold 100 % ethanol, and the samples were then placed at -80 °C for 15-20 min. The samples were centrifuged at 16,000 *g* and 4 °C for 10 min. The supernatant was discarded and the DNA pellet was air-dried for 10 min. The dry pellet was dissolved in an appropriate volume of dH_2O or TE buffer, pH 8.0.

4.2.1.5. Photometric determination of DNA and RNA concentrations

DNA and RNA concentrations were determined with the BioPhotometer (Eppendorf) as per manufacturer's protocol. The DNA and RNA concentrations are calculated by the following formulas:

$$1\ A_{260}\ \text{Unit of dsDNA} \approx 50\ \mu g/mL\ H_2O$$

$$1\ A_{260}\ \text{Unit of ssRNA} \approx 40\ \mu g/mL\ H_2O$$

The purity of DNA or RNA can be estimated by the following values:

$$\text{pure DNA: } A_{260}/A_{280} \geq 1.8$$

$$\text{pure RNA: } A_{260}/A_{280} \geq 2.0$$

4.2.1.6. Fill-in of 3'-recessed DNA ends

2 µL dNTPs (2.5 mM each) and 2 U Klenow fragment were added to the restriction endonuclease digested samples and incubated at 25 °C for 30 min. The DNA was purified by agarose gel electrophoresis and subsequent extraction (see 4.2.1.3.).

4.2.1.7. Dephosphorylation of vector DNA

Prior to ligation the vector DNA was dephosphorylated at the 5`-end with calf intestine phosphatase (CIP) (NEB). 1 µL CIP (1U/µL) was directly added to each 40 µL of restriction digest and incubated at 37 °C for up to 1 h. After gel electrophoresis the dephosphorylated vector DNA was extracted from agarose (see 4.2.1.3.).

4.2.1.8 Ligation of DNA fragments

For the ligation of linearized vectors and DNA fragments encoding proteins (inserts) the T4 DNA ligase was used (NEB). This enzyme catalyzes the formation of phosphodiester bonds between adjacent 3`-OH and 5`-P ends in dsDNA. For ligations of cohesive ends a molar ratio of 1:3 (vector : insert DNA) was chosen, for ligations of blunt ends a molar ratio of 1:5. In addition to vector and insert DNA the ligation reaction contained 0.5 µL T4 DNA ligase (NEB) and an appropriate volume of 10x ligase buffer (NEB). If necessary the

reaction volume was brought up to 10 µL with dH_2O. In order to check the ability of vector DNA to religate, one sample was set up without the addition of insert DNA. Ligation reactions were incubated at room temperature for 1h or at 16 °C overnight, and used directly for the transformation of competent bacteria.

4.2.1.9. Generation of transformation competent *E. coli* bacteria and transformation

5 mL LB medium were inoculated with the *E. coli* strain and incubated at 37 °C overnight with shaking (200 rpm). The next day 150 mL LB medium were inoculated with 900 µL overnight culture. The culture was grown until an OD_{600} value of 0.45-0.55 was reached. The bacteria suspension was put on ice for 10 min and then harvested at 2,000 rpm at 4 °C for 10 min. The supernatant was removed and the bacteria were resuspended with 30 mL TFB I. After 10 min incubation on ice, the bacteria were centrifuged and resuspended in 6 mL ice-cold TFB II. 50 µL portions of this cell suspension were transferred to a 1.5 mL Eppendorf tube and were flash frozen with liquid nitrogen. The competent bacteria were stored at -80 °C until usage.

LB medium……10 g tryptone; 5 g Yeast Extract; 10 g NaCl ad 1000 mL dH_2O; autoclaved; 4 °C storage

TFB I……50 mM $MnCl_2 \cdot 4\ H_2O$; 100 mM KCl; 10 mM $CaCl_2 \cdot 2\ H_2O$; 30 mM KOAc, pH 6.0; 15 % (v/v) glycerol; adjust to pH 6.1 with HOAc; autoclaved; 4 °C storage

TFB II……75 mM $CaCl_2 \cdot 2\ H_2O$; 10 mM KCl; 10 mM MOPS; 15 % (v/v) glycerol; adjust to pH 7.0 with KOH; autoclaved; 4 °C storage

Competent bacteria were thawed on ice. An appropriate amount of plasmid DNA or 5 µL of a ligation reaction, respectively were added to the bacteria and the suspension was mixed by stirring with a pipet tip. The transformation sample was incubated on ice for 15 min and then heat-shocked at 42 °C for 45-60 s. The bacteria was returned to ice for 2 min and then 300 µL LB medium were added, and incubated at 37 °C for 30 min. Subsequently the bacteria was spread onto LB plates containing an appropriate antibiotic and incubated at 37 °C overnight. Bacteria transformed with pCRII-Topo or pCR2.1-Topo constructs were spread on LB/ampicillin/IPTG/X-Gal plates for blue/white colour selection. The next day transformants were analyzed by PCR or plasmid miniprep cultures were inoculated (see 4.2.1.10.).

LB/agar……..20 g agar per 1000 mL LB; autoclaved and cooled to 60 °C; addition of antibiotic (see below); 4 °C storage

X-Gal/IPTG plates..... LB/ampicillin/agar, supplemented with 80 µg/mL X-Gal and 20 mM IPTG; 4 °C storage

Table 4.7: Selection of bacteria

antibiotic	final concentration
Ampicillin (Amp)	50-100 µg/mL
Kanamycin (Kan)	30-50 µg/mL
Chloramphenicol (Cmp)	100 µg/mL

4.2.1.10. Isolation of Plasmid-DNA

For the analytical plasmid isolation 5 mL LB/Amp or LB/Kan medium were inoculated with a single bacterial colony at 37 °C in a shaker (200 rpm) overnight. The next day the plasmid DNA was isolated using the *Nucleospin® Plasmid Kit* (Macherey-Nagel) or *Wizard® Plus SV Minipreps Kit* (Promega) as per manufacturer`s instructions. For the production of larger amounts of plasmid DNA, 50-250 mL LB medium supplemented with an appropriate antibiotic were inoculated and the culture was grown at 37 °C in a shaker (200 rpm) overnight. The preparation of plasmid DNA was carried out with the *NucleoBond® PC 100* or the *NucleoBond® PC 500 Kit* (Macherey-Nagel), respectively, as per manufacturer`s protocol.

4.2.1.11. Bacterial strain storage

For the long term strain storage, 1-2 mL of a freshly saturated bacterial culture were harvested at 3,000 rpm for 5 min. The supernatant was removed and the bacteria were resuspended in ¼ volume LB/antibiotic and ¼ volume glycerol (87 %). The bacterial stocks were stored at -80 °C.

4.2.1.12. Isolation of genomic DNA from tissue culture cells

For PCR applications (see section 4.2.1.16.), DT40 cells were washed once with PBS and resuspended in buffer K at a density of $5 \cdot 10^6$ cells/mL. The cell suspension was incubated at 56 °C for 1 h, and then the Proteinase K was heat-inactivated at 95 °C for 15 min. The genomic DNA within the cell lysate was directly used as template for PCR. Alternatively,

genomic DNA isolated with the *Automatic DNA Isolation System PI-50alpha* (Kurabo Industries, Japan) was used as template for PCRs.

buffer K.....10 mM Tris/HCl, pH 8.0; 50 mM KCl; 0.45 % NP-40; 0.45 % Tween-20; 100µg/mL Proteinase K

For Southern blot analysis, DT40 genomic DNA was isolated using the *Automatic DNA Isolation System PI-50alpha* as per manufacturer`s protocol.

4.2.1.13. Southern blotting

Southern blotting was performed for the identification of *ntal*$^{-/-}$ DT40 clones by digesting 20 µg of genomic DNA with 50 U restriction endonuclease overnight (300 µL total volume). The next day 50 U restriction endonuclease were added, and digestion was continued for 4 h at 37 °C. Then 1/25 volume 5 M NaCl were added and the sample was mixed by tapping. After addition of 2 volumes ice-cold 100 % EtOH, the samples were placed at -80 °C for 10 min. The samples were centrifuged at maximum speed and 4 °C for 15 min. The supernatant was discarded and the samples were re-centrifuged at maximum speed and 4 °C for 5 min. After removal of remaining liquid, the samples were dried with a speed vac for 3 min. The digested DNA was resuspended in 30 µL TE buffer and left at room temperature for at least 1 h. DNA fragments were resolved by agarose gel electrophoresis overnight (0.7 % agarose in 0.5 x TBE; running buffer: 0.5 x TBE). *Hind* III-digested λ-DNA was used as marker (MBI Fermentas). The gel was incubated with ethidium bromide and complete digestion was confirmed. Then the gel was incubated for 2 x 30 min with denaturing buffer under gentle agitation. After two brief washes with dH_2O, the gel was incubated for 2 x 30 min with neutralization buffer under gentle agitation. After two washes with dH_2O, the gel was blotted onto a nylon membrane by an upward capillary transfer. A spongy stone was placed in a reservoir tank filled with 20x SSC buffer. On the top of the stone, a transfer stack was assembled consisting of Whatmann 3MM paper, the gel, a Hybond-N^+ nylon membrane (Amersham Biosciences), and two pieces of Whatmann 3MM paper. As each layer was applied, it was wet with 20x SSC buffer and air-bubbles were removed. Finally a ~10 cm stack of paper towels, a glass plate and 0.2-0.4 kg weight were laid on the top of the stack. After over-night-transfer, the membrane was recovered and the position of the wells was marked. To confirm complete DNA transfer, the gel was re-stained with ethidium bromide. The nylon membrane was air-dried, baked for 1 h at 80 °C, UV-crosslinked and stored until hybridization.

denaturing buffer.....0.5 M NaOH; 1 M NaCl
neutralization buffer.....1 M Tris/HCl, pH 8.0; 1.5 M NaCl
20x SSC..... 3 M NaCl; 0.3 M sodium citrate dihydrate; adjust pH to 7.2 with 1 M HCl

Radioactive labelling of probes

DNA fragments generated by PCR or by restriction endonuclease digest served as probes. 30-50 ng of DNA (200-1000 bp length) were labelled with [α-^{32}P]dCTP (*Redivue*^{TM}; 370 MBq/mL; 10 mCi/mL; Amersham Biosciences) using the *Rediprime*^{TM} *DNA Labelling System* (Amersham Biosciences) and following the instructions of the manual. Unincorporated nucleotides were removed using *ProbeQuant*^{TM} *G-50 Micro Columns* (Amersham Biosciences). Successful [α-^{32}P]dCTP incorporation was confirmed using a *TriCarb* scintillation counter (Packard Instruments).

Hybridization & autoradiographie

Nylon membranes were soaked in 2x SSC and placed into a heat-sealable plastic bag. To block non-specific binding, pre-warmed pre-hybridization buffer with 0.1 mg/mL salmon sperm DNA (10 mg/mL stock; denatured by heating to 95 °C for 5 min) was added to the bag. After sealing the bag, the membrane was incubated in a water bath at 42 °C for 4 h or overnight. Subsequently salmon sperm DNA and the [α-^{32}P]dCTP-labelled probe were mixed, denatured by heating to 95 °C for 5 min, and added to pre-warmed hybridization buffer. The nylon membrane was incubated with this hybridization solution at 42 °C overnight. Different pre-hybridization and hybridization buffers were used according to the desired stringency conditions (see table 4.8). The next day the membrane was washed three times according to table 4.8. Subsequently the membrane was exposed for 1-3 h or overnight to an imaging plate, which was then analyzed using a phosphor-imager. Alternatively, the membrane was exposed to an X-ray film overnight at -80 °C. If the membrane was to be hybridized with an alternative probe, the membrane was stripped with a high stringency washing buffer (see table 4.8) two times for 15 min in the microwave. Probe removal was confirmed by exposing the membrane to an imaging plate for 1 h at RT.

pre-hybridization buffer……35-50 % Formamide (see table 4.8); 5x Denhardt's solution; 5x SSPE; 0.5 % SDS

50x Denhardt's solution……10 mg/mL Ficoll® 400; 10 mg/mL polyvinylpyrrolidone; 10 mg/mL BSA (fraction V); sterile filtered and stored at -20 °C

20x SSPE……..3 M NaCl; 0.2 M NaH_2PO_4; 20 mM EDTA; adjust to pH 7.0 with NaOH

hybridization buffer…….. pre-hybridization buffer containing 10 % (w/v) dextran sulphate

washing buffer…….. 0.1-2x SSC (see table 4.8); 0.1 % SDS

Table 4.8: Stringency conditions for hybridization and washing

step	component	high stringency	medium stringency	low stringency
pre-hybridization/ hybridzation	formamide	50 %	40 %	35 %
first wash (1x 10 min at RT)	SSC	2x		
second and third wash (2x 10 min at 50 °C)	SSC	0.1x	0.25x	0.4

4.2.1.14. Isolation of total RNA from eukaryotic cells

Total RNA was isolated by using the *RNeasy® Mini Kit* (Qiagen) according to the manufacturer's instructions. Disruption and homogenization of cell lysates was carried out using *QIAshredder™ columns* (Qiagen) as per manufacturer`s protocol.

Alternatively, total RNA was isolated by using RNAzol B (IsoTex Diagnostics) according to manufacturer's protocol. In brief, $7.5 \cdot 10^6$ cells were harvested and washed once with PBS. The cell pellet was briefly vortexed, 300 µL RNAzol B were added, and the cells were lysed by repeated pipetting. 1/10 volume $CHCl_3$ was added, and the sample was vortexed for 15 s and put on ice for 15 min. Phases were separated by centrifugation at 12,000 *g* for 15 min at 4 °C. The upper colorless aqueous phase was transferred to a new Eppendorf tube (~130 µL), and then 1 volume isopropanol was added. The sample was vortexed and placed on ice for 15 min. After centrifugation at 12,000 *g* and 4 °C for 15 min, the supernatant was discarded and the RNA precipitate was washed with 1 mL ice-cold 70 % EtOH. The sample was centrifuged at 12,000 *g* and 4 °C for 5 min and the supernatant discarded. The RNA pellet was air-dried 1-2 min and resuspended with 12 µL RNase-free dH_2O.

The isolated RNA was used directly for reverse transcription or stored at -80 °C.

4.2.1.15. Reverse transcription

First strand cDNAs were synthesized from RNA templates using the *RevertAid™ H Minus First Strand cDNA Synthesis Kit* (MBI Fermentas). The kit contains a genetically engineered version of the Moloney Murine Leukemia Virus Reverse Transcriptase which lacks ribonuclease H activity specific to RNA in RNA-DNA hybrids. For the reverse transcription, 10 ng - 5 µg of total RNA were brought up to a volume of 11 µL with RNase-free dH_2O. Then 1 µL oligo$(dT)_{18}$ primer (0.5 µg/µL stock) or 1 µL random hexamer primer (0.2 µg/µL stock) were added and gently mixed. The mixture was incubated at 70 °C for 5 min and subsequently chilled in an ice bath. The following components were added in the indicated order:

4 µL 5x reaction buffer
1 µL ribonuclease inhibitor (20 U/µL stock)
2 µL dNTP mix (10 mM stock)

The mixture was incubated at 37 °C for 5 min if oligo$(dT)_{18}$ primers were used, and at 25 °C for 5 min if random hexamer primers were used. Then 1 µL of *RevertAid™ H Minus M-MuLV reverse transcriptase* (200 U/µL stock) was added, and reverse transcription was carried out at 42 °C for 1 h. If random hexamer primers were used, the samples were incubated at 25 °C for 10 min and finally at 42 °C for 1 h. The reaction was stopped by heating at 70 °C for 10 min. The first strand cDNA was used directly for amplification by PCR (see section 4.2.1.16.)

4.2.1.16. Polymerase chain reaction (PCR)

General aspects

The Polymerase chain reaction is a technique for the selective in vitro amplification of specific DNA fragments (SAIKI et al., 1985; MULLIS et al., 1986; MULLIS and FALOONA, 1987). In table 4.9 the DNA polymerases used and their common features are listed.

Table 4.9: DNA polymerases and their application

DNA polymerase	supplier	Processivity [bases/min]	elongation T [°C]	3`-5`-proof-reading	overhang A's	application
Taq	NEB, Qiagen	1000	72	no	yes	analytical PCRs
Pfu	Promega	500	68	yes	no	cDNA amplification
Elongase	Invitrogen	1000-1300	68	yes	no	cDNA amplification
LA-Taq	Takara	1000	68-72	yes	yes	long range PCRs (genomic templates)
Primestar	Takara	1000	72	yes	no	cDNA amplification (GC-rich templates)

All PCRs were set up in a volume of 20-50 µL, containing up to 500 ng of genomic DNA or 10-50 ng plasmid as template. The synthetic oligonucleotides (primers) were designed with 40-60 % GC content, no internal structure or complementarity at the 3'-ends. The final primer concentration varied between 0.1 and 0.5 µM. Annealing temperatures were chosen ~5-10 °C lower than the melting temperature T_m. The final concentration of each dNTP was chosen between 50 and 500 µM (most commonly 200 µM). All DNA polymerases were used with supplied buffers. All PCRs were prepared on ice and immediately put into the 95 °C heating block (pseudo hot start). In table 4.10 the cycling parameters are summarized.

Table 4.10: Summary of cycling parameters

step	reaction	T [°C]	t	go to loops
1	initial denaturation	94-98	1-3 min	
2	denaturation	94-98	10-30 s	
3	annealing	55-68	0-30 s (*)	
4	elongation	68 or 72	see table 4.9	18-35x to step 2
5	final elongation	72	5-10 min	
6		12	∞	

* For 2-step-PCRs, the annealing was omitted.

If the amplicons were to be subcloned into the vectors pCR2.1-Topo or pCRII-Topo (see section 4.2.1.17.), single 3'-A overhangs had to be present. If the DNA polymerases were not capable of adding this 3'-A (see table 4.9), an A-tailing procedure was performed. For that 0.2 µL *Taq* DNA polymerase (NEB) and 1 µL dNTPs (10 mM) were added to the completed PCR reaction (50 µL) and incubated at 72 °C for 10 min.

Long distance PCR

LA-*Taq* (Takara) was used for long distance PCRs. The genomic templates were isolated and purified as described in section 4.2.1.12. The homologous sequences flanking the resistance cassettes of the targeting constructs pNTAL-neo/hisD and pDok-3-neo/hisD, respectively were amplified by long distance PCRs. PCR reactions containing LA-*Taq* were set up according to manufacturer's instructions.

Site-directed mutagenesis

The basic procedure of site-directed mutagenesis utilizes a supercoiled dsDNA vector with an insert of interest and two synthetic oligonucleotides containing the desired mutation. In these oligonucleotides, the desired mutation (substitution, deletion or insertion) is in the

middle with ~10-15 bases of correct sequence on both sides. The oligonucleotides are complementary to opposite strands of the vector and are extended during PCR with *Pfu* DNA polymerase. This generates a mutated plasmid containing staggered nicks. Following PCR, the sample is treated with *Dpn* I endonuclease, which is specific for methylated and hemimethylated DNA. Since plasmid DNA isolated from most *E. coli* strains is dam methylated, *Dpn* I digests the parental DNA template. The nicked, mutated plasmid is then transformed into competent bacteria (see 4.2.1.9.). The sample reactions were prepared as indicated below:

5-50 ng template DNA
2.5 µL 10 Pfu reaction buffer
65 ng forward mutagenesis oligonucleotide
65 ng reverse mutagenesis oligonucleotide
0.8 mM dNTPs
0.5 µL *Pfu* DNA polymerase (2.5 U/µL)
dH_2O to a final volume of 25 µL

In table 4.11 the cycling parameters for the site-directed mutagenesis PCR are listed.

Table 4.11: Cycling parameters for mutagenesis PCR

step	reaction	T [°C]	t	go to loops
1	initial denaturation	95	30 s	
2	denaturation	95	30 s	
3	annealing	55	1 min	
4	elongation	68	1 min/kb plasmid	12-18x to step 2
5		12	∞	

Following PCR, 1 µL of *Dpn* I restriction endonuclease is directly added to each amplification reaction and incubated at 37 °C for 1 h. 5 µL of this reaction were used for transformation. Successful site-directed mutagenesis was confirmed by DNA sequencing.

Bacterial PCR

Analysis of bacterial transformants was performed by analytical plasmid preparation (see 4.2.1.10.) or by PCR. Single colonies were picked from an agar plate, saved on a second agar plate and resuspended in 18.7 µL dH_2O. The suspension was heated to 95 °C for 5 min. Subsequently, 6.3 µL PCR mix were added, containing 250 µM dNTPs, 0.2 µM primers

(forward and reverse), buffer (for final volume of 25 µL), and 0.3 µL *Taq* DNA polymerase (NEB).

Splicing by overlap extension (SOE)/ Megaprime PCR

The cDNA encoding the NTAL/Grb2 chimeric protein described in section 5.1.12. was generated by SOE-PCR, alternatively called megaprime PCR. This method employs four different olignucleotides for the amplification of two different DNA fragments (*ntal* cDNA coding for amino acids 1-94 and *grb2* full length cDNA). The 3'-oligonucleotide of the 5'-fragment (bridge2rev; see table 4.5) and the 5'-oligonucleotide of the 3'-fragment (bridge2for) are complementary to each other. First two separate PCRs were performed, amplifying the partial *ntal* cDNA (oligonucleotides NTALfor and bridge2rev) and full length *grb2* cDNA (oligonucleotides bridge2for and Grb2rev). The fragments were purified (see 4.2.1.3.) and used for a second PCR, together with the two distal oligonucleotides NTALfor and Grb2rev. This results in the exponential amplification of *tm-grb2* cDNA.

4.2.1.17. Cloning of PCR products

Cloning of PCR products with 3'-A overhangs was carried out using the *TOPO TA Cloning® Kits* from Invitrogen, using either pCR2.1-Topo or pCRII-Topo. The ligation reactions were set up according to the manufacturer's instructions. The PCR product is ligated into a multiple cloning site within the α-peptide coding region of β-galactosidase, allowing for blue/white screening. Transformations of DH5α or Top10F' bacteria with the Topo ligation reactions are described in section 4.2.1.9. For Top10F' bacteria, IPTG has to be added to the plates, since this strain overexpresses the Lac repressor.

Alternatively, PCR amplicons were ligated into pENTR/SD/D-Topo to generate an entry vector for the Gateway® system (see 4.2.1.18.). This was also performed according to the manufacturer's instructions.

4.2.1.18. Gateway® System (Invitrogen)

The Gateway® Technology is based on the bacteriophage lambda site-specific recombination system which allows for the integration of lambda into the *E. coli* chromosome and the switch between the lytic and lysogenic pathways (PTASHNE et al. 1992). Lambda integration is an intermolecular DNA recombination mediated by lambda and *E. coli*-encoded recombination proteins. The recombination occurs between site-specific *att*achment (*att*) sites, i.e. *att*B on the *E. coli* chromosome and *att*P on the lambda chromosome. Recombination occurs between *att*B and *att*P sites and gives rise to *att*L and

*att*R sites. The lytic pathway (reaction: *att*L x *att*R → *att*B x *att*P) is catalyzed by the bacteriophage λ Integrase (Int) and Excisionase (Xis) proteins, and the *E. coli* Integration Host factor (IHF) protein. These three proteins are components of the *LR Clonase™ enzyme mix* (Invitrogen). The Gateway® Technology uses the lambda recombination system for the transfer of heterologous DNA sequences flanked by modified *att* sites between vectors. The *LR Clonase™ enzyme mix* catalyzes the recombination of an *att*L substrate (entry clone) with an *att*R substrate (destination vector), thereby generating an *att*B-containing expression clone. In table 4.12 common features of the Gateway® vectors are listed.

Table 4.12: Gateway® vectors

vector	*att* sites	propagated in	selection	vectors used in this thesis
Entry	*att*L	DH5α	Kan	pENTR/SD/D/chNTAL wt pENTR/SD/D/chNTAL wt HA pENTR/SD/D/chNTAL Y95F/Y136F/Y155F/Y184F HA pENTR/SD/D/chNTAL Y95only/Y136only/Y155only/Y184only HA pENTR/SD/D/chNTAL 4Y4F HA pENTR/SD/D/chNTAL C23,26A HA pENTR/SD/D/mNTAL
Destination	*att*R	DB3.1	Amp/Cmp	pApuroII/DEST A pMSCVpuro/DEST A
Expression	*att*B	DH5α	Amp	pApuroII/chNTAL wt pApuroII/chNTAL wt HA pMSCVpuro/chNTAL wt HA pMSCVpuro /chNTAL Y95F/Y136F/Y155F/Y184F HA pMSCVpuro /chNTAL Y95only/Y136only/Y155only/Y184only HA pMSCVpuro /chNTAL 4Y4F HA pMSCVpuro /chNTAL C23,26A HA pApuroII/mNTAL wt (for antibody check)

Chicken *ntal* cDNA and a PCR-generated expression cassette encoding C-terminally HA-tagged chicken NTAL were cloned into the entry vector *pENTR/SD/D-Topo* (Invitrogen). By site-directed mutagenesis of pENTR/SD/D/chNTAL wt HA the mutant entry constructs listed in the table above were obtained. The destination vectors pApuroII/DEST A and pMSCVpuro/DEST A were generated by insertion of the *Gateway® conversion cassette A* (Invitrogen) into the *Sma* I-site of pApuroII and the *Hpa* I-site of pMSCVpuro, respectively. The destination conversion cassettes contain the *ccd*B gene, encoding a protein which

interferes with *E. coli* DNA gyrase and thereby inhibiting growth of most *E. coli* strains. Destination vectors containing the *ccd*B gene have to be propagated in the DB3.1 *E. coli* strain, which is resistant to CcdB effects. Upon *LR Clonase™ enzyme mix*-catalyzed recombination the *ccd*B gene is replaced by the cDNA of interest. For LR-reaction, the following components were mixed:

5x LR reaction buffer	4 µL
supercoiled Entry-clone	100 ng
supercoiled Destination vector	300 ng
Topoisomerase (10 U/µL)	1.5 µL
TE-buffer	ad 16 µL

4 µL *LR Clonase™ enzyme mix* were added, and the reaction was incubated at 25 °C for 45 min. 2 µL Proteinase K (2µg/µL) were added, and the reaction was incubated at 37 °C for 10 min. 3 µL of the reaction mixture were used for transformation of competent DH5α *E. coli*.

4.2.1.19. DNA sequence analysis

Sequence analysis of DNA samples was performed by the dideoxy method (SANGER et al., 1977). Sequencing reactions were carried out with the *ABI PRISM® 3100 Genetic Analyser* (Applied Biosystems, Perkin-Elmer) and fluorescence-labelled dideoxy nucleotides (*ABI PRISM™ BigDye™ Terminator Cycle Sequencing Ready Reaction Kit*, Applied Biosystems, Perkin-Elmer) as per manufacturer`s instructions. Alternatively, sequencing was performed by MWG Biotech (Ebersberg, Germany).

4.2.2. Cell culturing

4.2.2.1. General aspects

Complement factors within fetal calf serum (FCS) and chicken serum (CS) were inactivated by heating to 56 °C for 30 min before usage. The cell density of a culture was determined with a Neubauer chamber slide. Cells were centrifuged with a refrigerated centrifuge (Heraeus Multifuge 3 S-R) for 4 min at 300 *g* and 4 °C (unless otherwise indicated)

4.2.2.2. Cell culturing conditions

All used cell lines were cultured in a 5 % CO_2 humidified atmosphere at 37 °C. Wild-type DT40 B lymphocytes and derivatives were cultured in RPMI 1640 containing 10 % FCS, 1 % CS, 3 mM L-glutamine, 50 µM β-mercaptoethanol, 50 U/mL penicillin, and 50 µg/mL streptomycin. Murine B cell lines K46, CH31, WEHI-231, TK μ^+, and TKμ^-, and the human B cell line Ramos were cultured in RPMI 1640 containing 10 % FCS, 2 mM L-glutamine, 2 mM pyruvate, 50 µM β-mercaptoethanol, 50 U/mL penicillin, and 50 µg/mL streptomycin. The murine B cell line IIA1.6 was cultured in RPMI 1640 containing 10 % FCS, 6 mM L-glutamine, 8 mM pyruvate, 50 µM β-mercaptoethanol, 50 U/mL penicillin, and 50 µg/mL streptomycin. HEK293T cells were cultured in DMEM containing 10 % FCS, 2 mM L-glutamine, 50 U/mL penicillin, 50 µg/mL streptomycin, and non-essential amino acids. Plat-E cells were cultured in DMEM containing 10 % FCS, 2 mM L-glutamine, 10 µg/mL blasticidin, 2.5 µg/mL puromycin, 50 U/mL penicillin, and 50 µg/mL streptomycin. The adherent growing HEK293T and Plat-E cells were split using Trypsin/EDTA solution.

4.2.2.3. Cell lines

DT40 (ATCC Number: CRL-2111)

The chicken DT40 B cell line is derived from an avian leucosis virus (ALV)-induced bursal lymphoma (BABA and HUMPHRIES, 1984; BABA et al., 1985). The original lymphoma was induced by viral infection of a 1 day old chicken with Rous associated virus 1 (RAV-1). DT40 cells express surface IgM and continue to undergo IgL gene conversion during *in vitro* cell culture (BUERSTEDDE et al., 1990; KIM et al., 1990). Stimulation of DT40 cells by anti-chicken IgM antibodies ultimately leads to apoptosis, mimicking the elimination of self-reactive B cells (TAKATA et al., 1995). The most unique feature of DT40 cells is the high ratio of targeted to random integration of exogenous DNA (reviewed in SONODA et al., 2001; WINDING and BERCHTOLD, 2001). Targeted integration occurs in frequencies similar to those of random integration (BUERSTEDDE and TAKEDA, 1991). Although the molecular basis for the high targeting efficiencies is unknown, it has been speculated that it may be related to the Ig gene conversion activity, since both processes are mediated by homologous recombination and presumably share the same enzymatic activities (SONODA et al., 2001). In table 4.13 the DT40 knock-out cell lines used in this thesis are listed.

Table 4.13: DT40 knock-out cell lines

DT40 knock-out cell line	reference
btk$^{-/-}$ DT40	TAKATA and KUROSAKI, 1996
dok-3$^{-/-}$ DT40	this thesis
grb2$^{-/-}$ DT40	HASHIMOTO et al., 1998
lyn$^{-/-}$ DT40	TAKATA et al., 1994
ntal$^{-/-}$ DT40	this thesis
p110α$^{-/-}$ DT40	INABE et al., 2002
plc-γ2$^{-/-}$ DT40	TAKATA et al., 1995
slp-65$^{-/-}$ DT40	ISHIAI et al., 1999b
syk$^{-/-}$ DT40	TAKATA et al., 1994

K46

The K46 cell line represents a murine B cell lymphoma and was established from BALB/c mice (KIM et al., 1979). In contrast to the originally described cell line, K46 cells express membrane IgG2a/κ.

IIA1.6

The IIA1.6 cell line is derived from the murine B cell lymphoma A20, which was established from a spontaneous reticulum cell neoplasm found in an old BALB/cAnN mouse (KIM et al., 1979). IIA1.6 cells express membrane IgG2a and do not express Fcγ receptors (JONES et al., 1986; VAN DEN HERIK-OUDIJK et al., 1994).

CH31

CH31 B cells belong to a series of 27 B-cell lymphomas (CH series), induced in B10.*H-2*^{a}*H-4*^{b}p/Wts mice by adoptive hyperimmunization with sheep erythrocytes (LANIER et al., 1982). CH31 cells express membrane IgM/κ (PENNELL et al., 1985).

WEHI-231 (ATCC Number: CRL-2111)

WEHI-231 B cells derive from a mineral-oil induced tumor in (Balb/c x NZB) F1 mice. They express surface IgM.

TKμ$^+$ and TKμ$^-$

TKμ$^-$ is an Ig-negative subclone of Abelson leukemia virus (AMuLV)-transformed pre-B cell line 18-81 (JACK and WABL, 1988). TKμ$^+$ cells were transfected with a μ-chain encoding vector and thus express a pre-BCR (KEYNA et al., 1995).

Ramos (ATCC Number: CRL-1596)

The Ramos B cell was established from an American Burkitt lymphoma (3 years old male patient) (KLEIN et al., 1975). The cells express surface IgM/λ.

HEK293T (ATCC Number: CRL-1573)

HEK 293 cells were generated by transformation of human embryonic kidney (HEK) cell cultures with sheared adenovirus 5 DNA (GRAHAM et al., 1977). HEK293T cells are higly transfectable derivatives of HEK293 cells into which the temperature sensitive gene for SV40 T-antigen was inserted.

Platinum-E (Plat-E)

Plat-E cells are a third generation retrovirus packaging cell line based on the HEK293T cell line. In Plat-E cells, the viral structural genes *gag-pol* and *env* are expressed under the control of the EF1α promotor, which is 100-fold more potent than the MuLV-LTR in 293T cells. Both *gag-pol* and *env* were joined to genes encoding selectable markers via an internal ribosome entry site (IRES) (MORITA et al., 2000).

4.2.2.4. Freezing and thawing of eukaryotic cells

For freezing, cells were harvested and resuspended in freezing medium. The cell density was adjusted to 1-1.5 · 10^7 cells/mL. 1 mL cell suspension was transferred into a cryo-tube and immediately put at -80 °C in a polysterene box, thereby guaranteeing a freezing rate of approximately -1 °C/min.

Cells were thawed rapidly at 37 °C and immediately put into 10 mL culture medium to dilute the DMSO. Then the cells were centrifuged, resuspended in fresh culture medium, and transferred to a Petri dish.

Freezing medium.....90 % (v/v) FCS; 10 % (v/v) DMSO

4.2.2.5. Transfection of DT40 lymphocytes by electroporation

$1 \cdot 10^7$ cells were harvested, washed with PBS, and resupended in 0.5 mL PBS. Then 10-25 µg of linearized DNA and the cell suspension were transferred to an electroporation cuvette (4 mm electrode gap, Peqlab Biotechnologie GmbH, Germany). After 10 min incubation on ice the cells were electroporated at 550 V and 25 µF or 250 V and 975 µF, respectively. The electroporated cells were incubated on ice for 10 min and resuspended in DT40 medium (see section 4.2.2.2.). The cells were incubated at 37 °C and 5 % CO_2 for 24 h and then resuspended in DT40 medium containing an appropriate concentration of antibiotic (see table 4.14). The cells were plated in two 96-well-dishes with 0.2 mL/well. After 5-7 days stable transfectants were visible and transferred to 24-well-dishes.

Table 4.14: Selection of DT40 cells

antibiotic	final concentration
G418	2 mg/mL [effective]
Histidinol	1 mg/mL
Hygromycin B	1.5-2.0 mg/mL
Puromycin	0.5 µg/mL
Blasticidin S	50 µg/mL

4.2.2.6. Transfection of Plat-E cells with FuGENE® for the production of recombinant viruses

Plat-E cells were used as packaging cell line for the production of recombinant, replication-incompetent retroviruses. These retroviruses were then used for the transduction of B lymphocytes (see 4.2.2.7.). Plat-E cells were split to about 50-60 % confluency prior to transfection (9 cm dish). The following components were mixed in the given order:

400 µL RPMI w/o supplements

15 µL FuGENE® (Roche Diagnostics) (directly pipetted into liquid)

3.6 µg retroviral expression vector

1.4 µg pHCMV-VSV-G (if viruses had to be pseudo-typed, i.e. for infection of DT40)

The components were mixed by tapping and left at RT for 15 min. The Plat-E medium was aspirated from the dish and fresh DT40 or K46 medium was given onto the cells. The transfection mixture was added dropwise to the cells. After 48 h incubation at 5 % CO_2 and 37 °C, the cell supernatant containing the retroviruses was used for transduction.

4.2.2.7. Transfection of lymphocytes by retroviral gene transfer

The retroviral gene transfer technology introduces efficiently stable, heritable genetic material into the genome of any dividing cell type (AUSUBEL et al. 1995; COFFIN et al. 1996). The retroviral gene transfer technology is based on the parallel design of packaging cell lines and retroviral expression vectors. Packaging cell lines package recombinant retroviral RNAs into infectious, replication-incompetent particles. In a packaging cell line, the viral *gag*, *pol*, and *env* genes are stably integrated into the genome.

The retroviral vectors p5N-M-IRES-hph and pMSCVpuro/blast used in this thesis are derived from Moloney murine leukemia virus (MMLV) and from PCC4-cell-passaged myeloproliferative sarcoma virus (PCMV, HILBERG et al., 1987; HAWLEY et al., 1994), respectively. Retroviral expression vectors provide the packaging signal Ψ^+, transcription and processing elements (5`- and 3`-long terminal repeats, LTRs), the target gene, and a selectable marker. Transfection of the retroviral vector into a packaging cell line produces replication-incompetent viruses, with the viral genomic transcript containing the target gene and the selectable marker.

The viral *env* gene expressed by the packaging cell line encodes the envelope protein. This protein determines the range of infectivity (tropism) of the packaged virus. Viral envelopes are classified according to the receptors used to enter the host cells. An overview is given in table 4.15.

Table 4.15: Retroviral tropism

tropism	viral entry mechanism
ecotropic	recognition of receptor on mouse and rat cells
amphotropic	recognition of receptor found on a broad range of mammalian cells
dualtropic	recognition of two different receptors found on a broad range of mammalian cells
pantropic	lipid binding and plasma membrane fusion, thereby infecting both mammalian and non-mammalian cells

In pantropic packaging cell lines, virions are pseudo-typed with the envelope glycoprotein from the vesicular stomatitis virus (VSV-G). Since stable expression of the VSV-G envelope protein is toxic, transient virus was produced by cotransfecting a retroviral expression vector and pHCMV-VSV-G into Plat-E cells (see section 4.2.2.6. for details).

Transfection of DT40 cells with recombinant retroviruses

DT40 cells were infected with VSV-G pseudo-typed recombinant retroviruses. In a 6 cm dish 1.5 mL fresh DT40 medium and 45 µL of a polybrene stock solution (final concentration 3 µg/mL) were mixed. The retroviral supernatant was centrifuged at 300 *g* and 4 °C for 4 min. Then $1 \cdot 10^6$ DT40 cells were resuspended with 3 mL retroviral supernatant and transferred to the 6 cm dish. After 24 h the DT40 cells were resuspended in fresh medium, and following an additional 24 h the antibiotic for selection was added to the cells (see 4.2.2.5.). All manipulations of pseudo-typed retroviruses were performed in compliance with the S2 standard and safety intructions.

polybrene stock solution..... 3 mg/mL polybrene in PBS; sterile filtered; freshly prepared prior to each infection

Transfection of K46 cells with recombinant retrovirus

Murine K46 cells were infected with ecotropic recombinant retroviruses, i.e. the virions do not harbor VSV-G. The infection procedure was identical to the protocol for DT40 cells (see above). K46 cells were selected with 10 µg/mL puromycin.

4.2.2.8. Calcium phosphate transfection of HEK293T cells

HEK293T cells were transfected with pApuroII-DEST/chNTAL or pApuroII-DEST/mNTAL by the calcium phosphate method. The cells were split to about 50-60 % confluency prior to transfection (6 cm dish). Then 15 µg plasmid DNA and 63 µL 2 M $CaCl_2$ were brought to a volume of 250 µL with TE buffer and incubated at RT for 10 min. While gently mixing, 250 µL 2x HBS were added dropwise to the DNA/$CaCl_2$ solution. After 15 min incubation on ice, the entire 500 µL were gradually and evenly added dropwise to the cell medium. After 14-16 h incubation the cells were lysed. The lysates were used for testing the specificity of the polyclonal rabbit-anti-chicken NTAL or rabbit-anti-mouse NTAL antibodies, respectively (see 4.2.3.1. and 4.2.3.2.).

2x HBS..... 50 mM HEPES; 280 mM NaCl; 1.5 mM $Na_2HPO_4 \cdot 2H_2O$; adjust pH to 7.0 with 1 M NaOH; sterile filter

4.2.2.9. Cloning of cell populations

For the subcloning of heterogenous eukaryotic cell populations the cell density was adjusted to 2.5 cells/mL in 20 mL complete medium. The cell suspension was spread on one 96-well-

dish in aliquots of 0.2 mL. Single clones were visible after 5-10 days and transferred to a 24-well-dish.

4.2.2.10. Confocal laser scanning microscopy

Confocal laser scanning microscopy of the Lyn/EGFP-positive transfectants (see section 5.2.5.) was performed on harvested cells washed twice with Krebs-Ringer solution containing Ca^{2+} (see 4.2.2.11.2.), and resuspended at a density of $1 \cdot 10^6$ cells/400 µL Krebs-Ringer solution with Ca^{2+}. Following cells sedimentation in 4-well chamber slides (Lab-Tek™, Nunc) the cells were subjected to confocal laser scanning microscopy using the Leica TCS SP2 microscope (kindly performed by I. Goldbeck; Leica objective PL APO 63x 1.3 Glycerol HCX CS; zoom 1-5). Images were exported to Adobe® Photoshop® CS2.

4.2.2.11. FACS analysis (flow cytometry)

4.2.2.11.1. Analysis of surface IgM expression on DT40 cells

For the analysis of surface IgM expression, $0.5\text{-}1 \cdot 10^6$ DT40 cells were transferred to a FACS tube, centrifuged, and washed twice with 2 mL cold PBS. The supernatant was removed and the cells were resuspended in ~200 µL PBS. After addition of 2 µL FITC-conjugated goat-anti-chicken IgM (Bethyl Laboratories), the cell suspension was incubated on ice for 15 min in the dark. Then the cells were washed once with 2 mL cold PBS, resuspended in 500 mL PBS and subjected to FACS analysis. Simultaneously unstained cells were analyzed. For each diagram 10,000 cells were monitored on a logarithmic scale.

4.2.2.11.2. Ca^{2+} mobilization analysis

The Ca^{2+} response in B lymphocytes after stimulation was determined by flow cytometry using the Ca^{2+}-sensitive fluorophors Fluo-3 or Indo-1, respectively. The acetoxymethyl ester derivatives of Fluo-3 (Fluo-3-AM) and Indo-1 (Indo-1-AM) are uncharged molecules that are capable of permeating cell membranes. Within the cell, the lipophilic blocking groups are cleaved by non-specific cytoplasmic esterases, resulting in a charged form which can permeate the plasma membrane far more slowly than its parent compound (“dye-trapping”). Fluo-3 shows an absorption spectrum compatible with excitation at 488 nm by argon-ion laser sources (e.g. FACSCalibur, Becton-Dickinson) and a typically >100 fold fluorescence intensity increase in response to Ca^{2+} binding. Emission is measured at 525 nm. Indo-1 can applied for ratio measurements, i.e. the emission shifts from about 475 nm (Indo-blue) without Ca^{2+} to about 400 nm (Indo-violet) with Ca^{2+} when excited at about 350 nm. The use of the 400/475 emission ratio considerably reduces the effects of unequal dye loading,

leakage of dye, photobleaching, and problems associated with measuring Ca^{2+} in cells of unequal size/thickness. Cell loading of the fluorophors is facilitated by the non-ionic, surfactant polyol Pluronic F-127. The detergent also prevents the compartimentation of the fluorophor within the cell membranes. For Ca^{2+} mobilization analysis, $1 \cdot 10^6$ cells were harvested at 300 *g* and 4 °C for 5 min. The cell pellet was resuspended in 700 µL of the corresponding medium with 5 % FCS. While vortexing mildly, the dye solution was added according to table 4.16.

Table 4.16: Loading conditions for Ca^{2+}-sensitive fluorophors

cell line	Pluronic F-127 (final)	Fluo-3-AM (final)	Indo-1-AM (final)
DT40 and derivatives	0.015 %	1.5 µM	1 µM
K46	0.02 %	1 µM	not applied
WEHI-231	0.02 %	1 µM	not applied

The cells were loaded for 25 min at 30 °C. Subsequently, the cell suspension was diluted with 700 µL of the corresponding prewarmed medium containing 10 % FCS. The cells were incubated for 10 min at 37 °C and were washed twice with Ca^{2+}-containing Krebs-Ringer solution. The cells were resuspended in Ca^{2+}-containing Krebs-Ringer solution and kept at 20 °C until measurement. Prior to measurements, cells were resuspended in Ca^{2+}-free/EGTA-containing Krebs-Ringer solution. The changes in fluorescence intensity of Fluo-3 were monitored on a FACSCalibur cytometer (Becton Dickinson), the ratio Indo-violet/Indo-blue was measured with an LSR II (Becton Dickinson). After 30 s, stimulation was performed with 10 µg/mL M4 (DT40), 20 µg/mL $F(ab')_2$ fragment goat anti-mouse IgG (K46), or 20 µg/mL $F(ab')_2$ fragment goat anti-mouse IgG + IgM (H+L) (WEHI-231), respectively. The extracellular Ca^{2+} level was restored to 1 mM after 6 min (DT40 cells) or after 5 min (K46, WEHI-231), respectively. Equal Fluo-3 loading of the cells was controlled by treatment with 100 nM ionomycin. The Ca^{2+} mobilization profiles were analyzed using FlowJo and Excel software. For comparative Fluo-3 measurements, loading levels were normalized if the deviations were <15 %.

Krebs-Ringer solution..... 10 mM HEPES, pH 7.0; 140 mM NaCl; 4 mM KCl; 1 mM $MgCl_2$; 10 mM glucose

Ca^{2+}-containing..... + 1 mM $CaCl_2$

Ca^{2+}-free/EGTA-containing..... + 0.5 mM EGTA

Pluronic F-127 stock.....5 % (w/v)
Fluo-3-AM stock.....1 mM in DMSO; store at -20 °C
Indo-1-AM stock.....1 mM in DMSO; store at -20 °C

4.2.3. Biochemical Methods

4.2.3.1. Production of recombinant GST fusion proteins with BL21 *E. coli*

Polyclonal antisera against chicken and murine NTAL were obtained by immunization of rabbits with recombinant GST fusion proteins. The cDNA sequences encoding the 49 C-terminal amino acids of chicken and murine NTAL were ligated into the pGEX-3X vector (Amersham Biosciences) at the *Eco*RI site. The resulting vectors pGEX-3X/chNTAL(aa150-198) and pGEX-3X/mNTAL(aa155-203) encode GST N-terminally fused to the 49 C-terminal amino acids of chicken and murine NTAL. These constructs were transformed into BL21 *E. coli*., and 500 mL LB/Amp medium were inoculated with 10 mL overnight culture of a single BL21 colony and grown until an OD_{600} of approximately 0.5 was reached. Expression of the GST/NTAL fusion proteins was induced with 1 mM IPTG. The bacteria was shaken at 37 °C for 2 hours, centrifuged at 3,000 *g* and 4 °C for 15 min, and the supernatant was discarded. The bacterial pellet was resuspended in 20 mL lysis buffer without Triton X-100. The bacteria were sonicated six times for 20 s, and Triton X-100 was added to a final concentration of 1 %. The lysate was incubated on ice for 10 min and centrifuged at 6,000 *g* and 4 °C for 20 min. The supernatant was transferred to two 15-mL-tubes, and 0.8 mL *Glutathione Sepharose® 4B* beads (Amersham Biosciences) equilibrated with Triton X-100-containing lysis buffer were added per tube. The lysate was rotated for 1 h at 4 °C, and the beads were washed two times with 5 mL Triton X-100-containing lysis buffer. The beads were resuspended with 1 mL Triton X-100-containing lysis buffer and transferred to a column. Elution of the GST/NTAL fusion proteins was carried out using 5 mL elution buffer and at 4 °C, and the eluate was collected in 10 fractions à 500 µL in 1.5 mL tubes. As determined by Coomassie staining, typically fractions 2 and 3 contained the highest amount of recombinant fusion protein (approximately 4-8 mg/mL) and were sent to the antibody production facility Medical & Biological Laboratories (MBL, Japan) (see section 4.2.3.2.).

lysis buffer (Japan).....25 mM Tris/HCl, pH 8.0; 10 % glycerol; 1 mM EDTA, pH 8.0; 100 mM NaCl; 1 mM DTT; 0.5 mM benzamidine; 100 ng/mL lysozyme; 0.2 mM PMSF; protease inhibitor

Triton X-100-containing..... to final 1 %

elution buffer.....50 mM Tris/HCl, pH 8.0; 10 mM Glutathione

Alternatively, GST fusion proteins were used for affinity purification experiments (see section 4.2.3.7). BL21(DE3) *E. coli* harboring the plasmids pGEX-4T-1, pGEX-4T-1/mGrb2[SH2], or pGEX-4T-1/mGrb2[cSH3], respectively, were kindly provided by Dr. A. Grabbe. 500 mL LB/Amp medium were inoculated with 5 mL overnight culture and grown until an OD_{600} of ~0.7 was attained. Expression of GST only or the GST/Grb2 fusion proteins was induced with 0.1 mM IPTG. The bacteria was shaken at 37 °C for 3 hours, centrifuged at 3,000 *g* and 4 °C for 20 min, and the supernatant was discarded. The bacterial pellet was resuspended in 50 mL lysis buffer without Triton X-100. The bacteria was sonicated three times for 30 s, and Triton X-100 was added to a final concentration of 0.5 %. The lysate was centrifuged at 6,000 *g* and 4 °C for 20 min. Aliquots of 2 mL were flash frozen in liquid N_2 until usage in affinity purification experiments.

lysis buffer (Germany).....50 mM Tris/HCl, pH 7.4; 150 mM NaCl; 5 mM DTT

4.2.3.2. Immunization of rabbits with GST fusion proteins

For the generation of polyclonal antibodies, rabbits were immunized with fusion proteins containing GST N-terminally fused to the 49 C-terminal amino acids of chicken or murine NTAL, respectively (performed by Medical & Biological Laboratories, MBL, Japan). The specificity of the obtained antibodies was tested by immunoblot analysis of lysates derived from HEK293T cells transfected with pApuroII-DEST/chNTAL or pApuroII-DEST/mNTAL, respectively (see 4.2.2.8.).

4.2.3.3. Stimulation of B lymphocytes via the BCR

B cells were harvested and washed once with RPMI 1640 medium without supplements and once with cold PBS. The cells were resuspended in RPMI 1640 medium without supplements at a density of $1\text{-}5 \cdot 10^7$ cells/mL and incubated at 37 °C for 10-25 min. For stimulation via the BCR 10 µg/mL M4 (DT40 cells), 20 µg/mL $F(ab')_2$ fragment goat anti-mouse IgG (K46/IIA1.6), 20 µg/mL $F(ab')_2$ fragment goat anti-mouse IgG + IgM (H+L)

(WEHI-231), or 20 µg/mL F(ab')$_2$ fragment goat anti-human IgM (Ramos) were added to the B cells. After vortexing the cell suspension was incubated at 37 °C for the desired time. Subsequently the cells were pelleted, 0.2-1 mL lysis buffer per $1 \cdot 10^7$ cells was added, and the lysates were rotated at 4 °C for 30 min. The lysates were cleared from insoluble cell debris by centrifugation at maximum speed and 4 °C for 10 min, and finally transferred to a fresh 1.5 mL Eppendorf tube. The cleared cellular lysates (CCLs) were mixed with 1/5 volume of 5x SDS sample buffer and heated to 95 °C for 5 min, or subjected to affinity purifications with GST fusion proteins or antibodies, respectively (see 4.2.3.6.).

lysis buffer.....20 mM Tris/HCl, pH 7.5; 150 mM NaCl; 0.5 mM EDTA; 10 mM NaF; 10 µM Na_2MoO_4; 1 mM Na_3VO_4; 0.5-1 % detergent (see below); protease inhibitor

detergent.....NP-40, Triton X-100, or laurylmaltoside

5x SDS sample buffer..... 156.25 mM Tris/HCl, pH 6.8; 50 mM DTT; 50 % glycerol; 15 % SDS; 0.05 % bromophenol blue

Alternatively, total cellular lysates were prepared. For that cells were washed once with PBS and directly lysed with 2x SDS sample buffer. The lysates were heated to 95 °C for 8-10 min, subjected to ultrasound for 5 min, and briefly centrifuged.

2x SDS sample buffer..... 62.5 mM Tris/HCl, pH 6.8; 20 mM DTT; 20 % glycerol; 6 % SDS; 0.02 % bromophenol blue

4.2.3.4. Preparation of membrane fractions

For the preparation of membrane fractions, DT40 cells were harvested, washed, starved, and if desired stimulated as described in 4.2.3.3. Protease inhibitor and 1 mM Na_3VO_4 were added and then the cells were flash frozen in liquid nitrogen. The samples were thawed on ice and homogenized with 20 strokes of a dounce homogenizer. The sample was centrifuged at 500 *g* and 4 °C for 5 min. The pellet (nuclei) was discarded and the sample centrifuged at 20,000 *g* and 4 °C for 1 h. The supernatant (cytosolic fraction) was placed on ice, and the pellet was resuspended with 600 µL 0.1 M Na_2CO_3. After centrifugation at 20,000 *g* and 4 °C for 45 min, the supernatant (membrane-associated fraction) was neutralized with 2 M HCl. The pellet (membrane fraction) was lysed with 1 mL lysis buffer (1 % NP-40; see 4.2.3.3.). After addition of NP-40 (1 % final concentration) to the cytosolic and the

membrane-associated fraction, all three fractions were subjected to immunopurification experiments (see 4.2.3.6.).

4.2.3.5. Preparation of lipid rafts

Lipid rafts were prepared by sucrose density gradient ultra centrifugation (modified from ISHIAI et al., 2000). $1 \cdot 10^8$ DT40 cells/lipid raft preparation were harvested and resuspended in 3 mL RPMI w/o supplements. The cells were starved at 37 °C for 5-10 min. If desired, stimulation was performed with 10 µg/mL M4. The cells were centrifuged at 500 *g* and 4 °C for 2 min and subsequently washed with 5 mL PBS-PI. After centrifugation at 2,500 *g* and 4 °C for 10 s, the supernatant was aspirated and the cells were lysed with 400 µL lysis buffer. The lysate was transferred into a homogenizer and homogenized with 20 strokes. The homogenate was transferred to a fresh 1.5 mL Eppendorf tube and placed on ice for 20 min. The samples were centrifuged at 1,500 *g* and 4 °C for 2 min, and 400 µL supernatant were transferred to an ultracentrifuge tube. Then 400 µL 80 % sucrose buffer were added and mixed by pipetting. After careful removal of air bubbles, the lysate was slowly overlaid with 2 mL 30 % and 1 mL 5 % sucrose buffer, respectively. The samples were ultracentrifuged at 200,000 *g* and 4 °C for at least 16 h. The next day, 12 fractions of 300 µL were taken from the top of the sample. Lipid rafts are visible as colourless "clouds", usually appearing in fraction 4. After addition of 60 µL 5x SDS sample buffer, the samples were heated to 95 °C for 8 min and subjected to SDS-PAGE (see 4.2.3.8.).

PBS-PI..... 1 mM Na_3VO_4; 3.75 mM EDTA; 7.5 mM $Na_4P_2O_7$ x 10 H_2O; in PBS

lysis buffer..... 1 mM Na_3VO_4; 10 µM Na_2MoO_4; 5 mM EDTA; 150 mM NaCl; 1 % Triton X-100; 25 mM Tris/HCl, pH 7.5; protease inhibitor

sucrose buffers..... 5, 30 or 80 % (w/v) sucrose; 1 mM Na_3VO_4; 10 µM Na_2MoO_4; 5 mM EDTA; 150 mM NaCl; 25 mM Tris/HCl, pH 7.5; add protease inhibitor prior to usage

4.2.3.6. Affinity purification experiments with GST fusion proteins or antibodies

Affinity purifications of proteins from CCLs were performed with GST fusion proteins containing either the murine Grb2 SH2 or the the C-terminal SH3 domain (see 4.2.3.1.). A 2 mL aliquot of the GST fusion protein was thawed on ice and centrifuged at maximum speed and 4 °C for 10 min. *Glutathione Sepharose® 4B* beads (Amersham Biosciences)

were added to the supernatant and rotated at 4 °C for at least 1 h (binding capacity ~10 mg recombinant GST/mL medium). The beads were washed three times with lysis buffer (see 4.2.3.1., lysis buffer Germany). 10-20 µL beads were added to the CCLs of 1-3 · 10^7 cells and rotated at 4 °C for at least 1 h. Then the beads were washed three times with NP-40- or Triton X-100-containing lysis buffer (see 4.2.3.3.). Subsequently 30-100 µL 2x SDS sample buffer were added and the samples were heated to 95 °C for 5 min. Purified proteins were resolved by SDS-PAGE (see 4.2.3.8.).

For immunopurifications of proteins from CCLs, 0.5-2 µg of the corresponding antibodies were added to the lysates and rotated at 4 °C for at least 1 h. Then 15-20 µL *Protein A/G Plus Agarose* beads (Santa Cruz) were added and proteins were immuno-purified while rotating at 4 °C for at least 1 h. Subsequently, the steps as described for affinity purifications were followed.

If necessary, GST fusion proteins or antibodies were covalently linked to glutathione sepharose or Protein A/G agarose beads, respectively. For that, GST fusion proteins together with glutathione sepharose beads or antibodies together with Protein A/G agarose beads were rotated at 4 °C for at least 1 h (usually overnight). Then the beads were washed two times with PBS and two times with 0.2 M triethanolamine, pH 8.2. Crosslinking was performed by rotating the beads in 0.2 M triethanolamine containing 3 mg/ml dimethyl pimelimidate (DMP; Uptima) at 4 °C overnight. To quench unreacted DMP, the beads were rotated with 10 mM ethanolamine, pH 8.2, at 4 °C for 30 min. After washing the beads three times with PBS, they were used for affinity or immunopurifications.

4.2.3.7. Deglycosylation of N-glycosylated polypeptides

Deglycosylation of proteins followed immunopurification experiments (see 4.2.3.6.) was carried out with PNGase F (NEB). Washed beads were incubated with 15 µL denaturing buffer at 95 °C for 15 min. Then the supernantant was transferred to a fresh 1.5 mL Eppendorf tube, and 2.5 µL G7 reaction buffer, 2.5 µL 10 % NP-40 and 3.5 µL PNGase F were added. The reaction was incubated at 37 °C overnight. After addition of 15 µL 5x SDS sample buffer and heating to 95 °C for 5 min, the samples were subjected to SDS-PAGE and subsequent western blotting (see 4.2.3.8. and 4.2.3.9.).

4.2.3.8. SDS polyacrylamide gel electrophoresis (SDS-PAGE)

Separation of proteins was carried out based principally on the method of one-dimensional, discontinuous electrophoresis in sodium dodecyl sulphate (WEBER and OSBORN, 1969; LAEMMLI, 1970). Laemmli gels are composed of an upper stacking gel, in which the protein

sample is concentrated, and a lower separating gel, in which the different proteins of a sample are separated. Polyacrylamide gels are an insoluble matrix of acrylamide monomers cross-linked with N,N`-methylene-bisacrylamide in the presence of polymerization catalysts (i.e. APS and TEMED). The final acrylamide concentration was 8-12.5 % for separating gels, and 4.8 % for stacking gels. *Rainbow™ coloured protein molecular weight markers* (2.5-45 kDa and 14.3-220 kDa, Amersham Biosciences) or *Prestained Protein Marker* (6.5-175 kDa, New England Biolabs) were used as standards. The electrophoretic separation was carried out at a constant current of 10-20 mA for stacking gels and 25-35 mA for separating gels. Subsequently gels were subjected to Coomassie staining (*Coomassie Brilliant Blue R-250*, Serva), silver staining, or western blot analysis (see section 4.2.3.9.).

separating gel..... 375 mM Tris/HCl, pH 8.8; 8-12.5 % acrylamide; 0.1 % SDS; 0.25 mM EDTA; 0.1 % TEMED; 0.1 % APS

stacking gel.....125 mM Tris/HCl, pH 6.8; 4.8 % acrylamide; 0.1 % SDS; 0.25 mM EDTA; 0.1 % TEMED; 0.1 % APS

SDS running buffer.....…25 mM Tris; 192 mM glycine; 0.1 % (w/v) SDS

4.2.3.9. Western blotting

Western blotting was performed with a semidry transfer unit (Bio-Rad or Amersham Biosciences). A sheet of transfer buffer-soaked filter paper was put in place on the anode. The filter paper was followed by the equilibrated nitrocellulose membrane, the gel and finally another sheet of transfer buffer-saturated filter paper. Air bubbles were rolled out as each component was added to the stack. The cathode was placed atop of the transfer stack and a current of max. 0.8 mA/cm^2 gel was applied for 45 min. After transfer the unit was dissassembled, and the membrane with transferred proteins was subjected to immunoprobing with primary and secondary horseradish-peroxidase (HRPO)-conjugated antibodies. The membrane was first incubated in blocking solution at room temperature for 1h or at 4 °C overnight on a rocking platform, and thereafter briefly washed three times with TBST. Specific proteins were detected with a specific primary antibody. The primary antibody dilution was typically 1/100 to 1/2000 in TBST with 1 % (w/v) BSA and 0.01 % (w/v) NaN_3. The membrane was incubated with the primary antibody at 4 °C for 1 h or overnight on a rocking platform. The membrane was washed with TBST three times by agitation on an orbital shaker, 7 to 10 min each time. The HRPO-conjugated anti-immunoglobulin antibody was diluted 1/5000 to 1/10,000 in TBST, and the membrane was incubated with the secondary antibody at room temperature or 4 °C for 0.5 to 1 h on a rocking platform. The membrane was washed with TBST three times by agitation on an

orbital shaker, 7 to 10 min each time. The immunoblot was visualized using the ECL® detection system (Amersham Biosciences). Detection of specific proteins was carried out by either exposure of the membrane to a film with variable exposure times (0.5-15 min) in the darkroom and subsequent automated film development (Optimax Typ TR, MS Laborgeräte, Germany), or direct exposure of the membrane to a digital imaging system (Chemi Lux Imager, Intas).

transfer buffer.....39 mM glycine; 48 mM Tris; 0.0375 % (w/v) SDS; 0.01 % (w/v) NaN3; 20 % MeOH
blocking solution.....5 % (w/v) nonfat dried milk or BSA in TBST
TBST.....0.1 % (v/v) Tween-20 in TBS

4.2.3.10. Stripping of immunoblot membranes

If nitrocellulose membranes had to be incubated with an alternative primary antibody derived from the same species, bound immunoglobulins were removed by incubating the nitrocellulose membranes with stripping buffer at 50 °C for 30 min. Then the membranes were washed 6-10 times for 10 min with TBST, followed by incubation in blocking solution and probing as described in 4.2.3.11.

Stripping buffer.....2 % SDS; 0.1 M β-MeOH; 62.5 mM Tris, pH 6.8

5. Results

5.1. Grb2 and NTAL regulate Ca^{2+} mobilization in B lymphocytes

Engagement of antigen receptors on lymphocytes results in the recruitment of adaptor molecules and kinases, leading to the activation of PLC-γ and an increase in $[Ca^{2+}]_i$. Lymphocytes generate their Ca^{2+} signals by using both intra- and extracellular sources. The first aim of this thesis was to investigate the regulation of Ca^{2+} mobilization in B lymphocytes and the roles of adaptor proteins in this process.

5.1.1. Differences in Ca^{2+} mobilization in immature and mature B lymphocytes

To discriminate between Ca^{2+} mobilization from intra- and extracellular sources, B cells were loaded with 1 µM Fluo3-AM/0.02% pluronic F127, and BCR stimulation was performed for 5 min in the presence of 0.5 mM EGTA to sequester extracellular Ca^{2+}-ions. After 5 min the extracellular Ca^{2+} concentration was restored to 1 mM, and the Ca^{2+} entry via ion channels in the plasma membrane was recorded. To further investigate the observation that the extent of extracellular Ca^{2+} entry depends on the developmental stage of the B lymphocyte (KONCZ et al., 2002; KOVESDI et al., 2002), Ca^{2+} flux was monitored in the immature murine B cell line WEHI-231 (figure 5.1, grey line) and the mature murine B cell line K46 (figure 5.1, black line). Whereas the Ca^{2+} release from intracellular stores is comparable in these two cell lines, Ca^{2+} entry across the plasma membrane is significantly higher in mature K46 B cells as compared to the immature WEHI-231 B cells. These results clearly confirm that the extent of extracellular Ca^{2+}-entry depends on the developmental stage of the B lymphocyte.

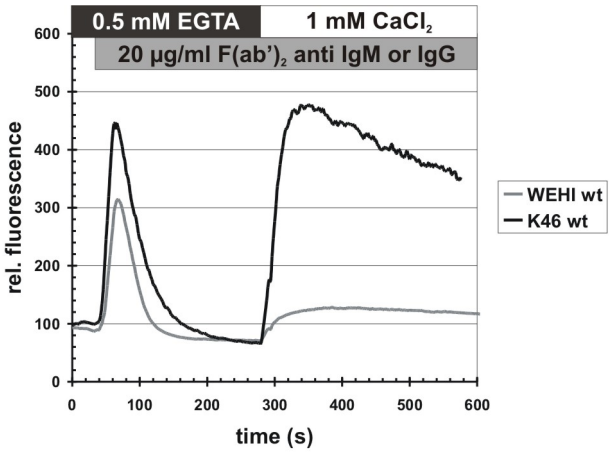

Figure 5.1: Ca^{2+} mobilization in B lymphocytes at different developmental stages
Upon loading of the immature B cell line WEHI-231 (grey line) and the mature B cell line K46 (black line) with 1 µM Fluo-3/0.02 % pluronic F127, BCR-induced release of intracellular Ca^{2+} was monitored for 5 min in the presence of 0.5 mM extracellular EGTA to sequester Ca^{2+} ions from the medium. Subsequently, the extracellular Ca^{2+} concentration was restored to 1 mM, and the influx of Ca^{2+} through plasma membrane channels was recorded. Ca^{2+} mobilization in these two cell lines was analysed in at least three independent measurements.

5.1.2. The adaptor protein Grb2 negatively regulates Ca^{2+} mobilization in B lymphocytes

In order to study whether the adaptor molecule Grb2 exhibits a Ca^{2+}-regulating role in B lymphocytes similar to the Grb2 family member Gads/GrpL in T lymphocytes, BCR-induced Ca^{2+} mobilization was analysed in the immature chicken B cell line DT40 and in genetic mutants that were rendered deficient for Grb2 expression by targeted gene disruption (HASHIMOTO et al., 1998). Reconstitution of wild-type Grb2 expression was achieved by retroviral gene transfer of the parental *grb2*$^{-/-}$ DT40 cell line with avian *grb2* cDNA. Avian *grb2* messenger RNA was isolated from DT40 wild-type cells by RT-PCR using the oligonucleotides chGrb2for and chGrb2rev, respectively. In figure 5.2 the deduced amino acid sequence of avian Grb2 is aligned to its murine and human orthologues. Grb2 is composed of three protein-protein interaction modules, i.e. an N-terminal SH3 domain (figure 5.2, amino acids 1-58), a central SH2 domain (amino acids 60-152), and a C-terminal SH3 domain (amino acids 156-215). The alignment shows a high degree of conservation of the ubiquitously expressed cytosolic adaptor among species with an overall identity of 97.2 %.

```
                    10        20        30        40        50        60
                     |         |         |         |         |         |
chicken     MEAIAKYDFKATADDELSFKRGDILKVLNEECDQNWYKAELNGKDGFIPKNYIEMKPHPW
mouse       MEAIAKYDFKATADDELSFKRGDILKVLNEECDQNWYKAELNGKDGFIPKNYIEMKPHPW
human       MEAIAKYDFKATADDELSFKRGDILKVLNEECDQNWYKAELNGKDGFIPKNYIEMKPHPW
            ************************************************************

                    70        80        90       100       110       120
                     |         |         |         |         |         |
chicken     FFGKIPRAKAEEMLGKQRHDGAFLIRESESAPGDFSLSVKFGNDVQHFKVLRDGAGKYFL
mouse       FFGKIPRAKAEEMLSKQRHDGAFLIRESESAPGDFSLSVKFGNDVQHFKVLRDGAGKYFL
human       FFGKIPRAKAEEMLSKQRHDGAFLIRESESAPGDFSLSVKFGNDVQHFKVLRDGAGKYFL
            **************.*********************************************

                   130       140       150       160       170       180
                     |         |         |         |         |         |
chicken     WVVKFNSLNELVDYHRSTSVSRNQQIFLRDIEQVPQQPTYVQALFDFDPQEEGELGFRRG
mouse       WVVKFNSLNELVDYHRSTSVSRNQQIFLRDIEQMPQQPTYVQALFDFDPQEDGELGFRRG
human       WVVKFNSLNELVDYHRSTSVSRNQQIFLRDIEQVPQQPTYVQALFDFDPQEDGELGFRRG
            *********************************:*****************:********

                   190       200       210
                     |         |         |
chicken     DFIQVLDNSDPNWWKGACHGQTGMFPRNYVTPVNRNI
mouse       DFIHVMDNSDPNWWKGACHGQTGMFPRNYVTPVNRNV
human       DFIHVMDNSDPNWWKGACHGQTGMFPRNYVTPVNRNV
            ***:*:*******************************:
```

Figure 5.2: Amino acid alignment of avian, murine, and human Grb2
The amino acid sequences of avian, murine (accession number NP_032189), and human Grb2 (accession number NP_002077) were aligned using the ClustalW algorithm (THOMPSON et al., 1994). Avian Grb2 amino acid sequence is deduced from multiple cDNA sequences. Amino acids are denoted by using the single letter code. Identical amino acids (*) are depicted in red, strongly similar amino acids (:) in green, and weakly similar amino acids (.) in blue.

Grb2 expression of reconstituted *grb2*$^{-/-}$ DT40 cells was confirmed by immunoblot analysis (see figure 5.4A). All retroviral gene transfers and Ca^{2+} mobilization measurements described in this thesis were performed in cooperation with Dr. M. Engelke (Cellular and Molecular Immunology, Georg-August University, Göttingen).

Wild-type DT40 cells, *grb2*$^{-/-}$ DT40 cells, and derivatives that upon retroviral gene transfer express wild-type Grb2 were loaded with 1.5 µM Fluo3-AM/0.015% pluronic F127. BCR-induced Ca^{2+} release from ER stores was monitored for 6 min in the presence of 0.5 mM EGTA to remove Ca^{2+} ions from the medium. Subsequently the extracellular Ca^{2+} concentration was restored to 1 mM and the influx of Ca^{2+} through plasma membrane ion channels was recorded. Wild-type DT40 cells show a response with internal Ca^{2+} elevation but no subsequent Ca^{2+} influx across the plasma membrane (figure 5.3, green line). The *grb2*$^{-/-}$ DT40 cell line exhibits a completely different Ca^{2+} signal, as these cells mobilize Ca^{2+} from both intra- and extracellular sources (black line). The Grb2-deficient cells also reveal an increased duration of Ca^{2+} efflux from the ER. It was demonstrated that both the prolonged Ca^{2+} release from intracellular stores, and the Ca^{2+} entry from extracellular sources is due solely to the absence of Grb2 since reconstitution of Grb2 expression results in a Ca^{2+} flux that resembles the signal in wild-type DT40 cells, i.e. shortened duration of intracellular Ca^{2+} release and inhibited Ca^{2+} influx across the plasma membrane (grey line). These experiments reveal a negative regulatory role for Grb2 in BCR-induced Ca^{2+} mobilization.

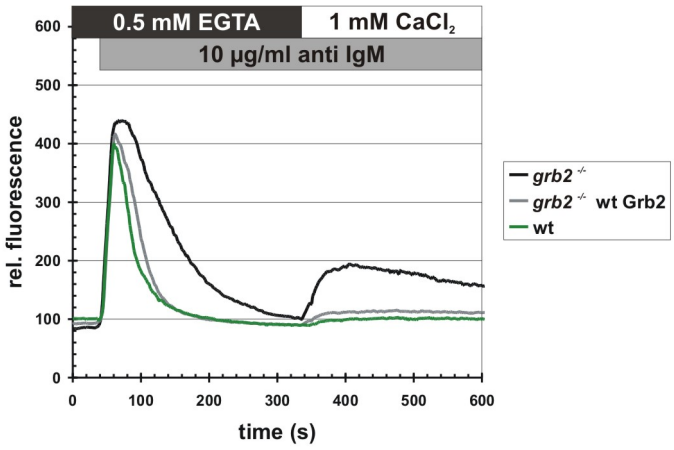

Figure 5.3: Grb2 negatively regulates Ca^{2+} mobilization in B lymphocytes
Wild-type DT40 B cells (green line), *grb2*$^{-/-}$ mutants (black line), and derivatives that upon retroviral gene transfer express wild-type Grb2 (grey line) were loaded with 1.5 µM Fluo-3/0.015 % pluronic F127, and BCR-induced Ca^{2+} release from intracellular stores was monitored for 6 min in the presence of 0.5 mM EGTA. Thereafter the extracellular Ca^{2+} concentration was restored to 1 mM and Ca^{2+} entry across the plasma membrane was recorded. Data represent the results obtained from 18 measurements of four independent retroviral infections.

5.1.3. The central SH2 domain and C-terminal SH3 domain are required for the inhibitory effect of Grb2 on Ca^{2+} mobilization

The contribution of the individual Grb2 domains to the inhibitory effect was investigated by mutational analysis. Chicken Grb2 proline 49 was substituted for leucine, arginine 86 was substituted for lysine, and tryptophane 193 was substituted for lysine to create SH2 or SH3 mutants, respectively. It has been previously described that these amino acid exchanges are loss-of-function substitutions for the corresponding interaction domain (MCPHERSON et al., 1994; TANAKA et al., 1995). Grb2 protein expression in wild-type DT40 cells and in *grb2*$^{-/-}$ DT40 cells reconstituted with wild-type Grb2 or non-functional variants was controlled by anti-Grb2 immunoblot analysis of total cellular lysates (figure 5.4A). Analysis of BCR-induced Ca^{2+} mobilization in *grb2*$^{-/-}$ DT40 cells reconstituted with these non-functional Grb2 variants reveal that the central SH2 domain and the C-terminal SH3 domain are required for the inhibitory effect of Grb2 on Ca^{2+} mobilization (figure 5.4B, blue and orange lines, respectively). In these cells, the prolonged Ca^{2+} release from intracellular stores and the increased Ca^{2+} entry is similar to the fluxes observed for *grb2*$^{-/-}$ DT40 cells. In contrast, the N-terminal SH3 domain is dispensable for this negative regulatory function (figure 5.4B, violet line), as the Ca^{2+} mobilization pattern of this cell line resembles the one observed for *grb2*$^{-/-}$ DT40 cells reconstituted with wild-type Grb2. In figure 5.4C the Ca^{2+} responses of *grb2*$^{-/-}$ DT40 cells and derivatives that were reconstituted with wild-type Grb2 or nonfunctional variants were depicted in one diagram. These measurements show that the inhibitory effect of Grb2 on Ca^{2+} mobilization is mediated by the central SH2 domain and the C-terminal SH3 domain.

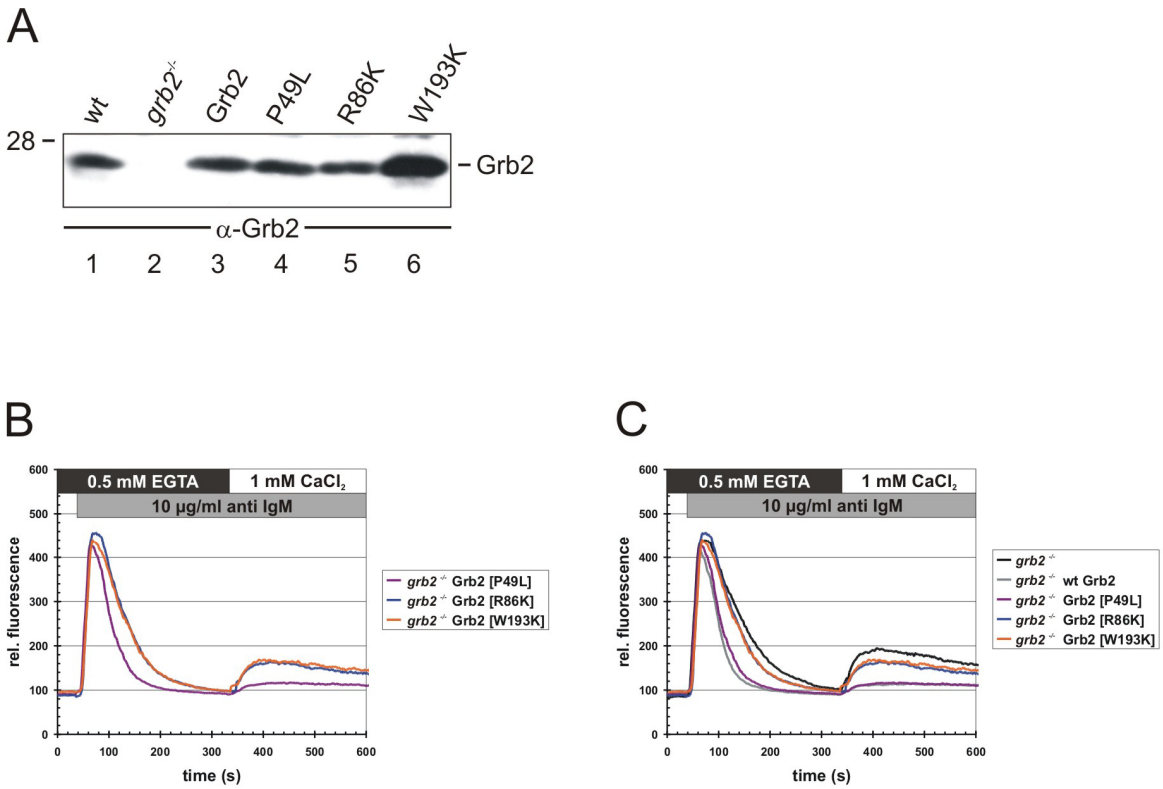

Figure 5.4: The inhibitory effect of Grb2 on Ca^{2+} mobilization depends on the SH2 and the C-terminal SH3 domain
(A) Grb2 protein expression in wild-type DT40 B cells (lane 1), *grb2*$^{-/-}$ mutants (lane 2), and derivatives that upon retroviral gene transfer express either wild-type Grb2 (lane 3) or variants with non-functional N-terminal SH3, central SH2, or C-terminal SH3 domains (lanes 4-6, respectively) was observed by anti-Grb2 immunoblot analysis of total cellular lysates. Amino acid substitutions present in variant Grb2 (P49L, R86K, or W193K) are specified by using the single letter code. Molecular mass protein standards (kDa) are indicated on the left. (B) Intra- and extracellular Ca^{2+} mobilization was recorded by flow cytometry (for details refer to figure 5.3 legend) in *grb2*$^{-/-}$ derivatives that upon retroviral infection express Grb2 variants with a non-functional N-terminal SH3 (violet line), central SH2 (blue line), or C-terminal SH3 domain (orange line). Data represent the results of five independent measurements. (C) Overlay of Ca^{2+} mobilization profiles described in figures 5.3 and 5.4B. Equivalent cellular loading with Fluo-3 was controlled by treatment of the cells with 100 nM ionomycin (data not shown).

5.1.4. Grb2 also exhibits inhibitory effects on Ca^{2+} mobilization in mature B lymphocytes

Thereafter the described negative signalling role of Grb2 was examined to determine if it is restricted to immature B lymphocytes such as DT40 since mature B cells show a more robust antigen-induced Ca^{2+} mobilization. Wild-type K46 cells were retrovirally infected with murine *grb2* cDNA, and overexpression of Grb2 was confirmed by anti-Grb2 immunoblot analysis of total cellular lysates (figure 5.5A, upper panel). As loading control the same membrane was analysed by anti-actin immunoblotting (figure 5.5A, lower panel). Analysis of Ca^{2+} mobilization showed that a moderate overexpression of wild-type Grb2 results in a significantly attenuated influx of extracellular Ca^{2+} ions (figure 5.5B, grey line).

These results confirm that the function of Grb2 as negative regulator of BCR-induced Ca^{2+} mobilization is not restricted to immature B cells such as DT40 but also plays a role in Ca^{2+} flux regulation in mature B lymphocytes.

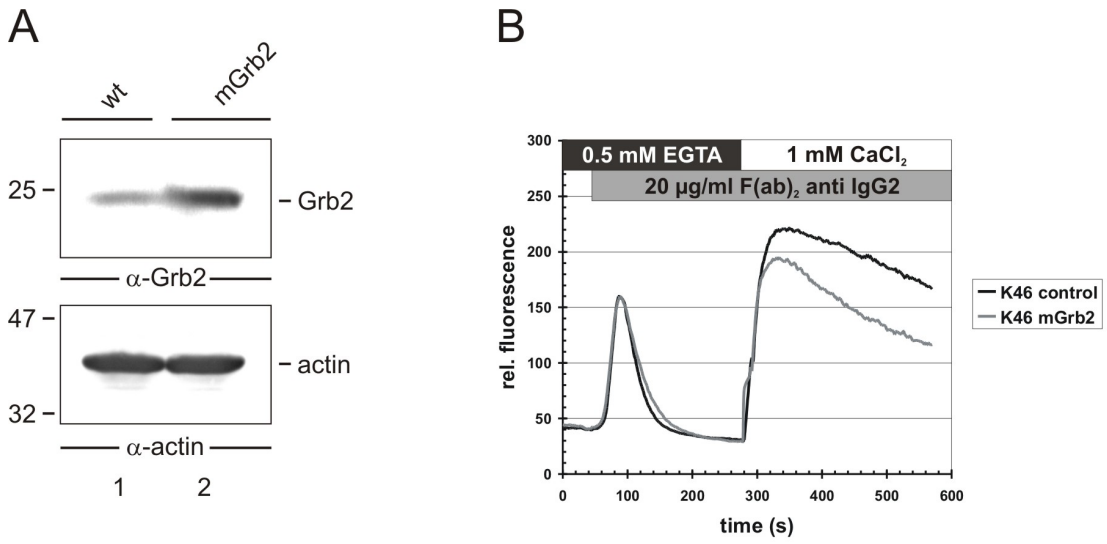

Figure 5.5: Grb2 also inhibits Ca^{2+} mobilization in mature B lymphocytes
(A) Grb2 protein expression in wild-type K46 B cells (lane 1) and derivatives that were retrovirally infected with murine *grb2* cDNA (lane 2) was observed by anti-Grb2 immunoblot analysis of total cellular lysates (upper panel). Anti-actin immunoblotting of the same membrane served as a loading control (lower panel). Molecular mass protein standards (kDa) are indicated on the left. (B) Intra- and extracellular Ca^{2+} mobilization was recorded by flow cytometry (refer to figure 5.1 legend for details) in wild-type K46 B cells (black line) and derivatives that upon retroviral infection overexpress Grb2 (grey line). Data represent the results of four independent measurements.

5.1.5. Grb2 deficiency does not alter the phosphorylation state of SLP-65 or PLC-γ2

One key hallmark of BCR-induced primary Ca^{2+} mobilization is the phosphorylation-dependent assembly of the Ca^{2+} initiation complex consisting of SLP-65, Btk and PLC-γ2 (KUROSAKI et al., 2000; WIENANDS, 2000b). In order to determine whether Grb2 directly affects the assembly of the Ca^{2+} initiation complex, the phosphorylation state of SLP-65 and PLC-γ2 was analysed. Wild-type and *grb2*$^{-/-}$ DT40 cells were left untreated or stimulated via their BCR with 10 µg/mL M4 antibodies for the indicated times and subjected to immunoprecipitation with antibodies to SLP-65 (figure 5.6, left panels) or PLC-γ2 (right panels). Purified proteins were analysed by anti-phospotyrosine (α-pTyr) immunoblotting (upper panels). It could be shown that Grb2 deficiency does not alter the phosphorylation state of SLP-65 or PLC-γ2. This data indicates that Grb2 might not affect the primary Ca^{2+} initiation complex directly.

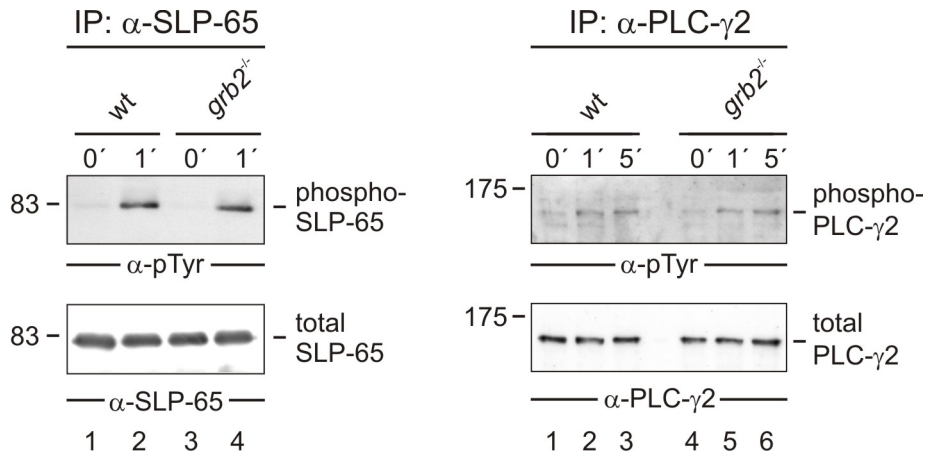

Figure 5.6: Grb2-deficiency does not alter phosphorylation state of SLP-65 or PLC-γ2
Wild-type and *grb2*$^{-/-}$ DT40 cells were untreated or stimulated through their BCR for the indicated times, and lysed. Following immunoprecipitation with antibodies to SLP-65 (left panels) or PLC-γ2 (right panels), the recovered proteins were analysed by anti-phosphotyrosine (α-pTyr) immunoblotting (upper panels). Equivalent protein recovery and loading was confirmed by reprobing the membranes with anti-SLP-65 and anti-PLC-γ2 antibodies (lower panels). Molecular mass protein standards (kDa) are indicated on the left.

5.1.6. The expression of the transmembrane adaptor NTAL in B lymphocytes is dependent on their developmental stage

Grb2 is expressed throughout all stages of B cell lymphopoesis. Therefore, it seemed likely that the differences in Ca^{2+} mobilization between immature, and mature B lymphocytes are evoked by an upstream regulator of Grb2 that is absent or expressed weakly in immature DT40 B cells. This regulator is capable of counter acting the inhibitory effects of Grb2 and thus permits a complete biphased Ca^{2+} response. In T lymphocytes LAT is the central transmembrane adaptor, and tyrosine phosphorylated LAT serves as a scaffold organizing the translocation of Ca^{2+}-regulating enzymes to the lipid raft fraction (reviewed in LINDQUIST et al., 2003; SIMEONI et al., 2005). Brdička et al. reported the identification of the non-T cell activation linker NTAL (BRDICKA et al., 2002) (alternatively called LAB, JANSSEN et al., 2003), which is closely related to LAT structurally and evolutionarily, and reported to bind Grb2 through phosphotyrosine-based binding motifs of the pYxN type (where x is any amino acid) in mammalian B cells. Using a panel of cDNAs derived from different immunorelevant cells and tissues, the *ntal* transcription pattern was analysed by RT-PCT using the oligonucleotides hNTALfor1 and hNTALrev1 (792 bp amplicon). Human *ntal* transcripts were mainly detected in spleen, lymph nodes, and periphal blood leukocytes (figure 5.7A, lanes 1, 2, 4). G*apdh*-specific oligonucleotides were used in this analysis for normalization (lanes 9 to 16).

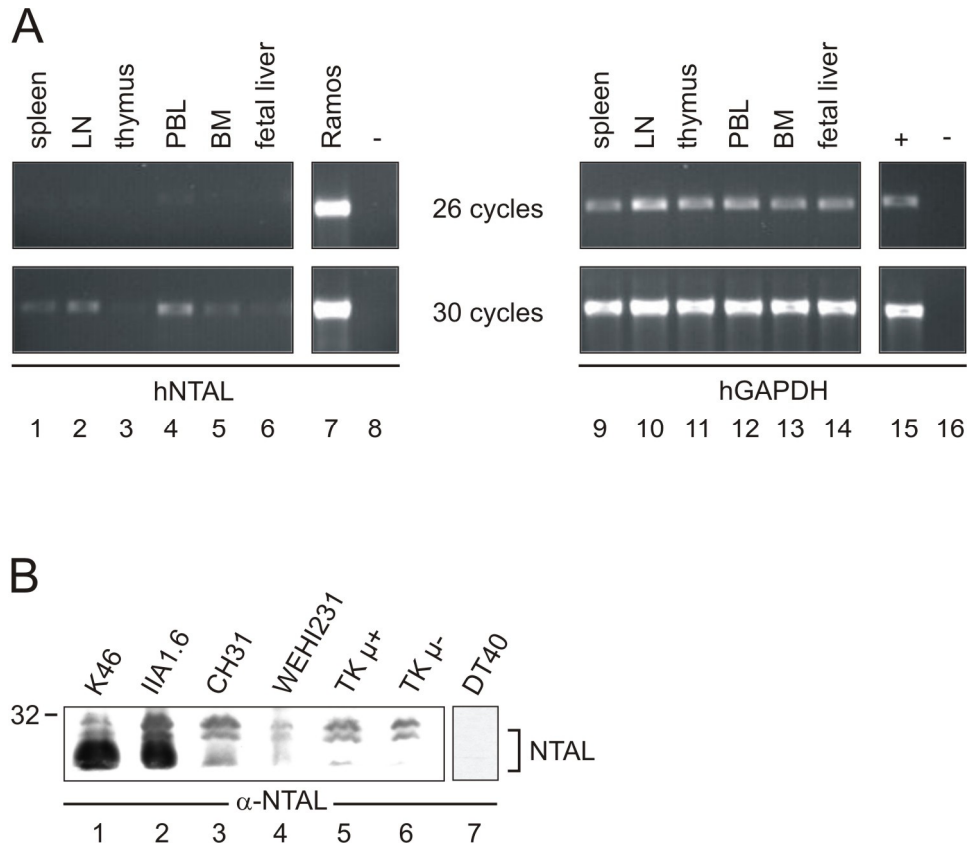

Figure 5.7: NTAL expression depends on the developmental stage of B lymphocytes
(A) Normalized first strand cDNA preparations (BD Human Immune System MTC™ Panel) from human spleen, lymph node (LN), thymus, peripheral blood leukocytes (PBL), bone marrow (BM), and fetal liver were used to analyse NTAL expression by RT-PCR. Oligonucleotides hNTALfor1 and hNTALrev1 are expected to yield a 792 bp amplicon (lanes 1-7). First strand cDNA prepared from human Ramos B lymphocytes was used as a positive control (lane 7). In addition *gapdh*-specific oligonucleotides were used for normalization (expected transcript size: 983 bp; lanes 9 to 16). Human control cDNA included in the panel served as positive control (lane 15), and negative controls (lanes 8 and 16) lacked the template. (B) Total cellular lysates were prepared from approximately 1 x 10^6 cells of B cell lines at various developmental stages and were subjected to anti-mouse (lanes 1-6) or anti-chicken NTAL (lane 7) immunoblotting. The mature B cell phenotype is represented by murine K46 (lane 1) and the A20-derivative IIA1.6 (lane 2); the immature phenotype is represented by murine CH31 (lane 3), WEHI-231 (lane 4), and chicken DT40 (lane 7), while the murine pre-B cell line TKμ$^+$ (lane 5) is a μm-positive variant of the pro-B cell line TKμ$^-$ (lane 6). Molecular mass protein standards are indicated on the left.

The next objective was to analyse the B lymphocyte-specific NTAL expression on the protein level. Thus antibodies specific for murine NTAL had to be generated for immunoblot analysis. This was achieved by immunization of rabbits with GST fusion proteins containing the 49 C-terminal amino acids of murine NTAL. The specificity of the antibodies was tested with lysates of HEK293T cells transfected with full length murine *ntal* cDNA (data not shown). Lysates from murine B cell lines representing different developmental stages were subjected to anti-mouse NTAL immunoblotting (figure 5.7B, maturation stages ascending from the right to the left). This analysis clearly demonstrates

that NTAL expression in B lymphocytes increases with maturation, and is expressed in mature B cell lines K46 and IIA1.6 at the highest levels (figure 5.7B, lanes 1 and 2, respectively).

5.1.7. Functional analysis of the palmitoylation and Grb2-binding motifs of avian NTAL

Cloning the avian *ntal* cDNA and subsequently characterizing its functional properties was then pursued. Three chicken expressed sequence tags (ESTs) were identified in the Biotechnology and Biological Sciences Research Council (BBSRC) repository (BOARDMAN et al., 2002; http://www.chick.umist.ac.uk) by a tblastx search with full length murine *ntal* cDNA sequence. These ESTs originated from chicken limbs, small intestine and liver, respectively, and displayed a high level of similarity to both the human and murine *ntal* cDNA sequences. Based on the identified chicken *ntal* sequences gene-specific oligonucleotides were designed, and *ntal* messenger RNA was isolated from wild-type DT40 cells by RT-PCR. The full length chicken *ntal* cDNA (deposited under accession number AY743659) was amplified using the oligonucleotides chNTALfor5 and chNTALrev2, respectively. Within the amplicon, 9 nucleotides at the 5'end and 19 nucleotides at the 3'end of chicken *ntal* cDNA are derived from the oligonucleotide sequences. The amplified avian *ntal* cDNA encodes a protein containing 198 amino acids with a calculated molecular mass of 22.4 kDa. In figure 5.8A the chicken NTAL amino acid sequence is aligned with its human and murine orthologues. The schematic representation of NTAL from different species and of human LAT depicted in figure 5.8B shows that the previously described cystein-containing palmitoylation motifs for raft localization and the tyrosine-based Grb2 binding sites (BRDICKA et al., 2002; JANSSEN et al., 2003) are also present in avian NTAL. For further functional studies polyclonal antibodies were generated in rabbits immunized with GST fusion proteins containing the 49 C-terminal amino acids of chicken NTAL. The specificity of the rabbit anti-chicken NTAL antibodies was tested with lysates of HEK293T cells transfected with full length chicken *ntal* cDNA (data not shown).
The functionality of the cystein-containing palmitoylation motifs of chicken NTAL was investigated. Raft localization of chicken NTAL was analysed in DT40 cells overexpressing chicken NTAL (transfectant N3-3) by sucrose gradient ultracentrifugation (figure 5.9A, upper panel). As a control for the isolated fractions, the same membrane was subjected to anti-Lyn immunoblotting (figure 5.9A, lower panel) since Lyn is a permanent resident of lipid rafts. These observations prove that chicken NTAL translocates to the lipid rafts since it is detected in fraction 4 containing raft-resident proteins.

A

```
                  10        20        30        40        50        60
                   |         |         |         |         |         |
chicken     -MAQPELLWAA--AGLMLLGVAVSACVRCQLYATKRGKDGSQGSRLERPQRFEVIRSCSA
mouse       MSAELELLWPVSGLLLLLLGATAWLCVHCSRPGVKRNEKIYEQRNRQENAQSSAAAQTYS
human       MSSGTELLWPG-AALLVLLGVAASLCVRCSRPGAKRSEKIYQQRSLREDQQSFTGSRTYS
              :  ****.     *:***.:.  **:*.  ..**.:.  :    ..  :  .     :

                  70        80        90       100       110       120
                   |         |         |         |         |         |
chicken     VTRRPERIKEPEHLARKAPEELSTSCHVGFESSAEPRYQNFLTEDCLHEDAAYVEPVPLD
mouse       LARQVWPGPQMDTAPNKSFERKNKMLFSHLEGPESPRYQNFYKGSNQEPDAAYVDPIPTN
human       LVGQAWPGPLADMAPTR--KDKLLQFYPSLEDPASSRYQNFSKGSRHGSEEAYIDPIAME
            :. :       :  . :  :      .  :*.. ..***** . .    : **::*:. :

                 130       140       150       160       170       180
                   |         |         |         |         |         |
chicken     YYSHNRFFSPPNDEDSHSYQNVIIGDPCSSELDD-------------------------
mouse       YYNWGCFQKPSEDDDSNSYENVLVCKPSTPESGV-------------------------
human       YYNWGRFSKPPEDDDANSYENVLICKQKTTETGAQQEGIGGLCRGDLSLSLALKTGPTSG
            **. . * .*.:*:*::**:**:: .  :.* .

                 190       200       210       220       230       240
                   |         |         |         |         |         |
chicken     ------------AEDYENSTAIEVWKVQQAKAMLY--AESQ------DEE---PDYVNTD
mouse       ----------EDFEDYQNSVSIHQWRESKRTMG----APMS-LSGSPDEE---PDYVNGD
human       LCPSASPEEDEESEDYQNSASIHQWRESRKVMGQLQREASPGPVGSPDEEDGEPDYVNGE
                     ***:**.:*. *: .:                 ***   ***** :

                 250
                   |
chicken     PTIDAVVLSK
mouse       VAAAENI---
human       VAATEA----
             :
```

B

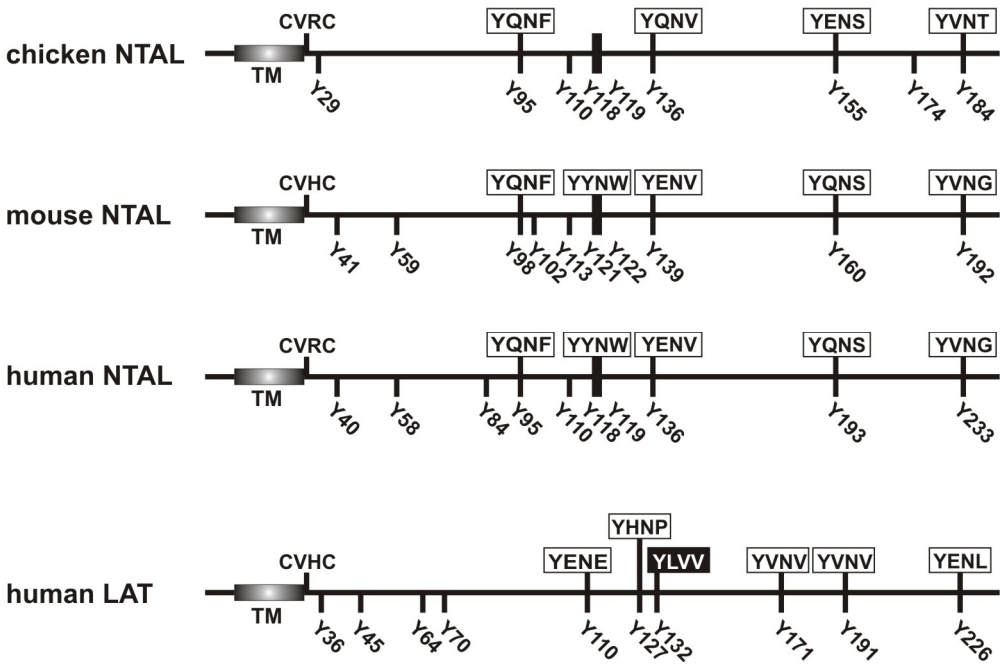

Figure 5.8: Alignments of avian, murine, and human NTAL
(A) The amino acid sequences of avian, murine (accession number NP_064428), and human NTAL (accession number NP_115852) were aligned using the ClustalW algorithm (THOMPSON et al., 1994). The avian NTAL amino acid sequence is deduced from multiple cDNA and genomic sequences, and its cDNA sequence is catalogued under GenBank accession number AY743659. Amino acids are denoted by using the single letter code. Identical amino acids (*) are depicted in red, strongly similar amino acids (:) in green, and weakly similar amino acids (.) in blue. Palmitoylation and Grb2 binding motifs are indicated in bold letters (B) Avian, murine, and human NTAL are schematically represented and compared to human LAT. The amino acid sequences of cystein-containing palmitoylation motifs for raft localization and tyrosine-based Grb2 binding sites are indicated above the respective schematics. Human LAT possess a unique PLC-γ binding site at amino acid position 132 (YLVV) that is highlighted by a black rectangle. TM, transmembrane regions.

Thereafter, the functionality of the tyrosine-based Grb2-binding motifs was examined. Four Grb2-binding sites are common amongst the NTAL proteins from different species (see figure 5.8A and B). BCR-induced tyrosine phosphorylation of avian NTAL was confirmed in two independent NTAL positive DT40 transfectants (transfectants N3-4 and N3-7) by immunoprecipitation with antibodies to chicken NTAL and subsequent anti-pTyr immunoblotting (figure 5.9B, lanes 4 and 6). The avian NTAL/Grb2 complex could be isolated from these two NTAL-positive transfectants following BCR stimulation by co-immunoprecipitation experiments with anti-Grb2 antibodies (figure 5.9C, upper panel, lanes 4 and 6).

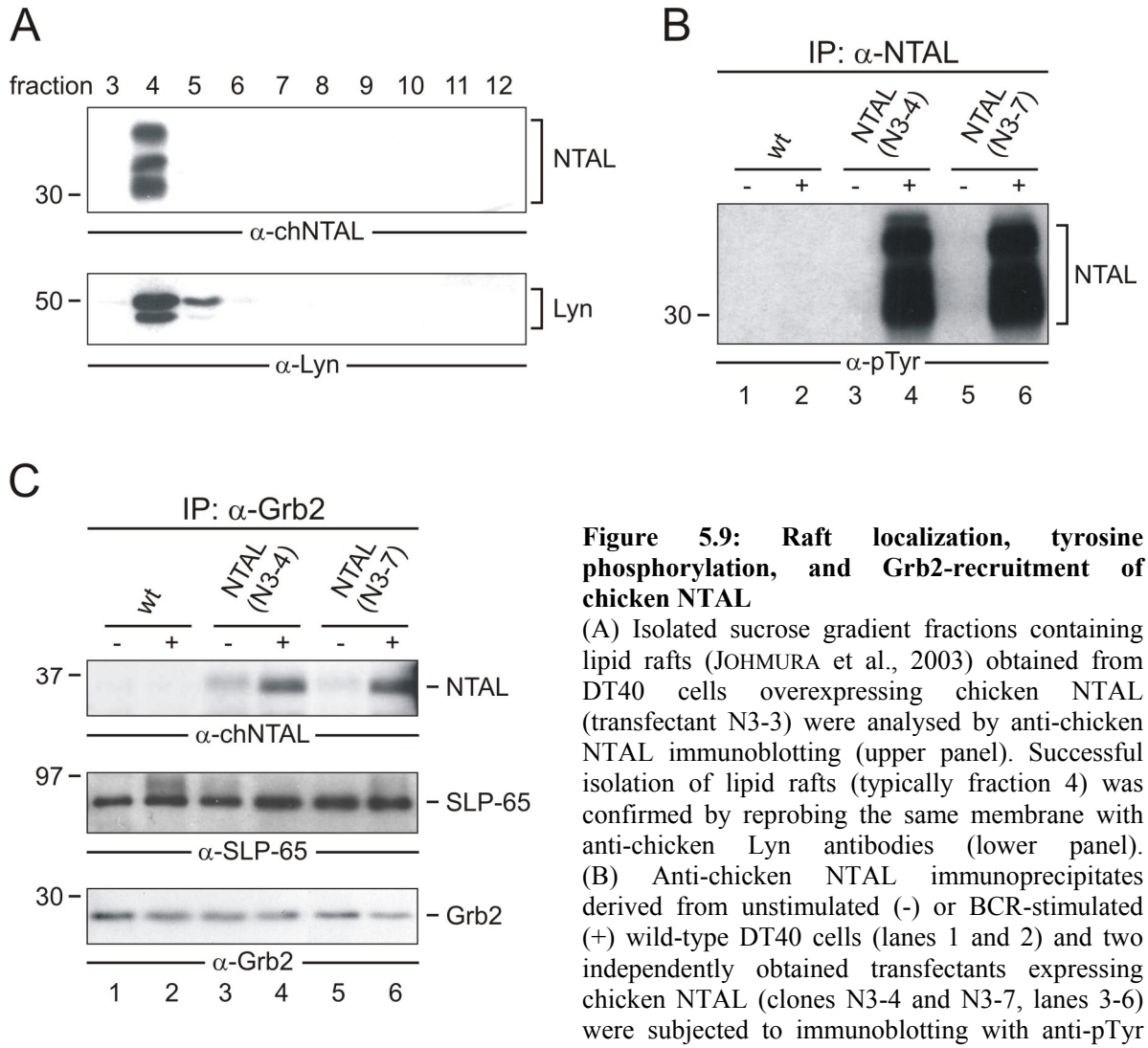

Figure 5.9: Raft localization, tyrosine phosphorylation, and Grb2-recruitment of chicken NTAL
(A) Isolated sucrose gradient fractions containing lipid rafts (JOHMURA et al., 2003) obtained from DT40 cells overexpressing chicken NTAL (transfectant N3-3) were analysed by anti-chicken NTAL immunoblotting (upper panel). Successful isolation of lipid rafts (typically fraction 4) was confirmed by reprobing the same membrane with anti-chicken Lyn antibodies (lower panel). (B) Anti-chicken NTAL immunoprecipitates derived from unstimulated (-) or BCR-stimulated (+) wild-type DT40 cells (lanes 1 and 2) and two independently obtained transfectants expressing chicken NTAL (clones N3-4 and N3-7, lanes 3-6) were subjected to immunoblotting with anti-pTyr antibodies. (C) Anti-Grb2 immunoprecipitates derived from unstimulated (-) or BCR-stimulated (+) wild-type DT40 cells (lanes 1 and 2) and two NTAL-positive transfectants decribed in (B) (lanes 3-6) were analysed by anti-chicken NTAL immunoblotting (upper panel). Equivalent protein recovery and co-immunoprecipitation conditions were verified by anti-Grb2 (lower panel) and anti-SLP-65 immunoblot analysis (middle panel). Molecular mass protein standards (kDa) are indicated on the left in the panels (A-C).

In wild-type DT40 cells, NTAL expression is not detectable by immunoblot analysis. The efficiency of the co-purification was monitored by reprobing the same membrane with both anti-SLP-65 (middle panel) and anti-Grb2 antibodies (lower panel). Together this data shows that NTAL is targeted to lipid rafts and recruits Grb2 following BCR engagement.

5.1.8. Generation of an *ntal*$^{-/-}$ DT40 cell line

NTAL function in BCR signalling pathways was further investigated by gene disruption in DT40 B lymphocytes. This cell line was employed since targeted integration of homologous DNA occurs in these cells at high frequencies (BUERSTEDDE and TAKEDA, 1991). *Ntal* messenger RNA was detected in DT40 B lymphocytes (see section 5.1.7). Therefore the generation of an *ntal*$^{-/-}$ DT40 cell line became necessary to exclude the possibility of endogenous NTAL expression dominantly affecting BCR-induced signalling in subsequent functional studies. The partial chicken *ntal* cDNA sequence obtained from the ESTs was employed to identify the *ntal* sequence within the genomic database (http://www.ncbi.nlm.nih.gov). The GenBank accession number of the chicken *ntal* locus is AC091726. Like its human and murine orthologues, the genomic locus of chicken *ntal* consists of 11 coding exons. Genomic clones of *ntal* were obtained by using the oligonucleotides genNTALfor and genNTALrev in a long range PCR. The targeting vectors pNTAL-neo and pNTAL-hisD were constructed by replacing a 4650 bp genomic fragment containing the exons corresponding to chicken NTAL amino acid residues 1-142 with neo or hisD cassettes, respectively. These cassettes were flanked by 3.2 and 2.3 kb of genomic sequence on the 5' and 3' sides, respectively (figure 5.10A). To disrupt one *ntal* allele, the targeting construct pNTAL-neo was transfected into wild-type DT40 cells. Homologous recombination was identified by PCR and Southern blot analysis (data not shown), and a targeted allele was detected in 13 out of 24 G418-resistant clones. Inactivation of the second allele was achieved by introducing pNTAL-hisD into the neo-targeted clone N2, and selection with both G418 and histidinol. For Southern blot analysis genomic DNA was digested with *Bgl*II and probed using a 841 bp fragment located in the 5' region exterior to the site of recombination, allowing a clear distinction between the 13 kb and 14.2 kb fragments corresponding to the neo- and hisD-targeted loci and the 5263 bp fragment of the wild-type locus. The generation of the *ntal*$^{-/-}$ DT40 clones N2-1, N2-15, N2-20, and N2-23 was confirmed by Southern blot analysis (figure 5.10B). The introduction of a single copy of each targeting vector was also verified by reprobing the blots with internal neo or hisD probes (data not shown).

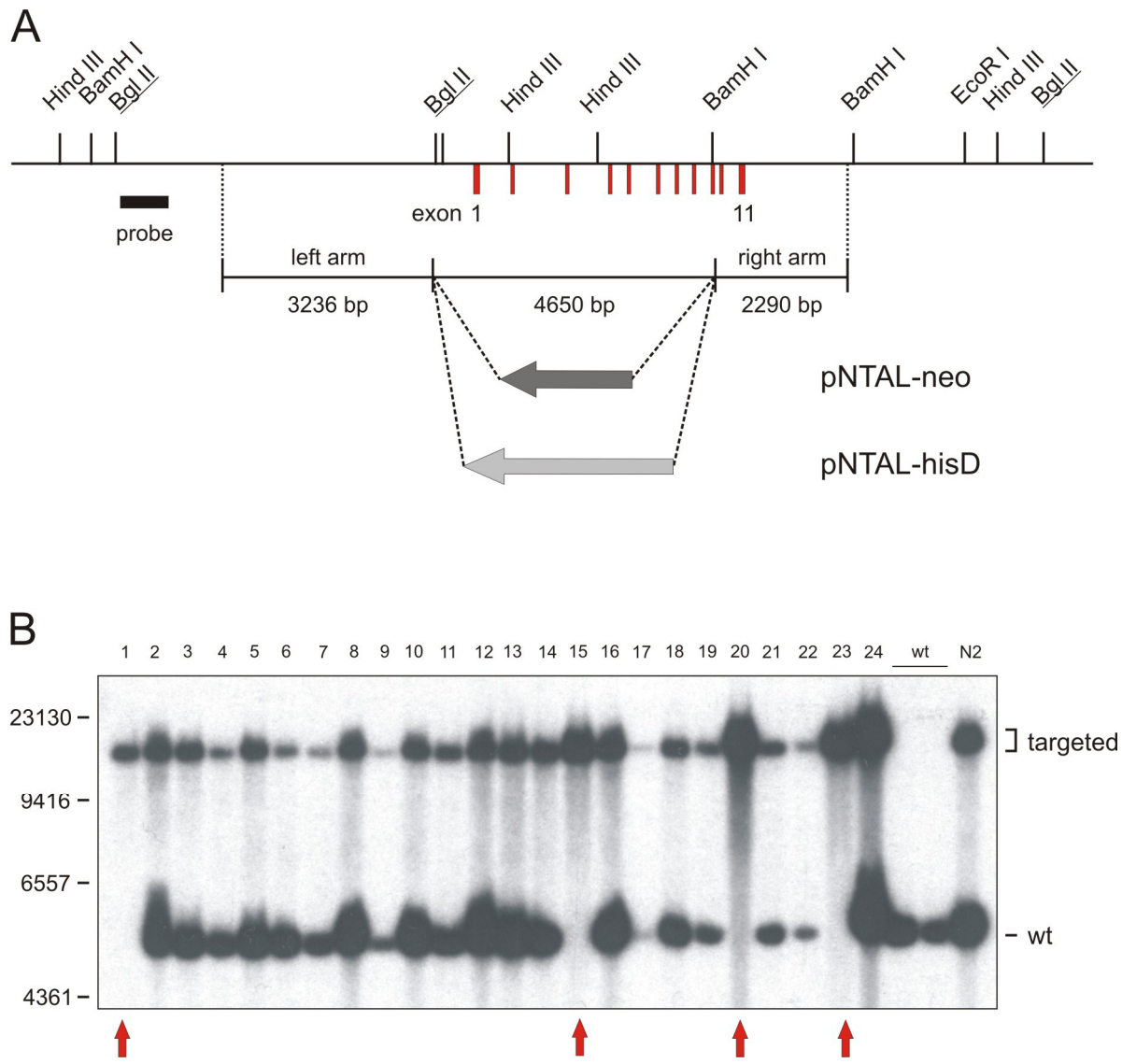

Figure 5.10: Generation of *ntal*$^{-/-}$ DT40 B lymphocytes
(A) Schematic representation of the chicken *ntal* genomic locus and targeting strategy. The targeting vectors pNTAL-neo and pNTAL-hisD were constructed by replacing the genomic fragment (4650 bp) containing exons corresponding to chicken NTAL amino acids 1-142 with neo, or hisD cassettes. The cassettes were flanked by 3236 bp and 2290 bp of genomic sequence on the 5' and 3' sides, respectively. The transcriptional direction of the resistance cassettes is opposite relative to *ntal*. Restriction endonuclease cleavage sites are denoted above the gene. Red boxes, *ntal* coding exons; black rectangle, probe for Southern blot analysis shown in (B). (B) Homologous recombination of pNTAL-neo and pNTAL-hisD at the *ntal* locus of DT40 B lymphocytes was determined by Southern blot analysis. The pNTAL-hisD was introduced into the neo-targeted clone N2 to obtain an NTAL deficient cell line. Genomic DNA from 24 selected clones was digested with *Bgl*II and probed using an 841 bp fragment located 5' to the targeted region. *Bgl*II-digested DNA derived from wild-type DT40 cells and the parental clone N2 served as controls. *Ntal*$^{-/-}$ clones N2-1, N2-15, N2-20, and N2-23 are marked by red arrows. DNA size markers (bp) are indicated on the left.

5.1.9. NTAL is a positive regulator of BCR-induced Ca^{2+} mobilization

To examine whether NTAL can counter act Grb2 in mature B lymphocytes, the direct impact of NTAL expression on the BCR-induced Ca^{2+} mobilization in DT40 B lymphocytes

was monitored. Like wild-type DT40 cells (figure 5.11, green line), the *ntal*$^{-/-}$ DT40 clone N2-1 retrovirally infected with an empty vector lacks Ca^{2+} influx from extracellular sources (blue line). In marked contrast, *ntal*$^{-/-}$ DT40 cells that express wild-type chicken NTAL following retroviral gene transfer (see figure 5.12A) display a prolonged intracellular Ca^{2+} release as well as significant extracellular Ca^{2+} entry (red line). Hence, the Ca^{2+} mobilization profile of NTAL-positive DT40 cells resembles the signal in Grb2-negative DT40 cells. Taken together, NTAL plays a positive regulatory role in BCR-induced Ca^{2+} mobilization.

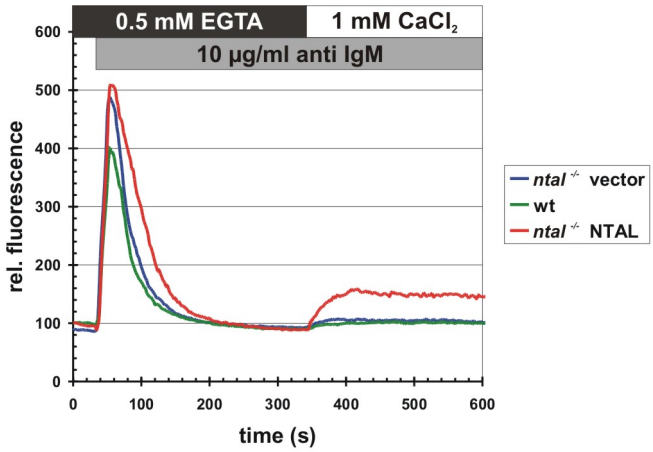

Figure 5.11: NTAL positively regulates BCR-induced Ca^{2+} mobilization
Intra- and extracellular Ca^{2+} mobilization was recorded by flow cytometry (described in figure 5.3 legend) in wild-type DT40 cells (green line) and *ntal*$^{-/-}$ mutants that were retrovirally infected with either empty pMSCVpuro vector (blue line) or pMSCVpuro containing chicken *ntal* cDNA (red line). Data represent the results obtained from 14 measurements of two independent retroviral infections.

5.1.10. The positive effect of NTAL on Ca^{2+} mobilization depends both on cysteine-containing palmitoylation motifs and tyrosine-based Grb2 binding sites

The positive regulatory role of NTAL on Ca^{2+} mobilization was further analysed in DT40 cells expressing NTAL mutants in which the amino acids responsible for raft localization or Grb2 binding were substituted. Alanine substitution of two cysteine residues within the NTAL palmitoylation motif (NTAL[C23/26A]) abrogates localization of the protein in lipid rafts (data not shown). Plasma membrane localization of this non-raft NTAL variant was confirmed by confocal laser scanning microscopy (data not shown). Equivalent expression of NTAL and NTAL derivatives in the different transfectants was controlled by anti-HA immunoblotting, respectively (figure 5.12A). Ca^{2+} mobilization analysis of *ntal*$^{-/-}$ DT40 cells reconstituted with NTAL[C23/26A] demonstrates that there is no extracellular Ca^{2+} influx (figure 5.12B). The same observation was made for NTAL mutants in which the four consensus Grb2 binding sites were inactivated by tyrosine-to-phenylalanine substitutions (figure 5.12B, NTAL[4Y4F]). Single Y-to-F substitutions rendering distinct Grb2 binding sites nonfunctional reveal that the membrane-proximal binding site (Y^{95}) is dispensable for

the positive effect of NTAL on Ca^{2+} mobilization (figure 5.12B, NTAL[Y95F]). In contrast, the three membrane-distal Grb2 binding sites (Y^{136}, Y^{155}, and Y^{184}) mediate elevated Ca^{2+} entry from extracellular sources (figure 5.12B, NTAL[Y136F], NTAL[Y155F], and NTAL[Y184F]). The closely related LAT molecule is capable of substituting NTAL function for Ca^{2+} mobilization in DT40 cells. This could be shown in *ntal*$^{-/-}$ DT40 cells expressing human LAT (figure 5.12B, LAT). Similar results were also obtained in *ntal*$^{-/-}$ DT40 cells expressing a LAT mutant lacking the PLC-γ binding site (figure 5.12B, LAT[Y132F]). The above results strongly suggest that raft-targeted NTAL positively regulates Ca^{2+} mobilization in B lymphocytes by means of its three membrane distal Grb2-binding motifs.

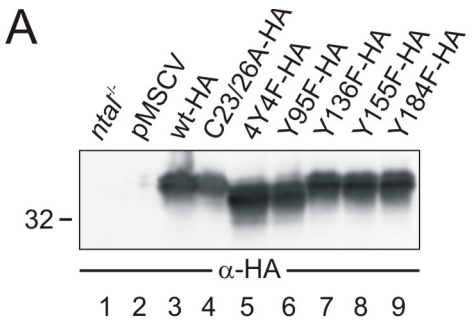

Figure 5.12: Effect of NTAL signalling motifs on the Ca^{2+} responses
(A) *Ntal*$^{-/-}$ clone N2-1 was transfected with either the empty pMSCVpuro vector or pMSCVpuro containing cDNA coding for either HA-tagged wild-type NTAL or NTAL variants containing the indicated C-to-A or Y-to-F amino acid substitutions. Expression of HA-tagged NTAL proteins was confirmed by anti-HA immunoblotting. (B) A summary of intra- and extracellular Ca^{2+} mobilization in *ntal*$^{-/-}$ N2-1 derivatives expressing HA-tagged NTAL proteins described in (A), wild-type human LAT, or a LAT Y-to-F mutant lacking the PLC-γ1 binding site (LAT[Y132F]). The control represents the Ca^{2+} response of empty pMSCVpuro vector control transfectants. Standard deviations were calculated for the maximal signal following restoration of extracellular Ca^{2+} (n = 4-17).

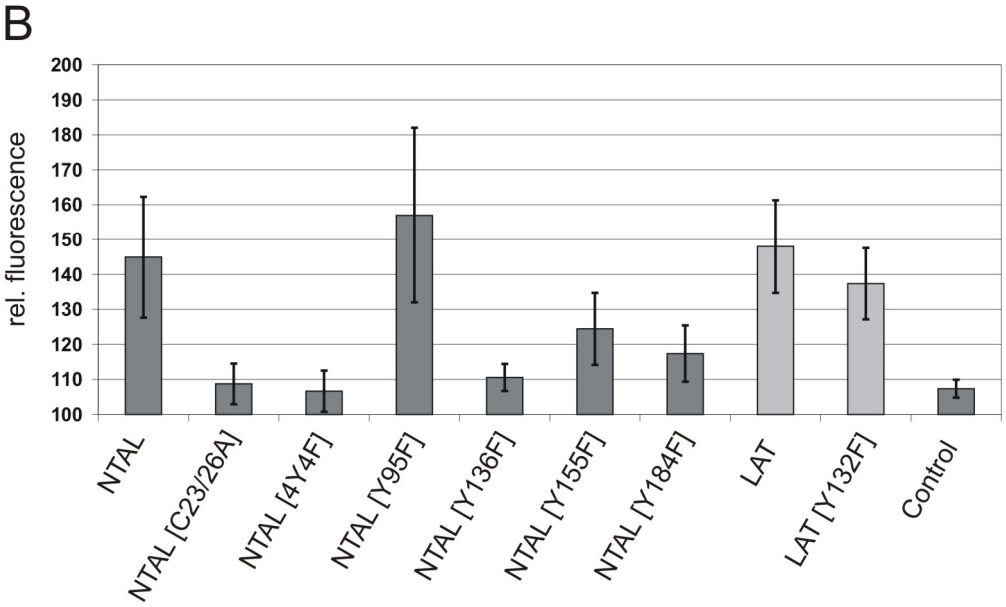

5.1.11. NTAL exerts its positive regulatory role on Ca^{2+} flux via phosphorylation-dependent Grb2 binding

The fact that the YxN motifs in NTAL are essential for Ca^{2+} regulation suggests a Grb2-dependent regulatory mechanism. To further analyse the role of NTAL/Grb2 interaction for the regulation of the Ca^{2+} response, single tyrosine residues were reintroduced into the NTAL[4Y4F] mutant. Phosphorylation of the four add-back mutants was analysed by anti-pTyr immunoblotting. In parallel the phosphorylation of wild-type NTAL, non-raft NTAL[C23/26A], NTAL[4Y4F], and human LAT was examined. Both wild-type NTAL and LAT are readily tyrosine phosphorylated upon BCR stimulation (figure 5.13A, lanes 2 and 18). However, tyrosine phosphorylation is not detectable for the non-raft mutant NTAL[C23/26] and the variant lacking the Grb2 binding sites (NTAL[4Y4F]) (lanes 5-8). Similarly, and in accordance with its less important role for NTAL-mediated Ca^{2+} elevation, tyrosine phosphorylation at the single Grb2 binding site Y^{95} is not observed (lanes 9 and 10). In marked contrast, tyrosine phosphorylation is readily detectable on the single add-back mutants Y^{136}, Y^{155}, and Y^{184}, which is consistent with their prominent role for Ca^{2+} mobilization (lanes 11-16).

Co-immunoprecipitation experiments were carried out in order to further assess the correlation between the tyrosine-phosphorylated Grb2 binding sites and the Grb2 SH2 domain. As shown above (figure 5.9C), wild-type Grb2 associates with NTAL in a stimulation-dependent manner (figure 5.13B, lanes 1 and 2). In contrast, wild-type Grb2 cannot be recruited by the phosphorylation-deficient NTAL mutants 4Y4F or C23/25A (figure 5.13B, lanes 3-6). Conversely, a Grb2 mutant with defective SH2 domain (Grb2[R86K]) does not bind to HA-tagged NTAL (lanes 9 and 10).

Taken together these observations clearly identify raft-localized NTAL and Grb2 as a stimulation-dependent regulatory module for Ca^{2+} mobilization in B lymphocytes. This function appears to be accomplished by SH2-mediated recruitment of Grb2 to tyrosine-phosphorylated NTAL, simultaneously preventing Grb2 from exerting its inhibitory effect on Ca^{2+} elevation.

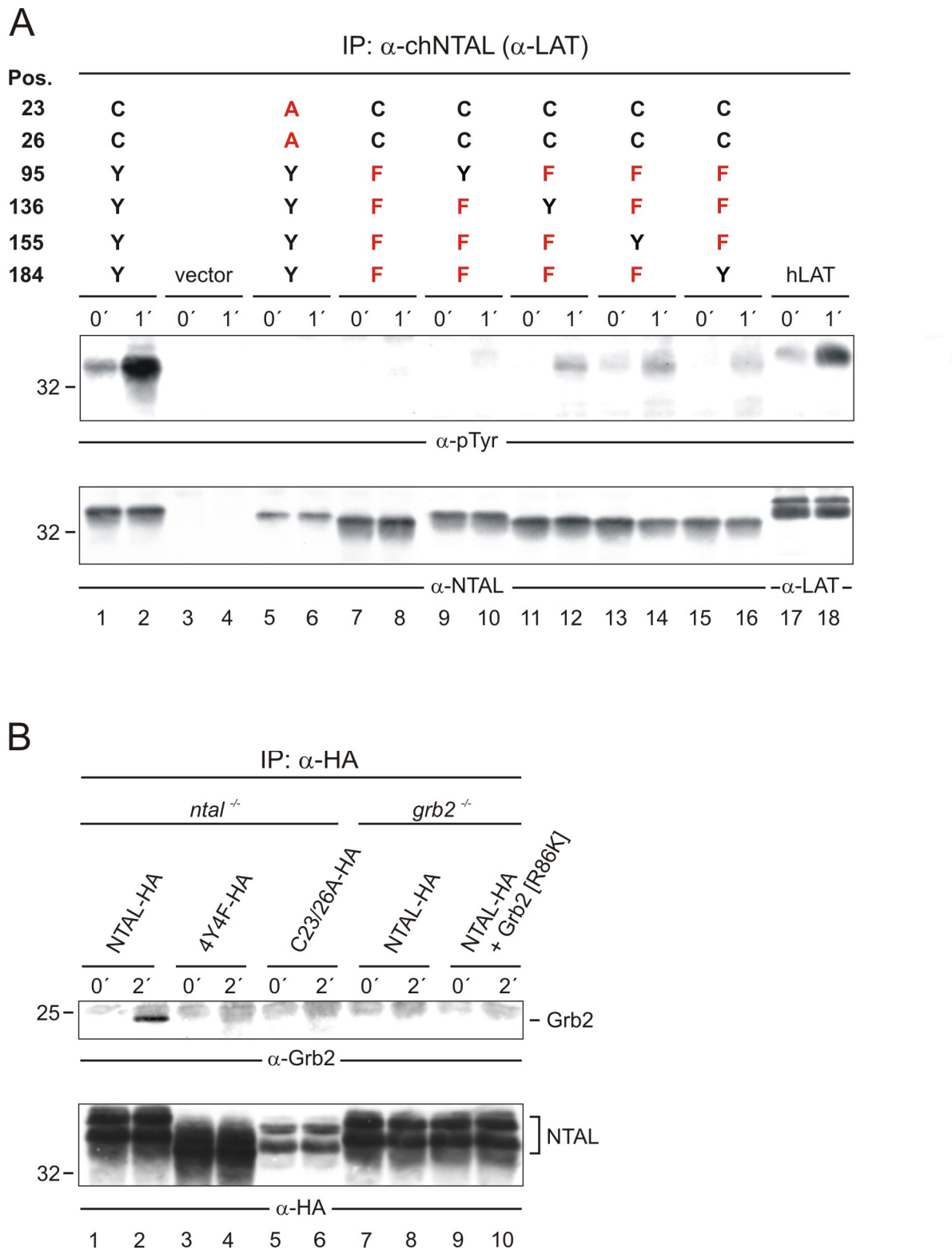

Figure 5.13: Tyrosine phosphorylation and Grb2 binding analysis of avian NTAL
(A) Unstimulated (0') or BCR-stimulated (1') *ntal*$^{-/-}$ DT40 (clone N2-1) transfectants expressing wild-type NTAL (lanes 1-2), no NTAL (empty pMSCVpuro vector transfectants, lanes 3-4), NTAL mutants as indicated (lanes 5-16), or wild-type human LAT (lanes 17-18) were subjected to immunoprecipitation experiments with anti-chicken NTAL (lanes 1-16) or anti-LAT (lanes 17-18) antibodies. The isolated proteins were analysed by immunoblotting with antibodies to phosphotyrosine (upper panel) or NTAL and LAT (lower panel). **(continued on next page)**

(legend to figure 5.13 continued) NTAL variants lack either a functional lipid raft targeting signal (C-to-A substitutions at positions 23 and 26, lanes 5-6) or one of the four Grb2 binding motifs (Y-to-F substitutions at positions 95, 136, 155, or 184, lanes 7-16). The amino acid positions refer to chicken NTAL protein sequence and are indicated on the left. (B) Anti-HA immunoprecipitates derived from unstimulated (0') or BCR-stimulated (2') *ntal*$^{-/-}$ (lanes 1-6) and *grb2*$^{-/-}$ (lanes 7-10) DT40 mutant cells that upon retroviral infection express HA-tagged versions of either wild-type NTAL (lanes 1-2 and lanes 7-8), 4Y4F NTAL (lanes 3-4), C23/26A NTAL (lanes 5-6), or wild-type NTAL plus SH2-domain-defective Grb2[R86K] (lanes 9-10) were analysed by immunoblotting with anti-Grb2 antibodies (upper panel). The faint background band visible in all lanes that nearly co-migrates with Grb2 emanates from the light chains of the precipitating antibodies. Equivalent NTAL protein recovery was confirmed by anti-HA immunoblot analysis (lower panel). Molecular mass protein standards (kDa) are indicted on the left (A-B), and data represent the results of three independent experiments.

5.1.12. Lipid raft targeting of Grb2 is sufficient for the inactivation of its negative regulatory role on Ca^{2+} mobilization

A transmembrane Grb2 fusion protein was generated to further investigate the model suggesting that NTAL/Grb2-mediated regulation of Ca^{2+} flux in B lymphocytes is dependent on subcellular re-localization of Grb2. By SOE-PCR using the oligonucleotides NTALfor, bridge2for, bridge2rev, and Grb2rev the cDNA fragment encoding the first 94 amino acids of chicken NTAL was added to the 5' end of the full length chicken *grb2* cDNA (see Materials and Methods, section 4.2.1.16.). By this method Grb2 was N-terminally equipped with the transmembrane region and the cyteine-containing palmitoylation motif (TM-Grb2). The fusion protein was expressed in *grb2*$^{-/-}$ DT40 cells in the absence of NTAL and was detected as a protein doublet of 35 and 36 kDa, respectively (figure 5.14A, lane 3). Multiple protein bands are typical for lipid raft residents such as NTAL (e.g. figures 5.9, 5.12, and 5.13) and LAT (ZHANG et al., 1998a). The chimeric TM-Grb2 is permanently targeted to lipid rafts as opposed to Grb2 which is isolated in the cytosolic fraction (figure 5.14B, upper and lower panel, compare figure 5.9A). The biochemical functionality of the fusion protein was confirmed by co-immunoprecipitation experiments performed by S. Laing. TM-Grb2 could be co-purified with endogenously expressed c-Cbl, and it also bound to a SLP-65-derived peptide encompassing the Grb2 binding site indicating that at least the C-terminal SH3 domain of the fusion protein is properly folded and functional (data not shown). However, the BCR-induced Ca^{2+} mobilization in TM-Grb2 transfectants is similar to the one observed for *grb2*$^{-/-}$ DT40 cells (figure 5.14C, orange and black line) indicating that unlike cytosolic wild-type Grb2 TM-Grb2 cannot suppress Ca^{2+} elevation (grey line). These experiments demonstrate that lipid raft localization is sufficient to prevent Grb2 from exerting its inhibitory function.

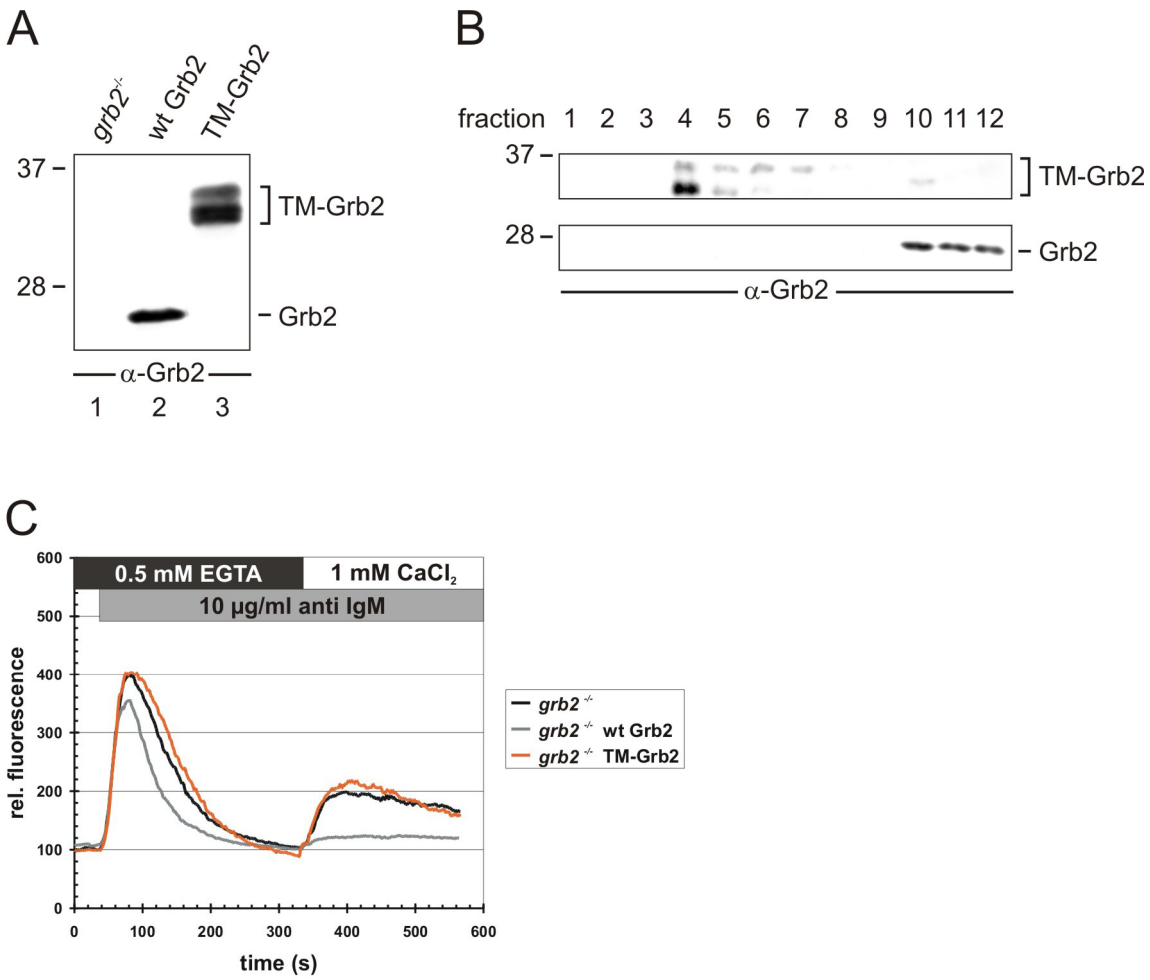

Figure 5.14: Lipid raft targeting of Grb2 inactivates its negative regulatory role on Ca^{2+} mobilization
(A-B) Grb2 protein expression and its subcellular localization were analysed, respectively by anti-Grb2 immunoblotting of (A) total cellular lysates and (B) isolated sucrose gradient fractions (JOHMURA et al., 2003) obtained from *grb2*$^{-/-}$ DT40 cells and transfectants reconstituted with either wild-type Grb2 or a Grb2 fusion protein constitutively targeted to lipid rafts (TM-Grb2). In TM-Grb2, the first 94 N-terminal amino acids of NTAL including the NTAL transmembrane region and the palmitoylation motif are fused to full length chicken Grb2. Molecular mass protein standards (kDa) are indicated on the left. (C) BCR-induced Ca^{2+} mobilization of DT40 cells described in (A-B) was analysed by flow cytometry (refer to figure 5.3 legend for details). Data represent the results of four independent measurements.

5.1.13. The NTAL/Grb2 module influences plasma membrane recruitment of PLC-γ2

To further elucidate the molecular mechanism of Grb2 action, K. Neumann in our group demonstrated that increased Ca^{2+} elevation in NTAL-positive or Grb2-negative DT40 B lymphocytes can be attributed to an increased intracellular IP3 concentration (PhD thesis in progress, unpublished results). Possible explanations for this observation are an enhancement of PLC-γ2 activity and/or an altered translocation of the lipase to the plasma membrane where its substrate resides. To further investigate this issue, *plc-γ2*$^{-/-}$ DT40 cells (TAKATA et al., 1995) were transfected with cDNA encoding a transmembrane PLC-γ2

chimera (TM-PLC-γ2) consisting of the extracellular CD16 domain (amino acids 1-208; RAVETCH and PERUSSIA, 1989), transmembrane CD3ζ domain (amino acids 31-58; WEISSMAN et al., 1988), and cytosolic full length rat PLC-γ2 (1265 amino acids; EMORI et al., 1989) (ISHIAI et al., 1999b). PLC-γ2 protein expression was confirmed by anti-PLC-γ2 immunoblot analysis (data not shown). *Plc-γ2*$^{-/-}$ DT40 B cells expressing TM- PLC-γ2 show a comparatively higher Ca^{2+} influx across the plasma membrane (figure 5.15, right panel). Interestingly, NTAL expression does not enhance Ca^{2+} mobilization in these cells upon the unique engagement of the BCR (figure 5.15), nor BCR/CD16 co-crosslinking (data not shown). In marked contrast, NTAL expression in cells reconstituted with cDNA encoding the wild-type cytosolic PLC-γ2 led to a slightly prolonged intracellular Ca^{2+} release, and a significantly elevated Ca^{2+} flux across the plasma membrane (figure 5.15, left panel). This set of experiments was conducted in collaboration with S. Alers and are part of his diploma thesis.

Collectively, during the work for this thesis a novel Ca^{2+}-regulating signalling pathway in B lymphocytes could be identified and characterized. This regulatory module is composed of the adaptor proteins NTAL and Grb2. It seems that the NTAL/Grb2 module influences the membrane localization of PLC-γ2 or its retention time at the membrane. This function is abolished in DT40 B lymphocytes expressing a PLC-γ2 chimeric protein that is constitutively associated with the plasma membrane.

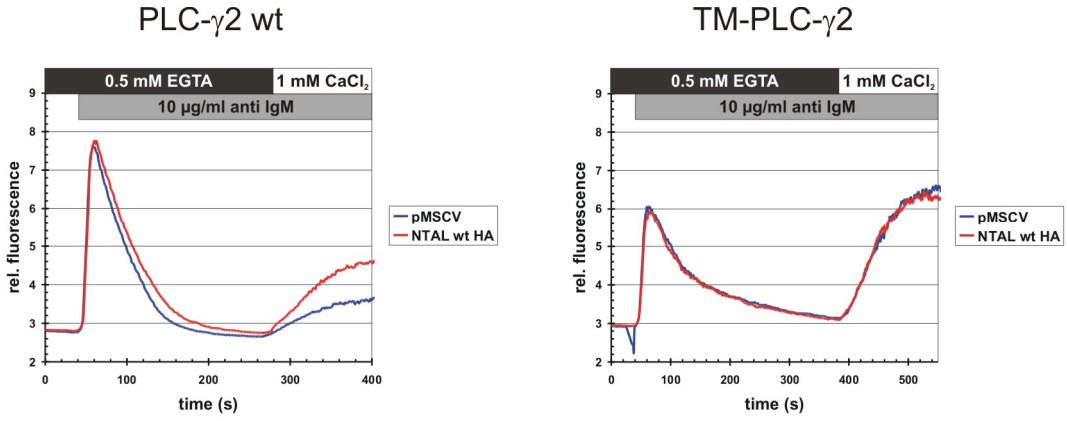

Figure 5.15: The NTAL/Grb2 module influences plasma membrane recruitment of PLC-γ2
Plc-γ2$^{-/-}$ DT40 cells were reconstituted with either wild-type rat PLC-γ2 (left panel), or the transmembrane PLC-γ2 chimera (TM-PLC-γ2, right panel) consisting of the extracellular CD16 domain (amino acids 1-208), transmembrane CD3ζ domain (amino acids 31-58) and cytosolic full length rat PLC-γ2 (1265 amino acids) (ISHIAI et al., 1999b). Intra- and extracellular Ca^{2+} mobilization was recorded by flow cytometry (refer to figure 5.3 legend for description) in these reconstituents that were retrovirally infected with either empty pMSCVpuro vector (blue line) or pMSCVpuro containing chicken *ntal* cDNA (red line).

5.2. Grb2 regulates tyrosine phosphorylation of p50/Dok-3

As shown in the first part of this thesis, the cytosolic adaptor molecule Grb2 acts as a central component of B cell signalling pathways. The *grb2*$^{-/-}$ DT40 B cell line represents an ideal tool to further elucidate the role of Grb2 in BCR signalling in general and to analyse the mechanism(s) underlying its negative regulatory function for Ca^{2+} mobilization in particular. As described above, a complex network of tyrosine phosphorylation and dephosphorylation catalyzed by specific kinases and phosphatases precedes the elevation of the intracellular Ca^{2+} concentration. Therefore, the second aim of this thesis was to analyse the role of Grb2 in BCR-induced tyrosine phosphorylation processes and how its involvement might contribute to the observed regulation of Ca^{2+} mobilization.

5.2.1. Tyrosine phosphorylation of p50 is dependent on Grb2 in DT40 B lymphocytes

Stimulation of the B cell antigen receptor initiates a biochemical cascade in which PTK acitivity is one of the earliest known events (WIENANDS, 2000b). Numerous cellular proteins become tyrosine phosphorlyated upon BCR engagement, many of which have yet to be chararacterized at the molecular level.

During the analysis of SLP-65 tyrosine phosphorylation upon BCR stimulation in wild-type and *grb2*$^{-/-}$ DT40 cells (see figure 5.6), the precipitating anti-SLP-65 antibodies cross-reacted with a tyrosine phosphorylated protein with a molecular weight of approximately 50 kDa (p50) (figure 5.16A, lower left panel, lane 2). Interestingly, tyrosine phosphorylation of p50 is only detectable in wild-type DT40 cells, indicating that this modification is dependent on Grb2 (lanes 2 and 4). The differences in the phosphorylation state of p50 between wild-type and *grb2*$^{-/-}$ DT40 cells were also demonstrated by immunoprecipitation experiments with anti-pTyr antibodies (figure 5.16A, lower right panel, lanes 6 and 8). Detection of phospho-SLP-65 served in each case as a loading control (upper panels). To further verify whether the absence of p50 tyrosine phosphorylation is solely due to the lack of Grb2, wild-type *grb2* cDNA was re-introduced into *grb2*$^{-/-}$ DT40 cells by retroviral gene transfer (compare figures 5.3 and 5.4). Indeed, reconstitution of wild-type Grb2 expression recapitulated tyrosine phosphorylation of p50 (figure 5.16B, lower panel, lane 10). Furthermore, p50 could also be purified from cleared cellular lysates of BCR-stimulated *slp-65*$^{-/-}$ DT40 cells (lane 6), demonstrating that the purification of p50 is due to the cross-reactivity of the anti-SLP-65 antibodies rather than a direct association with SLP-65. In marked contrast, tyrosine phosphorylation of p50 was not detected in *lyn*$^{-/-}$ DT40 cells (lane 4). P50 is one of the major tyrosine-phosphorylated proteins in DT40 B lymphocytes after BCR engagement, since it is prominently detected in cleared cellular lysates by anti-pTyr immunoblotting (figure 5.16C, lane 2). To summarize, p50 is a major substrate for

tyrosine kinases in DT40 B lymphocytes after BCR engagement, and tyrosine phosphorylation is dependent on the presence of the cytosolic adaptor molecule Grb2.

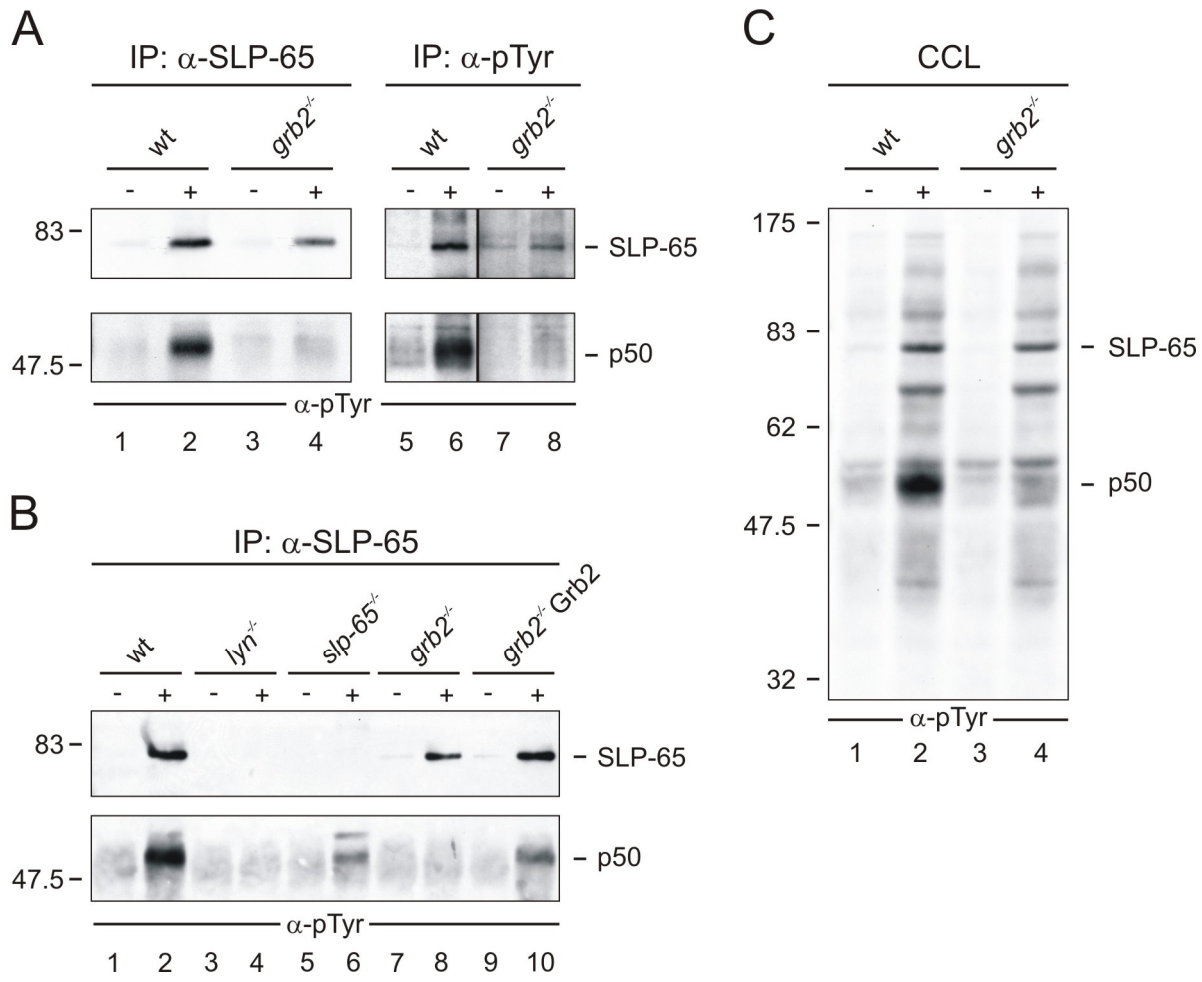

Figure 5.16: Grb2 regulates tyrosine phosphorylation of p50 in DT40 B cells
(A) Anti-chicken SLP-65 (left panels, lanes 1-4) and anti-pTyr immunoprecipitates (right panels, lanes 5-8) derived from unstimulated (-) or BCR-stimulated (+) wild-type (lanes 1-2 and lanes 5-6) and *grb2*$^{-/-}$ DT40 cells (lanes 3-4 and lanes 7-8) were analysed by anti-pTyr immunoblotting (lower panels). Equivalent protein recovery was confirmed by anti-SLP-65 immunoblot analysis (upper panels). Purification of p50 by anti-chicken SLP-65 antibodies is due to cross-reactivity. (B) Anti-chicken SLP-65 immunoprecipitates prepared from unstimulated (-) or BCR-stimulated (+) wild-type (lanes 1-2), *lyn*$^{-/-}$ (lanes 3-4), *slp-65*$^{-/-}$ (lanes 5-6), *grb2*$^{-/-}$ (lanes 7-8), and *grb2*$^{-/-}$ DT40 cells reconstituted with wild-type Grb2 (lanes 9-10) were analysed by anti-pTyr immunoblotting (lower panel). As a control for equal protein recovery anti-SLP-65 immunoblot analysis was performed (upper panel). (C) Cleared cellular lysates (CCLs) obtained from unstimulated (-) or BCR-stimulated (+) wild-type (lanes 1-2) and *grb2*$^{-/-}$ DT40 cells (lanes 3-4) were analysed by anti-pTyr immunoblotting. Molecular mass protein standards (kDa) are indicated on the left (A-C), and data represent the results of at least three independent experiments.

5.2.2. p50 is a cytosolic protein

The next aim was to further characterize p50 regarding its subcellular localization. Since the eukaryotic cell is a multicompartmental structure, it has to be ensured that newly synthesized proteins reach their ultimate destination. Protein targeting is achieved by a sophisticated system of labelling and sorting. N-glycosylation is one of the cotranslational modifications that distinguishes for proteins destined for cellular membranes, lysosomes, or secretion, and following glycosylation initiation in the lumen of the rough ER it proceeds throughout the smooth ER and various cisternae of the Golgi apparatus. To investigate whether N-linked oligosaccharides are attached to p50, cleared cellular lysates from *grb2*$^{-/-}$ and wild-type DT40 cells were treated with Peptide:N-glycosidase F (PNGase F) prior to immunoprecipitation with anti-SLP-65 antibodies. It appears that p50 does not aquire N-glycans since its mobility observed by SDS-PAGE is not altered by PNGase F treatment (figure 5.17A, lanes 5 and 6). Therefore, this suggests that p50 is neither a secreted nor an integral membrane protein. Detection of p50 was carried out by anti-pTyr immunoblotting. The subcellular localization of p50 was alternatively analysed by anti-pTyr immunoblot analysis of cytosolic, membrane-associated and membrane protein fractions subjected to immunoprecipitation experiments with anti-SLP-65 antibodies (figure 5.17B, lower panels). Detection of phospho-SLP-65 served as control for the enrichment of the cytosolic fraction (upper panels). P50 is prominently detected in the cytosolic protein fraction (lane 4). Taken together, these experiments indicate that p50 is likely to be a cytosolic protein.

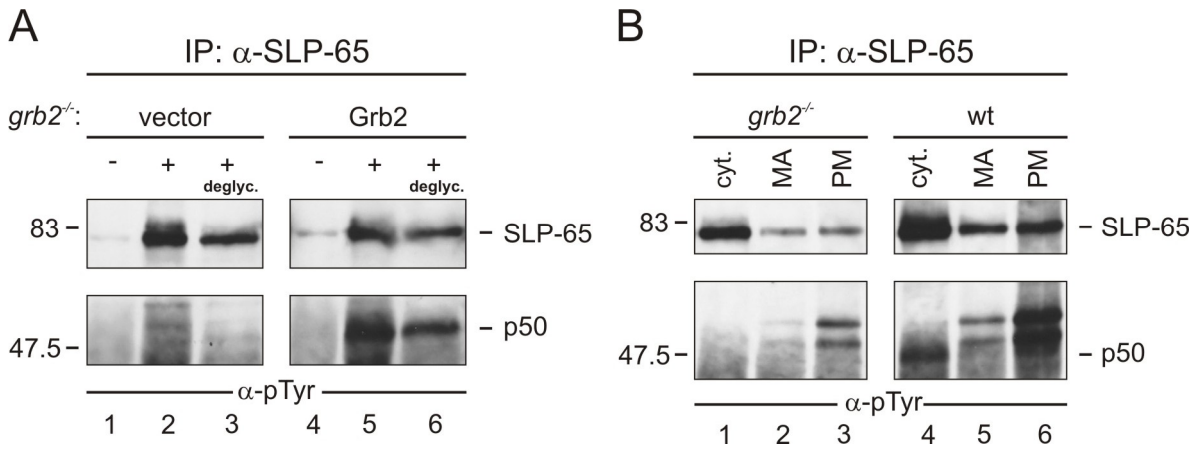

Figure 5.17 (legend see next page)

Figure 5.17: p50 is mainly localized in the cytosolic compartment
(A) Anti-chicken SLP-65 immunoprecipitates were prepared from unstimulated (-) or BCR-stimulated (+) *grb2*$^{-/-}$ DT40 cells transfected with either empty pMSCVpuro vector (left panels, lanes 1-3) or pMSCVpuro containing cDNA coding for wild-type Grb2 (right panels, lanes 4-6). N-linked oligosaccharides were removed from proteins in cleared cellular lysates from BCR-stimulated cells by treatment with Peptide:N-glycosidase F (PNGase F) prior to immunoprecipitation (lanes 3, 6). Immunoblot analysis was carried out with anti-pTyr (lower panels) and anti-SLP-65 antibodies (upper panels). (B) Cytosolic, membrane-associated and membrane protein fractions derived from BCR-stimulated *grb2*$^{-/-}$ (left panels, lanes 1-3), and wild-type DT40 cells (right panels, lanes 4-6) (as described in Material and Methods section 4.2.3.4.) were subjected to immunoprecipitation experiments with anti-SLP-65 antibodies, and analysed by anti-pTyr immunoblotting (lower panels). Detection of phospho-SLP-65 served as control for enrichment of the cytosolic fraction (upper panel). Molecular mass protein standards (kDa) are indicated on the left (A-B).

5.2.3. Tyrosine phosphorylation of p50 depends on both the Grb2 SH2 domain and the C-terminal SH3 domain

To further dissect the function of Grb2 in the regulation of p50 tyrosine phosphorylation, the importance of the three distinct Grb2 domains was analysed. The above described nonfunctional Grb2 mutants (see section 5.1.3) were tested for their capacity to support p50 tyrosine phosphorylation. Cleared cellular lysates from BCR-stimulated wild-type DT40 cells, *grb2*$^{-/-}$ DT40 cells, and derivatives reconstituted with either wild-type Grb2 or a nonfunctional variant were analysed by anti-pTyr immunoblotting (figure 5.18, lower panel). Detection of phospho-SLP-65 served as a loading control (upper panel). It appears that the N-terminal SH3 domain of Grb2 exhibits no influence on the phosphorylation state of p50 (lane 8). In marked contrast, the central SH2 domain and the C-terminal SH3 domain are mandatory for a maximal tyrosine phosphorylation of p50 (lower panel, lanes 10 and 12). A similar result indicating the importance of the three Grb2 interaction domains was obtained by purification of p50 with antibodies to SLP-65 (data not shown).

These results reveal that maximal tyrosine phosphorylation of p50 depends on both the central SH2 and the C-terminal SH3 domain of Grb2. It is noteworthy that both of these Grb2 domains are also responsible for the inhibitory effect of Grb2 on Ca^{2+} mobilization (see figure 5.4).

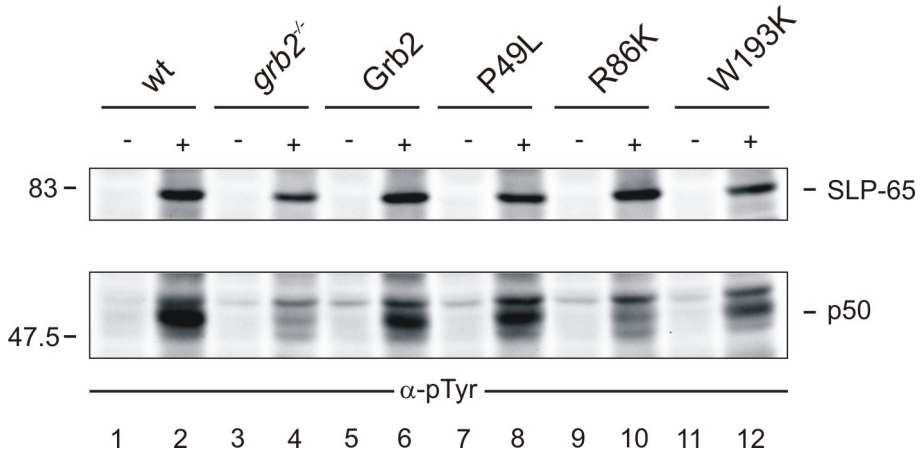

Figure 5.18: Tyrosine phosphorylation of p50 depends on both the Grb2 SH2 domain and the C-terminal SH3 domain
Cleared cellular lysates derived from unstimulated (-) or BCR-stimulated (+) wild-type DT40 cells (lanes 1-2), *grb2*$^{-/-}$ mutants (lanes 3-4) and derivatives that upon retroviral gene transfer express either wild-type Grb2 (lanes 5-6) or variants with a non-functional N-terminal SH3, central SH2, or C-terminal SH3 domain (lanes 7-12, refer to figure 5.4 legend) were subjected to anti-pTyr immunoblot analysis (lower panel). Equivalent protein loading was controlled by anti-SLP-65 immunoblotting (upper panel). Molecular mass protein standards (kDa) are indicated on the left. These results were confirmed by anti-pTyr immunoblot analysis of anti-SLP-65 precipitates obtained from cells described above (data not shown).

5.2.4. Tyrosine-phosphorylated p50 associates with the SH2 domain of Grb2

The next question was whether one of the two Grb2 domains directly associates with p50. Therefore, cleared cellular lysates from *grb2*$^{-/-}$ and reconstituted DT40 cells were subjected to affinity purification experiments with GST fusion proteins containing either the central SH2 domain or the C-terminal SH3 domain of Grb2. Subsequent anti-pTyr immunoblot analysis indeed revealed that p50 directly associates with the Grb2 SH2 domain (figure 5.19, lanes 7 and 15). Relatively lower levels of tyrosine-phosphorylated p50 were also purified from *grb2*$^{-/-}$ DT40 B lymphocytes by this method (lane 7).

These affinity purification experiments indicate that tyrosine phosphorylated p50 directly associates with the Grb2 SH2 domain. This observation strongly suggests the existence of at least one YxN phosphoacceptor site within the amino acid sequence of p50 (refer to section 5.1.6.). The direct interaction of the Grb2[SH2] domain with p50 must be emphasized since this domain is also required for p50 tyrosine phosphorylation (see section 5.2.3).

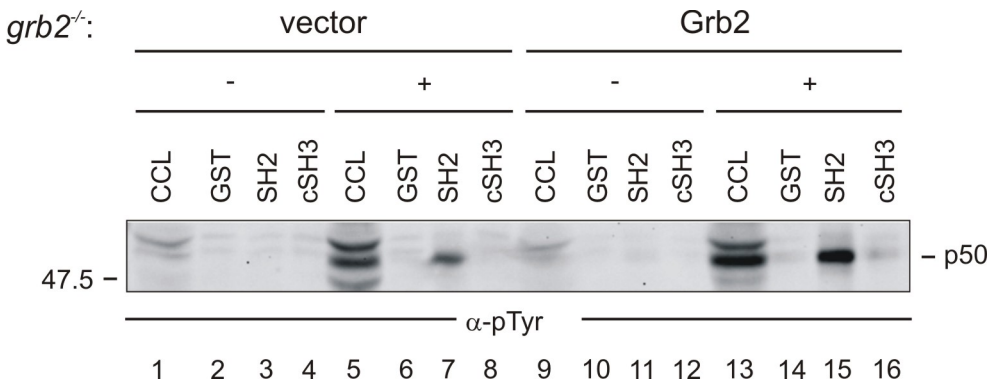

Figure 5.19: Tyrosine phosphorylated p50 associates with the central Grb2 SH2 domain
Cleared cellular lysates (CCL) prepared from unstimulated (-) or BCR-stimulated (+) *grb2*$^{-/-}$ DT40 mutant cells that were retrovirally infected with either empty pMSCVpuro vector (lanes 1-8) or pMSCVpuro containing wild-type chicken *grb2* cDNA (lanes 9-16) were subjected to affinity purification experiments with either GST (lanes 2, 6, 10, 14; GST) or GST fusion proteins containing the central SH2 (lanes 3, 7, 11, 15; SH2) or the C-terminal SH3 domain of murine Grb2 (lanes 4, 8, 12, 16; cSH3). Purified proteins were analysed by anti-pTyr immunoblotting. Molecular mass protein standards (kDa) are indicated on the left. Data represent the results of four independent affinity purification experiments.

5.2.5. PTK Lyn is mandatory for p50 tyrosine phosphorylation

PTK Lyn is expressed in two isoforms due to two alternative splicing variants, with molecular weights of 53 and 56 kDa in mice and humans (YI et al., 1991; YAMANASHI et al., 1989). Tyrosine phosphorylation of p50 does not occur in *lyn*$^{-/-}$ DT40 cells (figure 5.16C, lower panel). To exclude the possibility that the observed protein is Lyn itself, endogenous Lyn was purified from *grb2*$^{-/-}$ DT40 cells and derivatives expressing wild-type Grb2 with anti-Lyn antibodies (figure 5.20A, lanes 4-7). By immunoblot analysis with anti-pTyr antibodies it could be shown that the phospo-Lyn isoform doublet does not co-migrate with p50 purified from wild-type DT40 cells with anti-SLP-65 antibodies (lane 1). Furthermore, no differences in overall Lyn tyrosine phosphorylation are detectable in *grb2*$^{-/-}$ and reconstituted DT40 cells. Subsequently, *lyn*$^{-/-}$ DT40 cells were transfected with cDNA coding for murine Lyn with EGFP fused to its C terminus. This EGFP-tagged Lyn has a molecular weight of approximately 75 kDa (figure 5.20B, lane 2) and is located at the plasma membrane (figure 5.20C). Expression of the Lyn/EGFP fusion protein is capable of reconstituting tyrosine phosphorylation of p50 in *lyn*$^{-/-}$ cells (figure 5.20D, lane 6). Analysis of tyrosine phosphorylation in *syk*$^{-/-}$ and *btk*$^{-/-}$ DT40 B lymphocytes revealed that these two PTKs are dispensable for this process (data not shown). Taken together these observations clearly indicate that the Src kinase family member Lyn is obligatory for tyrosine phosphorylation of p50.

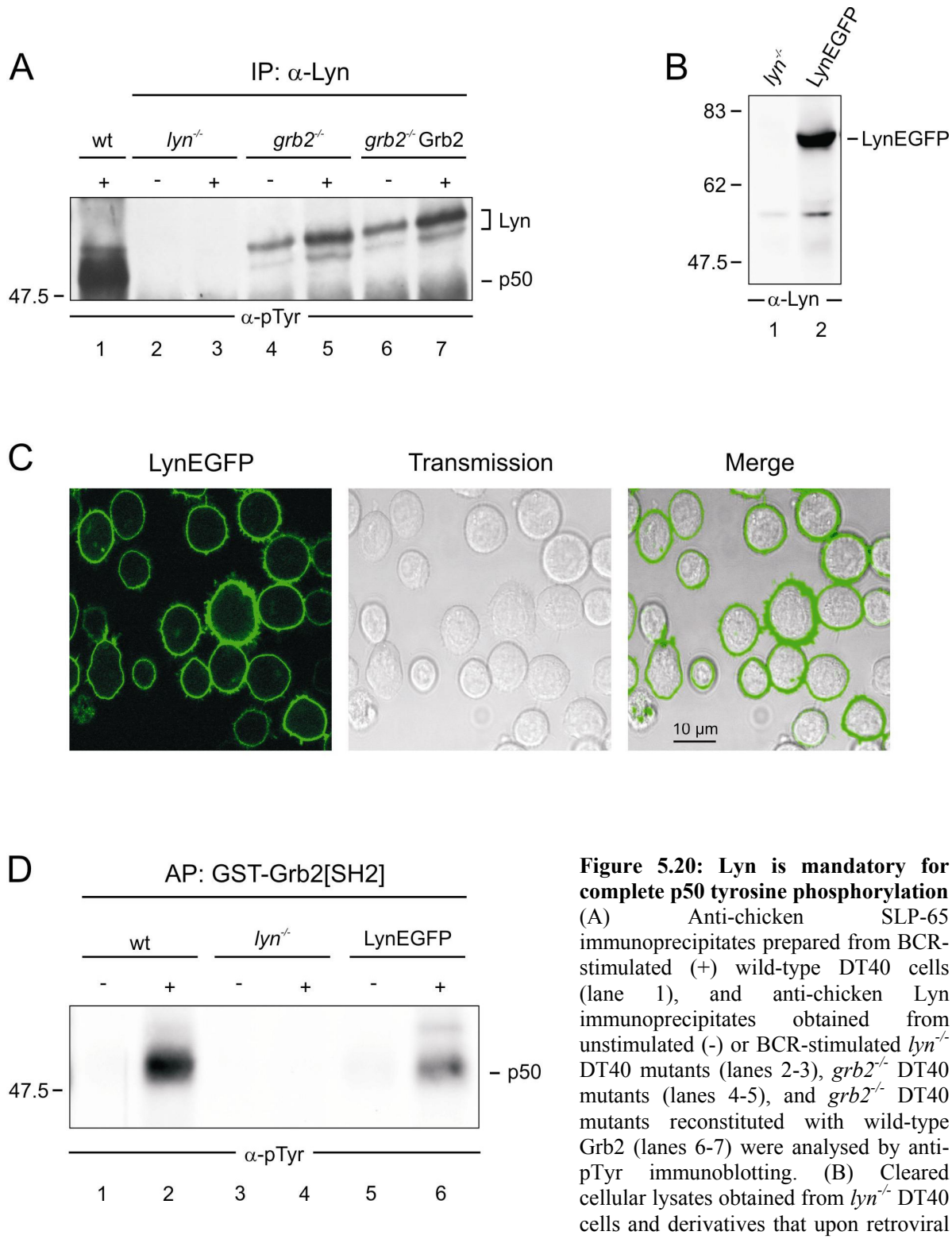

Figure 5.20: Lyn is mandatory for complete p50 tyrosine phosphorylation (A) Anti-chicken SLP-65 immunoprecipitates prepared from BCR-stimulated (+) wild-type DT40 cells (lane 1), and anti-chicken Lyn immunoprecipitates obtained from unstimulated (-) or BCR-stimulated *lyn*$^{-/-}$ DT40 mutants (lanes 2-3), *grb2*$^{-/-}$ DT40 mutants (lanes 4-5), and *grb2*$^{-/-}$ DT40 mutants reconstituted with wild-type Grb2 (lanes 6-7) were analysed by anti-pTyr immunoblotting. (B) Cleared cellular lysates obtained from *lyn*$^{-/-}$ DT40 cells and derivatives that upon retroviral gene transfer express C-terminally EGFP-tagged murine Lyn were subjected to anti-Lyn immunoblot analysis. (C) Expression of C-terminally EGFP-tagged murine Lyn in *lyn*$^{-/-}$ DT40 B lymphocytes was analysed by confocal laser scanning microscopy (kindly performed by I. Goldbeck). (D) Cleared cellular lysates prepared from unstimulated (-) or BCR-stimulated (+) wild-type DT40 cells (lanes 1-2), *lyn*$^{-/-}$ DT40 mutant cells (lanes 3-4) and derivatives that upon retroviral gene transfer express C-terminally EGFP-tagged murine Lyn (lanes 5-6) were subjected to affinity purification experiments with GST-Grb2[SH2] fusion proteins. Purified proteins were analysed by anti-pTyr immunoblotting. Molecular mass protein standards (kDa) are indicated on the left (A, B, D).

5.2.6. Kinetics of p50 phosphorylation

Following the identification of PTK Lyn as the kinase responsible for p50 tyrosine phosphorylation, the kinetics of this process were further analysed to determine whether the reduced tyrosine phosphorylation of p50 in *grb2*$^{-/-}$ DT40 cells is caused by either decreased phosphorylation, or increased dephosphorylation reactions. Therefore, wild-type and Grb2-deficient DT40 cells were stimulated with M4 antibodies for varying periods of time. P50 was purified by Grb2[SH2] affinity purification and tyrosine phosphorylation was analysed by anti-pTyr immunoblot analysis. It was shown that strong tyrosine phosphorylation of p50 is initiated after 30 s, lasting for 5-10 min (figure 5.21, upper panel, lanes 1-5). After 10 min p50 gradually becomes dephosphorylated (lanes 6-9). For *grb2*$^{-/-}$ DT40 cells, a clearly reduced tyrosine phosphorylation could be observed at all time points (figure 5.21, lower panel).

These results strongly suggest that the reduced p50 tyrosine phosphorylation in *grb2*$^{-/-}$ DT40 cells is due to a decreased phosphorylation rate in these cells and not caused by an increased and/or de-regulated dephosphorylation rate.

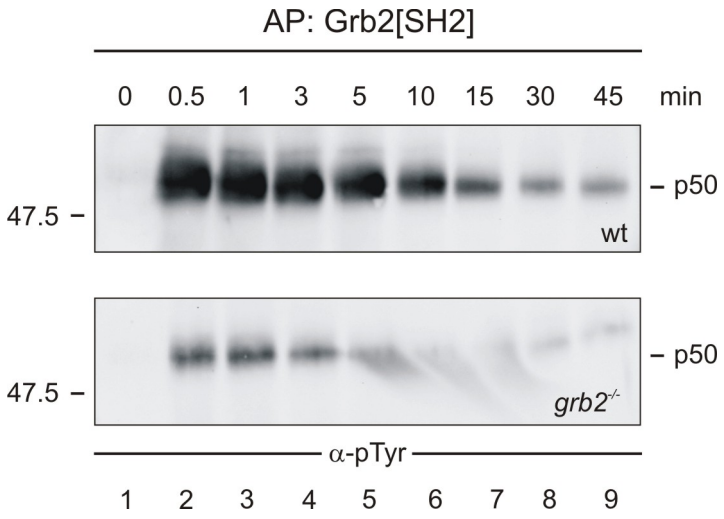

Figure 5.21: Kinetics of p50 tyrosine phosphorylation
Wild-type (upper panel) and *grb2*$^{-/-}$ DT40 cells (lower panel) were left untreated or stimulated through their BCR for the indicated times, lysed, and subjected to affinity purification with GST-mGrb2[SH2] fusion proteins. Purified proteins were analysed by anti-pTyr immunoblotting. Molecular mass protein standards (kDa) are indicated on the left. Data represents observations made in three independent experiments.

5.2.7. Identification of p50 by mass spectrometry and western blot analysis

The affinity purification with the GST-mGrb2[SH2] fusion protein was perfectly suitable for a large scale purification of p50 and subsequent analysis by mass spectrometry (kindly performed by Dr. T. Kähne, Institute of Experimental Internal Medicine, Otto-von-Guericke University, Magdeburg). P50 was purified from approximately 5 x 10^8 BCR-stimulated wild-type DT40 cells by GST-mGrb2[SH2] affinity purification. In parallel, p50 was purified from an identical number of unstimulated *grb2*$^{-/-}$ and wild-type DT40 cells as controls. The samples were separated by SDS-PAGE and purified proteins were visualized by silver staining (figure 5.22A, lanes 1-3). A prominent protein migrating at approximately 50 kDa was purified from the lysates of stimulated wild-type DT40 cells (lane 3, black arrow). Since lower levels of the protein were purified from unstimulated *grb2*$^{-/-}$ and wild-type DT40 cells (lanes 1 and 2, respectively) the association of this protein with the mGrb2[SH2] domain is stimulation-dependent. This observation is in accordance with the anti-pTyr immunoblotting data obtained for p50. The protein band was excised from the gel, and subsequently the samples were digested with trypsin. The resulting digest mixture was analysed by ESI-Ion Trap mass spectrometry including MS/MS analysis (Dr. T. Kähne, Magdeburg). An instrument with MS/MS capability can additionally provide structural information by monitoring the fragment ion spectrum of a peptide. The Mascot search engine (www.matrixscience.com) was searched with the fragment ion spectra of the obtained peptides, and the mass spectrometry data were matched to a partial chicken amino acid sequence (GenBank accession number: XP_427516). Subsequent database tblastx searches revealed that this protein is homologous to the mammalian Dok-3 adaptor protein. This adaptor belongs to the downstream of kinase (Dok) family, consisting so far of six members. Dok-3 was identified in 1999 (LEMAY et al., 2000) (Dok-L, CONG et al., 1999), and contains an N-terminal PH domain, followed by a PTB domain and a C-terminus with multiple phosphoacceptor sites. Since Dok-3 is a cytosolic adaptor protein, the identification of p50 as Dok-3 is in accordance with the data obtained for the subcellular localization of p50 (see section 5.2.2). Furthermore, Dok-3 also possess the above proposed YxN phosphoacceptor site (see section 5.2.4), which upon tyrosine phosphorylation is preferentially bound by the Grb2 SH2 domain.

To ultimately verify that p50 is chicken Dok-3, anti-Dok-3 immunoblot analysis was performed using antibodies to murine Dok-3 kindly provided by Dr. A. Veillette (Clinical Research Institute of Montréal, Canada). Unfortunately, these antibodies were not applicable for direct immunoblot detection of chicken Dok-3 (data not shown). Thus to determine if the antibodies recognize native chicken Dok-3, cleared cellular lysates from unstimulated and BCR-stimulated *grb2*$^{-/-}$ and wild-type DT40 cells were incubated with

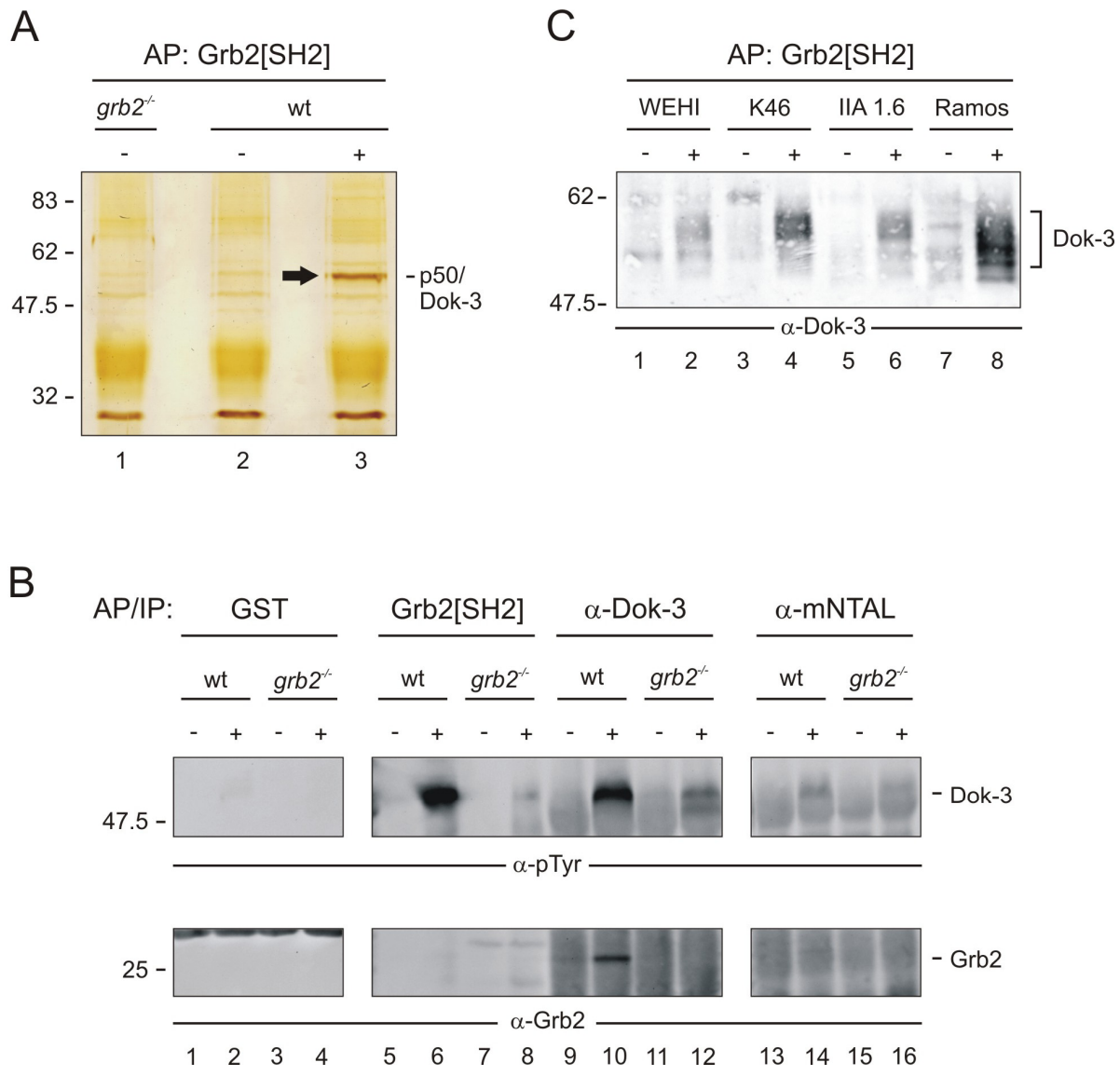

Figure 5.22: Identification of p50 by mass spectrometry and western blot analysis
(A) Approximately 5 x 10^8 *grb2*$^{-/-}$ (lane 1) and wild-type DT40 cells (lanes 2-3) were left untreated (-) or stimulated through their BCR (+), lysed, and subjected to affinity purifications with GST-mGrb2[SH2] fusion proteins. The samples were separated by SDS-PAGE and purified proteins were visualized by silver staining. A prominent protein migrating at approximately 50 kDa was purified from lysates of BCR-stimulated wild-type DT40 cells (lane 3, black arrow). Less of this protein was purified from unstimulated *grb2*$^{-/-}$ and wild-type DT40 cells (lanes 1 and 2). The protein band of interest was excised from the gel and subjected to mass spectrometric analysis (kindly performed by Dr. T. Kähne, Magdeburg). (B) Cleared cellular lysates prepared from unstimulated (-) or BCR-stimulated (+) wild-type DT40 cells and *grb2*$^{-/-}$ mutants were subjected to affinity purification experiments with GST-mGRB[SH2] fusion proteins (lanes 5-8), or rabbit-anti-Dok-3 antibodies (lanes 9-12). As control, purifications were performed with GST only (lanes 1-4) or non-relevant anti-mouse NTAL antibodies (lanes 13-16). Purified proteins were analyzed by immunoblotting with antibodies to pTyr (upper panels) or Grb2 (lower panels). (C) Cleared cellular lysates derived from unstimulated (-) or BCR-stimulated (+) murine WEHI-231 (lanes 1-2), K46 (lanes 3-4), IIA1.6 (lanes 5-6), and human Ramos B lymphocytes (lanes 7-8) were subjected to affinity purifications with GST-mGrb2[SH2] fusion proteins, and purified proteins were analyzed by rabbit-anti-Dok-3 immunoblotting. Molecular mass protein standards (kDa) are indicated on the left (A-C).

anti-mouse Dok-3 antibodies or GST-mGrb[SH2] fusion proteins, and affinity complexes were purified with glutathione-sepharose and ProteinA/G-agarose beads, respectively (figure 5.22B). Affinity purifications with irrelevant anti-mouse NTAL antibodies or GST only served as negative controls. Immunoblot analysis with anti-pTyr antibodies indeed revealed that p50 purified by the Grb2 SH2 domain co-migrates with a prominent tyrosine phosphorylated protein purified by anti-mouse Dok-3 antibodies from BCR-stimulated wild-type DT40 cells (figure 5.22B, upper middle panel, lanes 6 and 10). Reprobing the membrane with antibodies to Grb2 clearly shows that the protein purified by anti-mouse Dok-3 antibodies interacts with Grb2 in a stimulation-dependent manner (lower middle panel, lane 10). Interestingly Grb2 cannot be detected in the Grb2[SH2] affinity purifications (lanes 5-8), suggesting that the stoichiometry of the Grb2-Dok-3 interaction is 1:1.

To clarify whether the Grb2-Dok-3 association is a general mechanism in BCR-stimulated B lymphocytes, the formation of this complex was investigated in the three murine B cell lines WEHI-231, K46, and IIA1.6, and in the human B cell line Ramos (figure 5.22C). By affinity purification experiments with the Grb2 SH2 domain and subsequent anti-mouse Dok-3 immunoblotting it could indeed be demonstrated that Dok-3 is bound by the Grb2 SH2 domain in a stimulation-dependent manner in B lymphocytes originating from different species (lanes 2, 4, 6, and 8, respectively).

In summary, these observations show that Grb2 is obligatory for a complete Dok-3 tyrosine phosphorylation and that the Grb2-Dok-3 interaction is mediated via the Grb2-SH2 domain. The latter observation was confirmed in B lymphocytes of various species.

5.2.8. Cloning of chicken *dok-3* cDNA and generation of *dok-3*$^{-/-}$ DT40 cells

Isolation of the cDNA encoding full length chicken Dok-3 was then pursued since it is a major tyrosine phosphorylated protein and Grb2 interaction partner in activated DT40 B lymphocytes. The cDNA encoding the partial chicken Dok-3 protein described above included the coding exons 2, 3, and 4 of the chicken *dok-3* mRNA. Chicken *dok-3*-specific oligonucleotides, chDok-3cDNAfor3 and chDok-3cDNArev1, in combination with the oligonucleotides pJG4-5for and pJG4-5rev were used to amplify the missing 5' and 3' cDNA regions from the plasmid-based DT40 cDNA library pJG4-5/DT40 (kindly provided by Dr. T. Kurosaki). Oligonucleotides annealing in the 5`-UTR and the 3`-UTR of chicken *dok-3* were subsequently designed and used to amplify the full length chicken *dok-3* cDNA by RT-PCR. In figure 5.23A the deduced chicken Dok-3 amino acid sequence is aligned with its murine and human orthologs. Similar to its mammalian orthologs, chicken Dok-3 harbors an N-terminal PH domain followed by a PTB domain. The C-terminus contains two

PTB domain proximal tyrosines representing potential Csk and Grb2 binding motifs (Y^{307}ASI and Y^{331}ENI, repectively). The two distal tyrosines described for human and murine Dok-3 are not present in chicken Dok-3. Two tyrosines within the PH domain (Y^{11} and Y^{96}) and a single tyrosine between the PH and the PTB domain (Y^{140}) are predicted to be phosphorylated by an artificial neural network method (NetPhos 2.0 Server, BLOM et al., 1999). This method also predicts 17 serines/threonines of chicken Dok-3 are phosphoacceptor sites. Four core PxxP motifs exist in the C-terminal part of avian Dok-3 (see figure 5.23A; P^{296}VEP^{299}EAP, P^{322}GQP, and P^{398}SRP). These motifs represent potential SH3 domain binding sites, and two of them (RFPP^{296}VEP and RPCP^{322}GQP) conform to a class I ligand motif for SH3 domains, and share the consensus sequence (R/K)xxPxxP (FENG et al., 1994, 1995; SPARKS et al., 1996, 1998; MAYER, 2001; JIA et al., 2005).

Due to a single nucleotide polymorphism (SNP), the amino acid at position 122 of chicken Dok-3 can be either glutamate or alanine, as determined by analysis of multiple cDNA and genomic sequences.

The level of chicken *dok-3* messenger RNA in DT40 B lymphocytes was analysed by RT-PCR using the oligonucleotides chDok-3cDNAforSTART and chDok-3cDNArev1 (figure 5.23B; expected transcript size: 618 bp). The cDNA was synthesized from oligo-dT- or random hexamer-primed DT40 total RNA. It was shown that chicken *dok-3* transcripts are detectable after 22-26 cycles from both oligo-dT- and random hexamer-derived cDNA, and reach similar transcript levels as observed for chicken *gapdh*. The faint RT-PCR product running below the fragment corresponding to the main transcript may represent an alternative splice variant. For the human and murine orthologs indeed different isoforms were identified (www.expasy.org). Taken together, these RT-PCR experiments suggest a comparatively high concentration of chicken *dok-3* messenger RNA in DT40 B lymphocytes.

A

```
                    10        20        30        40        50        60        70        80
                    |         |         |         |         |         |         |         |
chicken     ----------------------------------------------------------MERPVKDGIIYVQHCKFGKRT
mouse       ----------------------------------------------------------MESVEPPVKDGILYQQHVKFGKKC
human       MTRGARLRSDARAQLNQLSLDGGTGSGQKGKCEEFPSSLSSVSPGLEAAALLLAVTMDPLETPIKDGILYQQHVKFGKKC
                                                                      :* *:****:* ** ****:

                    90        100       110       120       130       140       150       160
                    |         |         |         |         |         |         |         |
chicken     WRKIRAQLFAASPFGVARMEKFDARD--HGTVSDISL---QRCARRVIRLSDCVSVGPMGTESCPKATAAFYLTTTEKNY
mouse       WRKVWALLYAGGPSGVARLESWDVRDGGLGPAGDRSTGPSRRGERRVIRLADCVSVLPADGESCPRDTGAFLITTTERSH
human       WRKVWALLYAGGPSGVARLESWEVRDGGLGAAGDRSAGPGRRGERRVIRLADCVSVLPADGESCPRDTGAFLLTTTERSH
            ***: * *:*..* ****:*.::.**   *...* *    :*  ******:***** * . ****: *.** :****:.:

                    170       180       190       200       210       220       230       240
                    |         |         |         |         |         |         |         |
chicken     VLAAEQRDEWIEQLCQLAFQGKKEAEQSSSTGLQP----IPMEENCLYSSWQDLTEFPVLVLRTEAAARCELHGHYVLAA
mouse       LLAAQHRQSWVDPICQLAFPGTGECSSGSGQAESPKRGFVPMEENSIYSSWQEVTEFPVIVQRTEATSRCQLKGPYLLVL
human       LLAAQHRQAWMGPICQLAFPGTGEASSGSTDAQSPKRGLVPMEENSIYSSWQEVGEFPVVVQRTEAATRCQLKGPALLVL
            :***::*: *:  :***** *. *....*  . .*    :*****.:*****:: ****:* ****::**:*:*  :*.

                    250       260       270       280       290       300       310       320
                    |         |         |         |         |         |         |         |
chicken     LPHSLTLKDAQSQQPLLTWPYPFLRKFGQDQNIFSFEAGRRSDSGEGTFTFSTPRAAELCRAVAAAIACQQQ-----GQE
mouse       GQDDIQLRETSKPQACFSWPYRFLRKYGSDKGVFSFEAGRRCDSGEGLFAFSSPRAPDICGVVAAAIARQRERLPELAMS
human       GPDAIQLREAKGTQALYSWPYHFLRKFGSDKGVFSFEAGRRCHSGEGLFAFSTPCAPDLCRAVAGAIARQRERLPELTRP
              . : *:::.  *.  :*** ****:*.*:.:********..**** *:**:* *.::* .**.*** *::

                    330       340       350       360       370       380       390       400
                    |         |         |         |         |         |         |         |
chicken     SPQPSAQGLSNQPWGAEAEDPQCSPTLGRAHSGSHSASYP---SLNLLRFPPVEPEAPAPIVYASIARGQQPHFRPCPGQ
mouse       PPCPLPRALSLPSLEPPGELREVAPGFELPTPRKLPLTDPGPQSLPLLLSP--TQEGPASGLYASVCK----QTSKHTGT
human       QPCPLPRATSLPSLDTPGELREMPPGPEPPTSRKMHLAEPGPQSLPLLLGP--EPNDLASGLYASVCK----RASGPPG-
             * * .:. *  .  . .*  : .*    . . .   : *   ** **  *    :  *. :***:.:    :    .*

                    410       420       430       440       450       460       470       480
                    |         |         |         |         |         |         |         |
chicken     PLPEHLYENIFTAQPRP-LAEEEAEEEEGR-WELGCRQAPEGHSS-EAAVPYPARSAPQPHTQRWAPGGSRGGAEEPSRP
mouse       --AEHLYENVCMLEASPGLTNGGPEAQEGPPGGRSPLGSPIYHNTEDLSWPGSAQDSNLEAQYRRLLELELDEAGSAGRS
human       --NEHLYENLCVLEASPTLHGGEPEPHEGP-GSRSPTTSPIYHNGQDLSWPGPANDSTLEAQYRRLLELDQVEG--TGRP
               ******:   :. * *    .* .**     .   :*  *.  : : * .*..:      *     .   .  ..*.

                    490       500
                    |         |
chicken     KPQRTLRAKLVRLLSRD---GPGARDWS
mouse       GAQAGIKAKLVTLLTRERKKGPAPCDRP
human       DPQAGFKAKLVTLLSRERRKGPAPCDRP
             .*  ::**** **:*:   **.. * .
```

B

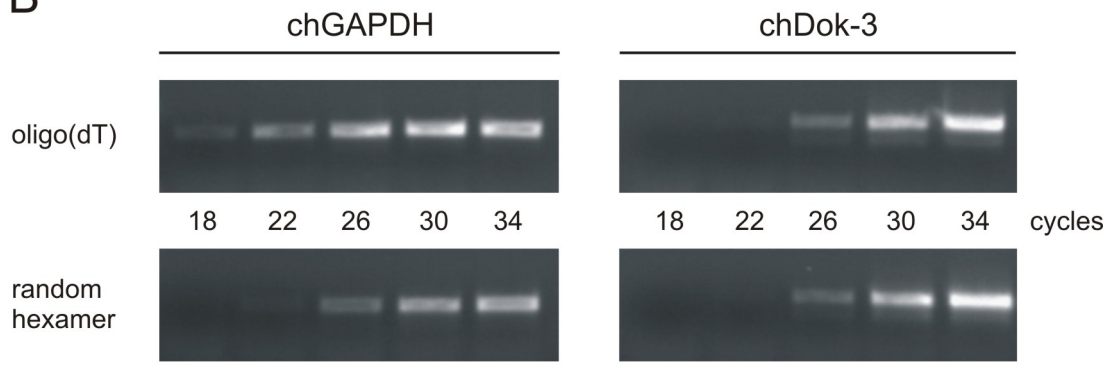

Figure 5.23: Avian Dok-3 amino acid sequence and messenger RNA levels in DT40 cells
(A) The amino acid sequences of avian, murine (accession number NP_038767), and human Dok-3 (accession number Q7L591) were aligned using the ClustalW algorithm (THOMPSON et al., 1994). The avian Dok-3 amino acid sequence is deduced from multiple cDNA and genomic sequences. Amino acids are described by using the single letter code. Identical amino acids (*) are denoted in red, strongly similar amino acids (:) in green, and weakly similar amino acids (.) in blue. Putative phosphoacceptor-tyrosines and class I ligand motifs for SH3 domains are indicated in bold letters (B) DT40 cDNA was synthesized from oligo-dT- (upper panels) or random hexamer-primed (lower panels) DT40 total RNA by reverse transcription. Chicken *dok-3* cDNA was amplified by PCR using the oligonucleotides chDok-3cDNAforSTART and chDok-3cDNArev1 (618 bp transcript), and amplicons were analyzed after the indicated number of cycles (right panels). As a control chicken *gapdh* cDNA was amplified (564 bp transcript; left panels).

For further functional analysis of Dok-3 in B lymphocyte signal transduction, the next aim was to generate a *dok-3*$^{-/-}$ DT40 cell line by gene targeting experiments. The genomic locus of chicken *dok-3* was identified by blastn searches of the chicken genomic database (www.ensembl.org) using the full length chicken *dok-3* cDNA sequence. The so far unidentified chicken *dok-3* locus was mapped to chicken chromosome 13 (Gga 13) (figure 5.24A). Two strategies were pursued in parallel for the gene targeting constructs (figure 5.24A). The first construct was designed as insertion vector, introducing the resistance encoding cassettes into intron 1 of chicken *dok-3* genomic sequence. Alternatively, a second targeting vector was generated by which 621 bp of intron 1 and the first 65 bp of exon 2 coding for chicken Dok-3 amino acids 19-40 were replaced upon homologous recombination. Exon 1 of chicken *dok-3* could not be inactivated by insertion or replacement since it is part of the 3`-UTR of the upstream chicken *ddx41* gene (figure 5.24A). Both the insertion and the replacement vector contain the functional polyadenylation site for chicken Ddx41 within intron 1 of the chicken *dok-3* genomic sequence. However, for both targeting approaches the ATG translation initiation codon of chicken *dok-3* was mutated to TTG, and a stop codon (TAG) was introduced immediately following the last in frame ATG of chicken *dok-3* coding sequence located within exon 3 (figure 5.24A). The neo and hisD cassettes were flanked by 1132 bp (replacement vector, REP) or 1798 bp (insertion vector, INS) at the 5`-site, and by 2858 bp at the 3`-site. To disrupt the *dok-3* locus, the targeting constructs pDok-3-neo(REP) and pDok-3-neo(INS) were transfected into wild-type DT40 cells. Homologous recombination was identified by PCR (data not shown). A targeted allele was detected in 4 out of 25 G418-resistant clones, i.e. clone D12 for the replacement vector, and clones D23, D27, and D28 for insertional inactivation. The pDok-3-hisD(REP) was introduced into the neo-targeted clone D12, and pDok-3-hisD(INS) was transfected into clones D23, D27, and D28, respectively. Transfectants were selected with both G418 and histidinol, and the generation of the *dok-3*$^{-/-}$ DT40 clones D12-15, D12-67, D12-90, D23-34, D23-38, and D27-30 was confirmed by PCR (figure 5.24B). The successful generation of *dok-3*$^{-/-}$ DT40 cells was also confirmed by immunoblot analysis (figure 5.24, C and D)

Taken together, the chicken *dok-3* cDNA was cloned and *dok-3* transcripts were detectable at relatively high levels in DT40 B lymphocytes. To exclude that the high expression of endogenous Dok-3 may dominantly affect signal transduction pathways in functional studies, *dok-3*$^{-/-}$ DT40 cells were generated by gene disruption experiments.

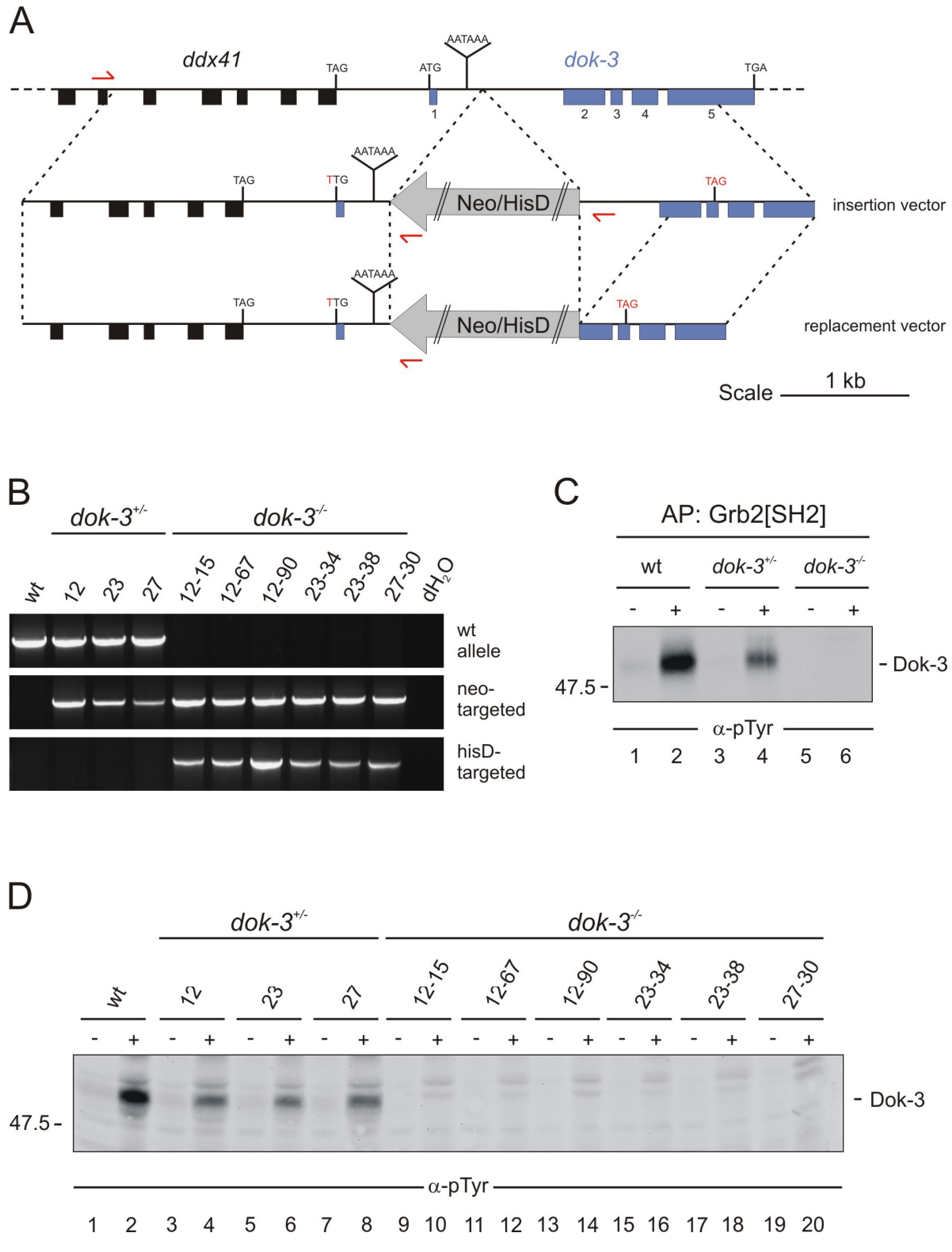

Figure 5.24: Generation of *dok-3*$^{-/-}$ DT40 B lymphocytes
(A) Schematic representation of the chicken *dok-3* genomic locus and targeting strategy. For gene disruption, two alternative targeting constructs were generated. The insertion vector (INS) introduces the resistance encoding cassettes into intron 1 of the chicken *dok-3* genomic sequence. The replacement vector (REP) deletes 621 bp in intron 1 and 65 bp in exon 2 (coding for amino acids 19-40) of the chicken *dok-3* genomic sequence. Exon 1 of chicken *dok-3* could not be inactivated by insertion or replacement since it is part of the 3`-UTR of the upstream chicken *ddx41* gene. **(continued on next page)**

(legend to figure 5.13 continued) Both the insertion and the replacement vector contain the functional polyadenylation site of chicken Ddx41 within intron 1 of the chicken *dok-3* genomic sequence. For both targeting vectors the ATG translation initiation codon of chicken *dok-3* was mutated to TTG, and immediately following the last in frame ATG within the chicken *dok-3* coding sequence (exon 3) a stop codon (TAG) was introduced. The neo and hisD cassettes were flanked by 1132 bp (replacement vector) or 1798 bp (insertion vector) at the 5`-site, and by 2858 bp at the 3`-site. Annnealing sites for the screening oligonuclotides are depicted as red half-arrows. (B) Homologous recombination of pDok-3-neo(REP/INS) and pDok-3-hisD(REP/INS) at the *dok-3* locus. The generation of *dok-3*$^{+/-}$ clones D12, D23, and D27 (lanes 2-4), and of *dok-3*$^{-/-}$ DT40 clones D12-15, D12-67, D12-90, D23-34, D23-38, and D27-30 (lanes 5-10) was confirmed by PCR. For the wild-type *dok-3* allele, the oligonucleotides screenLAfor2 and chDok-3rev2 were used. Neo- and HisD-targeted alleles were amplified using the oligonucleotides screenLAfor2 and Neo_rev or HisD_rev, respectively. Genomic DNA dervied from wild-type DT40 cells and dH_20 served as controls (lanes 1 and 11, respectively). (C) Cleared cellular lysates prepared from unstimulated (-) or BCR-stimulated (+) wild-type (lanes 1-2), *dok-3*$^{+/-}$ (clone D12; lanes 3-4), or *dok-3*$^{-/-}$ DT40 cells (clone D12-15, lanes 5-6) were subjected to affinity purification experiments with GST-mGRB[SH2] fusion proteins. Purified proteins were analyzed by immunoblotting with antibodies to pTyr. (D) Cleared cellular lysates of unstimulated (-) or BCR-stimulated (+) wild-type DT40 cells (lanes 1-2), *dok-3*$^{+/-}$ clones D12, D23, and D27 (lanes 3-8), and *dok-3*$^{-/-}$ clones D12-15, D12-67, D12-90, D23-34, D23-38, and D27-30 (lanes 9-20) were analyzed by anti-pTyr immunoblotting. Molecular mass protein standards (kDa) are indicated on the left (C, D).

5.2.9. Dok-3 negatively regulates BCR-induced Ca^{2+} mobilization

To elucidate whether Dok-3 is the downstream mediator of Grb2 in the negative regulation of BCR-induced Ca^{2+} mobilization, Ca^{2+} flux was analysed in *dok-3*$^{-/-}$ DT40 lymphocytes (clone D23-38). These cells show a prolonged intracellular Ca^{2+} release and a marked increase in extracellular Ca^{2+} entry (figure 5.25B, black line). In contrast, derivatives that were reconstituted with wild-type chicken Dok-3 (figure 5.25A, lane 6) display a Ca^{2+} flux profile similar to wild-type DT40 cells (figure 5.25B, grey and orange line, respectively). Hence, Ca^{2+} mobilization in Dok-3-deficient DT40 cells resembles that of Grb2-deficient DT40 cells (see figure 5.3). Taken together, Dok-3 appears to be the downstream mediator of Grb2 in the negative regulation of BCR-induced Ca^{2+} mobilization.

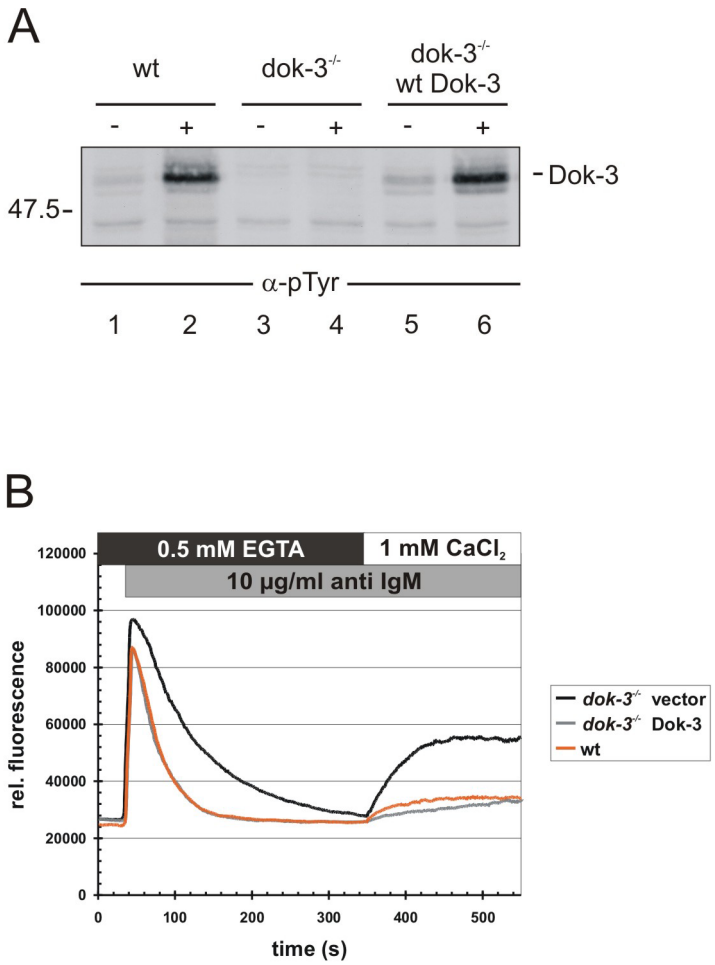

Figure 5.25: Enhanced Ca^{2+} mobilization in *dok-3*$^{-/-}$ DT40 cells
(A) Dok-3 protein expression in unstimulated (-) or BCR-stimulated (+) wild-type DT40 B cells (lanes 1-2), *dok-3*$^{-/-}$ mutants (lanes 3-4), and derivatives that upon electroporation express wild-type Dok-3 (lanes 5-6) were compared by anti-pTyr immunoblot analysis of cleared cellular lysates. Molecular mass protein standards (kDa) are indicated on the left.
(B) Wild-type DT40 B cells (orange line), *dok-3*$^{-/-}$ mutants (black line), and derivatives that were reconstituted with wild-type Dok-3 (grey line) were loaded with 1 µM Indo-1/0.015 % pluronic F127, and BCR-induced Ca^{2+} mobilization was monitored as described in the figure 5.3 legend. Data represent the results obtained from 3 independent measurements.

In summary, the studies presented in this thesis identify and characterize a novel Ca^{2+}-regulating signalling pathway in B lymphocytes. This pathway involves the transmembrane adaptor NTAL and the cytosolic adaptors Grb2 and Dok-3. Grb2 exhibits an inhibitory effect on BCR-induced Ca^{2+} elevation. This negative regulatory role is abolished by NTAL-mediated, phosphorylation-dependent recruitment of Grb2 to lipid rafts. Although the biochemical data does not reveal any differences in tyrosine phosphorylation of the Ca^{2+} flux regulators SLP-65 and PLC-γ2, the NTAL/Grb2 module appears to influence the activation and/or the membrane targeting of PLC-γ2. Dok-3, which is the major tyrosine phosphorylated protein in DT40 cells, was identified as the downstream mediator of Grb2 in the negative regulation of BCR-induced Ca^{2+} mobilization. It was shown that tyrosine phosphorylated Dok-3 is directly bound by the Grb2 SH2 domain, and the Ca^{2+} flux profiles in Grb2- and Dok-3-deficient DT40 cells are similar. Lyn-mediated tyrosine phosphorylation of Dok-3 depends on the presence of Grb2, whose central SH2 and C-terminal SH3 domain are a stringent requirement for maximal Dok-3 tyrosine phosphorylation. Notably, these two Grb2 domains are also responsible for the inhibitory

effect of Grb2 on Ca^{2+} mobilization. The direct association of the Grb2 SH2 domain with tyrosine phosphorylated Dok-3 is especially striking considering that in absence of a functional Grb2 SH2 domain tyrosine phosphorylation of Dok-3 is severely reduced. Chicken *dok-3* cDNA and *dok-3*$^{-/-}$ DT40 B lymphocytes are useful tools for the investigation of the mechanistic background of the Grb2-dependent Dok-3 phosphorylation and the involvement of Dok-3 in the Grb2-regulated Ca^{2+} mobilization in future experiments.

6. Discussion

B-cell signalling through the BCR occurs via a complex and highly regulated network of cytoplasmic protein tyrosine kinases and phosphatases, adaptor proteins and further effector enzymes. The BCR signal transduction is counterbalanced by an equally sophisticated inhibitory machinery. Inhibitory mechanisms involve a similar set of proteins, i.e. receptors, protein tyrosine kinases and phosphatases, lipid phosphatases, ubiquitin ligases, and inhibitory adaptor molecules.

Ca^{2+} is a universal second messenger and its concentration is precisely controlled within all cell types. A large electro-chemical gradient is maintained across the plasma membrane, and dynamic changes in intracellular Ca^{2+} release and Ca^{2+} entry through plasma membrane channels lead to broad range of short- and long-term cellular responses, e.g. secretory processes, cytoskeletal reorganizations, altered gene transcription, proliferation, and apoptosis. Key components of Ca^{2+} signalling pathways are members of the PLC superfamily. The PLC-catalyzed generation of the second messengers IP_3 and DAG initiates the Ca^{2+}-signal cascade. Downstream of the BCR, this process is coordinated by phosphorylation-dependent and successive recruitment of PLC-γ2 and Btk by the scaffolding molecule SLP-65.

Presently, one of the main questions in BCR signal transduction is how activation mechanisms and the inhibitory apparatus are choreographed for a dynamic Ca^{2+} mobilization in the cell. Intensive investigation is underway to determine (1) which mechanisms regulate membrane recruitment of the Ca^{2+} initiation complex comprised of PLC-γ2, SLP-65, and Btk, (2) what is the detailed mechanism of BCR-initiated PLC-γ2 activation, (3) how the intracellular Ca^{2+} release is connected to Ca^{2+} entry across the plasma membrane, and (4) how Ca^{2+} mobilization is differentially regulated in B lymphocytes of different developmental stages.

The above stated questions were addressed in this thesis by using the chicken DT40 B cell line and derivatives which were rendered deficient for central components of the Ca^{2+} mobilization machinery. The objective was to determine the role of the cytosolic adaptor molecule Grb2 in the regulation of BCR-induced Ca^{2+} signals.

The main findings of this thesis are:

1.) The adaptor molecule Grb2 is a negative regulator of BCR-induced Ca^{2+} mobilization, affecting both the Ca^{2+} release from intracellular stores, and the Ca^{2+} entry through plasma membrane channels. The central SH2 domain and the C-terminal SH3 domain are obligatory for this inhibitory role. This Grb2 function is controlled by its subcellular localization.

2.) The transmembrane adaptor molecule NTAL is a positive regulator of BCR-induced Ca^{2+} mobilization. Upon BCR engagement the three membrane-distal YxN sites of NTAL are tyrosine phosphorylated and are bound by the Grb2 SH2 domain. NTAL counter acts Grb2 by the stimulation-dependent recruitment of Grb2 to the lipid rafts. The NTAL/Grb2 module does not influence the phosphorylation state of central components of the Ca^{2+} initiation complex such as SLP-65 or PLC-γ2. There are indications that PLC-γ2 retention at the plasma membrane is prolonged in NTAL-positive cells.

3.) The tightly regulated expression of NTAL during B cell lymphopoiesis may explain the specificity of Grb2-regulated Ca^{2+} mobilization profiles at different stages of B cell development.

4.) In searching for Grb2 effector proteins, it was shown that the major tyrosine phosphorylated protein in DT40 B lymphocytes requires Grb2 for its phosphorylation. This protein was identified as the inhibitory adaptor molecule Dok-3, and was shown to bind to the Grb2 SH2 domain in a stimulation-dependent manner. The SH2 and the C-terminal SH3 domain of Grb2 are strictly required for complete Dok-3 tyrosine phosphorylation following BCR engagement.

5.) It was demonstrated that Dok-3 negatively regulates Ca^{2+} mobilization in B lymphocytes. Probably this function of Dok-3 is modified by the NTAL/Grb2 module through a competetive binding mechanism. It seems that NTAL promotes Ca^{2+} mobilization by SH2-mediated relocalization of Grb2 in order to prevent its phosphorylation-dependent interaction with Dok-3.

Collectively, in this scenario Grb2 seems to be a molecular switch of BCR-induced Ca^{2+} mobilization. The SH2-domain dependent binding of Grb2 to either tyrosine phosphorylated NTAL or Dok-3 ultimately results in positive or negative fine-tuning of antigen receptor-induced Ca^{2+} mobilization in B lymphocytes. Both the expression levels of NTAL and Dok-3 during B cell lymphopoiesis and the Grb2-dependent tyrosine phosphorylation of Dok-3 are critical factors in this mechanism.

6.1. Grb2 is a negative regulator of Ca^{2+} mobilization in B lymphocytes

The work presented in this thesis identifies Grb2 as a negative regulator of BCR-induced Ca^{2+} mobilization, both in immature and mature B lymphocytes. Grb2 deficiency affects both the release from intracellular stores and the Ca^{2+} entry across the plasma membrane. This negative regulatory function of Grb2 depends on the SH2 and the C-terminal SH3 domain. Interestingly, the overall tyrosine phosphorylation of the Ca^{2+} initiation complex components SLP-65 and PLC-γ2 was unaffected. This is supported by the observation that SLP-65 and Grb2 independently translocate to signalling competent lipid rafts (JOHMURA et al., 2003). It will be important to further address this question with phospho-specific antibodies to components of the Ca^{2+} initiation complex. It was previously suggested that Grb2 can indeed fulfill a role in PLC-γ regulation. Choi et al. reported that Grb2 directly binds phospho-Tyr^{783} of PLC-γ1 (rat sequence) in a HEK-293 cell-based system (CHOI et al., 2005). Downregulation of Grb2 in HEK-293 cells by RNA interference enhanced epidermal growth factor (EGF)-induced PLC-γ1 enzymatic activity and subsequent Ca^{2+} mobilization, while Grb2 overexpression inhibited PLC-γ1 activity. Interestingly, the EGF-induced tyrosine phosphorylation state of PLC-γ1 was unaffected (CHOI et al., 2005). In addition, it was reported that there is some level of association between PLC-γ1 and Grb2 which is independent of tyrosine phosphorylation, and probably mediated by a proline-rich motif of PLC-γ1 and one of the two SH3 domains of Grb2 (PEI et al., 1997). This data suggests that Grb2 directly influences PLC-γ recruitment and/or activity. However, it seems unlikely that similar interactions between Grb2 and PLC-γ2 are the cause of the observed negative regulation of Ca^{2+} mobilization in B lymphocytes. In our system, inducible or constitutive interactions between Grb2 and PLC-γ2 were not detected by immuno- or affinity purifications (I. Goldbeck, PhD thesis in progress). Furthermore, in PLC-γ2 neither Y^{753} nor Y^{759} are located within a motif similar to the postulated Grb2-binding motif in PLC-γ1 (Y^{783}).

Grb2 was shown to be a central component of many inhibitory signalling pathways by serving as scaffold for different negative regulators (reviewed in DIKIC and GIORDANO, 2003). The data reported herein is complementary to those studies and reveal for the first time a regulatory role of Grb2 for the essential process of Ca^{2+} mobilization in B lymphocytes.

6.2. NTAL positively regulates Ca^{2+} mobilization in B lymphocytes

Ca^{2+} mobilization differs significantly at different stages of B cell development. Since Grb2 is expressed throughout all stages of B cell lymphopoiesis, the requirement of an upstream

Grb2 regulator that may be differentially expressed during B cell maturation appeared to be obligatory. We focussed on the transmembrane adaptor NTAL, since it was previously shown that NTAL is capable of binding Grb2 through phosphotyrosine-based binding motifs of the pYxN type (BRDICKA et al., 2002; JANSSEN et al., 2003). The deduced amino acid sequence of avian NTAL indicates the importance of Grb2 binding since the evolutionary conservation is essentially restricted to these motifs. In this thesis it was demonstrated that tyrosine phosphorylation of the three membrane-distal YxN sites of NTAL leads to Grb2 recruitment via its SH2 domain. Thus, NTAL is a positive regulator of BCR-induced Ca^{2+} mobilization.

The results presented in this thesis clearly show that NTAL is not the B-cell homolog of LAT as previously assumed based on their structural similarity. NTAL lacks critical functional properties of LAT, most importantly it fails to recruit PLC-γ isoforms (BRDICKA et al., 2002; JANSSEN et al., 2003). Nevertheless, NTAL has been shown to activate Erk (BRDICKA et al., 2002) or to induce Ca^{2+} mobilization via an unknown pathway (JANSSEN et al., 2003). The hypothesis that NTAL does not exert its positive role in Ca^{2+} mobilization via a direct interaction with PLC-γ2 was further supported by the observation that a LAT variant which is incapable of binding PLC-γ (human LAT [$Y^{132}F$]) still leads to an increase in Ca^{2+} mobilization when expressed in DT40 B lymphocytes. Evidence for the functional equivalence of NTAL and the LAT [$Y^{132}F$] mutant was also obtained in other cell lines and mouse models. Both NTAL and LAT [$Y^{132}F$] were able to restore Ca^{2+} mobilization in LAT-deficient J.Cam2.5 Jurkat T cells, albeit to a reduced extent than variants expressing wild-type LAT (ZHANG et al., 2000; JANSSEN et al., 2004). In other studies both LAT [$Y^{136}F$] knock-in mice (murine LAT Y^{136} is the equivalent of human LAT Y^{132}) and *lat*$^{-/-}$ mice reconstituted with an *ntal* transgene under the control of the CD2 promotor show a T_H2 lymphoproliferative disorder characterized by a massive T cell infiltration and organomegaly (AGUADO et al., 2002; SOMMERS et al., 2002; JANSSEN et al., 2004), clearly emphasizing the importance of the association of LAT with PLC-γ1. It seems that this association determines the signalling threshold within the cells. If NTAL does not interact with PLC-γ isoforms, what is its function in B cells in general and how does it regulate Ca^{2+} mobilization in particular?

Mast cells isolated from *ntal*$^{-/-}$ mice show increased PLC-γ activity, increased IP3 production, and increased Ca^{2+} mobilization probably caused by enhanced LAT tyrosine phosphorylation (VOLNA et al., 2004; ZHU et al., 2004). Additionally, *ntal*$^{-/-}$ mice reveal slightly increased BCR-induced Ca^{2+} mobilization (ZHU et al., 2004; WANG et al., 2005). Thus, genetic deletion in mice reveals primarily an inhibitory function of NTAL. However,

a partial contributory role for NTAL in Ca^{2+} signalling has been deduced from studies in both T and B lymphocytes (BRDICKA et al., 2002; JANSSEN et al., 2003; 2004). Therefore, the increased LAT phosphorylation in *ntal-/-* mast cells might mask the positive regulatory role of NTAL in Ca^{2+} mobilization (VOLNA et al., 2004; ZHU et al., 2004). It must be noted that *ntal*$^{-/-}$ *lat*$^{-/-}$ mast cells are even less responsive than *lat*$^{-/-}$ mast cells (ZHU et al., 2004), clearly suggesting a stimulatory role for NTAL which could be mediated through its role in Ca^{2+} mobilization. Tkaczyk et al. indeed found a positive regulatory role for NTAL in Ca^{2+} signalling by using an RNAi approach in human mast cells (TKACZYK et al., 2004).

Further investigation is required to ultimately determine the redundancy (Grb2 binding) and/or difference (PLC-γ binding) of LAT and NTAL in immune cell signalling. The influence of other transmembrane adaptors capable of Grb2 recruitment (i.e. LAX and SIT) on NTAL-regulated signalling pathways has yet to be assayed. It must be considered that the genetic deletion of one transmemebrane adaptor may significantly alter the membrane distribution of the remaining transmembrane adaptors. The final assessment of overlapping functions of transmembrane adaptors is yet to come. Furthermore, the potential signalling capabilities of the highly conserved tyrosine motifs in NTAL, which are not Grb2-binding sites remains to be elucidated (Y^{110}, Y^{118}, and Y^{119} in avian NTAL).

Collectively, the data presented in this thesis lead to a bidentated model for Ca^{2+} mobilization in B lymphocytes. First, tyrosine phosphorylated SLP-65 serves as scaffold for the recruitment of PLC-γ2 and Btk, resulting in the formation of the Ca^{2+} initiation complex and the activation of PLC-γ2. Second, the tyrosine phosphorylated YxN sites of NTAL recruit Grb2 to the lipid rafts, thereby inactivating its negative regulatory role on Ca^{2+} mobilization and preventing a premature stop of the Ca^{2+} signal. This model is supported by the fact that a constitutive recruitment of Grb2 to the lipid rafts by virtue of a palmitoylated, transmembrane anchor leads to increased Ca^{2+} mobilization.

It appears that the NTAL/Grb2 module is one pathway to fine-tune the BCR-induced Ca^{2+} signal, allowing for specific cellular responses. Since both NTAL and Grb2 are expressed in various hematopoietic lineages, it can be assumed that the NTAL/Grb2 module also operates in the context of other receptor systems. The expression of other Grb2-recruiting transmembrane adaptors and their distribution in distinct plasma membrane microdomains are likely to be important factors influencing NTAL function.

6.3. The NTAL/Grb2 module: a regulator of PLC-γ2 function?

Over the course of this project it was demonstrated that the enhanced Ca^{2+} mobilization in NTAL-positive or Grb2-negative DT40 cells can be attributed to increased intracellular IP3

concentration (K. Neumann, PhD thesis in progress). This observation led to the assumption that the NTAL/Grb2 module affects PLC-γ2 activity. As outlined in the introduction, PLC-γ2 activity is regulated by tyrosine phosphorylation and its translocation to the plasma membrane. To further elucidate that hypthesis, the effect of NTAL overexpression was analysed in *plc-γ2*$^{-/-}$ DT40 cells reconstituted with either wild-type rat PLC-γ2 or a transmembrane chimera (diploma thesis S. Alers). Strikingly, forced expression of NTAL had no enhancing effect on Ca^{2+} mobilization in *plc-γ2*$^{-/-}$ DT40 cells expressing the transmembrane variant of PLC-γ2. Thus it appears that the NTAL/Grb2 module directly influences the membrane localization of PLC-γ2 or its retention time at the membrane. This function is abolished in DT40 B lymphocytes expressing a PLC-γ2 chimeric protein which is constitutively targeted to the plasma membrane. Collectively, these studies reveal a role of the NTAL/Grb2 module in the regulation of PLC-γ2 function. As demonstrated by the IP3 production assays discussed above and the data for the Ca^{2+} release from intracellular stores in NTAL-positive and Grb2-negative cells (shown in this thesis), it might be possible that the NTAL/Grb2 module directly affects PIP2 hydrolysis by an altered retention time of PLC-γ2 at the plasma membrane.

Although extensively studied, the regulation of Ca^{2+} permeable ion channels in the plasma membrane and exactly how receptor activation leads to channel activity remain obscure. Currently it seems to be evident that the same proteins participate in both Ca^{2+} release from intracellular stores and Ca^{2+} entry across the plasma membrane (PATTERSON et al., 2005). For example, this could be shown for IP_3R (FURUICHI et al., 1989; VAN ROSSUM et al., 2004), calmodulin (MICHIKAWA et al., 1999; ORDAZ et al., 2005), PKC (FERRIS et al., 1991; VENKATACHALAM et al., 2003), homer (TU et al., 1999; YUAN et al., 2003), and PLC-γ (SUGAWARA et al., 1997; PATTERSON et al., 2002).

B lymphocytes signal Ca^{2+} in response to antigen receptor engagement exclusively via PLC-γ2 (TAKATA et al., 1995; KUROSAKI et al., 2000; REBECCHI and PENTYALA, 2000; RHEE, 2001; WILDE and WATSON, 2001), and this is also the only isoform of PLC-γ expressed in DT40 B cells (TAKATA et al., 1995; REBECCHI and PENTYALA, 2000). Evidence is accumulating that PLC-γ2 has both lipase-dependent and lipase-independent functions in Ca^{2+} entry across the membrane (see introduction; BERRIDGE et al., 2000; PATTERSON et al., 2002; CLAPHAM, 2003; NISHIDA et al., 2003; PATTERSON et al., 2005; VAN ROSSUM et al., 2005). Nishida et al. convincingly demonstrated that PLC-γ2 acts to amplify the BCR-evoked Ca^{2+} signal. The amplification mechanism is a positive feedback cycle, in which the key event is the Ca^{2+} entry-mediated, lipase-independent translocation of PLC-γ2 towards

the plasma membrane via its C2 domain leading to PLC-γ2 activation, IP_3/DAG production, and finally to Ca^{2+} release and entry (NISHIDA et al., 2003). Interestingly, three recent reports provide clear evidence that PLC-γ also has a functional role in Ca^{2+} entry independent of its enzymatic activity. Patterson et al. reported experiments clearly showing that a lipase-inactive mutant of PLC-γ2 can elicit Ca^{2+} entry (PATTERSON et al., 2002). Yu et al. identified a point mutation in the murine *plc-γ2* gene leading to the gain-of-function substitution $D^{993}G$ (YU et al., 2005). The ability of this PLC-γ2 variant to interact and to remain at the plasma membrane is affected, and in turn causes an increased and sustained external Ca^{2+} entry (YU et al., 2005). Finally, van Rossum et al. reported that the C-terminal half of the split PH domain of PLC-γ1 interacts with a complementary partial PH-like domain in TRPC3, thereby eliciting lipid binding and cell-surface expression of TRPC3 (VAN ROSSUM et al., 2005). With regard to the data described above, one might speculate that the comparatively high Ca^{2+} influx from extracellular sources in DT40 cells expressing the transmembrane PLC-γ2 variant might be due to an increased cell-surface expression of Ca^{2+} channels. Collectively, as NTAL/Grb2 seem to control PLC-γ2 localization, it is likely that this module also regulates lipase-independent activities of PLC-γ2 in BCR-induced Ca^{2+} mobilization.

One important regulator of PLC-γ activation is PI3K, which plays a role in both Ca^{2+} release (BAE et al., 1998; BOLLAND et al., 1998; FALASCA et al., 1998; RAMEH et al., 1998; SCHARENBERG et al., 1998; SCHARENBERG and KINET, 1998; CLAYTON et al., 2002; JOU et al., 2002; OKKENHAUG et al., 2002; DONAHUE and FRUMAN, 2004) and Ca^{2+} influx (CHING et al., 2001; MACREZ et al., 2001; KAWANABE et al., 2003; LE BLANC et al., 2004; TSENG et al., 2004). However, the NTAL/Grb2 module seems to act independently of PI3K as concluded from three lines of evidence. First, Grb2-deficient DT40 cells continue to exhibit increased Ca^{2+} mobilization in the presence of the PI3K inhibitor wortmannin as compared to DT40 cells expressing Grb2. Second, forced expression of NTAL in *vav3*$^{-/-}$ DT40 cells similarly caused an augmentation in Ca^{2+} mobilization. Vav-3 was shown to modulate BCR responses as an upstream regulator of PI3K (INABE et al., 2002). Third, an enhanced Ca^{2+} flux was also observed in *p110α*$^{-/-}$ DT40 cells expressing either NTAL or the dominant negative Grb2 variant W193K (all data by K. Neumann, PhD thesis in progress). One major antagonist of PI3K activity is the 5′-phosphatase SHIP. However, the NTAL/Grb2 module seems to exert its function also in absence of SHIP, as deduced from an increased Ca^{2+} mobilization in *ship*$^{-/-}$ DT40 cells expressing NTAL (K. Neumann, PhD thesis in progress). Taken together, it seems that the role of the NTAL/Grb2 module in BCR-induced PLC-γ2

activation and subsequent Ca^{2+} mobilization cannot solely be attributed to an altered phosphoinositide metabolism catalyzed by PI3K and/or SHIP.

Since neither Grb2 nor NTAL directly associate with PLC-γ2 in B lymphocytes, the necessity of a further downstream effector molecule is apparent. Such a molecule might affect both the lipase-dependent and -independent activities of PLC-γ2. During the course of this project, different molecules known to interact with Grb2 and to be components of inhibitory signalling pathways in B lymphocytes were analysed for their sensitivity to the NTAL/Grb2 module. This was achieved by NTAL overexpression in DT40 cell lines rendered deficient for the corresponding negative regulators, i.e. *ship*$^{-/-}$, *shp1*$^{-/-}$, *shp2*$^{-/-}$, and *cbl*$^{-/-}$ DT40 cells (K. Neumann, PhD thesis in progress). However, in all these cell lines NTAL expression still led to an enhanced Ca^{2+} mobilization. Two conclusions may be drawn from these results. First, neither the lipid phosphatase SHIP, the tyrosine phosphatases SHP-1/-2 nor the ubiquitin ligase Cbl are the inhibitory molecule whose function is regulated by presence or absence of NTAL/Grb2. Rather an inhibitor that remains to be identified is controlled by the NTAL/Grb2 module. Second, the observed Ca^{2+} signal in NTAL-positive or Grb2-negative DT40 cells is composed of multiple Grb2-dependent pathways. Therefore, small differences might not be detectable in DT40 cells deficient for a single, Grb2-bound negative regulator.

6.4. Does the NTAL/Grb2 module influence store-operated Ca^{2+} entry?

In this thesis it was shown that the absence of Grb2 or the presence of NTAL increase the extent of Ca^{2+} entry across the plasma membrane. Some experiments not shown provided evidence that the NTAL/Grb2 module affects store-operated Ca^{2+} entry in DT40 B lymphocytes. Store-depletion with thapsigargin led to identical Ca^{2+} entry in Grb2-negative and Grb2-positive DT40 cells (data not shown). Identical Ca^{2+} mobilization from the extracellular space was also observed when BCRs were crosslinked after thapsigargin-mediated store-depletion (K. Neumann, PhD thesis in progress), indicating that a potential direct BCR-dependent coupling to the channels is unaffected by presence or absence of Grb2. This data agrees with the observation that PLC-γ depletion by RNAi or knockout in DT40 cells has no effect on Ca^{2+} entry following thapsigargin-induced store emptying (PATTERSON et al., 2002). It must be stated that the global store depletion induced by thapsigargin treatment may represent a pathophysiological state, bypassing important physiological regulatory elements (PATTERSON et al., 2002). However, it was shown that store depletion with thapsigargin results in the activation of I_{CRAC} in DT40 cells (PRAKRIYA and LEWIS, 2001). Interestingly, thapsigargin-induced Ca^{2+} entry is indeed potentiated upon

PLC-γ1 overexpression, suggesting that PLC-γ isoforms can indeed fulfill a functional role in SOC activation (PATTERSON et al., 2002).

Analogous to the lipase-dependent and -independent activity of PLC-γ2 in Ca^{2+} release and Ca^{2+} entry, evidence is accumulating that IP_3Rs have both release-dependent and release-independent functions in Ca^{2+} entry across the membrane. IP_3Rs are important components of the conformational/secretion-like coupling model for SOC-mediated Ca^{2+} entry. It could be shown that the IP_3R-mediated gating of TRPC3, an ion channel that is controversially disputed to be store-operated or not (see introduction; PAREKH and PUTNEY, 2005), is dependent on IP_3, but independent of Ca^{2+} release (KISELYOV et al., 1998; 1999). A similar dependence of endogenous SOCs on IP_3/IP_3R was reported in A431 cells (ZUBOV et al., 1999). Another group could demonstrate that capacitative Ca^{2+} entry could be rescued in *ip3r*$^{-/-}$ DT40 B cells reconstituted with a pore-dead mutant of IP_3R that is capable of binding IP_3. In marked contrast, Ca^{2+} entry could not be rescued using a mutant with a functional Ca^{2+} pore but defective IP_3 binding, simply suggesting that IP_3-binding to IP_3Rs, and not ER Ca^{2+} release triggers Ca^{2+} entry (VAN ROSSUM et al., 2004). Therefore, the possibility exists that increased IP_3 levels in NTAL-positive and Grb2-negative DT40 cells also directly influence IP_3R-gated Ca^{2+} entry channels, allocating the NTAL/Grb2 module an indirect role in the secretion-like coupling model. This could be further elucidated using *ip3r*$^{-/-}$ DT40 cells which are reconstituted with the IP_3R mutants described above and which are either positive for NTAL expression or deficient for Grb2. However, other studies do not support a requirement for IP_3 in TRPC3 and/or SOC gating (SUGAWARA et al., 1997; HOFMANN et al., 1999; BROAD et al., 2001; MA et al., 2001; VENKATACHALAM et al., 2001; TREBAK et al., 2003). It has been demonstrated that TRPC3 could be activated not by store-depletion but by DAG analogs (HOFMANN et al., 1999; VENKATACHALAM et al., 2001; TREBAK et al., 2003). In this scenario, channels would be activated contemporaneously with an increase in IP_3 and subsequent Ca^{2+} release, but it is the DAG produced as a result of PLC-γ activity and neither store depletion nor liganded IP_3Rs that opens the channels. Naturally, increased IP_3 levels in NTAL-positive or Grb2-negative DT40 cells are likely to reflect concomittantly increased DAG levels.

Physiologically, an increase in IP_3 or other Ca^{2+} mobilizing signals and subsequent Ca^{2+} release from the stores are the *sine qua non* of store-operated Ca^{2+} entry. Therefore, gating mechanisms for SOCs might differ between BCR signalling and pharmacological induced responses, e.g. the former might require IP_3/IP_3Rs whereas the latter does not. For example, receptor-mediated store depletion is spatially localized and temporally restricted, whereas thapsigargin globally depletes stores leading to an overriding stimulus independent of

PLC-γ2 activity. Further experiments will be necessary to determine the role of PLC-γ and/or IP_3 liganded IP_3Rs in gating Ca^{2+} channels of DT40 B lymphocytes and how the NTAL/Grb2 module may regulate this function.

Taken together, the studies and experiments described above allow for a refinement of the general principles underlying Ca^{2+} mobilization in B lymphocytes (figure 6.1; compare figure 2.2). (1) The BCR transmits information to the ER-resident IP_3Rs via the production of IP_3. This is mainly mediated by the Ca^{2+} initiation complex, and possibly fine-tuned by the NTAL/Grb2 module and further Grb2-dependent inhibitory effector molecule(s). (2) The ER transmits information back to the plasma membrane Ca^{2+} entry channels, e.g. via IP_3-liganded IP_3Rs or close interactions between the two membranes. (3) BCR engagement can also result in a "direct" modification of Ca^{2+} entry channels within the same membrane, e.g. via conformational changes. Alternatively, this "direct" modification is a result of lipase-dependent or -independent PLC-γ2 activities, e.g. via PLC-γ/TRP interactions or lipid mediators such as DAG. The last two steps might also be affected by the NTAL/Grb2 module and Grb2-dependent inhibitor(s), allowing for a dynamic Ca^{2+} signalling in response to antigen binding.

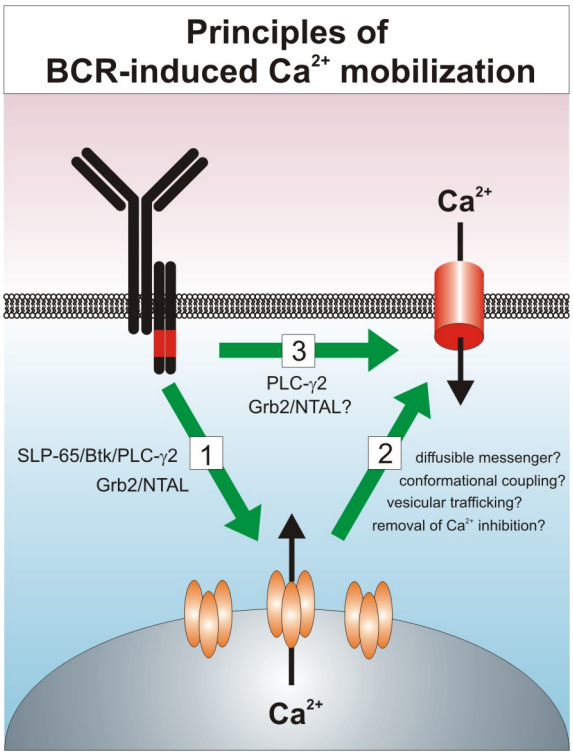

Figure 6.1: Ca^{2+} mobilization in B lymphocytes
Principle steps of the BCR-induced Ca^{2+} mobilization from intra- and extracellular sources (also refer to figure 2.1). (1) Antigen-binding by the BCR leads to the assembly of the Ca^{2+} initiation complex, PLC-γ2 activation, and subsequent IP3 production. This is possibly fine-tuned by the NTAL/Grb2 module and its downstream effector molecules. (2) The ER transmits information back to the plasma membrane Ca^{2+} entry channels, i.e. via a diffusible messenger, coupling processes (e.g. involving IP_3-liganded IP_3Rs), vesicular trafficking, or removal of Ca^{2+} inhibition. (3) BCR engagement can also lead to a direct activation of the Ca^{2+} entry channels. This may involve conformational changes or signalling molecules, e.g. PLC-γ2 itself or DAG. The last two steps could also be influenced by the NTAL/Grb2 module and Grb2-dependent inhibitor(s). (Modified from PATTERSON et al., 2005)

6.5. Dok-3 tyrosine phosphorylation is regulated by Grb2 in B lymphocytes

To achieve a deeper understanding of Grb2-dependent signalling pathways in DT40 B lymphocytes global tyrosine phosphorylation was analysed in Grb2-positive and -negative cells. Strikingly, the major tyrosine phosphorylated protein could not be detected by anti-pTyr immunoblot analysis in *grb2*$^{-/-}$ DT40 cells. During the course of this project, this protein was identified as Dok-3. Its complete tyrosine phosphorylation critically depends on the presence of Grb2, and the central SH2 domain and the C-terminal SH3 domain are particularly required.

The Grb2-dependent phosphorylation of Dok-3 was also confirmed in the murine system, using Grb2-deficient BAL17.TR mature B cells and variants in which wild-type Grb2 expression was reconstituted (HARMER and DEFRANCO, 1999; K. Neumann, PhD thesis in progress). Furthermore, it seems that Grb2 function concerning Dok-3 phosphorylation cannot be compensated by other members of the Grb2 adaptor family expressed in DT40 cells, e.g. Grap (HASHIMOTO et al., 1998) although Grb2 and Grap have highly related structures (59 % identity), and associate with the same proteins (FENG et al., 1996; TRUB et al., 1997). Dok-3 was reported to bind SHIP and Csk upon BCR stimulation, thus playing a role in the negative regulation of antigen receptor signalling in B cells (LEMAY et al., 2000). It has been proposed that the Dok-3/SHIP complex suppresses B-cell activation by selectively inhibiting the BCR-evoked activation of the Jun N-terminal protein kinase (Jnk) cascade (ROBSON et al., 2004).

The use of *lyn*$^{-/-}$ DT40 cells confirmed that PTK Lyn is capable of phosphorylating Dok-3 as reported previously (LEMAY et al., 2000). Lyn activity itself is regulated by various molecules. The best studied regulation mechanism involves the kinase-phosphatase pair Csk/CD45 that regulates the phosphorylation state of the C-terminal inhibitory tyrosine of Lyn. Yanagi et al. reported the generation of *chptpl*$^{-/-}$ DT40 cells which is the chicken homolog of CD45 (FANG et al., 1994; YANAGI et al., 1996). In these cells, BCR-induced tyrosine phosphorylation is almost completely abolished and resembles the pattern observed for *lyn*$^{-/-}$ cells (this thesis; TAKATA et al., 1994). Dok-3, the major tyrosine phosphorylated protein, also could not be detected by anti-pTyr immunoblot analysis in *chptpl*$^{-/-}$ DT40 cells (figure 3 in YANAGI et al., 1996). This observation provides further evidence that Lyn is the kinase responsible for Dok-3 phosphorylation along with the fact that Lyn is the only Src kinase expressed in DT40 B lymphocytes (TAKATA et al., 1994). Additionally, Dok-3 tyrosine phosphorylation was not altered in *syk*$^{-/-}$ or *btk*$^{-/-}$ DT40 cells (data not shown). Collectively, one might speculate that the Dok-3 phosphorylation by Lyn, the Csk binding by Dok-3 and the regulation of Lyn activity by Csk (see below) constitute a negative feedback loop in B lymphocytes which is independent of the transmembrane adaptor

PAG/Cbp. However, more experiments have to be performed to substantiate this hypothesis. Similar mechanisms were proposed for Dok-1 in the negative regulation of platelet-derived growth factor (PDGF)-induced mitogenesis (ZHAO et al., 2006) and Dok-2 in the attenuation of EGFR signalling (VAN SLYKE et al., 2005). Interestingly, these two reports revealed constitutive interactions between c-Src and Dok-1, and in greater detail between the c-Src SH3 domain and PxxP motifs in the C-terminal part of Dok-2 (VAN SLYKE et al., 2005; ZHAO et al., 2006). Whether such an association holds true for Lyn and Dok-3 in DT40 B lymphocytes awaits further clarification, but four core PxxP motifs also exist in avian Dok-3 (P^{296}VEP^{299}EAP, P^{322}GQP, and P^{398}SRP). Two of them (RFPP^{296}VEP and RPCP^{322}GQP) are indeed located within a class I ligand motif for SH3 domains, sharing the consensus motif (R/K)xxPxxP (FENG et al., 1994, 1995; SPARKS et al., 1996, 1998; MAYER, 2001; JIA et al., 2005). This is even more notable with regard to reports convincingly showing that Src family PTK activity is itself regulated by interactions with its SH3 domain, e.g. with the HIV accessory protein NEF, SHP-2 or UNC119 (MOAREFI et al., 1997; WALTER et al., 1999; CEN et al., 2003; GORSKA et al., 2004). This possibly suggests an even greater level of Dok-3-mediated regulation of Lyn activity. The SH3 domains of Src family PTKs bind preferentially to the (R/K)xxPxxP motif (RICKLES et al., 1994; ALEXANDROPOULOS et al., 1995), such as those found in avian Dok-3. The SH2-kinase linker region of Lyn has the canonical PxxP motif (amino acids 211-214) but lacks the flanking arginine. Therefore, this "imperfect" SH3 motif with low affinity binding can be easily displaced by a high affinity SH3 ligand (CEN et al., 2003). However, it seems that Grb2/Dok-3 complexes do not regulate Lyn activity by an all-or-nothing mechanism, since overall tyrosine phosphorylation patterns are not altered in *grb2*$^{-/-}$ or *dok-3*$^{-/-}$ DT40 cells. Interestingly, only two core PxxP motifs are present in the murine Dok-3 amino acid sequence and are not located within classical class I or II SH3 ligand motifs. Whether this difference contributes to the strong tyrosine phosphorylation of chicken Dok-3 in DT40 cells has to be investigated.

In summary, extensive Dok-3 tyrosine phosphorylation in DT40 B lymphocytes could be caused by two mechanisms, which are not mutually exclusive. First, Dok-3 is brought in perfect proximity to Lyn, e.g. via Grb2-supported plasma membrane recruitment (see below), direct interaction involving the Dok-3 PxxP motifs, or homotypic oligomerization processes. Homo- and heterotypic oligomerization processes were also described for Dok-1 and Dok-2 (SONGYANG et al., 2001; BOULAY et al., 2005). Second, the intense tyrosine phosphorylation signal is due to the massive expression of Dok-3 in DT40 cells, e.g. as indicated by the high levels of *dok-3* messenger RNA. Further experiments are currently underway to answer this question.

6.6. The phosphorylation-dependent Grb2-Dok-3 interaction: the hen-egg problem and beyond

In this thesis it was shown that the central SH2 domain of Grb2 binds to tyrosine phosphorylated Dok-3 upon BCR engagement in chicken, murine, and human B cells. This observation was somewhat unexpected since the SH2 domain itself together with the C-terminal SH3 domain are stringently required for Dok-3 tyrosine phosphorylation. The Grb2-dependent tyrosine phosphorylation of Dok-3 and the stimulation-dependent Grb2/Dok-3 interaction represent a typical hen-egg-problem.

In avian Dok-3 only two of the four tyrosines described for human and mouse amino acid sequences exist, i.e. the PTB domain proximal tyrosines Y^{307} and Y^{331}. The functional significance of the two PTB domain distal tyrosines is unclear, since substitution of these two residues with phenylalanine in murine Dok-3 had no impact on BCR-mediated signalling (ROBSON et al., 2004). Tyrosine Y^{331} represents a potential Grb2 SH2 domain binding site of the YxN type (Y^{331}ENI). Mutational analysis of this motif will ultimately determine if indeed it is the Grb2 interacting site (in progress). Weak Dok-3 tyrosine phosphorylation is also observed in *grb2*$^{-/-}$ DT40 cells. This Grb2-independent phosphorylation might occur at Y^{331} since the partially tyrosine phosphorylated Dok-3 is purified by GST-Grb2[SH2] fusion proteins. Robson et al. reported that the presence of the potential Grb2 binding site Y^{331}ENI is mandatory for Dok-3 phosphorylation (ROBSON et al., 2004). This was confirmed by overexpression studies of the chicken Dok-3 Y^{331}F variant in wild-type DT40 cells. In these cells, phosphorylation of the HA-tagged Dok-3 Y^{331}F variant was clearly diminished. A reduction in Dok-3 tyrosine phosphorylation was also observed in a derivative with a defective PTB domain (R197A). A complete lack of tyrosine phosphorylation was detected for a Dok-3 variant with deleted PH domain (ΔPH Dok-3), suggesting that the major contribution to subcellular localization is likely to be made by the Dok-3 PH domain (all data by K. Neumann, PhD thesis in progress).

A slightly increased tyrosine phosphorylation was seen in the Y^{307}F variant (K. Neumann, PhD thesis in progress). This is particularly notable with regard to the fact that an orthologous murine Dok-3 variant seemed to augment the inhibitory capacity in an interleukin (IL)-2 production assay in A20 cells (ROBSON et al., 2004). One might speculate that inhibition of the Dok-3/Csk interaction evoked by substitution of Y^{307} leads to enhanced Dok-3 global phosphorylation due to increased Lyn activity. The motif Y^{307}ASI reveals striking similarity to the Csk SH2 domain binding sites of SIT (YASV in human) and PAG/Cbp (YSSV in human) (BRDICKA et al., 2000; KAWABUCHI et al., 2000; PFREPPER et al., 2001). Previously it was shown by affinitiy purification experiments with GST Csk

[SH2] fusion proteins that the equivalent residue of murine Dok-3 (YASV) is necessary for Csk-Dok-3 interaction (ROBSON et al., 2004). It was also suggested that this interaction is enhanced by a functional Csk SH3 domain (LEMAY et al., 2000). Indeed it is necessary to note the striking similarities in the functional activities of the transmembrane adaptor SIT and the cytosolic adaptor Dok-3. Both molecules inducibly associate with Grb2 and Csk, and both molecules negatively regulate BCR-induced activation of the transcription factor NFAT (LEMAY et al., 2000; PFREPPER et al., 2001). Further studies are required to confirm whether these two adaptors fulfill overlapping or different functions in BCR-induced signalling. Both PTB domain proximal tyrosine residues of murine Dok-3 were shown to be bound by the SH2 domain of SHIP (ROBSON et al., 2004). A bidentated mechanism of Dok-3-SHIP interaction was suggested, since tyrosine phosphorylated SHIP could also be purified with GST-Dok-3 [PTB] fusion proteins (LEMAY et al., 2000). The exact interaction modes with known and possibly unknown binding partners are currently under investigation using wild-type Dok-3 and derivatives in immuno- and affinity purification experiments.

Interestingly, tyrosine phosphorylation is predicted by an artificial neural network method (NetPhos 2.0 Server, BLOM et al., 1999) for two tyrosines within the PH domain (Y^{11} and Y^{96}) and one tyrosine located in the PH-PTB interdomain (Y^{140}). It has been postulated that post-translational modifications (such as serine/threonine or tyrosine phosphorylation) or oligomerization might enable low affinity PH domain-containing molecules to bind membranes with more avidity (LEMMON and FERGUSON, 2000). Thus, Y^{11} and Y^{96} could regulate the affinity of the Dok-3 PH domain for membrane lipids. Phosphorylation of the tyrosine within the PH-PTB interdomain was proposed to be a critical step in hetero- and homotypic oligomerizations of the paralogs Dok-1 and Dok-2 (SONGYANG et al., 2001; BOULAY et al., 2005). Accordingly, Y^{140} might promote maximal Dok-3 tyrosine phosphorylation by supporting oligomerization processes. Recently it was reported that a pYxxY/F/W motif is bound by a C2 domain in a sequence-specific manner (BENES et al., 2005). Whether the putative pY^{140}SSW motif associates with molecules containing SH2, PTB or possibly C2 domains remains to be demonstrated. The relevance of these tyrosines for maximal Dok-3 tyrosine phosphorylation and for potential interactions with other molecules is also currently under study.

To shed light on the hen-egg-problem of the Grb2-dependent Dok-3 tyrosine phosporylation, the following mechanism is proposed. BCR engagement leads to tyrosine phosphorylation of Dok-3 at tyrosine Y^{331}. This site is then bound by the Grb2 SH2 domain, leading to a conformational “opening” of Dok-3. This in turn enables Dok-3 to localize at the plasma membrane probably via its PH domain and/or its PTB domain. Finally, membrane recruitment leads to complete tyrosine phosphorylation of Dok-3 catalyzed by

Lyn. Alternatively, the Grb2-mediated conformational "opening" of Dok-3 may only occur following its localization to the plasma membrane since tyrosine phosphorylation is completely abolished in the ΔPH Dok-3 variant (see above). It is likely that a Grb2-induced conformational "opening" of Dok-3 additionally facilitates homotypic oligomerization processes, leading to the maximal Dok-3 tyrosine phosphorylation observed in Grb2-positive cells. The C-terminal Grb2 SH3 domain may stabilize the association of Dok-3 with Lyn and/or the plasma membrane. This hypothesis is supported by several observations. First, Grb2 recruitment to the membrane according to this mechanism would depend on Dok-3 bringing Grb2 to the plasma membrane via a piggyback mechanism. Preliminary data reveals that recruitment of Grb2-EGFP is tremendously impaired in *dok-3*$^{-/-}$ DT40 cells (I. Goldbeck, PhD thesis in progress). Second, it was shown that a Dok-3-EGFP fusion protein is constitutively and Grb2-independently phosphorylated and permanently located at the plasma membrane (I. Goldbeck, PhD thesis in progress). This observation suggests that EGFP fusion to the C-terminus of chicken Dok-3 mimics binding of Grb2, thereby leading to membrane recruitment and complete tyrosine phosphorylation. Third, inducible plasma membrane recruitment via the PH domain was previously reported for Dok-1 (ZHAO et al., 2001). Collectively, the above hypothesis would explain the importance of Dok-3 Y^{331} and the SH2 domain of Grb2 for complete Dok-3 tyrosine phosphorylation. Intriguingly, this proposed mechanism represents a slight modification of a model published in 1995 (MAYER et al., 1995). The authors report that the substrate specificity of a non-receptor tyrosine kinase is dependent on the binding specificity of its associated SH2 domain. In this case, the SH2 domain binds to a subset of proteins tyrosine phosphorylated by its own catalytic domain, finally leading to a processive phosphorylation of those substrates. Strikingly, it was demonstrated that the non-receptor tyrosine kinase Abl can aquire an additional SH2 domain *in trans* by binding to the adaptor Crk through the Crk SH3 domain. In this case the bound adaptor serves as processivity factor initiating the processive phosphorylation (MAYER et al., 1995). The Grb2 SH2 domain binds with high affinity to partially tyrosine-phosphorylated Dok-3, and it could be shown that the C-terminal SH3 domain is also required for maximal Dok-3 tyrosine phosphorylation. It is tempting to speculate that Grb2 serves as processivity factor for Lyn-catalyzed Dok-3 tyrosine phosphorylation with the Grb2 SH3 domain holding Dok-3 in the vicinity of Lyn. In this scenario, the Grb2 SH3 domain may bind to Lyn directly or via further mediators, e.g. the Grb2-associated binder (Gab) family. It was shown that the C-terminal Grb2 SH3 domain can bind to sites containing either the canonical PxxP motif (e.g. present in Lyn) or

the atypical Px_3Rx_2KP motif (e.g. present in Gab proteins) (LOCK et al., 2000; SCHAEPER et al., 2000; LEWITZKY et al., 2001).

6.7. Do the Grb2-interacting adaptors Dok-3 and Shc have redundant functions in B cell signalling?

The next question that arises is the immunological relevance of the Grb2/Dok-3 interaction in B lymphocytes. To answer this question the scaffolding properties of Dok-3 and its interaction with catalytically active molecules have to be elucidated. Interestingly, Dok-3 is not the only molecule in B lymphocytes which is bound by the Grb2 SH2 domain upon BCR stimulation and whose tyrosine phosphorylation depends on Grb2. Both of these properties also apply to the adaptor molecule Shc (HARMER and DEFRANCO, 1999). Additionally, it was shown that Shc tyrosine phosphorylation strongly depends on Shc having a functional PTB domain, and the presence of SHIP (INGHAM et al., 1999). Harmer and DeFranco claimed that efficient binding of tyrosine phosphorylated SHIP and the Shc PTB domain requires Grb2, with Grb2 binding to Shc via its SH2 domain and to SHIP via its SH3 domains (HARMER and DEFRANCO, 1999). A ternary SHIP/Grb2/Shc complex would be analogous to the SOS/Grb2/Shc complex, which has been implicated in the regulation of the Ras/MAPK pathway (SAXTON et al., 1994; NAGAI et al., 1995; CROWLEY et al., 1996; HARMER and DEFRANCO, 1997). It has been proposed that SHIP may indirectly inhibit Ras activation by competing with SOS for binding to Shc and Grb2 (CHACKO et al., 1996; TRIDANDAPANI et al., 1997). However, whether SHIP may be involved in this function still remains unclear since the activation of the MAPK cascade seems to be unaffected in *ship*$^{-/-}$ DT40 cells (OKADA et al., 1998). Furthermore, it could be shown that Shc is not required for BCR-induced ERK response (HASHIMOTO et al., 1998). However, Hashimoto et al. suggested that Grb2 plays an important role in Ras activation, since the extent of ERK inhibition was comparable in DT40 cells expressing a dominant negative variant of Ras (RasN17) and in *grb2*$^{-/-}$ DT40 cells. Oh-hora et al. subsequently presented data that RasGRP3 couples PLC-γ2 to Ras after BCR engagement (OH-HORA et al., 2003). Therefore, it seems that the SOS/Grb2/Shc complex is not required for BCR-induced Ras/ERK activation. However, in the case of EGFR-mediated Ras activation it could indeed be demonstrated that the Grb2/SOS pathway also operates in the DT40 system (OH-HORA et al., 2003). Interestingly, the Dok family members Dok-1, Dok-2, and Dok-3 were all implicated in the regulation of Ras/ERK signalling (CONG et al., 1999; JONES and DUMONT, 1999; WICK et al., 2001; VAN SLYKE et al., 2005). This was also confirmed *in vivo* by using mice deficient for Dok-1 and/or Dok-2 (YAMANASHI et al., 2000; NIKI et al., 2004; YASUDA

et al., 2004; SHINOHARA et al., 2005). Both Dok-1 and Dok-2 have been shown to inducibly interact with p120 RasGAP via C-terminal phosphotyrosines (CARPINO et al., 1997; DI CRISTOFANO et al., 1998; NELMS et al., 1998; WICK et al., 2001). Dok-3 does not harbor a RasGAP-binding motif nor bind p120 RasGAP (CONG et al., 1999; LEMAY et al., 2000). Yet a role for Dok-3 in the activation of the Ras/ERK pathway was deduced from the following two observations. First, forced expression of Dok-3 in 293 cells inhibits ERK activation (CONG et al., 1999). Second, in a recent study using 293T cells it was suggested that Dok-3 sequesters Grb2 and SOS from Shc and thereby inhibits the Ras/ERK pathway downstream of PTKs (HONMA et al., 2006). Whether this mechanism functions in BCR-induced Ras/ERK activation in B lymphocytes is at best questionable for the reasons stated above. Nonetheless, given the fact that Grb2 plays a role in both BCR- and EGFR-induced Ras/ERK activation (HASHIMOTO et al., 1998; HASHIMOTO et al., 1999), it will be interesting to analyse these processes in the *dok-3*$^{-/-}$ DT40 cell lines. This is of particular importance in regard to the potential involvement of Dok-3 in the recruitment of Grb2 to the plasma membrane (see above).

It is tempting to speculate that a putative SHIP/Grb2/Dok-3 complex might play a similar functional role in B lymphocytes. However, several differences between Shc and Dok-3 must be considered. One important aspect is that Dok-3 becomes readily tyrosine-phosphorylated in *ship*$^{-/-}$ DT40 cells (data not shown). Efficient BCR-induced tyrosine phosphorylation of Shc requires kinase activity of Syk (NAGAI et al., 1995; RICHARDS et al., 1996), whereas Dok-3 phosphorylation is independent of Syk (this thesis; LEMAY et al., 2000). It seems that the Dok-3/SHIP interaction is mainly mediated by binding of the SHIP SH2 domain to phosphotyrosines of Dok-3 (LEMAY et al., 2000). The Dok-3 PTB domain binds phospho-SHIP only to a minor extent especially compared to the Shc PTB domain (LEMAY et al., 2000). Nevertheless, it is well accepted that the increase in BCR, FcεRI, or FcγR signalling observed in SHIP-deficient cells implies that SHIP can inhibit immunoreceptor signalling without the deliberate co-aggregation of the immunoreceptors with ITIM-bearing receptors like FcγRIIB (SAXTON et al., 1994; CROWLEY et al., 1996; BOLLAND et al., 1998; VEILLETTE et al., 2002). One might speculate that Dok-3 is involved in this FcγRIIB-independent process, e.g. by recruiting SHIP via its SH2 domain to the plasma membrane. In this scenario, it would be interesting to analyse whether membrane recruitment of SHIP is altered in *dok-3*$^{-/-}$ cells compared to wild-type DT40 cells. It is known that the 5'-phosphatase activity of SHIP is not regulated by tyrosine phosphorylation or interaction with adaptor proteins. Rather, it is commonly believed that its activity is determined by its localization (ROHRSCHNEIDER et al., 2000). Intriguingly, a

SHIP/Grb2/Dok-1 complex was proposed to play a role in FcεRI-mediated signalling in human mast cells (KEPLEY et al., 2004). However, the authors do not comment on the mode of Grb2-Dok-1 interaction. This would be interesting to elucidate, since Dok-1 lacks a classical YxN site for the interaction with the Grb2 SH2 domain.

Collectively, further studies are required to ultimately determine the interplay between the cytosolic adaptor molecules Grb2, Dok-3, and Shc. It is possible that both the Grb2/Shc complex and the Grb2/Dok-3 complex fulfill some redundant functions, but this is not necessarily the case. Current experiments are focused on the known Dok-3-bound effector molecules SHIP and Csk, but other unknown molecules may also participate in Dok-3-regulated pathways in B lymphocytes. In the future affinity purification experiments with GST fusion proteins containing either the PTB domain of Dok-3, or its tyrosine phosphorylated C-terminal part will hopefully give new insights how Dok-3 exerts its function in DT40 B lymphocytes. In this thesis it could be demonstrated that the negative regulation of BCR-induced Ca^{2+} mobilization belongs to those functions.

6.8. The NTAL/Grb2 module and Dok-3: shaping Ca^{2+} signals in B lymphocytes

The inhibitory adaptor molecule Dok-3 was demonstrated to negatively regulate Ca^{2+} mobilization in B lymphocytes. Dok-3 tyrosine phosphorylation depends on the central SH2 and the C-terminal SH3 domain of Grb2. Together with the fact that Dok-3 is also a major interacting partner for the Grb2 SH2 domain, it is likely that the NTAL/Grb2 module is connected to Dok-3. In this scenario, Grb2 seems to be a molecular switch in BCR-induced Ca^{2+} mobilization. The SH2-domain-dependent association of Grb2 with either tyrosine phosphorylated NTAL or Dok-3 ultimately leads to a positive or negative fine-tuning of antigen receptor-induced Ca^{2+} mobilization in B lymphocytes. Both the expression levels of NTAL and Dok-3 during B cell development and the Grb2-dependent tyrosine phosphorylation of Dok-3 are crucial parameters in this pathway.

Although more experiments are needed to confirm this hypothesis, some striking observations indicate a connection between these three adaptor molecules in BCR-induced Ca^{2+} mobilization. Firstly, for both the negative regulation of Ca^{2+} mobilization and Dok-3 tyrosine phosphorylation, the demands on Grb2 domains are identical, i.e. the central SH2 domain and the C-terminal SH3 domain are obligatory for both processes. Secondly, it seems that Dok-3 tyrosine phosphorylation is reduced in NTAL-overexpressing DT40 cells, whereas tyrosine phosphorylation of other PTK substrates is unaffected (data not shown). Third, in prelimenary experiments it was shown that forced expression of NTAL had no enhancing effect on BCR-induced Ca^{2+} mobilization in *dok-3*$^{-/-}$ DT40 cells (data not shown).

This is probably the strongest evidence for the assumption that Dok-3 is indeed the downstream inhibitory element which is regulated by the NTAL/Grb2 module.

Dok-3 tyrosine phosphorylation cannot be rescued in cells expressing the chimeric TM-Grb2 (data not shown and I. Goldbeck, PhD thesis in progress). These results were somewhat surprising since both TM-Grb2 and Lyn are located in lipid rafts. These observations indicate that enhanced Ca^{2+} mobilization in NTAL-positive DT40 cells may not be due to the sequestration of Grb2 to the lipid rafts, but as a consequence of the inability of this chimeric protein to support a conformational "opening" of Dok-3 and subsequent tyrosine phosphorylation. This could be due to restricted degrees of freedom in the chimeric protein. Therefore, to investigate if the targeting of Grb2 to lipid rafts causes the observed phenotypes, it could be useful to express a soluble form of NTAL consisting only of the cytoplasmatic domain and thus incapable of localizing in lipid rafts. A tyrosine phosphorylated soluble form of NTAL should be bound by the Grb2 SH2 domain with the same affinity as wild-type NTAL. A similar variant of LAT indeed became phosphorylated upon TCR stimulation and inhibited T-cell activation by recruiting PLC-γ1 and Grb2 (TORGERSEN et al., 2001). It might be that Grb2 sequestration by a soluble form of NTAL is sufficient to positively regulate BCR-induced Ca^{2+} mobilization.

Current experiments are aiming at the downstream effector molecule of Dok-3. As stated previously, Dok-3 associates with both SHIP and Csk (LEMAY et al., 2000). Intriguingly, a similarly increased Ca^{2+} mobilization from intra- and extracellular sources can be observed in *ship*$^{-/-}$, *grb2*$^{-/-}$, and *dok-3*$^{-/-}$ DT40 cells suggesting that SHIP is at least part of the effector machinery regulated by Grb2/Dok-3. Since NTAL expression in *ship*$^{-/-}$ DT40 cells still results in an enhanced BCR-induced Ca^{2+} mobilization (see section 6.3), it appears that this effect cannot solely be attributed to SHIP. The expression of dominant negative variants of Dok-3 in *ship*$^{-/-}$ DT40 cells will shed further light on other Grb2/Dok-3 regulated pathways influencing BCR-induced Ca^{2+} mobilization (K. Neumann, in progress). Alternatively, with the *dok-3* targeting constructs prepared during this thesis the generation of *dok-3*$^{-/-}$ *ship*$^{-/-}$ DT40 cells is possible. The double-deficient cell line and *ship*$^{-/-}$ DT40 cells could then be used to identify Dok-3-dependent, but SHIP-independent regulatory pathways.

As described above, the second known effector molecule bound by Dok-3 is Csk. It is reasonable to assume that Csk influences the extent of Ca^{2+} mobilization in B lymphocytes via the regulation of Lyn activity. However, to date *csk*$^{-/-}$ DT40 cells were not reported to reveal an altered Ca^{2+} mobilization (HATA et al., 1994). Definitely, these studies have to be extended. Interestingly, Ca^{2+} elevation was enhanced in primary B cells obtained from *lyn*$^{-/-}$ mice, although the initiation of the response showed a slightly longer delay (CHAN et al.,

1998). In *lyn*$^{-/-}$ DT40 cells, IP_3 production was slightly increased (TAKATA et al., 1994). However, crosslinking of BCR on *lyn*$^{-/-}$ DT40 cells evoked a considerably delayed and slow Ca^{2+} mobilization (TAKATA et al., 1994). Surprisingly, primary B cells expressing a gain-of-function Lyn tyrosine kinase mutant ($Y^{508}F$) show constitutive phosphorylation of Syk and PLC-γ2 and also a heightened Ca^{2+} mobilization in response to BCR stimulation (HARDER et al., 2001; HIBBS et al., 2002). As stated above, Lyn activity is regulated by multiple mechanisms, both tyrosine phosphorylation-dependent and -independent. Future experiments aiming at the phosphorylation state of the regulatory tyrosine residue of Lyn in *dok-3*$^{-/-}$ cells and also *in vitro* Lyn kinase assays will elucidate the importance of Dok-3/Csk complexes or even Lyn-Dok-3 associations (as discussed above) in BCR-induced Ca^{2+} mobilization.

However, SHIP and/or Csk may not be the only effector molecules regulated by Dok-3 and affecting BCR-induced Ca^{2+} mobilization. A connection between PTK Tec and Dok-1 or Dok-2 was reported in various cell lines (VAN DIJK et al., 2000; YOSHIDA et al., 2000; LIANG et al., 2002). Tec was shown both to associate with and to phosphorylate Dok-1 in Ramos B lymphocytes (VAN DIJK et al., 2000; YOSHIDA et al., 2000). It was further demonstrated that both the Tec/Dok-1 complex formation and Tec-dependent Dok-1 phosphorylation require PI3K activity (VAN DIJK et al., 2000). All of these characteristics were shown to be specific for Tec, since none of the other Tec family members (Btk, Bmx, Itk) phosphorylated Dok-1 as efficiently (YOSHIDA et al., 2000). This agrees with the observation that Dok-3 phosphorylation is not affected in *btk*$^{-/-}$ DT40 cells. However, a thorough assessment of the interplay of Dok-3 and Tec family PTKs in DT40 B lymphocytes has not yet come. Furthermore, the involvement of PI3K activity in Dok-3 tyrosine phosphorylation or in Dok-3-regulated pathways remains to be analysed.

The data obtained for the TM-PLC-γ2 chimera suggests an even more direct involvement of Dok-3 in the PLC-γ-Ca^{2+} pathway. A direct interaction between the PLC-γ1 SH2 domain and Dok-1 was demonstrated by affinity purification experiments (VAN DIJK et al., 2000). Dok-1-mediated inhibition of Ca^{2+} mobilization was observed upon CD2 crosslinking in Jurkat T cells and upon FcεRI-FcγRIIB coaggregation in RBL-2H3 cells (NEMORIN et al., 2001; OTT et al., 2002). A significant influence of Dok-3 on Ca^{2+} mobilization was also shown in A20 cells, albeit neglected by the authors (ROBSON et al., 2004). Forced expression of a murine Dok-3 variant in which all four PTB-domain distal tyrosines were replaced by phenylalanine caused an increased Ca^{2+} mobilization, suggesting a dominant negative effect of that derivative (figure 6F in ROBSON et al., 2004). However, overexpression of wild-type Dok-3 similarly led to an enhanced Ca^{2+} mobilization (figure

6F in ROBSON et al., 2004). These observations were confirmed in DT40 B cells by overexpression of the corresponding avian derivatives (K. Neumann, PhD thesis in progress). Interestingly, the overall phosphorylation state of PLC-γ2 seemed to be altered in A20 cells overexpressing wild-type or dominant negative Dok-3, but again the authors deemed it significance (figure 6C in ROBSON et al., 2004). Whether Dok-3 can indeed fulfill a direct regulatory role on PLC-γ2 activity remains to be proved. However, the observations that forced expression of wild-type Dok-3 can lead to enhanced Ca^{2+} mobilization suggest the importance of a tightly regulated Dok-3 expression level. Taken together, it is tempting to speculate that Dok-3 directly influences membrane recruitment or retention time of PLC-γ2 in DT40 B lymphocytes. A complete biochemical characterization of the *dok-3*$^{-/-}$ DT40 cell lines will hopefully give new insights into these functions.

In figure 6.2 the "revised Ca^{2+} signalling toolkit" of B lymphocytes is summarized. During this thesis new pathways fine-tuning the BCR-induced Ca^{2+} mobilization were identified and characterized. BCR crosslinking leads to the activation of PTKs and the subsequent assembly of the Ca^{2+} initiation complex. PLC-γ2-mediated IP_3 production leads to Ca^{2+} release from intracellular stores. Ca^{2+}-permeable channels in the plasma membrane are opened and allow for Ca^{2+} entry from extracellular sources. The regulation of those plasma membrane resident Ca^{2+} channels awaits further clarification. However, store depletion and/or "direct" modifications, e.g. by conformational changes and/or as a result of PLC-γ2 or lipid mediators, are likely to be involved in the regulated gating of the channels (see figure 6.1). In this revised model, BCR engagement and PTK activation also result in tyrosine phosphorylation of Dok-3, and plasma membrane recruitment of Dok-3/Grb2 complexes. Tyrosine phosphorylated Dok-3 exerts its inhibitory function via the previously described effector molecules SHIP and/or Csk, or possibly via so far unidentified Dok-3-associated molecule(s). Alternatively, Dok-3/Grb2 complexes directly influence the activity and/or membrane localization of components of the Ca^{2+} initiation complex (figure 6.2, left panel). The extent of this inhibitory regulation orchestrated by Dok-3 critically depends on the expression of NTAL. The presence of constitutively plasma membrane localized NTAL leads to tyrosine phosphorylation-dependent sequestration of Grb2, thereby preventing the association of Grb2 with Dok-3 and the subsequent membrane recruitment and tyrosine phosphorylation of Dok-3 (figure 6.2, right panel). The removal of these inhibitory elements in NTAL-positive cells ultimately results in enhanced Ca^{2+} mobilization, resembling the profiles observed for SHIP-, Grb2-, or Dok-3-negative cells. Obviously the balanced expression levels of NTAL and Dok-3 during B cell lymphopoiesis allow for a specific regulation of pathways dependent on the ubiquitous second messenger

Grb2. The revised BCR-induced Ca^{2+} mobilization model presented once again emphasizes the importance of a coordinated interplay of positive and negative signalling pathways.

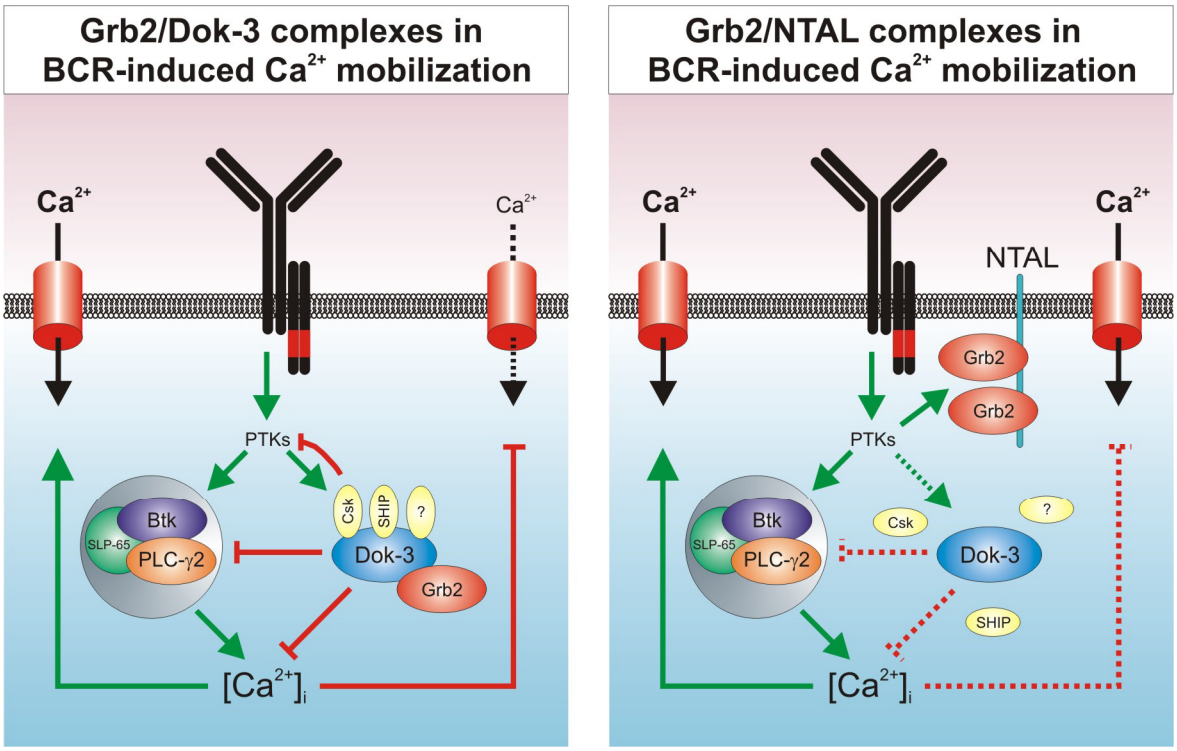

Figure 6.2: The "Ca^{2+} signalling toolkit" of B lymphocytes
BCR engagement leads to the activation of PTKs and the assembly of the Ca^{2+} initiation complex. PLC-γ2-mediated IP3 production leads to Ca^{2+} release from intracellular stores. Additionally, Ca^{2+}-permeable channels in the plasma membrane are opened and allow for Ca^{2+} entry from extracellular sources. BCR crosslinking and PTK activation also result in tyrosine phosphorylation of Dok-3 and plasma membrane recruitment of **Grb2/Dok-3 complexes**. Tyrosine phosphorylated Dok-3 exerts its inhibitory function via SHIP and/or Csk, or possibly via so far unknown Dok-3-associated molecule(s). Alternatively, Grb2/Dok-3 complexes directly influence the activity and/or membrane localization of components of the Ca^{2+} initiation complex (left panel). The presence of NTAL leads to tyrosine phosphorylation-dependent sequestration of Grb2. The formation of **Grb2/NTAL complexes** prevents the association of Grb2 with Dok-3 and the subsequent membrane recruitment and tyrosine phosphorylation of Dok-3. The removal of these inhibitory elements in NTAL-positive cells ultimately causes an enhanced Ca^{2+} mobilization (right panel).

6.9. Conclusions and outlook

In my opinion, two major fields are of particular interest to elucidate the biological relevance of the pathways described in this thesis. The first critical factor that should be considered is the connection between Ca^{2+} signalling and the cytoskeleton. There already exist many overlaps between components of the Ca^{2+} mobilization machinery and the cytoskeleton. For example, Grb2 was shown to bind dynamin via its SH3 domain (GOUT et

al., 1993; MIKI et al., 1994; SEEDORF et al., 1994). Members of the dynamin superfamily of large GTPases essentially participate in clathrin-mediated endocytosis (ORTH and MCNIVEN, 2003). Dynamin was also shown to interact with the SH3 domain of PLC-γ (SEEDORF et al., 1994; CHOI et al., 2004). Choi et al. could show that PLC-γ1 is a GEF for dynamin-1 and enhances dynamin-1-dependent EGFR endocytosis (CHOI et al., 2004). Vice versa, dynamin-2 is required for efficient Ca^{2+} mobilization and PLC-γ1 tyrosine phosphorylation in T cells (GOMEZ et al., 2005). PLC-γ isoforms were also reported to associate with the actin cytoskeleton during their translocation to the plasma membrane (REBECCHI and PENTYALA, 2000; RHEE, 2001). Close structural and functional links between PLC-γ and the Rho/Rac/Cdc42 family of GTPases, which participate in secretion and trafficking processes, were revealed (ARRIEUMERLOU et al., 2000; HONG-GELLER and CERIONE, 2000; ZENG et al., 2000). Strikingly, results obtained by Piechulek et al. suggest a novel mechanism of PLC-γ2 activation by Rac GTPases involving neither tyrosine phosphorylation nor PI3K-mediated $PI(3,4,5)P_3$ generation (PIECHULEK et al., 2005). Finally, it is known that store-operated Ca^{2+} channels are GTPase-dependent and are affected by actin cytoskeletal rearrangements (FASOLATO et al., 1993; FERNANDO et al., 1997; PATTERSON et al., 1999; YAO et al., 1999; ROSADO et al., 2000). All of the data described above indicate the importance of the cytoskeleton for Ca^{2+} mobilization, and future experimental set-ups should focus on the inputs that the Ca^{2+} signalling machinery receive from cytoskeletal components, and vice versa.

The second major issue is the role of Ca^{2+} signalling in B cell fate decision. Given the tightly regulated expression levels of NTAL during B cell development and the fundamentally different biological responses of immature and mature B lymphocytes to BCR stimulation (i.e. apoptosis versus activation), it is tempting to speculate that Grb2/NTAL/Dok-3-regulated Ca^{2+} signalling may be involved in processes such as tolerance induction. This is supported by the differences in Ca^{2+} mobilization between anergic and naïve B cells described in the introduction. Generally, Ca^{2+} responses can be subdivided into short-term, rapid responses and long-term modifications. The latter requires changes in gene expression, which ultimately govern B cell development and differentiation. Increased intracellular Ca^{2+} concentrations support nuclear translocation of two important sets of transcription factors, i.e. the NFAT and the NF-κB family (DOLMETSCH et al., 1997; HIKIDA and KUROSAKI, 2005). NF-κB activation occurs after a large transient Ca^{2+} rise, and NFAT activation is promoted by a slow but sustained Ca^{2+} elevation (DOLMETSCH et al., 1997; HIKIDA and KUROSAKI, 2005). The requirement for

differential Ca^{2+} signals for these two sets of transcription factors once again underlines the importance of adaptor-mediated regulation of Ca^{2+} mobilization in B lymphocytes.

In this thesis it was demonstrated that the adaptor molecules Grb2, NTAL, and Dok-3 are of particular importance for the modulation of BCR-induced Ca^{2+} mobilization. It will be fascinating to analyse whether this novel Ca^{2+} signalling pathway also functions in other immune cells. For example, all three adaptors are also expressed in myeloid lineages. The impact of this Ca^{2+} signalling pathway on the outcome of humoral immune responses must be supported by further experiments with currently available and future mouse models.

7. References

Aguado, E., Richelme, S., Nunez-Cruz, S., Miazek, A., Mura, A. M., Richelme, M., Guo, X. J., Sainty, D., He, H. T., Malissen, B., and Malissen, M. (2002). Induction of T helper type 2 immunity by a point mutation in the LAT adaptor. *Science* **296**, 2036-2040.

Alexandropoulos, K., Cheng, G., and Baltimore, D. (1995). Proline-rich sequences that bind to Src homology 3 domains with individual specificities. *Proc Natl Acad Sci U S A* **92**, 3110-3114.

Aman, M. J., and Ravichandran, K. S. (2000). A requirement for lipid rafts in B cell receptor induced Ca(2+) flux. *Curr Biol* **10**, 393-396.

Applegate, T. L., Karjalainen, A., and Bygrave, F. L. (1997). Rapid Ca2+ influx induced by the action of dibutylhydroquinone and glucagon in the perfused rat liver. *Biochem J* **323 (Pt 2)**, 463-467.

Arrieumerlou, C., Randriamampita, C., Bismuth, G., and Trautmann, A. (2000). Rac is involved in early TCR signaling. *J Immunol* **165**, 3182-3189.

Ausubel, F.M., Brent, R., Kingdom, R.E., Moore, D.M., Seidman, J.G., Smith, J.A., and Struhl, K., Eds. (1995). *Current Protocols in Molecular Biology*. (John Wiley & Sons, NY).

Baba, T. W., and Humphries, E. H. (1984). Differential response to avian leukosis virus infection exhibited by two chicken lines. *Virology* **135**, 181-188.

Baba, T. W., Giroir, B. P., and Humphries, E. H. (1985). Cell lines derived from avian lymphomas exhibit two distinct phenotypes. *Virology* **144**, 139-151.

Bae, Y. S., Cantley, L. G., Chen, C. S., Kim, S. R., Kwon, K. S., and Rhee, S. G. (1998). Activation of phospholipase C-gamma by phosphatidylinositol 3,4,5-trisphosphate. *J Biol Chem* **273**, 4465-4469.

Baeuerle, P. A., and Henkel, T. (1994). Function and activation of NF-kappa B in the immune system. *Annu Rev Immunol* **12**, 141-179.

Barritt, G. J. (1998). Does a decrease in subplasmalemmal Ca2+ explain how store-operated Ca2+ channels are opened? *Cell Calcium* **23**, 65-75.

Barritt, G. J. (1999). Receptor-activated Ca2+ inflow in animal cells: a variety of pathways tailored to meet different intracellular Ca2+ signalling requirements. *Biochem J* **337 (Pt 2)**, 153-169.

Bedirian, A., Baldwin, C., Abe, J., Takano, T., and Lemay, S. (2004). Pleckstrin homology and phosphotyrosine-binding domain-dependent membrane association and tyrosine phosphorylation of Dok-4, an inhibitory adapter molecule expressed in epithelial cells. *J Biol Chem* **279**, 19335-19349.

Bell, S. E., Vigorito, E., McAdam, S., Reynolds, H. M., Caraux, A., Colucci, F., and Turner, M. (2004). PLCgamma2 regulates Bcl-2 levels and is required for survival rather than differentiation of marginal zone and follicular B cells. *Eur J Immunol* **34**, 2237-2247.

Benes, C. H., Wu, N., Elia, A. E., Dharia, T., Cantley, L. C., and Soltoff, S. P. (2005). The C2 domain of PKCdelta is a phosphotyrosine binding domain. *Cell* **121**, 271-280.

Benschop, R. J., Aviszus, K., Zhang, X., Manser, T., Cambier, J. C., and Wysocki, L. J. (2001). Activation and anergy in bone marrow B cells of a novel immunoglobulin transgenic mouse that is both hapten specific and autoreactive. *Immunity* **14**, 33-43.

Berridge, M. J. (1993). Inositol trisphosphate and calcium signalling. *Nature* **361**, 315-325.

Berridge, M. J. (1997a). The AM and FM of calcium signalling. *Nature* **386**, 759-760.

Berridge, M. J. (1997b). Elementary and global aspects of calcium signalling. *J Exp Biol* **200**, 315-319.

Berridge, M. J., Lipp, P., and Bootman, M. D. (2000). The versatility and universality of calcium signalling. *Nat Rev Mol Cell Biol* **1**, 11-21.

Berry, D. M., Nash, P., Liu, S. K., Pawson, T., and McGlade, C. J. (2002). A high-affinity Arg-X-X-Lys SH3 binding motif confers specificity for the interaction between Gads and SLP-76 in T cell signaling. *Curr Biol* **12**, 1336-1341.

Bezprozvanny, I., and Ehrlich, B. E. (1993). ATP modulates the function of inositol 1,4,5-trisphosphate-gated channels at two sites. *Neuron* **10**, 1175-1184.

Bird, G. S., Rossier, M. F., Hughes, A. R., Shears, S. B., Armstrong, D. L., and Putney, J. W., Jr. (1991). Activation of Ca2+ entry into acinar cells by a non-phosphorylatable inositol trisphosphate. *Nature* **352**, 162-165.

Blom, N., Gammeltoft, S., and Brunak, S. (1999). Sequence and structure-based prediction of eukaryotic protein phosphorylation sites. *J Mol Biol* **294**, 1351-1362.

Blomberg, N., Baraldi, E., Nilges, M., and Saraste, M. (1999). The PH superfold: a structural scaffold for multiple functions. *Trends Biochem Sci* **24**, 441-445.

Boardman, P. E., Sanz-Ezquerro, J., Overton, I. M., Burt, D. W., Bosch, E., Fong, W. T., Tickle, C., Brown, W. R., Wilson, S. A., and Hubbard, S. J. (2002). A comprehensive collection of chicken cDNAs. *Curr Biol* **12**, 1965-1969.

Bobe, R., Wilde, J. I., Maschberger, P., Venkateswarlu, K., Cullen, P. J., Siess, W., and Watson, S. P. (2001). Phosphatidylinositol 3-kinase-dependent translocation of phospholipase Cgamma2 in mouse megakaryocytes is independent of Bruton tyrosine kinase translocation. *Blood* **97**, 678-684.

Bolland, S., Pearse, R. N., Kurosaki, T., and Ravetch, J. V. (1998). SHIP modulates immune receptor responses by regulating membrane association of Btk. *Immunity* **8**, 509-516.

Bonilla, F. A., Fujita, R. M., Pivniouk, V. I., Chan, A. C., and Geha, R. S. (2000). Adapter proteins SLP-76 and BLNK both are expressed by murine macrophages and are linked to signaling via Fcgamma receptors I and II/III. *Proc Natl Acad Sci U S A* **97**, 1725-1730.

Bootman, M. D., and Lipp, P. (1999). Ringing changes to the 'bell-shaped curve'. *Curr Biol* **9**, R876-878.

Borg, J. P., Ooi, J., Levy, E., and Margolis, B. (1996). The phosphotyrosine interaction domains of X11 and FE65 bind to distinct sites on the YENPTY motif of amyloid precursor protein. *Mol Cell Biol* **16**, 6229-6241.

Borg, J. P., and Margolis, B. (1998). Function of PTB domains. *Curr Top Microbiol Immunol* **228**, 23-38.

Boulay, G., Brown, D. M., Qin, N., Jiang, M., Dietrich, A., Zhu, M. X., Chen, Z., Birnbaumer, M., Mikoshiba, K., and Birnbaumer, L. (1999). Modulation of Ca(2+) entry by polypeptides of the inositol 1,4, 5-trisphosphate receptor (IP3R) that bind transient receptor potential (TRP): evidence for roles of TRP and IP3R in store depletion-activated Ca(2+) entry. *Proc Natl Acad Sci U S A* **96**, 14955-14960.

Boulay, I., Nemorin, J. G., and Duplay, P. (2005). Phosphotyrosine binding-mediated oligomerization of downstream of tyrosine kinase (Dok)-1 and Dok-2 is involved in CD2-induced Dok phosphorylation. *J Immunol* **175**, 4483-4489.

Brauweiler, A., Tamir, I., Dal Porto, J., Benschop, R. J., Helgason, C. D., Humphries, R. K., Freed, J. H., and Cambier, J. C. (2000). Differential regulation of B cell development, activation, and death by the src homology 2 domain-containing 5' inositol phosphatase (SHIP). *J Exp Med* **191**, 1545-1554.

Brdicka, T., Pavlistova, D., Leo, A., Bruyns, E., Korinek, V., Angelisova, P., Scherer, J., Shevchenko, A., Hilgert, I., Cerny, J., Drbal, K., Kuramitsu, Y., Kornacker, B., Horejsi, V., and Schraven, B. (2000). Phosphoprotein associated with glycosphingolipid-enriched microdomains (PAG), a novel ubiquitously expressed transmembrane adaptor protein, binds the protein tyrosine kinase csk and is involved in regulation of T cell activation. *J Exp Med* **191**, 1591-1604.

Brdicka, T., Imrich, M., Angelisova, P., Brdickova, N., Horvath, O., Spicka, J., Hilgert, I., Luskova, P., Draber, P., Novak, P., Engels, N., Wienands, J., Simeoni, L., Osterreicher, J., Aguado, E., Malissen, M., Schraven, B., and Horejsi, V. (2002). Non-T cell activation linker (NTAL): A transmembrane adaptor protein involved in immunoreceptor signaling. *Journal of Experimental Medicine* **196**, 1617-1626.

Brdickova, N., Brdicka, T., Angelisova, P., Horvath, O., Spicka, J., Hilgert, I., Paces, J., Simeoni, L., Kliche, S., Merten, C., Schraven, B., and Horejsi, V. (2003). LIME: a new membrane Raft-associated adaptor protein involved in CD4 and CD8 coreceptor signaling. *J Exp Med* **198**, 1453-1462.

Briggs, S. D., Sharkey, M., Stevenson, M., and Smithgall, T. E. (1997). SH3-mediated Hck tyrosine kinase activation and fibroblast transformation by the Nef protein of HIV-1. *J Biol Chem* **272**, 17899-17902.

Broad, L. M., Cannon, T. R., and Taylor, C. W. (1999). A non-capacitative pathway activated by arachidonic acid is the major Ca2+ entry mechanism in rat A7r5 smooth muscle cells stimulated with low concentrations of vasopressin. *J Physiol* **517 (Pt 1)**, 121-134.

Broad, L. M., Braun, F. J., Lievremont, J. P., Bird, G. S., Kurosaki, T., and Putney, J. W., Jr. (2001). Role of the phospholipase C-inositol 1,4,5-trisphosphate pathway in calcium release-activated calcium current and capacitative calcium entry. *J Biol Chem* **276**, 15945-15952.

Brown, D. A., and Rose, J. K. (1992). Sorting of GPI-anchored proteins to glycolipid-enriched membrane subdomains during transport to the apical cell surface. *Cell* **68**, 533-544.

Brown, D. A., and London, E. (2000). Structure and function of sphingolipid- and cholesterol-rich membrane rafts. *J Biol Chem* **275**, 17221-17224.

Buday, L., and Downward, J. (1993). Epidermal growth factor regulates p21ras through the formation of a complex of receptor, Grb2 adapter protein, and Sos nucleotide exchange factor. *Cell* **73**, 611-620.

Buerstedde, J. M., Reynaud, C. A., Humphries, E. H., Olson, W., Ewert, D. L., and Weill, J. C. (1990). Light chain gene conversion continues at high rate in an ALV-induced cell line. *Embo J* **9**, 921-927.

Buerstedde, J. M., and Takeda, S. (1991). Increased ratio of targeted to random integration after transfection of chicken B cell lines. *Cell* **67**, 179-188.

Cai, D., Dhe-Paganon, S., Melendez, P. A., Lee, J., and Shoelson, S. E. (2003). Two new substrates in insulin signaling, IRS5/DOK4 and IRS6/DOK5. *J Biol Chem* **278**, 25323-25330.

Cambier, J. C. (1995). Antigen and Fc receptor signaling. The awesome power of the immunoreceptor tyrosine-based activation motif (ITAM). *J Immunol* **155**, 3281-3285.

Campbell, M. A., and Sefton, B. M. (1992). Association between B-lymphocyte membrane immunoglobulin and multiple members of the Src family of protein tyrosine kinases. *Mol Cell Biol* **12**, 2315-2321.

Cantrell, D. A. (2001). Phosphoinositide 3-kinase signalling pathways. *J Cell Sci* **114**, 1439-1445.

Carpino, N., Wisniewski, D., Strife, A., Marshak, D., Kobayashi, R., Stillman, B., and Clarkson, B. (1997). p62(dok): a constitutively tyrosine-phosphorylated, GAP-associated protein in chronic myelogenous leukemia progenitor cells. *Cell* **88**, 197-204.

Cen, O., Gorska, M. M., Stafford, S. J., Sur, S., and Alam, R. (2003). Identification of UNC119 as a novel activator of SRC-type tyrosine kinases. *J Biol Chem* **278**, 8837-8845.

Chacko, G. W., Tridandapani, S., Damen, J. E., Liu, L., Krystal, G., and Coggeshall, K. M. (1996). Negative signaling in B lymphocytes induces tyrosine phosphorylation of the 145-kDa inositol polyphosphate 5-phosphatase, SHIP. *J Immunol* **157**, 2234-2238.

Chan, V. W., Lowell, C. A., and DeFranco, A. L. (1998). Defective negative regulation of antigen receptor signaling in Lyn-deficient B lymphocytes. *Curr Biol* **8**, 545-553.

Chardin, P., Camonis, J. H., Gale, N. W., van Aelst, L., Schlessinger, J., Wigler, M. H., and Bar-Sagi, D. (1993). Human Sos1: a guanine nucleotide exchange factor for Ras that binds to GRB2. *Science* **260**, 1338-1343.

Charest, A., Wagner, J., Jacob, S., McGlade, C. J., and Tremblay, M. L. (1996). Phosphotyrosine-independent binding of SHC to the NPLH sequence of murine protein-tyrosine phosphatase-PEST. Evidence for extended phosphotyrosine binding/phosphotyrosine interaction domain recognition specificity. *J Biol Chem* **271**, 8424-8429.

Chen, C. L., Lehmeyer, J. E., and Cooper, M. D. (1982). Evidence for an IgD homologue on chicken lymphocytes. *J Immunol* **129**, 2580-2585.

Cheng, P. C., Dykstra, M. L., Mitchell, R. N., and Pierce, S. K. (1999). A role for lipid rafts in B cell antigen receptor signaling and antigen targeting. *J Exp Med* **190**, 1549-1560.

Chien, C. T., Wang, S., Rothenberg, M., Jan, L. Y., and Jan, Y. N. (1998). Numb-associated kinase interacts with the phosphotyrosine binding domain of Numb and antagonizes the function of Numb in vivo. *Mol Cell Biol* **18**, 598-607.

Ching, T. T., Hsu, A. L., Johnson, A. J., and Chen, C. S. (2001). Phosphoinositide 3-kinase facilitates antigen-stimulated Ca(2+) influx in RBL-2H3 mast cells via a phosphatidylinositol 3,4,5-trisphosphate-sensitive Ca(2+) entry mechanism. *J Biol Chem* **276**, 14814-14820.

Chiu, C. W., Dalton, M., Ishiai, M., Kurosaki, T., and Chan, A. C. (2002). BLNK: molecular scaffolding through 'cis'-mediated organization of signaling proteins. *EMBO J* **21**, 6461-6472.

Choi, J. H., Park, J. B., Bae, S. S., Yun, S., Kim, H. S., Hong, W. P., Kim, I. S., Kim, J. H., Han, M. Y., Ryu, S. H., Patterson, R. L., Snyder, S. H., and Suh, P. G. (2004). Phospholipase C-gamma1 is a guanine nucleotide exchange factor for dynamin-1 and enhances dynamin-1-dependent epidermal growth factor receptor endocytosis. *J Cell Sci* **117**, 3785-3795.

Choi, J. H., Hong, W. P., Yun, S., Kim, H. S., Lee, J. R., Park, J. B., Bae, Y. S., Ryu, S. H., and Suh, P. G. (2005). Grb2 negatively regulates epidermal growth factor-induced phospholipase C-gamma1 activity through the direct interaction with tyrosine-phosphorylated phospholipase C-gamma1. *Cell Signal* **17**, 1289-1299.

Chong, Y. P., Ia, K. K., Mulhern, T. D., and Cheng, H. C. (2005a). Endogenous and synthetic inhibitors of the Src-family protein tyrosine kinases. *Biochim Biophys Acta* **1754**, 210-220.

Chong, Y. P., Mulhern, T. D., and Cheng, H. C. (2005b). C-terminal Src kinase (CSK) and CSK-homologous kinase (CHK)--endogenous negative regulators of Src-family protein kinases. *Growth Factors* **23**, 233-244.

Clapham, D. E. (1995). Calcium signaling. *Cell* **80**, 259-268.

Clapham, D. E. (2003). TRP channels as cellular sensors. *Nature* **426**, 517-524.

Clark, S. G., Stern, M. J., and Horvitz, H. R. (1992). C. elegans cell-signalling gene sem-5 encodes a protein with SH2 and SH3 domains. *Nature* **356**, 340-344.

Clayton, E., Bardi, G., Bell, S. E., Chantry, D., Downes, C. P., Gray, A., Humphries, L. A., Rawlings, D., Reynolds, H., Vigorito, E., and Turner, M. (2002). A crucial role for the p110delta subunit of phosphatidylinositol 3-kinase in B cell development and activation. *J Exp Med* **196**, 753-763.

Coffin, J.M., and Varmus, H.E., Ed. (1996) Retroviruses (Cold Spring Harbor Laboratory Press, NY).

Cong, F., Yuan, B., and Goff, S. P. (1999). Characterization of a novel member of the DOK family that binds and modulates Abl signaling. *Mol Cell Biol* **19**, 8314-8325.

Cooke, M. P., Heath, A. W., Shokat, K. M., Zeng, Y., Finkelman, F. D., Linsley, P. S., Howard, M., and Goodnow, C. C. (1994). Immunoglobulin signal transduction guides the specificity of B cell-T cell interactions and is blocked in tolerant self-reactive B cells. *J Exp Med* **179**, 425-438.

Crabtree, G. R., and Clipstone, N. A. (1994). Signal transmission between the plasma membrane and nucleus of T lymphocytes. *Annu Rev Biochem* **63**, 1045-1083.

Crabtree, G. R., and Olson, E. N. (2002). NFAT signaling: choreographing the social lives of cells. *Cell* **109 Suppl**, S67-79.

Crowder, R. J., Enomoto, H., Yang, M., Johnson, E. M., Jr., and Milbrandt, J. (2004). Dok-6, a Novel p62 Dok family member, promotes Ret-mediated neurite outgrowth. *J Biol Chem* **279**, 42072-42081.

Crowley, M. T., Harmer, S. L., and DeFranco, A. L. (1996). Activation-induced association of a 145-kDa tyrosine-phosphorylated protein with Shc and Syk in B lymphocytes and macrophages. *J Biol Chem* **271**, 1145-1152.

Dekker, L. V., and Parker, P. J. (1994). Protein kinase C--a question of specificity. *Trends Biochem Sci* **19**, 73-77.

Di Cristofano, A., Carpino, N., Dunant, N., Friedland, G., Kobayashi, R., Strife, A., Wisniewski, D., Clarkson, B., Pandolfi, P. P., and Resh, M. D. (1998). Molecular cloning and characterization of p56dok-2 defines a new family of RasGAP-binding proteins. *J Biol Chem* **273**, 4827-4830.

Dikic, I., and Giordano, S. (2003). Negative receptor signalling. *Curr Opin Cell Biol* **15**, 128-135.

Dillon, S. R., Mancini, M., Rosen, A., and Schlissel, M. S. (2000). Annexin V binds to viable B cells and colocalizes with a marker of lipid rafts upon B cell receptor activation. *J Immunol* **164**, 1322-1332.

Dolmetsch, R. E., Lewis, R. S., Goodnow, C. C., and Healy, J. I. (1997). Differential activation of transcription factors induced by Ca2+ response amplitude and duration. *Nature* **386**, 855-858.

Dolmetsch, R. E., Xu, K., and Lewis, R. S. (1998). Calcium oscillations increase the efficiency and specificity of gene expression. *Nature* **392**, 933-936.

Donahue, A. C., and Fruman, D. A. (2004). PI3K signaling controls cell fate at many points in B lymphocyte development and activation. *Semin Cell Dev Biol* **15**, 183-197.

Douglass, A. D., and Vale, R. D. (2005). Single-molecule microscopy reveals plasma membrane microdomains created by protein-protein networks that exclude or trap signaling molecules in T cells. *Cell* **121**, 937-950.

Downward, J. (1994). The GRB2/Sem-5 adaptor protein. *FEBS Lett* **338**, 113-117.

Egan, S. E., Giddings, B. W., Brooks, M. W., Buday, L., Sizeland, A. M., and Weinberg, R. A. (1993). Association of Sos Ras exchange protein with Grb2 is implicated in tyrosine kinase signal transduction and transformation. *Nature* **363**, 45-51.

Ellis, C., Moran, M., McCormick, F., and Pawson, T. (1990). Phosphorylation of GAP and GAP-associated proteins by transforming and mitogenic tyrosine kinases. *Nature* **343**, 377-381.

Emori, Y., Homma, Y., Sorimachi, H., Kawasaki, H., Nakanishi, O., Suzuki, K., and Takenawa, T. (1989). A second type of rat phosphoinositide-specific phospholipase C containing a src-related sequence not essential for phosphoinositide-hydrolyzing activity. *J Biol Chem* **264**, 21885-21890.

Engels, N., Wollscheid, B., and Wienands, J. (2001). Association of SLP-65/BLNK with the B cell antigen receptor through a non-ITAM tyrosine of Ig-alpha. *Eur J Immunol* **31**, 2126-2134.

Facchetti, F., Chan, J. K., Zhang, W., Tironi, A., Chilosi, M., Parolini, S., Notarangelo, L. D., and Samelson, L. E. (1999). Linker for activation of T cells (LAT), a novel immunohistochemical marker for T cells, NK cells, mast cells, and megakaryocytes: evaluation in normal and pathological conditions. *Am J Pathol* **154**, 1037-1046.

Falasca, M., Logan, S. K., Lehto, V. P., Baccante, G., Lemmon, M. A., and Schlessinger, J. (1998). Activation of phospholipase C gamma by PI 3-kinase-induced PH domain-mediated membrane targeting. *Embo J* **17**, 414-422.

Fang, K. S., Sabe, H., Saito, H., and Hanafusa, H. (1994). Comparative study of three protein-tyrosine phosphatases. Chicken protein-tyrosine phosphatase lambda dephosphorylates c-Src tyrosine 527. *J Biol Chem* **269**, 20194-20200.

Fanger, C. M., Hoth, M., Crabtree, G. R., and Lewis, R. S. (1995). Characterization of T cell mutants with defects in capacitative calcium entry: genetic evidence for the physiological roles of CRAC channels. *J Cell Biol* **131**, 655-667.

Fasolato, C., Hoth, M., and Penner, R. (1993). A GTP-dependent step in the activation mechanism of capacitative calcium influx. *J Biol Chem* **268**, 20737-20740.

Favre, C., Gerard, A., Clauzier, E., Pontarotti, P., Olive, D., and Nunes, J. A. (2003). DOK4 and DOK5: new Dok-related genes expressed in human T cells. *Genes Immun* **4**, 40-45.

Feng, G. S., Ouyang, Y. B., Hu, D. P., Shi, Z. Q., Gentz, R., and Ni, J. (1996). Grap is a novel SH3-SH2-SH3 adaptor protein that couples tyrosine kinases to the Ras pathway. *J Biol Chem* **271**, 12129-12132.

Feng, S., Chen, J. K., Yu, H., Simon, J. A., and Schreiber, S. L. (1994). Two binding orientations for peptides to the Src SH3 domain: development of a general model for SH3-ligand interactions. *Science* **266**, 1241-1247.

Feng, S., Kasahara, C., Rickles, R. J., and Schreiber, S. L. (1995). Specific interactions outside the proline-rich core of two classes of Src homology 3 ligands. *Proc Natl Acad Sci U S A* **92**, 12408-12415.

Fernando, K. C., Gregory, R. B., Katsis, F., Kemp, B. E., and Barritt, G. J. (1997). Evidence that a low-molecular-mass GTP-binding protein is required for store-activated Ca2+ inflow in hepatocytes. *Biochem J* **328 (Pt 2)**, 463-471.

Ferris, C. D., Huganir, R. L., Bredt, D. S., Cameron, A. M., and Snyder, S. H. (1991). Inositol trisphosphate receptor: phosphorylation by protein kinase C and calcium calmodulin-dependent protein kinases in reconstituted lipid vesicles. *Proc Natl Acad Sci U S A* **88**, 2232-2235.

Finco, T. S., Kadlecek, T., Zhang, W., Samelson, L. E., and Weiss, A. (1998). LAT is required for TCR-mediated activation of PLCgamma1 and the Ras pathway. *Immunity* **9**, 617-626.

Finn, J. T., Grunwald, M. E., and Yau, K. W. (1996). Cyclic nucleotide-gated ion channels: an extended family with diverse functions. *Annu Rev Physiol* **58**, 395-426.

Fluckiger, A. C., Li, Z., Kato, R. M., Wahl, M. I., Ochs, H. D., Longnecker, R., Kinet, J. P., Witte, O. N., Scharenberg, A. M., and Rawlings, D. J. (1998). Btk/Tec kinases regulate sustained increases in intracellular Ca2+ following B-cell receptor activation. *Embo J* **17**, 1973-1985.

Forman-Kay, J. D., and Pawson, T. (1999). Diversity in protein recognition by PTB domains. *Curr Opin Struct Biol* **9**, 690-695.

Frantz, B., Nordby, E. C., Bren, G., Steffan, N., Paya, C. V., Kincaid, R. L., Tocci, M. J., O'Keefe, S. J., and O'Neill, E. A. (1994). Calcineurin acts in synergy with PMA to inactivate I kappa B/MAD3, an inhibitor of NF-kappa B. *Embo J* **13**, 861-870.

Fruman, D. A., Meyers, R. E., and Cantley, L. C. (1998). Phosphoinositide kinases. *Annu Rev Biochem* **67**, 481-507.

Fu, C., Turck, C. W., Kurosaki, T., and Chan, A. C. (1998). BLNK: A central linker protein in B cell activation. *Immunity* **9**, 93-103.

Furuichi, T., Yoshikawa, S., Miyawaki, A., Wada, K., Maeda, N., and Mikoshiba, K. (1989). Primary structure and functional expression of the inositol 1,4,5-trisphosphate-binding protein P400. *Nature* **342**, 32-38.

Fusaki, N., Tomita, S., Wu, Y., Okamoto, N., Goitsuka, R., Kitamura, D., and Hozumi, N. (2000). BLNK is associated with the CD72/SHP-1/Grb2 complex in the WEHI231 cell line after membrane IgM cross-linking. *Eur J Immunol* **30**, 1326-1330.

Futterer, K., Wong, J., Grucza, R. A., Chan, A. C., and Waksman, G. (1998). Structural basis for Syk tyrosine kinase ubiquity in signal transduction pathways revealed by the crystal structure of its regulatory SH2 domains bound to a dually phosphorylated ITAM peptide. *J Mol Biol* **281**, 523-537.

Gale, N. W., Kaplan, S., Lowenstein, E. J., Schlessinger, J., and Bar-Sagi, D. (1993). Grb2 mediates the EGF-dependent activation of guanine nucleotide exchange on Ras. *Nature* **363**, 88-92.

Gallo, E. M., Cante-Barrett, K., and Crabtree, G. R. (2006). Lymphocyte calcium signaling from membrane to nucleus. *Nat Immunol* **7**, 25-32.

Gangi-Peterson, L., Peterson, S. N., Shapiro, L. H., Golding, A., Caricchio, R., Cohen, D. I., Margulies, D. H., and Cohen, P. L. (1998). bca: an activation-related B-cell gene. *Mol Immunol* **35**, 55-63.

Gauld, S. B., Benschop, R. J., Merrell, K. T., and Cambier, J. C. (2005). Maintenance of B cell anergy requires constant antigen receptor occupancy and signaling. *Nat Immunol* **6**, 1160-1167.

Gibbins, J. M., Briddon, S., Shutes, A., van Vugt, M. J., van de Winkel, J. G., Saito, T., and Watson, S. P. (1998). The p85 subunit of phosphatidylinositol 3-kinase associates with the Fc receptor gamma-chain and linker for activitor of T cells (LAT) in platelets stimulated by collagen and convulxin. *J Biol Chem* **273**, 34437-34443.

Goitsuka, R., Fujimura, Y.-I., Mamada, H., Umeda, A., Morimura, T., Uetsuka, K., Doi, K., Tsuji, S., and Kitamura, D. (1998). BASH, a novel signaling molecule preferentially expressed in B cells of the Bursa of Fabricius. *J Immunol* **161**, 5804-5808.

Gomes, B., Savignac, M., Moreau, M., Leclerc, C., Lory, P., Guery, J. C., and Pelletier, L. (2004). Lymphocyte calcium signaling involves dihydropyridine-sensitive L-type calcium channels: facts and controversies. *Crit Rev Immunol* **24**, 425-447.

Gomez, T. S., Hamann, M. J., McCarney, S., Savoy, D. N., Lubking, C. M., Heldebrant, M. P., Labno, C. M., McKean, D. J., McNiven, M. A., Burkhardt, J. K., and Billadeau, D. D. (2005). Dynamin 2 regulates T cell activation by controlling actin polymerization at the immunological synapse. *Nat Immunol* **6**, 261-270.

Gorska, M. M., Stafford, S. J., Cen, O., Sur, S., and Alam, R. (2004). Unc119, a novel activator of Lck/Fyn, is essential for T cell activation. *J Exp Med* **199**, 369-379.

Gout, I., Dhand, R., Hiles, I. D., Fry, M. J., Panayotou, G., Das, P., Truong, O., Totty, N. F., Hsuan, J., Booker, G. W., and et al. (1993). The GTPase dynamin binds to and is activated by a subset of SH3 domains. *Cell* **75**, 25-36.

Grafton, G., Stokes, L., Toellner, K. M., and Gordon, J. (2003). A non-voltage-gated calcium channel with L-type characteristics activated by B cell receptor ligation. *Biochem Pharmacol* **66**, 2001-2009.

Graham, F. L., Smiley, J., Russell, W. C., and Nairn, R. (1977). Characteristics of a human cell line transformed by DNA from human adenovirus type 5. *J Gen Virol* **36**, 59-74.

Grimm, J., Sachs, M., Britsch, S., Di Cesare, S., Schwarz-Romond, T., Alitalo, K., and Birchmeier, W. (2001). Novel p62dok family members, dok-4 and dok-5, are substrates of the c-Ret receptor tyrosine kinase and mediate neuronal differentiation. *J Cell Biol* **154**, 345-354.

Harden, T. K., and Sondek, J. (2006). Regulation of phospholipase C isozymes by ras superfamily GTPases. *Annu Rev Pharmacol Toxicol* **46**, 355-379.

Harder, K. W., Parsons, L. M., Armes, J., Evans, N., Kountouri, N., Clark, R., Quilici, C., Grail, D., Hodgson, G. S., Dunn, A. R., and Hibbs, M. L. (2001). Gain- and loss-of-function Lyn mutant mice define a critical inhibitory role for Lyn in the myeloid lineage. *Immunity* **15**, 603-615.

Harmer, S. L., and DeFranco, A. L. (1997). Shc contains two Grb2 binding sites needed for efficient formation of complexes with SOS in B lymphocytes. *Mol Cell Biol* **17**, 4087-4095.

Harmer, S. L., and DeFranco, A. L. (1999). The Src homology domain 2-containing inositol phosphatase SHIP forms a ternary complex with Shc and Grb2 in antigen receptor-stimulated B lymphocytes. *Journal of Biological Chemistry* **274**, 12183-12191.

Hashimoto, A., Okada, H., Jiang, A., Kurosaki, M., Greenberg, S., Clark, E. A., and Kurosaki, T. (1998). Involvement of guanosine triphosphatases and phospholipase C-gamma 2 in extracellular signal-regulated kinase, c-Jun NH2-terminal kinase, and p38 mitogen-activated protein kinase activation by the B cell antigen receptor. *Journal of Experimental Medicine* **188**, 1287-1295.

Hashimoto, A., Kurosaki, M., Gotoh, N., Shibuya, M., and Kurosaki, T. (1999a). Shc regulates epidermal growth factor-induced activation of the JNK signaling pathway. *J Biol Chem* **274**, 20139-20143.

Hashimoto, A., Takeda, K., Inaba, M., Sekimata, M., Kaisho, T., Ikehara, S., Homma, Y., Akira, S., and Kurosaki, T. (2000). Cutting edge: essential role of phospholipase C-gamma 2 in B cell development and function. *J Immunol* **165**, 1738-1742.

Hashimoto, S., Iwamatsu, A., Ishiai, M., Okawa, K., Yamadori, T., Matsushita, M., Baba, Y., Kishimoto, T., Kurosaki, T., and Tsukada, S. (1999b). Identification of the SH2 domain binding protein of Bruton's tyrosine kinase as BLNK: Functional significance of Btk-SH2 domain in B-cell antigen receptor-coupled calcium signaling. *Blood* **94**, 2357-2364.

Hata, A., Sabe, H., Kurosaki, T., Takata, M., and Hanafusa, H. (1994). Functional analysis of Csk in signal transduction through the B-cell antigen receptor. *Mol Cell Biol* **14**, 7306-7313.

Hawley, R. G., Lieu, F. H., Fong, A. Z., and Hawley, T. S. (1994). Versatile retroviral vectors for potential use in gene therapy. *Gene Ther* **1**, 136-138.

Healy, J. I., Dolmetsch, R. E., Timmerman, L. A., Cyster, J. G., Thomas, M. L., Crabtree, G. R., Lewis, R. S., and Goodnow, C. C. (1997). Different nuclear signals are activated by the B cell receptor during positive versus negative signaling. *Immunity* **6**, 419-428.

Healy, J. I., and Goodnow, C. C. (1998). Positive versus negative signaling by lymphocyte antigen receptors. *Annu Rev Immunol* **16**, 645-670.

Hibbs, M. L., Harder, K. W., Armes, J., Kountouri, N., Quilici, C., Casagranda, F., Dunn, A. R., and Tarlinton, D. M. (2002). Sustained activation of Lyn tyrosine kinase in vivo leads to autoimmunity. *J Exp Med* **196**, 1593-1604.

Hikida, M., Johmura, S., Hashimoto, A., Takezaki, M., and Kurosaki, T. (2003). Coupling between B cell receptor and phospholipase C-gamma2 is essential for mature B cell development. *J Exp Med* **198**, 581-589.

Hikida, M., and Kurosaki, T. (2005). Regulation of Phospholipase C-gamma2 Networks in B Lymphocytes. *Adv Immunol* **88**, 73-96.

Hilberg, F., Stocking, C., Ostertag, W., and Grez, M. (1987). Functional analysis of a retroviral host-range mutant: altered long terminal repeat sequences allow expression in embryonal carcinoma cells. *Proc Natl Acad Sci U S A* **84**, 5232-5236.

Hofmann, T., Obukhov, A. G., Schaefer, M., Harteneck, C., Gudermann, T., and Schultz, G. (1999). Direct activation of human TRPC6 and TRPC3 channels by diacylglycerol. *Nature* **397**, 259-263.

Homma, Y., and Takenawa, T. (1992). Inhibitory effect of src homology (SH) 2/SH3 fragments of phospholipase C-gamma on the catalytic activity of phospholipase C isoforms. Identification of a novel phospholipase C inhibitor region. *J Biol Chem* **267**, 21844-21849.

Hong-Geller, E., and Cerione, R. A. (2000). Cdc42 and Rac stimulate exocytosis of secretory granules by activating the IP(3)/calcium pathway in RBL-2H3 mast cells. *J Cell Biol* **148**, 481-494.

Honma, M., Higuchi, O., Shirakata, M., Yasuda, T., Shibuya, H., Iemura, S., Natsume, T., and Yamanashi, Y. (2006). Dok-3 sequesters Grb2 and inhibits the Ras-Erk pathway downstream of protein-tyrosine kinases. *Genes Cells* **11**, 143-151.

Hope, H. R., and Pike, L. J. (1996). Phosphoinositides and phosphoinositide-utilizing enzymes in detergent-insoluble lipid domains. *Mol Biol Cell* **7**, 843-851.

Hoth, M., and Penner, R. (1992). Depletion of intracellular calcium stores activates a calcium current in mast cells. *Nature* **355**, 353-356.

Howell, B. W., Lanier, L. M., Frank, R., Gertler, F. B., and Cooper, J. A. (1999). The disabled 1 phosphotyrosine-binding domain binds to the internalization signals of transmembrane glycoproteins and to phospholipids. *Mol Cell Biol* **19**, 5179-5188.

Hur, E. M., Son, M., Lee, O. H., Choi, Y. B., Park, C., Lee, H., and Yun, Y. (2003). LIME, a novel transmembrane adaptor protein, associates with p56lck and mediates T cell activation. *J Exp Med* **198**, 1463-1473.

Iino, M. (1991). Effects of adenine nucleotides on inositol 1,4,5-trisphosphate-induced calcium release in vascular smooth muscle cells. *J Gen Physiol* **98**, 681-698.

Ikura, M. (1996). Calcium binding and conformational response in EF-hand proteins. *Trends Biochem Sci* **21**, 14-17.

Inabe, K., Ishiai, M., Scharenberg, A. M., Freshney, N., Downward, J., and Kurosaki, T. (2002). Vav3 modulates B cell receptor responses by regulating phosphoinositide 3-kinase activation. *J Exp Med* **195**, 189-200.

Ingham, R. J., Okada, H., Dang-Lawson, M., Dinglasan, J., van Der Geer, P., Kurosaki, T., and Gold, M. R. (1999). Tyrosine phosphorylation of shc in response to B cell antigen receptor engagement depends on the SHIP inositol phosphatase. *J Immunol* **163**, 5891-5895.

Irvin, B. J., Williams, B. L., Nilson, A. E., Maynor, H. O., and Abraham, R. T. (2000). Pleiotropic contributions of phospholipase C-gamma1 (PLC-gamma1) to T-cell antigen receptor-mediated signaling: reconstitution studies of a PLC-gamma1-deficient Jurkat T-cell line. *Mol Cell Biol* **20**, 9149-9161.

Irvine, R. F. (1990). 'Quantal' Ca2+ release and the control of Ca2+ entry by inositol phosphates--a possible mechanism. *FEBS Lett* **263**, 5-9.

Ishiai, M., Sugawara, H., Kurosaki, M., and Kurosaki, T. (1999a). Association of phospholipase C-γ2 Src homology 2 domain with BLNK is critical for B cell antigen receptor signaling. *J Immunol* **163**, 1746-1749.

Ishiai, M., Kurosaki, M., Pappu, R., Okawa, K., Ronko, I., Fu, C., Shibata, M., Iwamatsu, A., Chan, A. C., and Kurosaki, T. (1999b). BLNK required for coupling Syk to PLCγ2 and Rac1-JNK in B cells. *Immunity* **10**, 1-20.

Ishiai, M., Kurosaki, M., Inabe, K., Chan, A. C., Sugamura, K., and Kurosaki, T. (2000). Involvement of LAT, Gads, and Grb2 in compartmentation of SLP-76 to the plasma membrane. *J Exp Med* **192**, 847-856.

Jack, H. M., and Wabl, M. (1988). Immunoglobulin mRNA stability varies during B lymphocyte differentiation. *Embo J* **7**, 1041-1046.

Jacobs, A. R., LeRoith, D., and Taylor, S. I. (2001). Insulin receptor substrate-1 pleckstrin homology and phosphotyrosine-binding domains are both involved in plasma membrane targeting. *J Biol Chem* **276**, 40795-40802.

Janssen, E., Zhu, M. H., Zhang, W. J., Koonpaew, S., and Zhang, W. G. (2003). LAB: A new membrane-associated adaptor molecule in B cell activation. *Nature Immunology* **4**, 117-123.

Janssen, E., Zhu, M., Craven, B., and Zhang, W. (2004). Linker for activation of B cells: a functional equivalent of a mutant linker for activation of T cells deficient in phospholipase C-gamma1 binding. *J Immunol* **172**, 6810-6819.

Jayaraman, T., Ondrias, K., Ondriasova, E., and Marks, A. R. (1996). Regulation of the inositol 1,4,5-trisphosphate receptor by tyrosine phosphorylation. *Science* **272**, 1492-1494.

Jia, C. Y., Nie, J., Wu, C., Li, C., and Li, S. S. (2005). Novel Src homology 3 domain-binding motifs identified from proteomic screen of a Pro-rich region. *Mol Cell Proteomics* **4**, 1155-1166.

Johmura, S., Oh-hora, M., Inabe, K., Nishikawa, Y., Hayashi, K., Vigorito, E., Kitamura, D., Turner, M., Shingu, K., Hikida, M., and Kurosaki, T. (2003). Regulation of Vav localization in membrane rafts by adaptor molecules Grb2 and BLNK. *Immunity* **18**, 777-787.

Jones, B., Tite, J. P., and Janeway, C. A., Jr. (1986). Different phenotypic variants of the mouse B cell tumor A20/2J are selected by antigen- and mitogen-triggered cytotoxicity of L3T4-positive, I-A-restricted T cell clones. *J Immunol* **136**, 348-356.

Jones, N., and Dumont, D. J. (1998). The Tek/Tie2 receptor signals through a novel Dok-related docking protein, Dok-R. *Oncogene* **17**, 1097-1108.

Jones, N., and Dumont, D. J. (1999). Recruitment of Dok-R to the EGF receptor through its PTB domain is required for attenuation of Erk MAP kinase activation. *Curr Biol* **9**, 1057-1060.

Jou, S. T., Carpino, N., Takahashi, Y., Piekorz, R., Chao, J. R., Carpino, N., Wang, D., and Ihle, J. N. (2002). Essential, nonredundant role for the phosphoinositide 3-kinase p110delta in signaling by the B-cell receptor complex. *Mol Cell Biol* **22**, 8580-8591.

Jumaa, H., Wollscheid, B., Mitterer, M., Wienands, J., Reth, M., and Nielsen, P. J. (1999). Abnormal development and function of B lymphocytes in mice deficient for the signaling adaptor protein SLP-65. *Immunity* **11**, 547-554.

Kabak, S., Skaggs, B. J., Gold, M. R., Affolter, M., West, K. L., Foster, M. S., Siemasko, K., Chan, A. C., Aebersold, R., and Clark, M. R. (2002). The direct recruitment of BLNK to immunoglobulin alpha couples the B-cell antigen receptor to distal signaling pathways. *Mol Cell Biol* **22**, 2524-2535.

Katan, M., Rodriguez, R., Matsuda, M., Newbatt, Y. M., and Aherne, G. W. (2003). Structural and mechanistic aspects of phospholipase Cgamma regulation. *Adv Enzyme Regul* **43**, 77-85.

Kawabuchi, M., Satomi, Y., Takao, T., Shimonishi, Y., Nada, S., Nagai, K., Tarakhovsky, A., and Okada, M. (2000). Transmembrane phosphoprotein Cbp regulates the activities of Src-family tyrosine kinases. *Nature* **404**, 999-1003.

Kawanabe, Y., Hashimoto, N., and Masaki, T. (2003). Role of phosphoinositide 3-kinase in the nonselective cation channel activation by endothelin-1/endothelinB receptor. *Am J Physiol Cell Physiol* **284**, C506-510.

Kaznacheyeva, E., Zubov, A., Nikolaev, A., Alexeenko, V., Bezprozvanny, I., and Mozhayeva, G. N. (2000). Plasma membrane calcium channels in human carcinoma A431 cells are functionally coupled to inositol 1,4,5-trisphosphate receptor-phosphatidylinositol 4,5-bisphosphate complexes. *J Biol Chem* **275**, 4561-4564.

Kepley, C. L., Taghavi, S., Mackay, G., Zhu, D., Morel, P. A., Zhang, K., Ryan, J. J., Satin, L. S., Zhang, M., Pandolfi, P. P., and Saxon, A. (2004). Co-aggregation of FcgammaRII with FcepsilonRI on human mast cells inhibits antigen-induced secretion and involves SHIP-Grb2-Dok complexes. *J Biol Chem* **279**, 35139-35149.

Kessels, H. W., Ward, A. C., and Schumacher, T. N. (2002). Specificity and affinity motifs for Grb2 SH2-ligand interactions. *Proc Natl Acad Sci U S A* **99**, 8524-8529.

Keyna, U., Beck-Engeser, G. B., Jongstra, J., Applequist, S. E., and Jack, H. M. (1995). Surrogate light chain-dependent selection of Ig heavy chain V regions. *J Immunol* **155**, 5536-5542.

Kim, K. J., Kanellopoulos-Langevin, C., Merwin, R. M., Sachs, D. H., and Asofsky, R. (1979). Establishment and characterization of BALB/c lymphoma lines with B cell properties. *J Immunol* **122**, 549-554.

Kim, S., Humphries, E. H., Tjoelker, L., Carlson, L., and Thompson, C. B. (1990). Ongoing diversification of the rearranged immunoglobulin light-chain gene in a bursal lymphoma cell line. *Mol Cell Biol* **10**, 3224-3231.

Kim, Y. J., Sekiya, F., Poulin, B., Bae, Y. S., and Rhee, S. G. (2004). Mechanism of B-cell receptor-induced phosphorylation and activation of phospholipase C-gamma2. *Mol Cell Biol* **24**, 9986-9999.

Kimura, T., Sakamoto, H., Appella, E., and Siraganian, R. P. (1996). Conformational changes induced in the protein tyrosine kinase p72syk by tyrosine phosphorylation or by binding of phosphorylated immunoreceptor tyrosine-based activation motif peptides. *Mol Cell Biol* **16**, 1471-1478.

Kiselyov, K., Xu, X., Mozhayeva, G., Kuo, T., Pessah, I., Mignery, G., Zhu, X., Birnbaumer, L., and Muallem, S. (1998). Functional interaction between InsP3 receptors and store-operated Htrp3 channels. *Nature* **396**, 478-482.

Kiselyov, K., Mignery, G. A., Zhu, M. X., and Muallem, S. (1999). The N-terminal domain of the IP3 receptor gates store-operated hTrp3 channels. *Mol Cell* **4**, 423-429.

Klein, G., Giovanella, B., Westman, A., Stehlin, J. S., and Mumford, D. (1975). An EBV-genome-negative cell line established from an American Burkitt lymphoma; receptor characteristics. EBV infectibility and permanent conversion into EBV-positive sublines by in vitro infection. *Intervirology* **5**, 319-334.

Kohler, F., Storch, B., Kulathu, Y., Herzog, S., Kuppig, S., Reth, M., and Jumaa, H. (2005). A leucine zipper in the N terminus confers membrane association to SLP-65. *Nat Immunol* **6**, 204-210.

Koncz, G., Bodor, C., Kovesdi, D., Gati, R., and Sarmay, G. (2002). BCR mediated signal transduction in immature and mature B cells. *Immunology Letters* **82**, 41-49.

Koretzky, G. A., Abtahian, F., and Silverman, M. A. (2006). SLP76 and SLP65: complex regulation of signalling in lymphocytes and beyond. *Nat Rev Immunol* **6**, 67-78.

Kovesdi, D., Koncz, G., Ivanyi-Nagy, R., Caspi, Y., Ishiai, M., Kurosaki, T., Gergely, J., Haimovich, J., and Sarmay, G. (2002). Developmental differences in B cell receptor-induced signal transduction. *Cell Signal* **14**, 563-572.

Kurosaki, T., Takata, M., Yamanashi, Y., Inazu, T., Taniguchi, T., Yamamoto, T., and Yamamura, H. (1994). Syk activation by the Src-family tyrosine kinase in the B cell receptor signaling. *J Exp Med* **179**, 1725-1729.

Kurosaki, T., Johnson, S. A., Pao, L., Sada, K., Yamamura, H., and Cambier, J. C. (1995). Role of the Syk autophosphorylation site and SH2 domains in B cell antigen receptor signaling. *J Exp Med* **182**, 1815-1823.

Kurosaki, T., Maeda, A., Ishiai, M., Hashimoto, A., Inabe, K., and Takata, M. (2000). Regulation of the phospholipase C-gamma2 pathway in B cells. *Immunol Rev* **176**, 19-29.

Kurosaki, T., and Tsukada, S. (2000). BLNK: Connecting Syk and Btk to calcium signals. *Immunity* **12**, 1-5.

Kurosaki, T. (2002). Regulation of B-cell signal transduction by adaptor proteins. *Nat Rev Immunol* **2**, 354-363.

Laemmli, U. K. (1970). Cleavage of structural proteins during the assembly of the head of bacteriophage T4. *Nature* **227**, 680-685.

Langlet, C., Bernard, A. M., Drevot, P., and He, H. T. (2000). Membrane rafts and signaling by the multichain immune recognition receptors. *Curr Opin Immunol* **12**, 250-255.

Lanier, L. L., Arnold, L. W., Raybourne, R. B., Russell, S., Lynes, M. A., Warner, N. L., and Haughton, G. (1982). Transplantable B-cell lymphomas in B10. H-2aH-4bp/Wts mice. *Immunogenetics* **16**, 367-371.

Latour, S., and Veillette, A. (2001). Proximal protein tyrosine kinases in immunoreceptor signaling. *Curr Opin Immunol* **13**, 299-306.

Le Blanc, C., Mironneau, C., Barbot, C., Henaff, M., Bondeva, T., Wetzker, R., and Macrez, N. (2004). Regulation of vascular L-type Ca2+ channels by phosphatidylinositol 3,4,5-trisphosphate. *Circ Res* **95**, 300-307.

Lemay, S., Davidson, D., Latour, S., and Veillette, A. (2000). Dok-3, a novel adapter molecule involved in the negative regulation of immunoreceptor signaling. *Mol Cell Biol* **20**, 2743-2754.

Lemmon, M. A., and Ferguson, K. M. (1998). Pleckstrin homology domains. *Curr Top Microbiol Immunol* **228**, 39-74.

Lemmon, M. A., and Ferguson, K. M. (2000). Signal-dependent membrane targeting by pleckstrin homology (PH) domains. *Biochem J* **350 Pt 1**, 1-18.

Lemmon, M. A. (2004). Pleckstrin homology domains: not just for phosphoinositides. *Biochem Soc Trans* **32**, 707-711.

Lenz, T., and Kleineke, J. W. (1997). Hormone-induced rise in cytosolic Ca2+ in axolotl hepatocytes: properties of the Ca2+ influx channel. *Am J Physiol* **273**, C1526-1532.

Lewitzky, M., Kardinal, C., Gehring, N. H., Schmidt, E. K., Konkol, B., Eulitz, M., Birchmeier, W., Schaeper, U., and Feller, S. M. (2001). The C-terminal SH3 domain of the adapter protein Grb2 binds with high affinity to sequences in Gab1 and SLP-76 which lack the SH3-typical P-x-x-P core motif. *Oncogene* **20**, 1052-1062.

Li, N., Batzer, A., Daly, R., Yajnik, V., Skolnik, E., Chardin, P., Bar-Sagi, D., Margolis, B., and Schlessinger, J. (1993). Guanine-nucleotide-releasing factor hSos1 binds to Grb2 and links receptor tyrosine kinases to Ras signalling. *Nature* **363**, 85-88.

Liang, X., Wisniewski, D., Strife, A., Shivakrupa, Clarkson, B., and Resh, M. D. (2002). Phosphatidylinositol 3-kinase and Src family kinases are required for phosphorylation and membrane recruitment of Dok-1 in c-Kit signaling. *J Biol Chem* **277**, 13732-13738.

Lichtenberg, D., Goni, F. M., and Heerklotz, H. (2005). Detergent-resistant membranes should not be identified with membrane rafts. *Trends Biochem Sci* **30**, 430-436.

Lin, J., Weiss, A., and Finco, T. S. (1999). Localization of LAT in glycolipid-enriched microdomains is required for T cell activation. *J Biol Chem* **274**, 28861-28864.

Lin, J., and Weiss, A. (2001). Identification of the minimal tyrosine residues required for linker for activation of T cell function. *J Biol Chem* **276**, 29588-29595.

Lindquist, J. A., Simeoni, L., and Schraven, B. (2003). Transmembrane adapters: attractants for cytoplasmic effectors. *Immunol Rev* **191**, 165-182.

Liou, J., Kim, M. L., Heo, W. D., Jones, J. T., Myers, J. W., Ferrell, J. E., Jr., and Meyer, T. (2005). STIM is a Ca2+ sensor essential for Ca2+-store-depletion-triggered Ca2+ influx. *Curr Biol* **15**, 1235-1241.

Liu, Q., Berry, D., Nash, P., Pawson, T., McGlade, C. J., and Li, S. S. (2003). Structural basis for specific binding of the Gads SH3 domain to an RxxK motif-containing SLP-76 peptide: a novel mode of peptide recognition. *Mol Cell* **11**, 471-481.

Lock, L. S., Royal, I., Naujokas, M. A., and Park, M. (2000). Identification of an atypical Grb2 carboxyl-terminal SH3 domain binding site in Gab docking proteins reveals Grb2-dependent and -independent recruitment of Gab1 to receptor tyrosine kinases. *J Biol Chem* **275**, 31536-31545.

Lowenstein, E. J., Daly, R. J., Batzer, A. G., Li, W., Margolis, B., Lammers, R., Ullrich, A., Skolnik, E. Y., Bar-Sagi, D., and Schlessinger, J. (1992). The SH2 and SH3 domain-containing protein GRB2 links receptor tyrosine kinases to ras signaling. *Cell* **70**, 431-442.

Ma, H. T., Patterson, R. L., van Rossum, D. B., Birnbaumer, L., Mikoshiba, K., and Gill, D. L. (2000). Requirement of the inositol trisphosphate receptor for activation of store-operated Ca2+ channels. *Science* **287**, 1647-1651.

Ma, H. T., Venkatachalam, K., Li, H. S., Montell, C., Kurosaki, T., Patterson, R. L., and Gill, D. L. (2001). Assessment of the role of the inositol 1,4,5-trisphosphate receptor in the activation of transient receptor potential channels and store-operated Ca2+ entry channels. *J Biol Chem* **276**, 18888-18896.

Macrez, N., Mironneau, C., Carricaburu, V., Quignard, J. F., Babich, A., Czupalla, C., Nurnberg, B., and Mironneau, J. (2001). Phosphoinositide 3-kinase isoforms selectively couple receptors to vascular L-type Ca(2+) channels. *Circ Res* **89**, 692-699.

Manji, S. S., Parker, N. J., Williams, R. T., van Stekelenburg, L., Pearson, R. B., Dziadek, M., and Smith, P. J. (2000). STIM1: a novel phosphoprotein located at the cell surface. *Biochim Biophys Acta* **1481**, 147-155.

Margolis, B., and Skolnik, E. Y. (1994). Activation of Ras by receptor tyrosine kinases. *J Am Soc Nephrol* **5**, 1288-1299.

Marshall, A. J., Niiro, H., Yun, T. J., and Clark, E. A. (2000). Regulation of B-cell activation and differentiation by the phosphatidylinositol 3-kinase and phospholipase Cgamma pathway. *Immunol Rev* **176**, 30-46.

Mason, D. Y., Jones, M., and Goodnow, C. C. (1992). Development and follicular localization of tolerant B lymphocytes in lysozyme/anti-lysozyme IgM/IgD transgenic mice. *Int Immunol* **4**, 163-175.

Mayer, B. J., Hirai, H., and Sakai, R. (1995). Evidence that SH2 domains promote processive phosphorylation by protein-tyrosine kinases. *Curr Biol* **5**, 296-305.

Mayer, B. J. (2001). SH3 domains: complexity in moderation. *J Cell Sci* **114**, 1253-1263.

McKinsey, T. A., Zhang, C. L., and Olson, E. N. (2000). Activation of the myocyte enhancer factor-2 transcription factor by calcium/calmodulin-dependent protein kinase-stimulated binding of 14-3-3 to histone deacetylase 5. *Proc Natl Acad Sci U S A* **97**, 14400-14405.

McPherson, P. S., Czernik, A. J., Chilcote, T. J., Onofri, F., Benfenati, F., Greengard, P., Schlessinger, J., and De Camilli, P. (1994). Interaction of Grb2 via its Src homology 3 domains with synaptic proteins including synapsin I. *Proc Natl Acad Sci U S A* **91**, 6486-6490.

Means, A. R. (2000). Regulatory cascades involving calmodulin-dependent protein kinases. *Mol Endocrinol* **14**, 4-13.

Meyer, D., Liu, A., and Margolis, B. (1999). Interaction of c-Jun amino-terminal kinase interacting protein-1 with p190 rhoGEF and its localization in differentiated neurons. *J Biol Chem* **274**, 35113-35118.

Michell, R. H. (1975). Inositol phospholipids and cell surface receptor function. *Biochim Biophys Acta* **415**, 81-47.

Michikawa, T., Hirota, J., Kawano, S., Hiraoka, M., Yamada, M., Furuichi, T., and Mikoshiba, K. (1999). Calmodulin mediates calcium-dependent inactivation of the cerebellar type 1 inositol 1,4,5-trisphosphate receptor. *Neuron* **23**, 799-808.

Mignen, O., and Shuttleworth, T. J. (2000). I(ARC), a novel arachidonate-regulated, noncapacitative Ca(2+) entry channel. *J Biol Chem* **275**, 9114-9119.

Miki, H., Miura, K., Matuoka, K., Nakata, T., Hirokawa, N., Orita, S., Kaibuchi, K., Takai, Y., and Takenawa, T. (1994). Association of Ash/Grb-2 with dynamin through the Src homology 3 domain. *J Biol Chem* **269**, 5489-5492.

Miyakawa, T., Maeda, A., Yamazawa, T., Hirose, K., Kurosaki, T., and Iino, M. (1999). Encoding of Ca2+ signals by differential expression of IP3 receptor subtypes. *Embo J* **18**, 1303-1308.

Miyakawa, T., Mizushima, A., Hirose, K., Yamazawa, T., Bezprozvanny, I., Kurosaki, T., and Iino, M. (2001). Ca(2+)-sensor region of IP(3) receptor controls intracellular Ca(2+) signaling. *Embo J* **20**, 1674-1680.

Moarefi, I., LaFevre-Bernt, M., Sicheri, F., Huse, M., Lee, C. H., Kuriyan, J., and Miller, W. T. (1997). Activation of the Src-family tyrosine kinase Hck by SH3 domain displacement. *Nature* **385**, 650-653.

Morita, S., Kojima, T., and Kitamura, T. (2000). Plat-E: an efficient and stable system for transient packaging of retroviruses. *Gene Ther* **7**, 1063-1066.

Mullis, K., Faloona, F., Scharf, S., Saiki, R., Horn, G., and Erlich, H. (1986). Specific enzymatic amplification of DNA in vitro: the polymerase chain reaction. *Cold Spring Harb Symp Quant Biol* **51 Pt 1**, 263-273.

Mullis, K. B., and Faloona, F. A. (1987). Specific synthesis of DNA in vitro via a polymerase-catalyzed chain reaction. *Methods Enzymol* **155**, 335-350.

Munro, S. (2003). Lipid rafts: elusive or illusive? *Cell* **115**, 377-388.

Nada, S., Yagi, T., Takeda, H., Tokunaga, T., Nakagawa, H., Ikawa, Y., Okada, M., and Aizawa, S. (1993). Constitutive activation of Src family kinases in mouse embryos that lack Csk. *Cell* **73**, 1125-1135.

Nagai, K., Takata, M., Yamamura, H., and Kurosaki, T. (1995). Tyrosine phosphorylation of Shc is mediated through Lyn and Syk in B cell receptor signaling. *J Biol Chem* **270**, 6824-6829.

Nakade, S., Rhee, S. K., Hamanaka, H., and Mikoshiba, K. (1994). Cyclic AMP-dependent phosphorylation of an immunoaffinity-purified homotetrameric inositol 1,4,5-trisphosphate receptor (type I) increases Ca2+ flux in reconstituted lipid vesicles. *J Biol Chem* **269**, 6735-6742.

Negulescu, P. A., Shastri, N., and Cahalan, M. D. (1994). Intracellular calcium dependence of gene expression in single T lymphocytes. *Proc Natl Acad Sci U S A* **91**, 2873-2877.

Nelms, K., Snow, A. L., Hu-Li, J., and Paul, W. E. (1998). FRIP, a hematopoietic cell-specific rasGAP-interacting protein phosphorylated in response to cytokine stimulation. *Immunity* **9**, 13-24.

Nemorin, J. G., Laporte, P., Berube, G., and Duplay, P. (2001). p62dok negatively regulates CD2 signaling in Jurkat cells. *J Immunol* **166**, 4408-4415.

Neuberger, M. S., Patel, K. J., Dariavach, P., Nelms, K., Peaker, C. J., and Williams, G. T. (1993). The mouse B-cell antigen receptor: definition and assembly of the core receptor of the five immunoglobulin isotypes. *Immunol Rev* **132**, 147-161.

Newton, A. C. (1997). Regulation of protein kinase C. *Curr Opin Cell Biol* **9**, 161-167.

Niki, M., Di Cristofano, A., Zhao, M., Honda, H., Hirai, H., Van Aelst, L., Cordon-Cardo, C., and Pandolfi, P. P. (2004). Role of Dok-1 and Dok-2 in leukemia suppression. *J Exp Med* **200**, 1689-1695.

Nishida, M., Sugimoto, K., Hara, Y., Mori, E., Morii, T., Kurosaki, T., and Mori, Y. (2003). Amplification of receptor signalling by Ca2+ entry-mediated translocation and activation of PLCgamma2 in B lymphocytes. *Embo J* **22**, 4677-4688.

Oancea, E., and Meyer, T. (1998). Protein kinase C as a molecular machine for decoding calcium and diacylglycerol signals. *Cell* **95**, 307-318.

Oh-Hora, M., Johmura, S., Hashimoto, A., Hikida, M., and Kurosaki, T. (2003). Requirement for Ras guanine nucleotide releasing protein 3 in coupling phospholipase C-gamma 2 to Ras in B cell receptor signaling. *Journal of Experimental Medicine* **198**, 1841-1851.

Okada, H., Bolland, S., Hashimoto, A., Kurosaki, M., Kabuyama, Y., Iino, M., Ravetch, J. V., and Kurosaki, T. (1998). Role of the inositol phosphatase SHIP in B cell receptor-induced Ca2+ oscillatory response. *J Immunol* **161**, 5129-5132.

Okada, T., Inoue, R., Yamazaki, K., Maeda, A., Kurosaki, T., Yamakuni, T., Tanaka, I., Shimizu, S., Ikenaka, K., Imoto, K., and Mori, Y. (1999). Molecular and functional characterization of a novel mouse transient receptor potential protein homologue TRP7. Ca(2+)-permeable cation channel that is constitutively activated and enhanced by stimulation of G protein-coupled receptor. *J Biol Chem* **274**, 27359-27370.

Okada, T., Maeda, A., Iwamatsu, A., Gotoh, K., and Kurosaki, T. (2000). BCAP: the tyrosine kinase substrate that connects B cell receptor to phosphoinositide 3-kinase activation. *Immunity* **13**, 817-827.

Okkenhaug, K., Bilancio, A., Farjot, G., Priddle, H., Sancho, S., Peskett, E., Pearce, W., Meek, S. E., Salpekar, A., Waterfield, M. D., Smith, A. J., and Vanhaesebroeck, B. (2002). Impaired B and T cell antigen receptor signaling in p110delta PI 3-kinase mutant mice. *Science* **297**, 1031-1034.

Okkenhaug, K., and Vanhaesebroeck, B. (2003). PI3K in lymphocyte development, differentiation and activation. *Nat Rev Immunol* **3**, 317-330.

Olivier, J. P., Raabe, T., Henkemeyer, M., Dickson, B., Mbamalu, G., Margolis, B., Schlessinger, J., Hafen, E., and Pawson, T. (1993). A Drosophila SH2-SH3 adaptor protein implicated in coupling the sevenless tyrosine kinase to an activator of Ras guanine nucleotide exchange, Sos. *Cell* **73**, 179-191.

Ong, S. H., Guy, G. R., Hadari, Y. R., Laks, S., Gotoh, N., Schlessinger, J., and Lax, I. (2000). FRS2 proteins recruit intracellular signaling pathways by binding to diverse targets on fibroblast growth factor and nerve growth factor receptors. *Mol Cell Biol* **20**, 979-989.

Ordaz, B., Tang, J., Xiao, R., Salgado, A., Sampieri, A., Zhu, M. X., and Vaca, L. (2005). Calmodulin and calcium interplay in the modulation of TRPC5 channel activity. Identification of a novel C-terminal domain for calcium/calmodulin-mediated facilitation. *J Biol Chem* **280**, 30788-30796.

Orth, J. D., and McNiven, M. A. (2003). Dynamin at the actin-membrane interface. *Curr Opin Cell Biol* **15**, 31-39.

Ott, V. L., Tamir, I., Niki, M., Pandolfi, P. P., and Cambier, J. C. (2002). Downstream of kinase, p62(dok), is a mediator of Fc gamma IIB inhibition of Fc epsilon RI signaling. *J Immunol* **168**, 4430-4439.

Parekh, A. B., and Penner, R. (1997). Store depletion and calcium influx. *Physiol Rev* **77**, 901-930.

Parekh, A. B., and Putney, J. W., Jr. (2005). Store-operated calcium channels. *Physiol Rev* **85**, 757-810.

Park, D. J., Rho, H. W., and Rhee, S. G. (1991). CD3 stimulation causes phosphorylation of phospholipase C-gamma 1 on serine and tyrosine residues in a human T-cell line. *Proc Natl Acad Sci U S A* **88**, 5453-5456.

Parsons, S. A., Millay, D. P., Wilkins, B. J., Bueno, O. F., Tsika, G. L., Neilson, J. R., Liberatore, C. M., Yutzey, K. E., Crabtree, G. R., Tsika, R. W., and Molkentin, J. D. (2004). Genetic loss of calcineurin blocks mechanical overload-induced skeletal muscle fiber type switching but not hypertrophy. *J Biol Chem* **279**, 26192-26200.

Patterson, R. L., van Rossum, D. B., and Gill, D. L. (1999). Store-operated Ca2+ entry: evidence for a secretion-like coupling model. *Cell* **98**, 487-499.

Patterson, R. L., van Rossum, D. B., Ford, D. L., Hurt, K. J., Bae, S. S., Suh, P. G., Kurosaki, T., Snyder, S. H., and Gill, D. L. (2002). Phospholipase C-gamma is required for agonist-induced Ca2+ entry. *Cell* **111**, 529-541.

Patterson, R. L., van Rossum, D. B., Nikolaidis, N., Gill, D. L., and Snyder, S. H. (2005). Phospholipase C-gamma: diverse roles in receptor-mediated calcium signaling. *Trends Biochem Sci* **30**, 688-697.

Pei, Z., Maloney, J. A., Yang, L., and Williamson, J. R. (1997). A new function for phospholipase C-gamma1: coupling to the adaptor protein GRB2. *Arch Biochem Biophys* **345**, 103-110.

Pennell, C. A., Arnold, L. W., Lutz, P. M., LoCascio, N. J., Willoughby, P. B., and Haughton, G. (1985). Cross-reactive idiotypes and common antigen binding specificities expressed by a series of murine B-cell lymphomas: etiological implications. *Proc Natl Acad Sci U S A* **82**, 3799-3803.

Petrie, R. J., Schnetkamp, P. P., Patel, K. D., Awasthi-Kalia, M., and Deans, J. P. (2000). Transient translocation of the B cell receptor and Src homology 2 domain-containing inositol phosphatase to lipid rafts: evidence toward a role in calcium regulation. *J Immunol* **165**, 1220-1227.

Pfrepper, K. I., Marie-Cardine, A., Simeoni, L., Kuramitsu, Y., Leo, A., Spicka, J., Hilgert, I., Scherer, J., and Schraven, B. (2001). Structural and functional dissection of the cytoplasmic domain of the transmembrane adaptor protein SIT (SHP2-interacting transmembrane adaptor protein). *Eur J Immunol* **31**, 1825-1836.

Piechulek, T., Rehlen, T., Walliser, C., Vatter, P., Moepps, B., and Gierschik, P. (2005). Isozyme-specific stimulation of phospholipase C-gamma2 by Rac GTPases. *J Biol Chem* **280**, 38923-38931.

Prakriya, M., and Lewis, R. S. (2001). Potentiation and inhibition of Ca(2+) release-activated Ca(2+) channels by 2-aminoethyldiphenyl borate (2-APB) occurs independently of IP(3) receptors. *J Physiol* **536**, 3-19.

Ptashne, M. (1992). A Genetic Switch: Phage (Lambda) and Higher Organsims. (Cambridge, MA: Cell Press).

Putney, J. W., Jr., Broad, L. M., Braun, F. J., Lievremont, J. P., and Bird, G. S. (2001). Mechanisms of capacitative calcium entry. *J Cell Sci* **114**, 2223-2229.

Rajendran, L., and Simons, K. (2005). Lipid rafts and membrane dynamics. *J Cell Sci* **118**, 1099-1102.

Rameh, L. E., Rhee, S. G., Spokes, K., Kazlauskas, A., Cantley, L. C., and Cantley, L. G. (1998). Phosphoinositide 3-kinase regulates phospholipase Cgamma-mediated calcium signaling. *J Biol Chem* **273**, 23750-23757.

Rameh, L. E., and Cantley, L. C. (1999). The role of phosphoinositide 3-kinase lipid products in cell function. *J Biol Chem* **274**, 8347-8350.

Rao, A. (1994). NF-ATp: a transcription factor required for the co-ordinate induction of several cytokine genes. *Immunol Today* **15**, 274-281.

Ravetch, J. V., and Perussia, B. (1989). Alternative membrane forms of Fc gamma RIII(CD16) on human natural killer cells and neutrophils. Cell type-specific expression of two genes that differ in single nucleotide substitutions. *J Exp Med* **170**, 481-497.

Ravichandran, K. S., Zhou, M. M., Pratt, J. C., Harlan, J. E., Walk, S. F., Fesik, S. W., and Burakoff, S. J. (1997). Evidence for a requirement for both phospholipid and phosphotyrosine binding via the Shc phosphotyrosine-binding domain in vivo. *Mol Cell Biol* **17**, 5540-5549.

Rebecchi, M. J., and Pentyala, S. N. (2000). Structure, function, and control of phosphoinositide-specific phospholipase C. *Physiol Rev* **80**, 1291-1335.

Reth, M. (1989). Antigen receptor tail clue. *Nature* **338**, 383.

Reth, M. (1992). Antigen Receptors on B Lymphocytes. *Annual Review of Immunology* **10**, 97-121.

Reth, M., Wienands, J., and Schamel, W. W. (2000). An unsolved problem of the clonal selection theory and the model of an oligomeric B-cell antigen receptor. *Immunol Rev* **176**, 10-18.

Rhee, S. G., and Choi, K. D. (1992a). Regulation of inositol phospholipid-specific phospholipase C isozymes. *J Biol Chem* **267**, 12393-12396.

Rhee, S. G., and Choi, K. D. (1992b). Multiple forms of phospholipase C isozymes and their activation mechanisms. *Adv Second Messenger Phosphoprotein Res* **26**, 35-61.

Rhee, S. G., and Bae, Y. S. (1997). Regulation of phosphoinositide-specific phospholipase C isozymes. *J Biol Chem* **272**, 15045-15048.

Rhee, S. G. (2001). Regulation of phosphoinositide-specific phospholipase C. *Annu Rev Biochem* **70**, 281-312.

Richards, J. D., Gold, M. R., Hourihane, S. L., DeFranco, A. L., and Matsuuchi, L. (1996). Reconstitution of B cell antigen receptor-induced signaling events in a nonlymphoid cell line by expressing the Syk protein-tyrosine kinase. *J Biol Chem* **271**, 6458-6466.

Rickles, R. J., Botfield, M. C., Weng, Z., Taylor, J. A., Green, O. M., Brugge, J. S., and Zoller, M. J. (1994). Identification of Src, Fyn, Lyn, PI3K and Abl SH3 domain ligands using phage display libraries. *Embo J* **13**, 5598-5604.

Robson, J. D., Davidson, D., and Veillette, A. (2004). Inhibition of the Jun N-terminal protein kinase pathway by SHIP-1, a lipid phosphatase that interacts with the adaptor molecule Dok-3. *Mol Cell Biol* **24**, 2332-2343.

Rogge, R. D., Karlovich, C. A., and Banerjee, U. (1991). Genetic dissection of a neurodevelopmental pathway: Son of sevenless functions downstream of the sevenless and EGF receptor tyrosine kinases. *Cell* **64**, 39-48.

Rohrschneider, L. R., Fuller, J. F., Wolf, I., Liu, Y., and Lucas, D. M. (2000). Structure, function, and biology of SHIP proteins. *Genes Dev* **14**, 505-520.

Roos, J., DiGregorio, P. J., Yeromin, A. V., Ohlsen, K., Lioudyno, M., Zhang, S., Safrina, O., Kozak, J. A., Wagner, S. L., Cahalan, M. D., Velicelebi, G., and Stauderman, K. A. (2005). STIM1, an essential and conserved component of store-operated Ca2+ channel function. *J Cell Biol* **169**, 435-445.

Rosado, J. A., Jenner, S., and Sage, S. O. (2000). A role for the actin cytoskeleton in the initiation and maintenance of store-mediated calcium entry in human platelets. Evidence for conformational coupling. *J Biol Chem* **275**, 7527-7533.

Rosado, J. A., Brownlow, S. L., and Sage, S. O. (2002). Endogenously expressed Trp1 is involved in store-mediated Ca2+ entry by conformational coupling in human platelets. *J Biol Chem* **277**, 42157-42163.

Rowley, R. B., Burkhardt, A. L., Chao, H. G., Matsueda, G. R., and Bolen, J. B. (1995). Syk protein-tyrosine kinase is regulated by tyrosine-phosphorylated Ig alpha/Ig beta immunoreceptor tyrosine activation motif binding and autophosphorylation. *J Biol Chem* **270**, 11590-11594.

Rozakis-Adcock, M., Fernley, R., Wade, J., Pawson, T., and Bowtell, D. (1993). The SH2 and SH3 domains of mammalian Grb2 couple the EGF receptor to the Ras activator mSos1. *Nature* **363**, 83-85.

Runnels, L. W., Yue, L., and Clapham, D. E. (2002). The TRPM7 channel is inactivated by PIP(2) hydrolysis. *Nat Cell Biol* **4**, 329-336.

Sadighi Akha, A. A., Willmott, N. J., Brickley, K., Dolphin, A. C., Galione, A., and Hunt, S. V. (1996). Anti-Ig-induced calcium influx in rat B lymphocytes mediated by cGMP through a dihydropyridine-sensitive channel. *J Biol Chem* **271**, 7297-7300.

Saiki, R. K., Scharf, S., Faloona, F., Mullis, K. B., Horn, G. T., Erlich, H. A., and Arnheim, N. (1985). Enzymatic amplification of beta-globin genomic sequences and restriction site analysis for diagnosis of sickle cell anemia. *Science* **230**, 1350-1354.

Salcini, A. E., McGlade, J., Pelicci, G., Nicoletti, I., Pawson, T., and Pelicci, P. G. (1994). Formation of Shc-Grb2 complexes is necessary to induce neoplastic transformation by overexpression of Shc proteins. *Oncogene* **9**, 2827-2836.

Sanger, F., Nicklen, S., and Coulson, A. R. (1977). DNA sequencing with chain-terminating inhibitors. *Proc Natl Acad Sci U S A* **74**, 5463-5467.

Sarkar, S. (1998). Tyrosine phosphorylation and translocation of LAT in platelets. *FEBS Lett* **441**, 357-360.

Satterthwaite, A. B., Li, Z., and Witte, O. N. (1998). Btk function in B cell development and response. *Semin Immunol* **10**, 309-316.

Sauer, K., Liou, J., Singh, S. B., Yablonski, D., Weiss, A., and Perlmutter, R. M. (2001). Hematopoietic progenitor kinase 1 associates physically and functionally with the adaptor proteins B cell linker protein and SLP-76 in lymphocytes. *J Biol Chem* **276**, 45207-45216.

Saxton, T. M., van Oostveen, I., Bowtell, D., Aebersold, R., and Gold, M. R. (1994). B cell antigen receptor cross-linking induces phosphorylation of the p21ras oncoprotein activators SHC and mSOS1 as well as assembly of complexes containing SHC, GRB-2, mSOS1, and a 145-kDa tyrosine-phosphorylated protein. *J Immunol* **153**, 623-636.

Schaeper, U., Gehring, N. H., Fuchs, K. P., Sachs, M., Kempkes, B., and Birchmeier, W. (2000). Coupling of Gab1 to c-Met, Grb2, and Shp2 mediates biological responses. *J Cell Biol* **149**, 1419-1432.

Schamel, W. W., and Reth, M. (2000). Monomeric and oligomeric complexes of the B cell antigen receptor. *Immunity* **13**, 5-14.

Scharenberg, A. M., El-Hillal, O., Fruman, D. A., Beitz, L. O., Li, Z., Lin, S., Gout, I., Cantley, L. C., Rawlings, D. J., and Kinet, J. P. (1998). Phosphatidylinositol-3,4,5-trisphosphate (PtdIns-3,4,5-P3)/Tec kinase-dependent calcium signaling pathway: a target for SHIP-mediated inhibitory signals. *Embo J* **17**, 1961-1972.

Scharenberg, A. M., and Kinet, J. P. (1998). PtdIns-3,4,5-P3: a regulatory nexus between tyrosine kinases and sustained calcium signals. *Cell* **94**, 5-8.

Schlessinger, J., and Lemmon, M. A. (2003). SH2 and PTB domains in tyrosine kinase signaling. *Sci STKE* **2003**, RE12.

Secrist, J. P., Karnitz, L., and Abraham, R. T. (1991). T-cell antigen receptor ligation induces tyrosine phosphorylation of phospholipase C-gamma 1. *J Biol Chem* **266**, 12135-12139.

Seedorf, K., Kostka, G., Lammers, R., Bashkin, P., Daly, R., Burgess, W. H., van der Bliek, A. M., Schlessinger, J., and Ullrich, A. (1994). Dynamin binds to SH3 domains of phospholipase C gamma and GRB-2. *J Biol Chem* **269**, 16009-16014.

Sekiya, F., Bae, Y. S., and Rhee, S. G. (1999). Regulation of phospholipase C isozymes: activation of phospholipase C-gamma in the absence of tyrosine-phosphorylation. *Chem Phys Lipids* **98**, 3-11.

Shibasaki, F., Price, E. R., Milan, D., and McKeon, F. (1996). Role of kinases and the phosphatase calcineurin in the nuclear shuttling of transcription factor NF-AT4. *Nature* **382**, 370-373.

Shinohara, H., Inoue, A., Toyama-Sorimachi, N., Nagai, Y., Yasuda, T., Suzuki, H., Horai, R., Iwakura, Y., Yamamoto, T., Karasuyama, H., Miyake, K., and Yamanashi, Y. (2005). Dok-1 and Dok-2 are negative regulators of lipopolysaccharide-induced signaling. *J Exp Med* **201**, 333-339.

Simeoni, L., Smida, M., Posevitz, V., Schraven, B., and Lindquist, J. A. (2005). Right time, right place: the organization of membrane proximal signaling. *Semin Immunol* **17**, 35-49.

Simons, K., and Toomre, D. (2000). Lipid rafts and signal transduction. *Nat Rev Mol Cell Biol* **1**, 31-39.

Skolnik, E. Y., Batzer, A., Li, N., Lee, C. H., Lowenstein, E., Mohammadi, M., Margolis, B., and Schlessinger, J. (1993). The function of GRB2 in linking the insulin receptor to Ras signaling pathways. *Science* **260**, 1953-1955.

Sommers, C. L., Park, C. S., Lee, J., Feng, C., Fuller, C. L., Grinberg, A., Hildebrand, J. A., Lacana, E., Menon, R. K., Shores, E. W., Samelson, L. E., and Love, P. E. (2002). A LAT mutation that inhibits T cell development yet induces lymphoproliferation. *Science* **296**, 2040-2043.

Songyang, Z., Shoelson, S. E., Chaudhuri, M., Gish, G., Pawson, T., Haser, W. G., King, F., Roberts, T., Ratnofsky, S., Lechleider, R. J., and et al. (1993). SH2 domains recognize specific phosphopeptide sequences. *Cell* **72**, 767-778.

Songyang, Z., Yamanashi, Y., Liu, D., and Baltimore, D. (2001). Domain-dependent function of the rasGAP-binding protein p62Dok in cell signaling. *J Biol Chem* **276**, 2459-2465.

Sonoda, E., Morrison, C., Yamashita, Y. M., Takata, M., and Takeda, S. (2001). Reverse genetic studies of homologous DNA recombination using the chicken B-lymphocyte line, DT40. *Philos Trans R Soc Lond B Biol Sci* **356**, 111-117.

Sparks, A. B., Rider, J. E., Hoffman, N. G., Fowlkes, D. M., Quillam, L. A., and Kay, B. K. (1996). Distinct ligand preferences of Src homology 3 domains from Src, Yes, Abl, Cortactin, p53bp2, PLCgamma, Crk, and Grb2. *Proc Natl Acad Sci U S A* **93**, 1540-1544.

Sparks, A. B., Rider, J. E., and Kay, B. K. (1998). Mapping the specificity of SH3 domains with phage-displayed random-peptide libraries. *Methods Mol Biol* **84**, 87-103.

Su, Y.-W., Zhang, Y., Schweikert, J., Koretzky, G. A., Reth, M., and Wienands, J. (1999). Interaction of SLP adaptors with the SH2 domain of Tec family kinases. *Eur J Immunol* **29**, 3702-3711.

Su, Y. W., and Jumaa, H. (2003). LAT links the pre-BCR to calcium signaling. *Immunity* **19**, 295-305.

Sugawara, H., Kurosaki, M., Takata, M., and Kurosaki, T. (1997). Genetic evidence for involvement of type 1, type 2 and type 3 inositol 1,4,5-trisphosphate receptors in signal transduction through the B-cell antigen receptor. *Embo J* **16**, 3078-3088.

Takata, M., Sabe, H., Hata, A., Inazu, T., Homma, Y., Nukada, T., Yamamura, H., and Kurosaki, T. (1994). Tyrosine Kinases Lyn and Syk Regulate B-Cell Receptor-Coupled Ca2+ Mobilization through Distinct Pathways. *Embo Journal* **13**, 1341-1349.

Takata, M., Homma, Y., and Kurosaki, T. (1995). Requirement of Phospholipase C-Gamma-2 Activation in Surface-Immunoglobulin M-Induced B-Cell Apoptosis. *Journal of Experimental Medicine* **182**, 907-914.

Takata, M., and Kurosaki, T. (1996). A role for Bruton's tyrosine kinase in B cell antigen receptor-mediated activation of phospholipase C-gamma 2. *J Exp Med* **184**, 31-40.

Tamir, I., Stolpa, J. C., Helgason, C. D., Nakamura, K., Bruhns, P., Daeron, M., and Cambier, J. C. (2000). The RasGAP-binding protein p62dok is a mediator of inhibitory FcgammaRIIB signals in B cells. *Immunity* **12**, 347-358.

Tanaka, M., Gupta, R., and Mayer, B. J. (1995). Differential inhibition of signaling pathways by dominant-negative SH2/SH3 adapter proteins. *Mol Cell Biol* **15**, 6829-6837.

Thompson, J. D., Higgins, D. G., and Gibson, T. J. (1994). CLUSTAL W: improving the sensitivity of progressive multiple sequence alignment through sequence weighting, position-specific gap penalties and weight matrix choice. *Nucleic Acids Res* **22**, 4673-4680.

Timmerman, L. A., Clipstone, N. A., Ho, S. N., Northrop, J. P., and Crabtree, G. R. (1996). Rapid shuttling of NF-AT in discrimination of Ca2+ signals and immunosuppression. *Nature* **383**, 837-840.

Tkaczyk, C., Horejsi, V., Iwaki, S., Draber, P., Samelson, L. E., Satterthwaite, A. B., Nahm, D. H., Metcalfe, D. D., and Gilfillan, A. M. (2004). NTAL phosphorylation is a pivotal link between the signaling cascades leading to human mast cell degranulation following Kit activation and Fc epsilon RI aggregation. *Blood* **104**, 207-214.

Tong, Q., Chu, X., Cheung, J. Y., Conrad, K., Stahl, R., Barber, D. L., Mignery, G., and Miller, B. A. (2004). Erythropoietin-modulated calcium influx through TRPC2 is mediated by phospholipase Cgamma and IP3R. *Am J Physiol Cell Physiol* **287**, C1667-1678.

Torgersen, K. M., Vaage, J. T., Rolstad, B., and Tasken, K. (2001). A soluble LAT deletion mutant inhibits T-cell activation: reduced recruitment of signalling molecules to glycolipid-enriched microdomains. *Cell Signal* **13**, 213-220.

Trebak, M., St, J. B. G., McKay, R. R., Birnbaumer, L., and Putney, J. W., Jr. (2003). Signaling mechanism for receptor-activated canonical transient receptor potential 3 (TRPC3) channels. *J Biol Chem* **278**, 16244-16252.

Tridandapani, S., Kelley, T., Cooney, D., Pradhan, M., and Coggeshall, K. M. (1997). Negative signaling in B cells: SHIP Grbs Shc. *Immunol Today* **18**, 424-427.

Trub, T., Frantz, J. D., Miyazaki, M., Band, H., and Shoelson, S. E. (1997). The role of a lymphoid-restricted, Grb2-like SH3-SH2-SH3 protein in T cell receptor signaling. *J Biol Chem* **272**, 894-902.

Tseng, P. H., Lin, H. P., Hu, H., Wang, C., Zhu, M. X., and Chen, C. S. (2004). The canonical transient receptor potential 6 channel as a putative phosphatidylinositol 3,4,5-trisphosphate-sensitive calcium entry system. *Biochemistry* **43**, 11701-11708.

Tu, C. L., Chang, W., and Bikle, D. D. (2005). Phospholipase cgamma1 is required for activation of store-operated channels in human keratinocytes. *J Invest Dermatol* **124**, 187-197.

Tu, J. C., Xiao, B., Naisbitt, S., Yuan, J. P., Petralia, R. S., Brakeman, P., Doan, A., Aakalu, V. K., Lanahan, A. A., Sheng, M., and Worley, P. F. (1999). Coupling of mGluR/Homer and PSD-95 complexes by the Shank family of postsynaptic density proteins. *Neuron* **23**, 583-592.

Turner, M., Schweighoffer, E., Colucci, F., Di Santo, J. P., and Tybulewicz, V. L. (2000). Tyrosine kinase SYK: essential functions for immunoreceptor signalling. *Immunol Today* **21**, 148-154.

Tuveson, D. A., Carter, R. H., Soltoff, S. P., and Fearon, D. T. (1993). CD19 of B cells as a surrogate kinase insert region to bind phosphatidylinositol 3-kinase. *Science* **260**, 986-989.

Van Den Herik-Oudijk, I. E., Westerdaal, N. A., Henriquez, N. V., Capel, P. J., and Van De Winkel, J. G. (1994). Functional analysis of human Fc gamma RII (CD32) isoforms expressed in B lymphocytes. *J Immunol* **152**, 574-585.

van der Geer, P., Wiley, S., Gish, G. D., and Pawson, T. (1996). The Shc adaptor protein is highly phosphorylated at conserved, twin tyrosine residues (Y239/240) that mediate protein-protein interactions. *Curr Biol* **6**, 1435-1444.

van Dijk, T. B., van Den Akker, E., Amelsvoort, M. P., Mano, H., Lowenberg, B., and von Lindern, M. (2000). Stem cell factor induces phosphatidylinositol 3'-kinase-dependent Lyn/Tec/Dok-1 complex formation in hematopoietic cells. *Blood* **96**, 3406-3413.

van Rossum, D. B., Patterson, R. L., Kiselyov, K., Boehning, D., Barrow, R. K., Gill, D. L., and Snyder, S. H. (2004). Agonist-induced Ca2+ entry determined by inositol 1,4,5-trisphosphate recognition. *Proc Natl Acad Sci U S A* **101**, 2323-2327.

van Rossum, D. B., Patterson, R. L., Sharma, S., Barrow, R. K., Kornberg, M., Gill, D. L., and Snyder, S. H. (2005). Phospholipase Cgamma1 controls surface expression of TRPC3 through an intermolecular PH domain. *Nature* **434**, 99-104.

Van Slyke, P., Coll, M. L., Master, Z., Kim, H., Filmus, J., and Dumont, D. J. (2005). Dok-R mediates attenuation of epidermal growth factor-dependent mitogen-activated protein kinase and Akt activation through processive recruitment of c-Src and Csk. *Mol Cell Biol* **25**, 3831-3841.

Vanhaesebroeck, B., Leevers, S. J., Panayotou, G., and Waterfield, M. D. (1997). Phosphoinositide 3-kinases: a conserved family of signal transducers. *Trends Biochem Sci* **22**, 267-272.

Vazquez, G., Lievremont, J. P., St, J. B. G., and Putney, J. W., Jr. (2001). Human Trp3 forms both inositol trisphosphate receptor-dependent and receptor-independent store-operated cation channels in DT40 avian B lymphocytes. *Proc Natl Acad Sci U S A* **98**, 11777-11782.

Vazquez, G., Wedel, B. J., Trebak, M., St John Bird, G., and Putney, J. W., Jr. (2003). Expression level of the canonical transient receptor potential 3 (TRPC3) channel determines its mechanism of activation. *J Biol Chem* **278**, 21649-21654.

Veillette, A., Latour, S., and Davidson, D. (2002). Negative regulation of immunoreceptor signaling. *Annual Review of Immunology* **20**, 669-707.

Venkatachalam, K., Ma, H. T., Ford, D. L., and Gill, D. L. (2001). Expression of functional receptor-coupled TRPC3 channels in DT40 triple receptor InsP3 knockout cells. *J Biol Chem* **276**, 33980-33985.

Venkatachalam, K., Zheng, F., and Gill, D. L. (2003). Regulation of canonical transient receptor potential (TRPC) channel function by diacylglycerol and protein kinase C. *J Biol Chem* **278**, 29031-29040.

Volna, P., Lebduska, P., Draberova, L., Simova, S., Heneberg, P., Boubelik, M., Bugajev, V., Malissen, B., Wilson, B. S., Horejsi, V., Malissen, M., and Draber, P. (2004). Negative regulation of mast cell signaling and function by the adaptor LAB/NTAL. *J Exp Med* **200**, 1001-1013.

Walter, A. O., Peng, Z. Y., and Cartwright, C. A. (1999). The Shp-2 tyrosine phosphatase activates the Src tyrosine kinase by a non-enzymatic mechanism. *Oncogene* **18**, 1911-1920.

Wang, D., Feng, J., Wen, R., Marine, J. C., Sangster, M. Y., Parganas, E., Hoffmeyer, A., Jackson, C. W., Cleveland, J. L., Murray, P. J., and Ihle, J. N. (2000). Phospholipase Cgamma2 is essential in the functions of B cell and several Fc receptors. *Immunity* **13**, 25-35.

Wang, Y., Horvath, O., Hamm-Baarke, A., Richelme, M., Gregoire, C., Guinamard, R., Horejsi, V., Angelisova, P., Spicka, J., Schraven, B., Malissen, B., and Malissen, M. (2005). Single and combined deletions of the NTAL/LAB and LAT adaptors minimally affect B-cell development and function. *Mol Cell Biol* **25**, 4455-4465.

Weber, K., and Osborn, M. (1969). The reliability of molecular weight determinations by dodecyl sulfate-polyacrylamide gel electrophoresis. *J Biol Chem* **244**, 4406-4412.

Weinstein, H., and Mehler, E. L. (1994). Ca(2+)-binding and structural dynamics in the functions of calmodulin. *Annu Rev Physiol* **56**, 213-236.

Weintraub, B. C., Jun, J. E., Bishop, A. C., Shokat, K. M., Thomas, M. L., and Goodnow, C. C. (2000). Entry of B cell receptor into signaling domains is inhibited in tolerant B cells. *J Exp Med* **191**, 1443-1448.

Weissman, A. M., Hou, D., Orloff, D. G., Modi, W. S., Seuanez, H., O'Brien, S. J., and Klausner, R. D. (1988). Molecular cloning and chromosomal localization of the human T-cell receptor zeta chain: distinction from the molecular CD3 complex. *Proc Natl Acad Sci U S A* **85**, 9709-9713.

Wen, R., Chen, Y., Schuman, J., Fu, G., Yang, S., Zhang, W., Newman, D. K., and Wang, D. (2004). An important role of phospholipase Cgamma1 in pre-B-cell development and allelic exclusion. *Embo J* **23**, 4007-4017.

White, M. F., and Yenush, L. (1998). The IRS-signaling system: a network of docking proteins that mediate insulin and cytokine action. *Curr Top Microbiol Immunol* **228**, 179-208.

White, S. P., Scott, D. L., Otwinowski, Z., Gelb, M. H., and Sigler, P. B. (1990). Crystal structure of cobra-venom phospholipase A2 in a complex with a transition-state analogue. *Science* **250**, 1560-1563.

Wick, M. J., Dong, L. Q., Hu, D., Langlais, P., and Liu, F. (2001). Insulin receptor-mediated p62dok tyrosine phosphorylation at residues 362 and 398 plays distinct roles for binding GTPase-activating protein and Nck and is essential for inhibiting insulin-stimulated activation of Ras and Akt. *J Biol Chem* **276**, 42843-42850.

Wienands, J., Freuler, F., and Baumann, G. (1995). Tyrosine-phosphorylated forms of Ig beta, CD22, TCR zeta and HOSS are major ligands for tandem SH2 domains of Syk. *Int Immunol* **7**, 1701-1708.

Wienands, J., Schweikert, J., Wollscheid, B., Jumaa, H., Nielsen, P. J., and Reth, M. (1998). SLP-65: A new signaling component in B lymphocytes which requires expression of the antigen receptor for phosphorylation. *J Exp Med* **188**, 791-795.

Wienands, J. (2000a). Signal transduction elements of the B cell antigen receptor and their role in immunodeficiencies. *Immunobiology* **202**, 120-133.

Wienands, J. (2000b). The B-cell antigen receptor: formation of signaling complexes and the function of adaptor proteins. *Curr Top Microbiol Immunol* **245**, 53-76.

Wilde, J. I., and Watson, S. P. (2001). Regulation of phospholipase C gamma isoforms in haematopoietic cells: why one, not the other? *Cell Signal* **13**, 691-701.

Williams, R. T., Senior, P. V., Van Stekelenburg, L., Layton, J. E., Smith, P. J., and Dziadek, M. A. (2002). Stromal interaction molecule 1 (STIM1), a transmembrane protein with growth suppressor activity, contains an extracellular SAM domain modified by N-linked glycosylation. *Biochim Biophys Acta* **1596**, 131-137.

Winding, P., and Berchtold, M. W. (2001). The chicken B cell line DT40: a novel tool for gene disruption experiments. *J Immunol Methods* **249**, 1-16.

Wollscheid, B., Wienands, J., and Reth, M. (1999). The adaptor protein SLP-65/BLNK controls the calcium response in activated B cells. *Curr Top Microbiol Immunol* **246**, 283-288; discussion 288-289.

Xavier, R., Brennan, T., Li, Q., McCormack, C., and Seed, B. (1998). Membrane compartmentation is required for efficient T cell activation. *Immunity* **8**, 723-732.

Yamanashi, Y., Mori, S., Yoshida, M., Kishimoto, T., Inoue, K., Yamamoto, T., and Toyoshima, K. (1989). Selective expression of a protein-tyrosine kinase, p56lyn, in hematopoietic cells and association with production of human T-cell lymphotropic virus type I. *Proc Natl Acad Sci U S A* **86**, 6538-6542.

Yamanashi, Y., Kakiuchi, T., Mizuguchi, J., Yamamoto, T., and Toyoshima, K. (1991). Association of B cell antigen receptor with protein tyrosine kinase Lyn. *Science* **251**, 192-194.

Yamanashi, Y., and Baltimore, D. (1997). Identification of the Abl- and rasGAP-associated 62 kDa protein as a docking protein, Dok. *Cell* **88**, 205-211.

Yamanashi, Y., Tamura, T., Kanamori, T., Yamane, H., Nariuchi, H., Yamamoto, T., and Baltimore, D. (2000). Role of the rasGAP-associated docking protein p62(dok) in negative regulation of B cell receptor-mediated signaling. *Genes Dev* **14**, 11-16.

Yanagi, S., Sugawara, H., Kurosaki, M., Sabe, H., Yamamura, H., and Kurosaki, T. (1996). CD45 modulates phosphorylation of both autophosphorylation and negative regulatory tyrosines of Lyn in B cells. *J Biol Chem* **271**, 30487-30492.

Yao, Y., Ferrer-Montiel, A. V., Montal, M., and Tsien, R. Y. (1999). Activation of store-operated Ca2+ current in Xenopus oocytes requires SNAP-25 but not a diffusible messenger. *Cell* **98**, 475-485.

Yasuda, T., Shirakata, M., Iwama, A., Ishii, A., Ebihara, Y., Osawa, M., Honda, K., Shinohara, H., Sudo, K., Tsuji, K., Nakauchi, H., Iwakura, Y., Hirai, H., Oda, H., Yamamoto, T., and Yamanashi, Y. (2004). Role of Dok-1 and Dok-2 in myeloid homeostasis and suppression of leukemia. *J Exp Med* **200**, 1681-1687.

Yi, T. L., Bolen, J. B., and Ihle, J. N. (1991). Hematopoietic cells express two forms of lyn kinase differing by 21 amino acids in the amino terminus. *Mol Cell Biol* **11**, 2391-2398.

Yoshida, K., Yamashita, Y., Miyazato, A., Ohya, K., Kitanaka, A., Ikeda, U., Shimada, K., Yamanaka, T., Ozawa, K., and Mano, H. (2000). Mediation by the protein-tyrosine kinase Tec of signaling between the B cell antigen receptor and Dok-1. *J Biol Chem* **275**, 24945-24952.

Yu, P., Constien, R., Dear, N., Katan, M., Hanke, P., Bunney, T. D., Kunder, S., Quintanilla-Martinez, L., Huffstadt, U., Schroder, A., Jones, N. P., Peters, T., Fuchs, H., de Angelis, M. H., Nehls, M., Grosse, J., Wabnitz, P., Meyer, T. P., Yasuda, K., Schiemann, M., Schneider-Fresenius, C., Jagla, W., Russ, A., Popp, A., Josephs, M., Marquardt, A., Laufs, J., Schmittwolf, C., Wagner, H., Pfeffer, K., and Mudde, G. C. (2005). Autoimmunity and inflammation due to a gain-of-function mutation in phospholipase C gamma 2 that specifically increases external Ca2+ entry. *Immunity* **22**, 451-465.

Yuan, J. P., Kiselyov, K., Shin, D. M., Chen, J., Shcheynikov, N., Kang, S. H., Dehoff, M. H., Schwarz, M. K., Seeburg, P. H., Muallem, S., and Worley, P. F. (2003). Homer binds TRPC family channels and is required for gating of TRPC1 by IP3 receptors. *Cell* **114**, 777-789.

Zeng, L., Sachdev, P., Yan, L., Chan, J. L., Trenkle, T., McClelland, M., Welsh, J., and Wang, L. H. (2000). Vav3 mediates receptor protein tyrosine kinase signaling, regulates GTPase activity, modulates cell morphology, and induces cell transformation. *Mol Cell Biol* **20**, 9212-9224.

Zhang, S. L., Yu, Y., Roos, J., Kozak, J. A., Deerinck, T. J., Ellisman, M. H., Stauderman, K. A., and Cahalan, M. D. (2005). STIM1 is a Ca2+ sensor that activates CRAC channels and migrates from the Ca2+ store to the plasma membrane. *Nature* **437**, 902-905.

Zhang, W., Trible, R. P., and Samelson, L. E. (1998a). LAT palmitoylation: its essential role in membrane microdomain targeting and tyrosine phosphorylation during T cell activation. *Immunity* **9**, 239-246.

Zhang, W., Sloan-Lancaster, J., Kitchen, J., Trible, R. P., and Samelson, L. E. (1998b). LAT: the ZAP-70 tyrosine kinase substrate that links T cell receptor to cellular activation. *Cell* **92**, 83-92.

Zhang, W., Sommers, C. L., Burshtyn, D. N., Stebbins, C. C., DeJarnette, J. B., Trible, R. P., Grinberg, A., Tsay, H. C., Jacobs, H. M., Kessler, C. M., Long, E. O., Love, P. E., and Samelson, L. E. (1999a). Essential role of LAT in T cell development. *Immunity* **10**, 323-332.

Zhang, W. G., Trible, R. P., Zhu, M. H., Liu, S. K., McGlade, J., and Samelson, L. E. (2000). Association of Grb2 Gads, and phospholipase C-gamma 1 with phosphorylated LAT tyrosine residues - Effect of LAT tyrosine mutations on T cell antigen receptor-mediated signaling. *Journal of Biological Chemistry* **275**, 23355-23361.

Zhao, M., Schmitz, A. A., Qin, Y., Di Cristofano, A., Pandolfi, P. P., and Van Aelst, L. (2001). Phosphoinositide 3-kinase-dependent membrane recruitment of p62(dok) is essential for its negative effect on mitogen-activated protein (MAP) kinase activation. *J Exp Med* **194**, 265-274.

Zhao, M., Janas, J. A., Niki, M., Pandolfi, P. P., and Van Aelst, L. (2006). Dok-1 independently attenuates Ras/mitogen-activated protein kinase and Src/c-myc pathways to inhibit platelet-derived growth factor-induced mitogenesis. *Mol Cell Biol* **26**, 2479-2489.

Zhu, M., Janssen, E., and Zhang, W. (2003). Minimal requirement of tyrosine residues of linker for activation of T cells in TCR signaling and thymocyte development. *J Immunol* **170**, 325-333.

Zhu, M., Liu, Y., Koonpaew, S., Granillo, O., and Zhang, W. (2004). Positive and negative regulation of FcepsilonRI-mediated signaling by the adaptor protein LAB/NTAL. *J Exp Med* **200**, 991-1000.

Zhu, M., Rhee, I., Liu, Y., and Zhang, W. (2006). Negative regulation of Fcepsilon RI-mediated signaling and mast cell function by the adaptor protein LAX. *J Biol Chem*.

Zubov, A. I., Kaznacheeva, E. V., Nikolaev, A. V., Alexeenko, V. A., Kiselyov, K., Muallem, S., and Mozhayeva, G. N. (1999). Regulation of the miniature plasma membrane Ca(2+) channel I(min) by inositol 1,4,5-trisphosphate receptors. *J Biol Chem* **274**, 25983-25985.

8. Addendum

8.1. List of Figures

8.2. List of Tables

Curriculum vitae

Personal Data

Name	Björn Stork	
Date/Place of birth	1975/08/25 in Herford	
Marital status	single	
Nationality	German	
Address	Private: Hannoversche Str. 137, App. 8 37077 Göttingen Ph: 0170 3448368	Office: Cellular and Molecular Immunology University of Göttingen Humboldtallee 34 37073 Göttingen Ph: 0551 3913854 bstork@gwdg.de

School

1982 – 1986	Elementary School, Eilshausen, Germany
1986 – 1995	Gymnasium am Markt, Bünde, Germany
Degree	Allgemeine Hochschulreife

Civilian Service

1995/08-1996/08	Diakonie II, Herford, Germany

University

1996 – 2001	Studies of Biochemistry at the University of Bielefeld, Germany
2000	Internship at McGill University, Montréal, Canada

Diploma

2001/08-2002/04	Department of Biochemistry & Molecular Immunology at the University of Bielefeld; Supervisor Prof. J. Wienands Title of diploma thesis: How does the antigen receptor on B lymphocytes organize the Ca^{2+} initiation complex?

Work experience

2002/07-2004/12	Scientific assistant in the Dept. of Biochemistry & Molecular Immunology at the University of Bielefeld, Prof. J. Wienands
2002/07-2003/04	Research stay at the Kansai Medical University, Osaka, Japan (Prof. T. Kurosaki)
since 2005/01	Scientific assistant in the Dept. of Cellular & Molecular Immunology at the University of Göttingen, Prof. J. Wienands

Bielefeld, 2006/07/12

Eidesstattliche Erklärung

Hiermit erkläre ich an Eides Statt, die vorliegende Dissertation selbständig und ohne unzulässige Hilfe Dritter unter ausschließlicher Nutzung der aufgeführten Materialien, Methoden und Literaturquellen an der Universität Bielefeld, an der Kansai Medical University (Osaka, Japan) und an der Georg-August-Universität Göttingen unter der Leitung von Prof. Dr. J. Wienands und Prof. Dr. T. Kurosaki angefertigt zu haben.

Bielefeld, den 12.07.2006 Björn Stork

Gedruckt auf alterungsbeständigem Papier nach ISO 9706